Development of Graft Copolymeric Carrier Networks for Controlled Drug Delivery and its Evaluation

A dissertation submitted in partial

fulfillment of the requirements for the degree of

DOCTOR OF PHILOSOPHY

(Pharmaceutics)

by

Ume Ruqia Tulain

B. Pharm,. M.Phil.

Department of Pharmacy

Faculty of Pharmacy and Alternative Medicine,

The Islamia University of Bahawalpur,

Pakistan

(2012-2015)

In the name of Allah, Most Gracious, Most Merciful

DEDICATION

Dedicated to,

My Dearest Parents
For their endless support, appreciation, encouragement and ever sincere prayers

My Dearest Son
Ahmed Abdullah
For his love, care and affiliation,

My Husband
Nazir Ahmad
For his cooperation, care, confidence and encouragement

My Dearest Brothers& Sisters
For their love, care, confidence and giving me strength to chase my dreams

DECLARATION

I, Ume Ruqia Tulain, Ph.D Scholar of Department of Pharmacy, The Islamia University of Bahawalpur, hereby declare that the research work entitled “Development of Graft Copolymeric Carrier Networks for Controlled Drug Delivery and its Evaluation” is done by me. I also certify that nothing has been incorporated in this research work without acknowledgement and that to the best of my knowledge and belief it does not contain any material previously published or written by any other person or any material previously submitted for a degree in any university where due reference is not made in the text.

Ume Ruqia Tulain

CERTIFICATE

It is hereby certified that this dissertation entitled **"Development of Graft Copolymeric Carrier Networks for Controlled Drug Delivery and its Evaluation"** is based upon the results of experiments carried out by **Ms. Ume Ruqia Tulain** under my supervision. No portion of this work has previously been presented for higher degree in this university or any other institute of learning and to the best of the knowledge, no material has been used in this dissertation which is not her own work except where due acknowledgement has been made. She has fulfilled all the requirements and is qualified to submit this dissertation for the Degree of Doctor of Philosophy in Pharmaceutics.

Prof. Dr. Mahmood Ahmad
Supervisor,
Dean Faculty of Pharmacy and Alternative medicines,
The Islamia University of Bahawalpur

Ph.D. DISSERTATION (PHARMACEUTICS) OPEN DEFENSE/VIVA VOCE EXAMIANTION OF **MS. UME RUQIA TULAIN** HELD ON 14TH SEPTEMBER 2015

Candidate _____

Supervisor/Internal Examiner
(Prof. Dr. Mahmood Ahmad) _____ 14/9/15

External Examiner I
(Prof. Dr. Muhammad Jamshaid) _____ 14/09/15

External Examiner II
(Prof. Dr. Abdullah Dayo) _____ 14/09/15

Chairman
Department of Pharmacy _____

Dean
Faculty of Pharmacy & Alternative Medicine _____ 14/9/15

ACKNOWLEDGEMENT

All praises to **Allah Almighty** who created the universe and knows whatever is in it, hidden or evident, and who bestowed upon me the intellectual ability and wisdom to search for its secrets.

All respects, blessings and love to the last **Holy Prophet MUHAMMAD**, (Sal-Allaho-alaihe-wa-aalehee-wasallam), who enabled me to recognize Creator and His creations and changed me from man to Muslim by teaching, "Seek knowledge from cradle to grave."

I feel ample pleasure in expressing my heartiest gratitude to my ever affectionate supervisor Prof. Dr. Mahmood Ahmad for his supervision and constant support. His precious assistance of constructive comments and suggestions throughout the experimental and thesis works have contributed to the success of this research.

I would like to encompass my deep felt gratitude and appreciations to Dr. Naveed Akhtar, Chairman Department of Pharmacy for his support to the completion of this milestone.

I will record my sincere thanks and appreciation for my seniors, particularly Assistant Professors Dr. Muhammad Usman Minhas, and Assistant Professors Dr. Imran Masood, Assistant Professors Dr. Raees Muhammad Akhter and Mr. Muhammad Zubair Malik for their valuable guidance and support.

I would like to thank Ayesha Rashid, who as a good friend, was always willing to help and give her best suggestions. It would have been a lonely lab without her. It would like to acknowledge cooperation and support of my class fellows Mrs. Ayesha Yakoob, and Mr. Furqan Muhammad Iqbal.

Also I would like to acknowledge Hafiz Muhammad Saleem, peon Dean Office and Mukhtar Ahmad, Lab attendant, M.Phil/Ph.D Research Lab. 25 for their services and cooperation during whole of my research work.

I express my heartfelt gratitude to my mother, father, husband, my son and all other family members. Their unlimited love and affection served me a beacon of light. It is through their benevolent help and wholehearted prayers that enabled me to complete my studies. I am also indebted to all those people who prayed for my success.

UME RUQIA TULAIN

Abbreviations

CMAX	Carboxymethyl Arabinoxylan
AA	Acrylic acid
CMC	Carboxy methyl cellulose
MAA	Methacrylic acid
PEG	Polyethylene glycol
HEMA	2-Hydroxyethyl methacrylate
MBA	N,N/ methylene-bis-acrylamide
KPS	Potassium per sulphate
FTIR	Fourier transform infrared spectroscopy
XRD	X-ray diffraction
SEM	Scanning electron microscopy
TGA	Thermal gravimetric analysis
DSC	Differential scanning calorimetry
A	CMAX-g-AA hydrogel
M	CMAX-g-MAA hydrogel
CA	CMC-g-AA hydrogel
CMA	CMC-g-MAA hydrogel
PMA	PEG-g-MAA
PHA	PEG (HEMA-co-AA) hydrogel
Hrs	Hours
UV	Ultraviolet
$AUC_{0-\infty}$	Area Under the Curve from zero to infinity
$AUMC_{0-\infty}$	Area Under the Moment Curve from zero to infinity
C_{max}	Maximum Plasma Concentration
HPLC	High Performance Liquid Chromatography
GIT	Gastro-intestinal Tract
MRT	Mean Residence Time
T_{max}	Time for Maximum Plasma Concentration
$t_{1/2}$	Half life
b.w	Body weight

ALT	Alanine transaminase
AST	Aspartate transaminase
MCH	Mean corpuscular hemoglobin
MCV	Mean corpuscular volume
MCHC	Mean corpuscular hemoglobin concentration
Hb	Hemoglobin

CONTENTS

List of Tables

List of Figures

Abstract

Background: Rabeprazole sodium, a proton pump inhibitor, is expedient for the preclusion and management of ulcers, gastro esophageal reflux disease (GERD) and other disorders encompassing extreme acid secretion. Numerous methodologies have been employed to prepare substantial formulation of rabeprazole sodium. However during development process of other drug carriers several complications are challenged such as unpredictability and failure to localize the API within preferred region of the GIT for desired time and this variability may cause arbitrary bioavailability.

Purpose of study: Present generous work deals with synthesis and characterization of an innovative drug delivery carriers for highly acid labile drug, to overcome the problems of acidic degradation, extensive pre systemic metabolism, shorter half life (frequent dosing) and relatively low bioavailability (52%) for rabeprazole sodium controlled release at specific site in GIT.

Experimental design: Free radical polymerization technique was employed to synthesize crosslinked polymeric networks of varying composition by using carboxymethyl arabinoxylan, carboxymethyl cellulose and polyethylene glycol (polymer), methacrylic acid and acrylic acid (monomer), potassium persulfate (initiator) and N,N Methylene bisacrylamide (crosslinker). Prepared crosslinked polymeric networks were characterized by swelling analysis at acidic and basic pH, instrumental analysis (SEM, FTIR and thermal analysis) and pH responsive *in vitro* drug release of model drug rabeprazole sodium. Acute oral toxicity study of prepared hydrogels were implemented consistent with the "Organization of Economic Co-operation and Development (OECD) guideline for chemicals toxicity study. On the basis of preliminary characterization and *in vitro* release analysis investigations two formulations (CA5 and A6) with maximum *in vitro* cumulative drug release were selected for *in vivo* evaluation. Healthy rabbits having weight greater than 2.5 ± 0.61 Kg were used for *in vivo* study. Rabbit plasma was analyzed by HPLC. Mobile phase consisted of 60 % of 100 mM Ammonium acetate buffer & 40% Acetonitrile and eluted at a flow rate of 1.0 ml/min. The pharmacokinetic parameters of Rabeprazole sodium from CMAX-g-AA, CMC-g-

AA hydrogels and drug solution were analyzed from the plasma levels in rabbits by non compartmental pharmacokinetic analysis using the software package kinetica v 4.4. Pharmacokinetic data was statistically analyzed by one way ANOVA.

Results: Carboxymethyl arabinoxyllan anionic polysaccharide obtained from Ispaghola husk by alkali extraction, exhibited variety of ideal characteristics for controlled drug delivery carrier. Free radical polymerization by KPS can be successfully employed to formulate pH responsive copolymeric network of carboxymethyl arabin oxylan with acrylic acid and methacrylic acid. FTIR, SEM and thermo gravimetric analysis verify graft copolymerization. Porous structure of hydrogel become more prominent at pH 7.4 by increasing contents of acrylic acid, as compared to methacrylic acid contents. CMAX-g-AA and CMAX-g-MAA underwent morphological changes during grafting which modified its structure and properties as well, which shows more thermal stability as compared to the raw back bone. Graft copolymers revealed highly pH responsive swelling, consequently drug release. At acidic pH cumulative drug release from CMAX-g-AA hydrogels decreased (11.52 %, 7.64 %, and 3.91 %) with progressive increase of acrylic acid (10 %, 15 % and 20 %) contents. At higher pH carboxylic acid group present in graft copolymer became progressively more ionized, hydrogels swelled more rapidly ultimately cumulative drug release enhanced (93.18 %, 85.51 % and 79.77 % with progressive decreasing acrylic acid contents). As swelling of CMAX-g-AA hydrogel increased by increasing concentration of CMAX, swelling was directly proportional to drug release (92.83 %, 96.76 %, and 98.44 % at CMAX concentration 1 %, 1.5 % and 2 %, respectively at basic pH). It has been observed that overall swelling ratio (q) (20.85, 16.70, and 14.28; 20 %w/w, 30 %w/w and 35 %w/w methacrylic contents respectively) of CMAX-g-MAA reduced by increasing concentration of methacrylic acid. Hydrophobic nature of methacrylic acid is responsible for reduce swelling. *In vitro* release study has revealed that as contents of methacrylic acid raised (20 %, 30 % and 35 %), pH sensitivity enhanced (% CDR at basic pH is 84.19 %, 75.9 %, 71.26 % and at acidic pH % CDR 10.3 %, 7.7 % and 5.33 %) but overall swelling reduced so percent cumulative drug release has been declined. Degree of swelling depends on crosslinked monomer concentration, polymer concentration and also on crosslinking density of hydrogels. Swelling of such hydrogels in the stomach is minimal so drug release

consequently low at acidic pH. Values of R^2 obtained using zero order release model were viewed higher than other order release model, thus depicting that drug release from the series of hydrogels at varying amount of polymer, monomer and crosslinker was zero order.

It was observed that swelling ratio (q) of graft copolymer (CMC-g-AA) increased (35.3, 37.8, and 43.3) with an increasing concentration of CMC (0.5 %, 1 %, and 1.5 %) respectively but decreased (31.6) at 2 % concentration of CMC. pH sensitive % cumulative drug release from CMC-g-Acrylic hydrogel ranges from 3.12% to 10.66% during early 24 hrs of dissolution release in simulated acidic pH medium of stomach (i.e. pH 1.2) while it range from 50.68% to 80.75% depending upon varying amounts of CMC, acrylic acid and cross linker. It was viewed that maximum drug released from CMC-g-MAA hydrogel at pH 1.2 was (11.69 %, 7.80 %, and 5.59 % respectively) after 24 hrs with increasing contents of methacrylic acid (from 20- 35 %w/w). However, 63.11 % to 71.85 % of the total drug loaded was released at pH 8 in 24 hrs**.** These results are correlated with pH responive swelling of CMC-g-MAA hydrogels.

PEG-g-MAA hydrogels showed the rabeprazole sodium release profile of the hydrogels, it was noticed that by increasing PEG contents from 5 %-20 % cumulative drug release enhanced from 73 % to 93 %. Methacrylic acid act as swelling retardant because of hydrophobic methyl group, by increasing methacrylic acid contents hydrogels exhibited highly pH sensitive response but cumulative drug release was reduced due to low degree of swelling. Water absorbing property of hydrogel is attractive for their biomedical application. The effect of HEMA and AA on the swelling curve of prepared hybrid hydrogels PEG (HEMA-co-AA) at acidic and basic pH were studied by varying concentrations. Swelling analysis of PEG (HEMA-co-AA) polymeric network exhibited that with varying contents of AA (7.5 %, 10 %, 12.5 % and 15 %) swelling ratio (q) in acidic medium decreased gradually (3.58, 3.30, 2.66, and 2.24) but at alkaline pH swelling ratio (12.89, 14.07, 16.13 and 19.72 respectively) increased. Hydrogels prepared with varying contents of HEMA (1 %, 1.5 %, 2 % and 3 %) show low swelling ratio (4.03, 3.34, 3.16, 2.24 at acidic pH and 26.94, 24.65, 21.42 and 16.35 at high pH) with increasing its contents and concentration of other constituents keeping constant. Present

study also investigated that by increasing HEMA contents while PEG and acrylic acid contents kept constant, drug release declined. These findings were correlated with swelling analysis of PEG (HEMA-co-AA). As HEMA is neutral monomer, which has no ionize able groups and exhibited very small swelling in buffer solution. But water swelling properties of HEMA could be improved by co-polymerization with more hydrophilic monomer like acrylic acid

Acute toxicity study of hydrogel is the knowledge of interaction of chemical composition of the biomaterial and tissue exposure. Acute oral toxicity study of prepared hydrogels suggested that no mortality was found within study period. No signs of illness (vomiting, eye secretion, running nose, salivation) were observed after hydrogels administration. According to globally harmonized system (GHS), LD50 value of testing chemical is higher than the 2000 mg/kg dose then it will be categorize under the "Category 5" and toxicity score will be "zero." Therefore, prepared hydrogels can be categorized under the Category 5 and toxicity grade is zero.

The peak plasma concentration (C_{max}) and time to reach peak plasma concentration (T_{max}) was obtained from the visual inspection of the plasma concentration-time curves. The area under the plasma concentration curve (AUC_{0-t}) was determined using the trapezoidal rule. C_{max} values of (CMC-g-AA) CA and (CMAX-g-AA) A and same oral dose of rabeprazole sodium were 87.28±12.671, 103.71±16.081 and 61.263±5.37 ng/ml, respectively. Observed mean plasma AUC_{0-24} values for CA (952.25±191 ng.h/ml) and A (1084.57±148.68 ng.h/ml) was significantly ($P < 0.05$) higher than drug solution (83.67±8.28 ng.h/ml). The T_{max} value of graft copolymer matrices CA (4.43 h) and A (4h) was significantly ($P < 0.05$) higher than drug solution (1h). The relative bioavailability of hydrogel formulations (CA and A) containing rabeprazole sodium than free rabeprazole sodium in drug solution, containing the same dose of the same drug, is obtained by comparing their respective AUCs (952.25 ng.l/hr for CA and 1084.57 ng.l/hr for A hydrogel) were higher.

Conclusion: The concept of formulating graft copolymer containing Rabeprazole sodium offered an appropriate, sensible approach to accomplish a lingering therapeutic

outcome by continuously releasing the drug over extended period of time. Prepared hydrogels were nontoxic, safe and biocompatible following oral administration and it might be auspicious candidate as innovative oral drug carrier. Graft copolymerization is faster and more cost-effective technique to modify imperative properties of the existing drugs than developing new drug entities hence this research work will be windfall to novel drug carrier system.

CHAPTER # 1

INTRODUCTION

1. INTRODUCTION

This significant and substantial piece of research work includes development, characterization and evaluation of various polymeric formulations for stable delivery of acid labile drug. Rabeprazole sodium having very short half-life (1-1.5 hr), and is highly acid-labile so low bioavailability (52%), presents many formulation challenges.

Low bioavailability is a major imperfection in efficacious drug delivery by oral route of administration. To comprehend the reason behind, low bioavailability is essential before developing drug delivery system (Thakar *et al*., 2010). Rabeprazole sodium is an inhibitor of gastric proton pump. It restrain gastric acid secretion by particularly blocking the H^+/K^+- ATPase enzyme system at the secretory surface of gastric parietal cell considerably plummeting gastric acid levels and allowing acid-related disorders to cure, as well as mitigate symptoms of chronic conditions, like gastric and duodenal ulceration and also in Zollinger Ellison syndrome and reflux esophagitis (Williams and Pounder, 1999).

The proton pump inhibitors have closely similar mechanism of action, yet important pharmacological differences exist, which can significantly impact certain aspects of their clinical efficacy. Rabeprazole has an early onset of effective acid inhibition compared with other proton pump inhibitors, exhibit faster response and shorter duration of action (Stedman & Barclay, 2000).

Researchers have struggled to engineer the controlled drug delivery system to regulate the bioavailability of drugs. The most striking way to improve bioavailability of acid sensitive drugs is pH responsive release. Hydrogels having such desired characteristics, make them an ideal vehicle for intelligent drug delivery system (Narayan *et al*., 2010).

Latest progressions in hydrogel synthesis techniques have fabricated a new replica in the use of these systems for the improvement of new pharmaceutical forms, predominantly of those hydrogels that reveal an intelligent behavior (David *et al*., 2008).

Intelligent hydrogels can recognize and respond to small alteration in external circumstances such as pH, temperature, light, and ionic strength. The smart drug delivery systems hold some vital characteristic such as predetermined rate, self controlled, targeted, predefined time and monitor the delivery (Subham *et al*,. 2010).

Hydrogels are three-dimensional, cross-linked networks of water-soluble polymers, which imbibe a large quantity of water while maintaining their dimensional stability by either physical or chemical crosslinking (Lin and Metters, 2006). Chemically, crosslinked hydrogels (as compared to physical hydrogels) are mechanically stable due to the covalent bond. These hydrogels can be prepared by radical polymerization of low molecular weight monomers/polymers in the presence of a crosslinking agent (Chauhan *et al*., 2012)

The distinctive features of hydrogels have promoted meticulous attention in their use in drug delivery applications. Highly porous structure can be regulated by crosslinking density of hydrogels. Porosity imparts affinity with aqueous medium to swell, thus allows drug loading and subsequent release through gel matrix (Hoare and Daniel, 2008).

For a polymer system to become "sensitive", a sharp phase volume-transition must happen. The foremost prerequisite of the system is the presence of ionizable weak acidic or basic moieties attached to a backbone. Transition from collapsed state to expanded state also modified by electrostatic repulsion in response to alterations in environmental states like pH, temperature, ionic contents etc. Proper selection between polyacid or polybase is essential for desired application. Polyacidic polymers will be unswollen at low pH, since the acidic groups will be protonated and unionized. When increasing the pH, a negatively charged polymer will swell. The opposite behaviour is exhibited in polybasic polymers, since the ionization of basic groups will increase when decreasing the pH. Typical examples of pH sensitive polymers with anionic groups are poly (carboxylic acids) as poly (acrylic acid) (PAA) or poly (methacrylic acid) (Qui and Park, 2001).

The pH - responsive hydrogels contain hydrophilic functional groups i.e. -OH, -CONH-, -CONH2, -COOH and -SO_3H, responsible for water gulping ability of polymer (Hoare and Kohane, 2008).These ionic moieties perceive and respond alteration in external pH results in sudden volume transition by generating electrostatic repulsive forces between ionized groups, which builds a great osmotic swelling force. Swelling of anionic hydrogels in the stomach is least, level of swelling increases as the hydrogel passes down the intestinal tract due to increase in pH leading to the ionization of carboxylic groups. The nature of the ionic groups, the polymer composition, the hydrophobicity of polymer backbone, and the crosslinking density modulate the vital characteristics of smart

hydrogels (Qiu and Park 2001). Water intake and holding capability made polymeric networks to resemble more closely to natural living tissues than synthetic polymers. Such smart polymers guide drug release upon variations in external environment either by phase alteration or by changes in their bulk (Soppimath *et al.,* 2002).

Hydrogels can be designed as per desired functionalities, like swelling and mechanical properties, qualifying their diversity of biomedical uses, from contact lenses to controlled-release drug delivery and tissue engineering (Susana *et al*., 2012). In fact, smart hydrogels behave like a natural system in its speed, function, and repeatability. Design and composition of hydrogels are the key factors to define their functionalities. They can be fabricated from natural and synthetic polymer materials (Davis and Anseth, 2002). Hydrogels can be prepared by several methods by combining distinctive properties of natural and synthetic polymers/monomers. Many researchers have been proved that copolymerization is most appropriate method to achieve desired mechanical properties of hydrogels. The mechanical properties of hydrogels are essential to maintain its physical texture during the delivery of therapeutic moieties for the predetermined period of time (Das, 2013).

In modern era, copolymers have originated new and extremely progressing horizons in front of the precincts of conventional drug delivery system to develop into one of the focal compounds as drug delivery vehicles. Copolymers are heteropolymers of miscellaneous types of monomers and with varying length of structural repeating units. The amalgamation of different chemical units in copolymer structures consequences in new materials with numerous novel features (Mehrdad *et al*., 2012).

Graft copolymerization is versatile technique to improve compatibility between synthetic polymers and natural polymer. Graft copolymer offer additional advantages, especially stimuli responsive polymer, like higher acid base and thermal resistance, lower crystallinity of natural polymers (Kumar *et al*., 2014). Graft copolymers are prepared by first generating free radicals on the biopolymer backbone and then allowing these radicals to serve as macroinitiators. The chemical and radiation initiating systems are employed to graft copolymerize monomers onto polymers (Sabyasachi *et al.,* 2010).

A graft copolymer is a macromolecular chain with one or more species connected to the main chain as side chain(s). The general structure consist of the main polymer backbone,

commonly referred to as the trunk polymer, has branches of another polymeric chain emanating from different points along its length. Grafting of synthetic polymer is a convenient method to impart desired new properties to a natural polymer with minimum loss of the initial properties of substrate (Sabyasachi *et al.,* 2010).

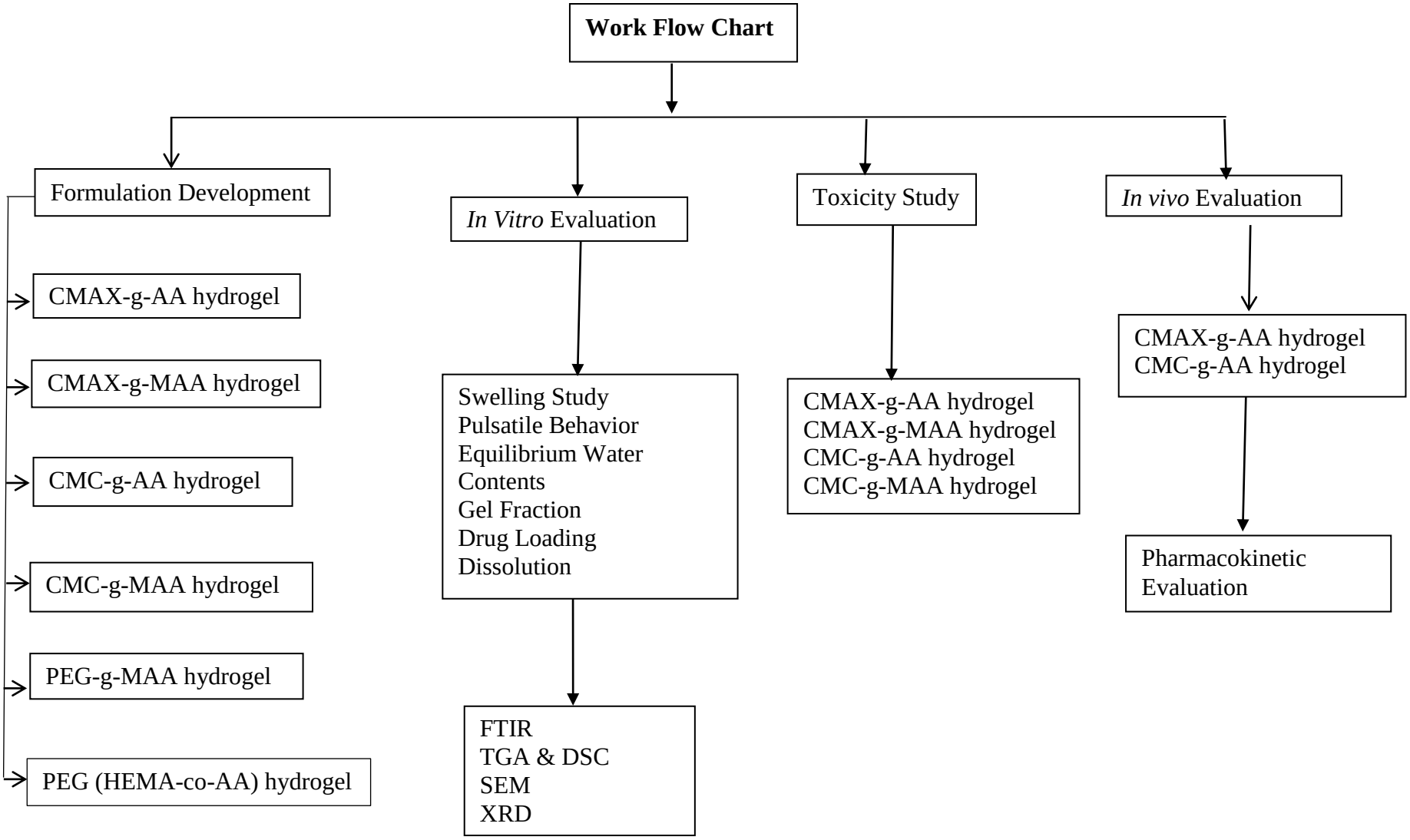
Work Flow Chart
Formulation Development
CMAX-g-AA hydrogel
CMAX-g-MAA hydrogel
CMC-g-AA hydrogel
CMC-g-MAA hydrogel
PEG-g-MAA hydrogel
PEG (HEMA-co-AA) hydrogel
In Vitro Evaluation
Swelling Study
Pulsatile Behavior
Equilibrium Water Contents
Gel Fraction
Drug Loading
Dissolution
FTIR
TGA & DSC
SEM
XRD
Toxicity Study
CMAX-g-AA hydrogel
CMAX-g-MAA hydrogel
CMC-g-AA hydrogel
CMC-g-MAA hydrogel
In vivo Evaluation
CMAX-g-AA hydrogel
CMC-g-AA hydrogel
Pharmacokinetic Evaluation

CHAPTER # 2

LITERATURE REVIEW

2. *Literature review*

2.1 Controlled release drug delivery system

Low bioavailability of drugs by oral route is a major imperfection in efficacious drug delivery. To comprehend the reason behind low bioavailability is essential before developing drug delivery system ((Beierle *et al*. 1999; Bardelmeijer *et al*., 2000; Katsura and Inui, 2003). In last few decades modern drug delivery techniques have revolutionized the entire approaches to defeat shortcomings of conventional dosage forms. Numerous efforts have been made to control the factors like influence of pharmacokinetic processes on drug efficacy, as well as the importance of dosing frequency and of drug targeting to the site of action. In the mid to late 1960s, the term "controlled drug delivery" came about to illustrate new perceptions of drug delivery design. "Class of drug delivery system which release drug in a premeditated, predictable, and sustained manner". Controlled release systems designed to create more steadfast absorption and to improve bioavailability and augment patient compliance (Kovanya *et al*., 2012).

Some of challenges with use of conventional drug delivery system, poor bioavailability, *in vivo* stability, solubility, intestinal absorption, sustained and targeted delivery to site of action, therapeutic effectiveness, generalized side effects, and plasma fluctuations of drugs require tool for research and development of such system to achieve unmet clinical requirements. Following attributes of controlled drug release technique like improve bioavailability of drug product, reduction in the dose frequency and prolong duration of effective blood levels, reduces the fluctuation of peak trough concentration and side effects and possibly improves the specific distribution of drug making more attractive approach for rational therapy (Vilar *et al*., 2012).

One of the major challenges in pharmaceutical research is site targeted dosage form design for acid labile drugs. These formulations can release active substance in the proximal part of small intestine (duodenum) through the enteric coating to treat bowel diseases by improving the systemic absorption of drugs, which are unstable in gastric juice or low pH conditions, thus must be protected from the gastric acid by the coating with high pH soluble polymers or aqueous soluble polymers (enteric coated polymers) when given orally (Vilar *et al*., 2012).

2.2 Role of polymers in CRDDS

Naturapolyceutics is based on interdisciplinary approaches that combine natural polymer and pharmaceutics for advancement in drug delivery design **(**Ndidi *et al*., 2014**)**.

Polymers have historically a massive function in drug delivery systems. Novelty in polymer science has led to the development of new drug delivery systems. Natural polymers can be chemically modified for desired applications. Synthetic polymers can be produced on the basis of required functionalities depending on needs of drug delivery system (Veeran and Betageri, 2011). Biomedical applications of polymers range from their use as binders, thickening agent, film coating material, stabilizer, release modifier, solubilizer and barrier properties depending upon unique characteristics of polymers (Swathimutyam and Bala, 2013).

Natural polymers are an attractive class of excipients for successful, stable and effective drug delivery system. These are economical and easily available, safe, biodegradable, and ecofriendly and can be modified according to need (Kavitha *et al*., 2011; Prakash and Kumar, 2013). Pharmaceutical applications of natural polymers include, manufacture of solid monolithic matrix systems, implants, films, beads, microparticles, nanoparticles, as well as for parenteral use.Various natural polymers like cellulose, pectin, inulin, alginate, carrageenan, rosin, guar gum, locust bean gum, gum arabic, psyllium, starch, aloe gel, xanthan and chitosan have been used for the development of controlled or sustained release drug delivery system (Carien *et al*., 2009) .

Polymers utilized for safe and effective controlled drug delivery must possess following characteristics (Javad and Zarnegar, 2014).

- Polymer and its degradation products must be biocompatible
- Satisfactory mechanical strength
- Must be degradable and degradation kinetics matching a biological process
- Processibility using available equipment.
- Must be soluble in diverse solvents.
- Having chemical, structural and application diversity.
- Cost-effective and eco friendly
- Acceptable shelf life

Table 2.1: Classification of biodegradable polymers used in drug delivery systems (Coulembiera *et al*., 2006).

Synthetic biodegradable polymers		**Natural biodegradable polymers**
Polyesters	Polyoxalates	Starch
Polyorthoesters	Polyiminocarbonates	Hyaluronic acid
Polyanhydrides	Polyurethanes	Heparin
Polydioxanones	Polyphosphazenes	Gelatin
Poly(cyanoacrylates)		Albumin
		Dextran
		Chitosan

2.3 Polymer modifications

Polymer modifications are necessary to transform supreme characters to natural materials, such as improve thermal stability, multiphase physical responses, compatibility, impact response, flexibility, rigidity and aqeous solubility. Thus polymer modification perk ups the processibility of polymers (Ndidi *et al*., 2014). Chemical modification of polymer provides multifunctional characteristics like swelling and solubilization depends upon addition of functional group (Dodi *et al.,* 2011). Polar functionalities can be introduced into natural polymers by chemical or enzymatic reactions to enhance their biodegradation profile (Dey *et al*., 2011). Polymer modification may cause alterations in physical characteristic of polymer like, mechanical strength, permeation, solubility, swellability and surface features.

The diverse chemical modifications helpful to control drug delivery are:

a) Grafting b) Carboxymethylation

a) Grafting

Grafting is an attractive tool to add valuable features to natural polymer with minimum loss of its innate properties**.** Due to abundant availability, economical source, water solubility, safe and biocompatibility, natural polymers could be appealing starting materials for the synthesis of graft copolymers**.** Grafting involves the random branching of a monomer on the backbone of a polymer. Chemical reagents like initiators or high energy radiations are used to create active sites on polymers and functional monomers are crosslinked on these sites (Madolia and Maurya, 2013).

b) Carboxymethylation

Carboxymethylation is an extensively used technique for polymer modification to produce a variety of promising characters in polymer. Carboxymethylation adds carboxymethyl groups to the natural polymers thereby augmenting their solubility and solution clarity renders more suitable candidate for food, cosmetics and pharmaceutical applications (Yuen *et al*., 2009). Carboxymethylation is a flexible conversion of natural polymer to water-soluble polymers with a range of imperative traits (Adeyanju *et al*., 2014).

General mechanism of carboxymethylation involves Williamson's ether synthesis procedure. In this technique polymer is alkalized with sodium hydroxide and converted with monochloroacetic acid or its salt to its ether derivatives. Carboxymethyl cellulose, Carboxymethyl starch, Carboxymethyl chitosan and many other derivatives may be produced depending on starting material (Nawaz *et al*., 2011).

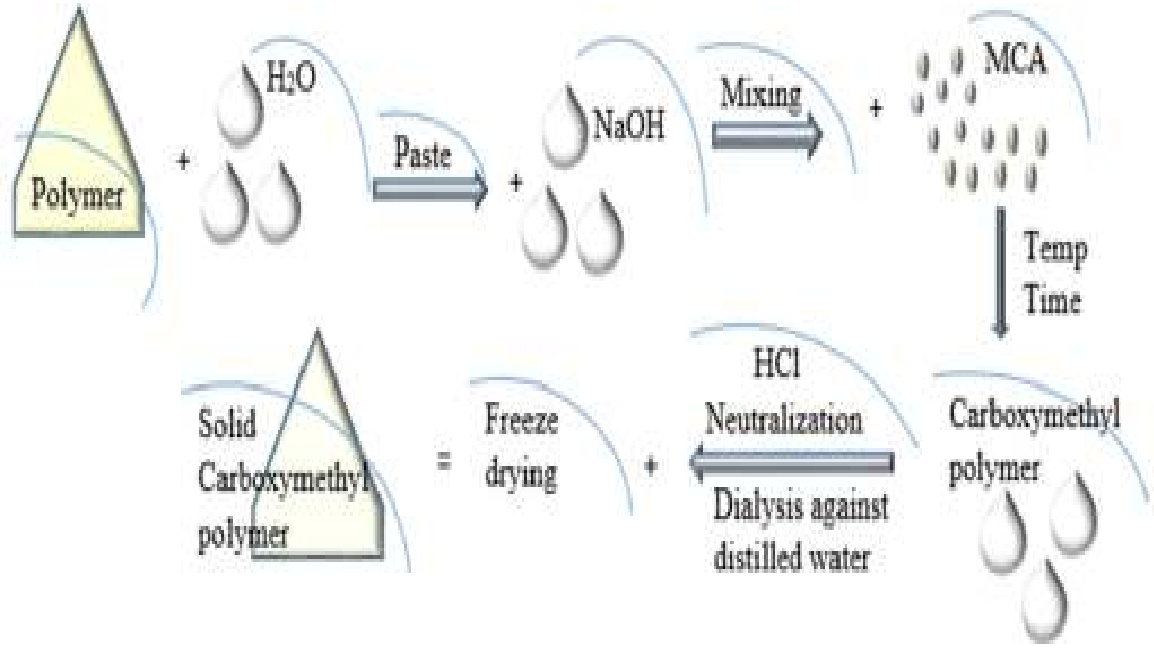

Figure 2.1: General procedure of carboxymethylation of polymer

2.4 Graft copolymerization

Graft copolymerization is expected to be a potential tool for polymer modifications to impart desired characteristics (Arpit *et al*., 2011). Components of graft copolymerization may include initiator, polymer and monomer. Nature of the graft copolymer depends on time of reaction, polymer and monomer nature. Initiator in very small amount creates active sites either on polymer or monomer. Various initiator systems may be used for graft copolymer like, potassium persulfate, ammonium persulfate, benzoyl peroxide, azobisisobutyronitrile and ceric ammonium nitrate (Onishi *et al*., 2004; Sadeghi and Hosseinzadeh, 2010; Sadeghi *et al*., 2011).

- ***Techniques of graft copolymerization***

Extensive efforts have been made to build up diverse techniques of graft copolymerization of various monomers on polymeric backbone. These techniques include chemical, radiation and photochemical polymerization for drug delivery design.

- ***Chemical graft co polymerization/Free radical polymerization***

  In chemical graft copolymerization, generally polymers react with initiator and generate free radicals. These free radicals start the graft polymerization of monomers and cross-linker on the substrate. Free radical generation mechanism depends on characteristics of initiator used. Initiator may generate free radicals by direct or indirect method. Nature, concentration and solubility of initiator determine the mechanism of free radical polymerization (Misra *et al*., 1980; Misra *et al*., 1984).

- ***Radiation polymerization***

  The irradiation of polymer cause homolytic fission and generate free radicals on the polymer. Initiator is not required for this technique. Medium of polymerization is critical for this method e.g, if irradiation is carried out in air, peroxides may be formed on the polymer. Free radical life span depends on nature of the backbone polymer (Chen *et al*., 2003).

- ***Photochemical grafting***

  This technique requires chromophore on polymer backbone to absorb light. After light absorption, polymer goes into an excited state and converted into reactive free-radicals, hence the grafting process is initiated. Photosensitizers may be used for free radical generation e.g. benzoin ethyl ether, dyes, such as Na-2,7 anthraquinone sulphonate or acrylated azo dye, aromatic ketones (such as benzophenone, xanthone) or metal ions. Photochemical grafting can be proceed in two ways, with or without sensitizer depend on photosensitive nature of polymer (Bellobono *et al*., 1981)

2.5 Intelligent drug delivery system

Biocompatible materials having capability to respond certain physiological variables or external physicochemical stimuli designed to deliver therapeutic agent are intelligent drug delivery system (You *et al*., 2010). Smart polymers simulate biological systems in a rudimentary way where an external signal (e.g. change in pH or temperature) results in an alteration in properties. This leads to a conformational change for the soluble polymers and a change in the swelling behavior of the hydrogels when ionisable groups are linked to the polymer structure results in release of bioactive molecule from the drug delivery system (Dirk, 2006).

Polymer scientists have been striving for preparing such polymers, having capability to perceive physiological stimuli and respond accordingly. Smart polymers may undergo physical or chemical transformations in response to fluctuations of environmental conditions like pH, temperature, light, magnetic or electric field, ionic factors, biological molecules etc. These polymers by exhibiting changes in their physical or chemical behavior, release entrapped drug in controlled manner (Snezana *et al*., 2011).

- ***Types of intelligent drug delivery system***
  - *Biological stimuli responsive drug delivery system:* (pH Sensitive System, Thermo-responsive Systems, Inflammation Responsive Systems, Glucose Sensitive Systems, Ionic Cross - linking *In Situ* Gelling System, Enzymatic Cross - linking *In Situ* Gelling System)

- *Magnetically controlled drug delivery system*
- *Electrically controlled drug delivery system*
- *Photo-responsive drug delivery system*
- *Ultrasonically modulated system* (Nihar *et al*., 2013)

2.6 Hydrogels

Hydrogels are cross-linked polymeric networks comprise of high number of hydrophilic domains, capable of imbibing large amount of water, but do not dissolving in water at physiological pH and temperature because of their net work structure (Yong and Kinam, 2001). In swollen state hydrogels due to high water contents and soft consistency resemble natural living tissue and are biocompatible (Satish *et al*., 2006). Equilibrium swelling capacity of hydrogels depends on hydrogel structure, crosslinking density, ionic contents and hydrophilicity of hydrogel (Omidian and Park, 2008). Hydrogels used for biomedical applications must be stable after swelling and maintain their structural integrity (Dumitriu, 2002).

Hydrogels have hydrophilic domains, which do not dissolve in aqueous media but swell at specific physiological conditions. Swelling of polymeric network governs the release mechanism of drug however, its elasticity regulate mechanical strength and stability (Peppas *et al*., 2000).Three dimensional networks of hydrogels can retain large amount of water making it biocompatible, elastic and stable drug carrier system. Presence of hydrophilic functional groups like $-SO_3H$, $-CONH_2$, -COOH, and –OH are responsible for above characteristics (Wang *et al*., 2006).

2.6.1 *Hydrogels applications as controlled drug-delivery carriers*

Hydrogels polymeric network has distinctive swelling behavior, which extensively dictates the pattern of drug delivery. By controlling few crucial aspects like, polymer concentration, composition, initiator and cross linker nature and concentration which direct density and degree of cross linking hydrogel properties can be ideally modified for their desired application. Chemical and physical connections are vital for the improvement of enviable interfacial strength (Peppas *et al*., 2006).

Researchers have made it possible to achieve unattainable task of ideal drug delivery by hydrogel discovery. Researchers have engineered their physical and chemical properties at the molecular level to optimize their properties, for attractive applications;

- Control permeability for sustained-release applications
- Made environment-responsive nature for pulsatile-release applications
- Modify surface functionality for PEG coatings for stealth release
- Biodegradability for bioresorbable applications
- Surface biorecognition sites for targeted release and bioadhesion applications for controlled drug-delivery applications (Peppas *et al*., 2004).

2.6.2 *Hydrogel classification*

Hydrogels can be classified on the basis of various parameters:

1) Types of hydrogels based on the method of preparation

A) Homopolymer hydrogels
B) Co-polymer hydrogels
C) Multi polymer hydrogels

2) Types of hydrogels on the basis of ionic contents hydrogels

A) Neutral hydrogels
B) Anionic hydrogels
C) Cationic hydrogels
D) Ampholytic hydrogels

3) Structure based types of hydrogels

A) Amorphous hydrogels
B) Semi-crystalline hydrogels
C) Hydrogen bonded hydrogels

4) Drug release mechanism based classes of hydrogels

A) Diffusion controlled release systems
B) Swelling controlled release systems
C) Chemically controlled release systems
D) Environment responsive systems (Bindu *et al*., 2012)

2.6.3 *Technologies adopted in hydrogel preparation*

- ***Physical hydrogels***

  Nature of association in physical hydrogels is physical. These hydrogels can be achieved by hydrophobic association, hydrogen bonding, chain aggregation and polymer-polymer complexation. For example, acrylic-based hydrogels treated with calcium, aluminum, iron; sodium alginate treated with calcium and aluminum; poly (vinyl alcohol) treated with borax. All of these interactions are reversible, and can be disrupted by changes in physical conditions or application of stress (Rosiak & Yoshii, 1999).

Table 2.2: Methods for preparation of physical and chemical hydrogels

Physically crosslinked hydrogels **(**Yoshida *et al*., 1995; Gacesa, 1988; Goosen *et al*., 1985; Gombotz and Wee, 1998; Mumper *et al*., 1994)
• Ionic interactions (alginate etc.) • Hydrophobic interactions (PEO–PPO–PEO etc.) • Hydrogen bonding interactions (PAAc etc.) • Stereocomplexation (enantiomeric lactic acid etc.) • Supramolecular chemistry (inclusion complex etc.)
Chemically crosslinked hydrogels **(**Matsuo and Tanaka,1992; Yoshida *et al*.,1995; Edman *et al*., 1980; Tanaka *et al*., 1987)
• Polymerization (acryloyl group etc.) • Radiation (γ-ray etc.) • Small-molecule crosslinking (glutaraldehyde etc.) • Polymer–polymer crosslinking (condensation reaction etc.)

- ***Chemical hydrogels***

  Chemical crosslinking is involved in formation of chemical hydrogels. On the contrary, a chemical process, i.e., chemical crosslinking is utilized to prepare a chemical hydrogel (Hennink & Nostrum, 2002). They exhibit equilibrium swelling, depends on the polymer-water interaction parameter and the crosslink density (Rosiak & Yoshii, 1999).

2.6.4 *Drug release mechanisms from hydrogel formulations*

Hydrogels have a distinctive blend of traits which render them valuable in drug delivery system. Owing hydrophilic characteristics hydrogels can hold huge amount of water than

its own weight. Consequently, drug release phenomenon of hydrogels is awfully special as compared to other biomaterials. Both straightforward and complicated models have not been developed before to calculate the release of drug from a hydrogel system as a function of time.

Therefore, physicochemical nature of network and method of drug loading will dictate release pattern from polymeric matrix.

Generally two method of drug loading applied

- ***Post-loading***

  In this technique dried hydrogels are soaked in definite strength of drug solution until equilibrium swelling achieved. This procedure promotes the maximum amount of liquid uptaken during swelling. In inert network system diffusion is chief driving force for drug loading and release will be by diffusion/swelling mechanism (Oprea *et al.*, 2010)

- ***In situ loading***:

  This method involves simultaneous addition of drug during synthesis of hydrogel. In these systems, the release of drugs can be controlled by diffusion, hydrogel swelling, drug–polymer interactions, or degradation of labile covalent bonds (Lin and Metters, 2006).

➢ ***Diffusion-controlled delivery systems***

Drug transfer from polymeric matrix to its surrounding is basic mechanism of drug release. To find out the pattern and recognize the main controlling factors that direct drug release from hydrogels is the key point to predict release profile. Drug diffusion coefficients of porous and non porous hydrogels and mesh size of polymeric network. Diffusion controlled hydrogel delivery systems can be either reservoir or matrix.

In hydrogel reservoir system polymeric membrane surround drug molecules. Fick's law of diffusion can be used to describe drug release through polymeric boundary.

$$J_A = -\frac{DdC_A}{dx} \qquad (1)$$

Where:

J_A - flux of the drug,

D - Drug diffusion coefficient

C_A - drug concentration.

In many cases, the drug diffusion coefficient is assumed to be constant to simplify the modeling. Generally drug diffusion coefficient is function of drug concentration, used to predict drug flux and correlate the concentration and diffusivity of drug.

For a matrix system release mechanism cane explained by Fick's second law of diffusion.

$$\frac{dC_A}{dt} = \frac{Dd^2C_A}{dx^2} \qquad (2)$$

Drug diffusion coefficient in this case is again assumed as a constant (Lowman and Peppas 1999).

Additionally for hydrogel systems diffusivities of encapsulated molecules will depend on the degree of swelling and crosslinking density of the gels. Therefore , diffusion coefficient used to describe drug release will be sensitive to environmental changes or degradation of the polymer network and may vary over the timescale of release.

- ***Swelling controlled release systems***

Hydrophilic polymeric hydrogels absorb water and exhibit swelling. In these systems, the polymer matrix begins to swell and two distinct phases can be observed in the polymer; the inner glassy phase and the swollen rubbery phase. The drug molecules are able to diffuse out of the rubbery phase of the polymer. Drug release will be swelling controlled. Since no drug diffuses out of the glassy region of the polymer.

Empirical power law may explain the release mechanism in the swelling-controlled delivery systems:

$$\frac{M_t}{M_\infty} = kt^n \qquad (3)$$

Here, M_t and M_∞ describe the amounts of drug released at time t, and at equilibrium respectively, k is proportionality constant, and n is the diffusional exponent. Ritger and Peppas described Fickian and non-Fickian diffusional behavior of drug release of hydrogels in terms of the value of the coefficient “n” (Siepmann and Peppas, 2001; Ritger and Peppas, 1987).

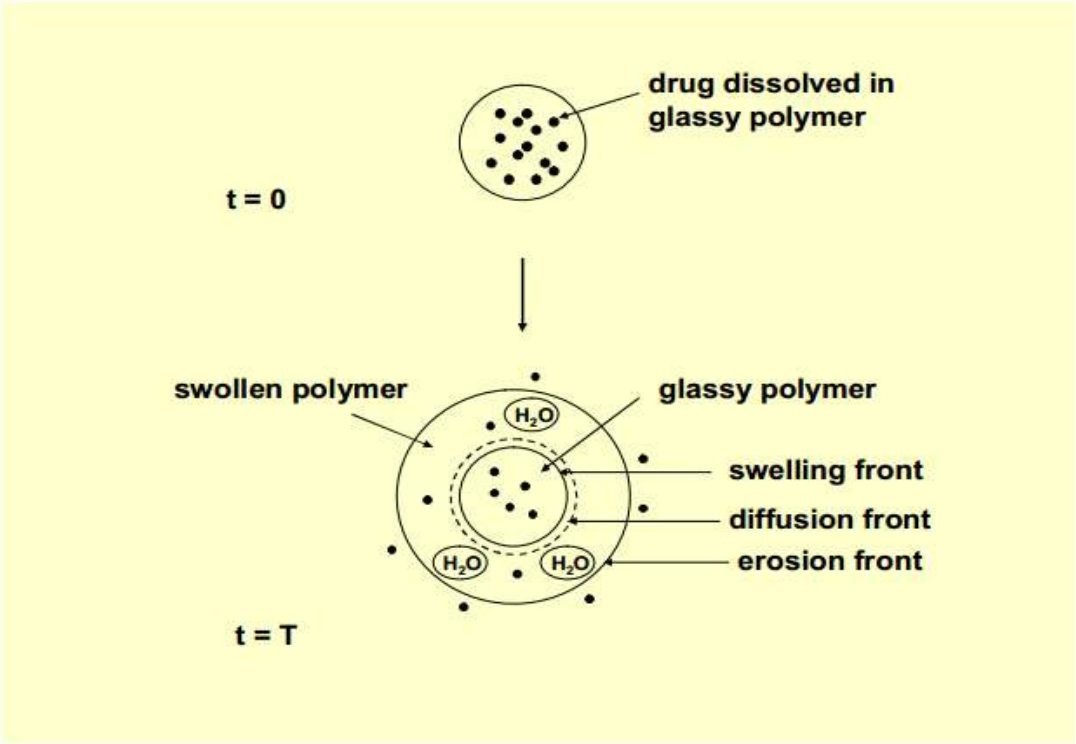

Figure 2.2: Swelling-controlled drug delivery system

- ***Chemically-controlled delivery systems***

This system is further classified on bases of release mechanism into two classes:

- ***Erodible systems:*** Drug release is controlled by degradation and dissolution of polymer. Erosion or diffusion is rate controlling step. If erosion is constant than there will be zero order release. Erosion may either be heterogeneous or homogeneous depending on polymer hydrophilic or hydrophobic nature.
- ***Pendent chain systems:*** Drug is attached with polymer hydrolytically or enzymatically labile linkage. Drug release is controlled by degradation of linkage (Peppas *et al*., 2000).

2.7 Responsive hydrogels

By fabricating their molecular structure, polymer networks can interact with their environment in a preplanned and smart manner. These smart polymers are capable of delivering their contents in response to fluctuations in environmental conditions

according to physiological requirements at the right time and suitable place (Peppas *et al*., 2006). Response mechanism based on chemical composition and structure of polymeric network and external environmental conditions like pH or temperature or enzyme level etc. Responsive or smart hydrogels may undergo structure conformations in response to external stimuli. Swelling of these hydrogels dictates the release of drug. Swelling in response to stimuli may allow these polymers to serve as self-regulated and pulsatile drug delivery systems (Susana *et al*., 2012).

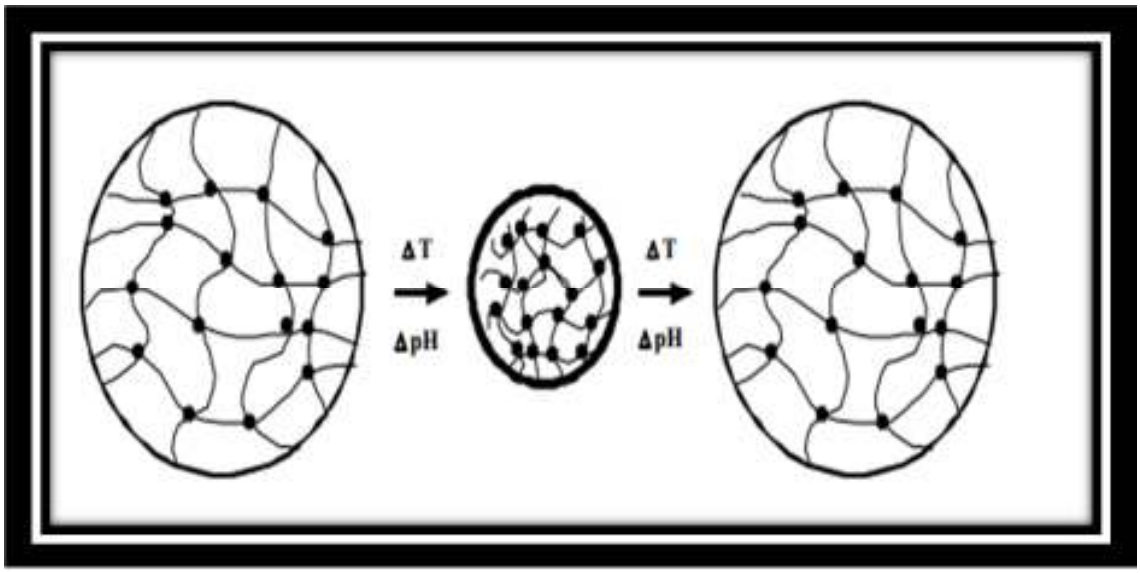

Figure 2.3: Responsive Hydrogels

2.7.1 Temperature sensitive

Responsive or smart hydrogels may be temperature sensitive exhibit a volume phase transition at a certain temperature which causes a sudden change in their state. These polymers have lower critical solution temperature (LCST). Poly (N-isopropyl acrylamide) (PNIPA) is the most commonly used as temperature responsive polymer (Mallikarjuna *et al*., 2011).

2.7.2 pH sensitive hydrogels.

pH sensitive hydrogels containing ionic network (ionizable side groups e.g., carboxylic or amine group), which perceive physiological signals and respond (swell), accordingly. In these hydrogels pH transition is responsible to expand or collapse the polymeric network in aqueous medium. Swelling of pH sensitive hydrogels protects the drug from harsh environment of stomach, may release drug in intestinal medium and may release the drug

in stomach to optimize therapy depends on composition of hydrogels. Swelling force of ionic hydrogels is stronger than non ionic biomaterial. Swelling cause structure modification by absorbing fluid and direct the release of drug from polymeric network (Soppimath *et al.*, 2002).

pH responsive hydrogels are ionic in nature containing ionizeable acidic or basic group renders hydrogel more hydrophilic. Examples of several frequently studied ionic polymers include poly (acrylic acid), poly (methacrylic acid), polyacrylamide (PAAm), poly (diethylaminoethyl methacrylate), and poly (dimethylaminoethyl methacrylate). Polmers with large numbers of ionizeable groups are polyelectrolytes. Polyacidic polymers will be unswollen at electrostatic repulsion forces. With increase in pH polyacidic polymers will ionize and show swelling. The reverse action is initiated in polybasic polymers, since the ionization of basic groups will increase when decreasing the pH (Yong and Kinam, 2001). Hydrogels can swell to beneficial rates when placed into an appropriate environment, exhibiting pH-sensitive swelling behavior. Ionic hydrogels may either be anionic or cationic depending upon the attached group. Transition in external pH ionize the acidic or basic group, electrostatic repulsion increase uptake of solvent in the network causing expansion of polymer (Fariba and Ebrahim, 2009).

Type of polymer, functional group, crosslinking density, porosity and drying are some effective parameters for swelling (Omidian and Park, 2008). Expansion of polymer as a result of change in pH of external environment is reversible. This property of rapid expansion and collapse of responsive hydrogel promote the controlled release of drug from system (Bajpai, 2001).

2.7.3 Electric signal-sensitive hydrogels

Electric signals can also be used as stimuli for hydrogels response. Polymeric network respond to electric signals containing polyelectrolytes. These hydrogels undergo volume transition when exposed to electrodes (in a bathing solution) under an externally applied electric field. The hydrogels may expand/collapse and bend due to osmotic pressures variation resulting from the difference in the ionic concentrations between the hydrogels and the external solutions. The alterations in shape and structure of hydrogels under an externally applied electric field can result in the release of entrenched drug molecule. For example, ketoprofen was released from poly (AAm-grafted-xanthan gum) (poly (AAm-g-XG) hydrogels (Murdan, 2003; Kulkarni and Sa, 2009)

2.7.4 Light-sensitive hydrogels

Photo-sensitive hydrogels have been developed for optical switches and ophthalmology drug delivery devices. The magic behind this technique describe that hydrogels absorb energy from light and convert it into heat and increase temperature of hydrogel above its LCST results in hydrogel shrinking and release of drug from polymeric net work. Light-sensitive hydrogels can be used in the development of photo-responsive artificial muscle or as the in situ forming gels for cartilage tissue engineering (Averitt *et al*., 1996).

2.7.5 Glucose-responsive hydrogels

Management of blood glucose fluctuations in diabetic patients is most imperative task for researchers. Delivery of insulin to regulate blood glucose is different from other drugs in a sense release of insulin time and physiological need dependent. Glucose oxidase is extensively used enzyme for glucose level detection and release insulin from hydrogels in a pulsatile fashion (Yong and Kinam, 2001)

2.8 Polymers and monomers used in this study

2.8.1 *Carboxymethyl cellulose*

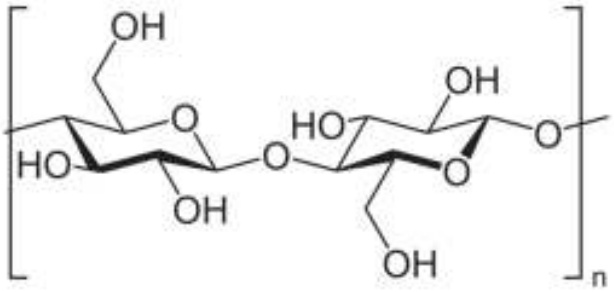

Figure 2.4: Structural formula of Carboxymethyl cellulose

CMC is produced by reacting alkali cellulose with sodium monochloroacetate under rigidly controlled conditions. Carboxymethyl cellulose (SCMC) is a cellulose ether hydrophilic polymer. It is pale yellow in appearance, odorless, safe, stable in wide range of pH and insoluble in organic solvents**.** CMC is long-chain polymer. Solution properties of CMC depend on average chain length or degree of substitution. As molecular weight of polymer increased viscosity of solution increased (Togrul and Arslan, 2003).

Carboxymethyl cellulose has diverse applications in a numerous fields because of some complimentary characteristics. It is economical, water soluble but insoluble in organic solvents used in cosmetics and pharmaceutical products as emulsifier **(**Arion, 2001**).** Various significant properties of this polymer make it an ideal thickener, suspending aid, stabilizer, binder, and film former for numerous formulations (Rowe *et al*., 2009). Sodium Carboxymethyl cellulose is the only smart (show pH responsive behavior) derivative of cellulose. It increases swelling of hydrogels. The polyelectrolyte nature of NaCMC makes it ideal for the development of superabsorbent hydrogels with a smart behavior (Alessandro *et al*., 2009).

2.8.2 *Polyethylene glycol*

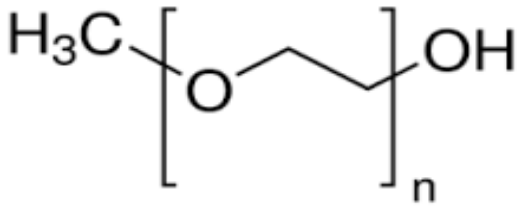

Figure 2.5: Structural formula of Polyethylene glycol

Polyethylene glycol is FDA accepted polymer for diverse biomedical functions because of biocompatibility, biodegradability, low toxicity, and non immunogenic nature (Veronese and Pasut, 2005). PEG is non ionic hydrophilic and also soluble in organic solvents. Its hydrophilic nature improves the drug's hydrophobicity when conjugated with them. It augments the physical and chemical stability of drugs as well (Knop *et al*., 2010). Various drugs require alteration in their pharmacokinetic and pharmacodynamic properties for safe and efficient therapeutic use. Conjugation of PEG with such drug molecules is forthcoming tactic for development of more efficient drug delivery system (Marina *et al*., 2011).

2.8.3 *Carboxymethyl arabinoxylan*

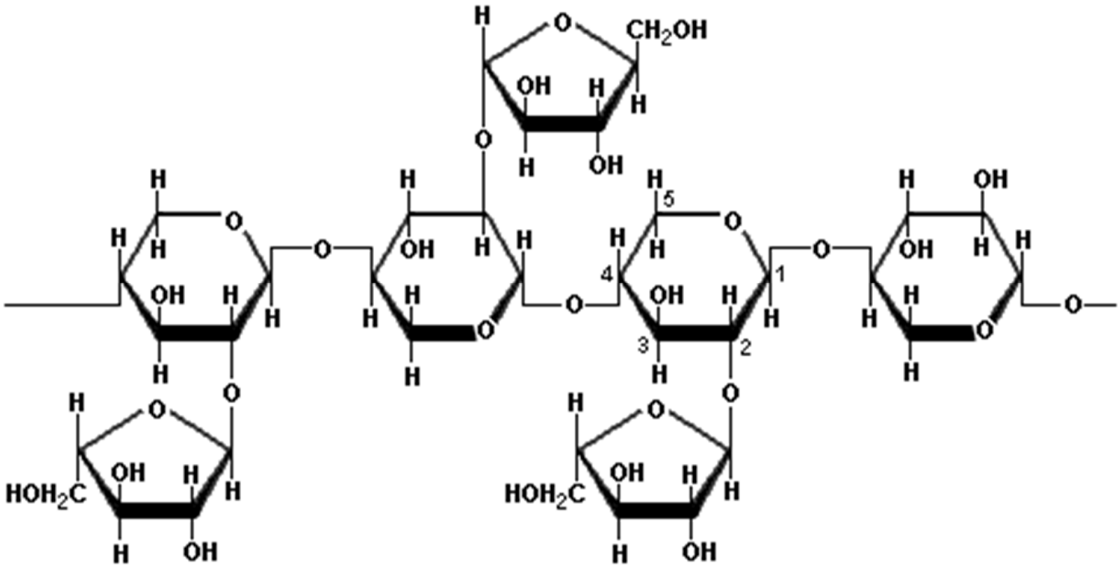

Figure 2.6: Structural formula of Arabinoxylan

The seed husk of Ispaghula (*Plantago ovata*) is chief source of xylan (arabinoxylan) and minor amount of other sugar components Rhap and Galp (Fischer *et al*., 2004) Arabinoxylan (AX) extracted from Ispaghula (Plantago ovata) containing 74.8% Xylp and 23.2% Araf. Extraction was carried out by immersing the seed husk in water overnight, treated with aqueous sodium hydroxide and finally acetic acid is used to coagulate the product. The Arabin oxylan has molecular weight 364,470 g/mol exhibit extreme swelling in aqueous medium. The carboxymethylation of arabinoxylane was converted by treatment with sodium monochloroacetate in aqueous alkaline medium into carboxymethyl arabinoxylan. Various factors, (time and temperature of reaction, molar ratio, and alkali concentration) control water solubility and ionic characters of product. Aqueous solubility of carboxymethyl arabinoxylan depends upon degree of substitution. (Saghir *et al*., 2008). Carboxymethylation of psyllium arabinoxylan modified its fundamental properties. It reduces viscosity of solution; improve crystallinity and thermal stability of arabinoxylan (Meenakshi and Munish, 2015). It has been reported that carboxymethylated xylan obtained from birch, beech-, and eucalyptus wood, oat husk, rye bran, and corn cob posses anionic properties (Petzold *et al*., 2006a; Petzold *et al*., 2006b) Arabinoxylans are the foremost polysaccharides obtained by alkali extraction from numerous cereal plants. Structural composition of arabinoxylan contain b-(1,4)-linked D-

xylopyranosyl residues to which arabinofuranosyl moieties are attached. Intestinal bacteria are capable to degrade arabinofuranosyl moieties (Grootaert *et al*., 2007).

2.8.4 *Methacrylic acid*

IUPAC name: 2-propenoic acid, 2-methyl

Synonyms: Methacrylic acid (MAA)

Molecular weight: 86.09 g/mol

Molecular formula: $C_4H_6O_2$

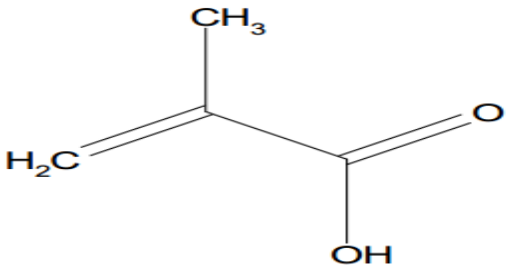

Figure 2.7: Structural formula of Methacrylic acid

According to CEFIC (European Chemical Industry Council) (1995), MAA is used in chemical industry for manufacturing of a variety of polymers mainly its ester derivatives. Hydrogels comprises of poly (methacrylic acid) (PMA) grafted with poly (ethylene glycol) (PEG) exhibit pH responsive behavior (Peppas and Klier, 1991). Methacrylic acid controls the hydrolytic and swelling behavior of hydrogels. High contents of methacrylic acid increase swelling of hydrogel in alkaline/ intestinal medium and vice versa. (Davaran *et al*., 2001).

2.8.5 *Acrylic acid*

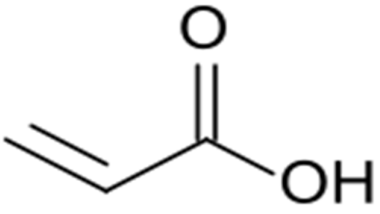

Figure 2.8: Structural formula of Acrylic acid

Acrylic acid is a colorless liquid with an acrid odor at room temperature. It is miscible with water and most organic solvents. Acrylic acid is highly reactive so polymerize very easily. The polymerization is catalysed by heat, light, and peroxides and inhibited by stabilizers, such as monomethyle ether of hydroquinone or hydroquinone itself. Acrylic acid is hydrophilic and become ionize at high pH due to carboxylic group. Acrylic acid based hydrogels also having electro sensitive properties (Tanaka *et al*., 1982). Hydrogels prepared with acrylic acid broadly used in mucoadhesive system for drug delivery (Young *et al*., 2014). Acrylic acid has capability to build up different intermolecular contacts to produce hydrogels with other polymers. Swelling capacity mainly depend upon acrylic acid intermolecular forces. (Bromberg *et al*., 2004; Devine and Higginbotham, 2005).

2.8.6 *Hydroxyethyl methacrylate*

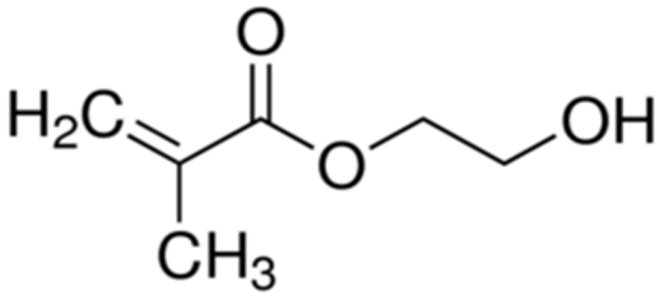

Figure 2.9: Structural formula of hydroxyethyl methacrylate

HEMA (2-hydroxyethylmethacrylate) was the former monomer for the preparation of hydrogels for drug delivery system. Its swellability may be modified by grafting of hydrophilic monomers with HEMA (Wichterle and Lim, 1960). HEMA belongs to esters of methacrylic acid. However, HEMA is unique in its hydrophilic nature and relatively low volatility. Copolymers of HEMA, as implant hydrogel employed for controlled delivery of drugs (Kuzma *et al*., 1996).

Numerous HEMA based hydrogels characterized by various techniques have been used as iontophoretic drug delivery, biomedical membrane, potential transdermal antibiotic carrier, as orthopedic carrier, drugs for ocular delivery (Arica *et al*., 2005; Eljarrat *et al*., 2005; Eljarrat *et al*., 2004)

2.9 Peptic ulcer

A peptic ulcer is a sore on the inner lining of the esophagus, stomach or duodenum. Damage of protective lining of stomach may be superficial or deep if remain untreated. Peptic ulcer grows by disturbance in protective mechanism of GI mucosa e.g., mucus and bicarbonate secretion imbalance plagued by harmful effect of gastric acid and pepsin. It has been reported that 95 percent of peptic ulcer is caused by H. pylori and NSAIDs are responsible for remaining present (Mynatt *et al*., 2009).

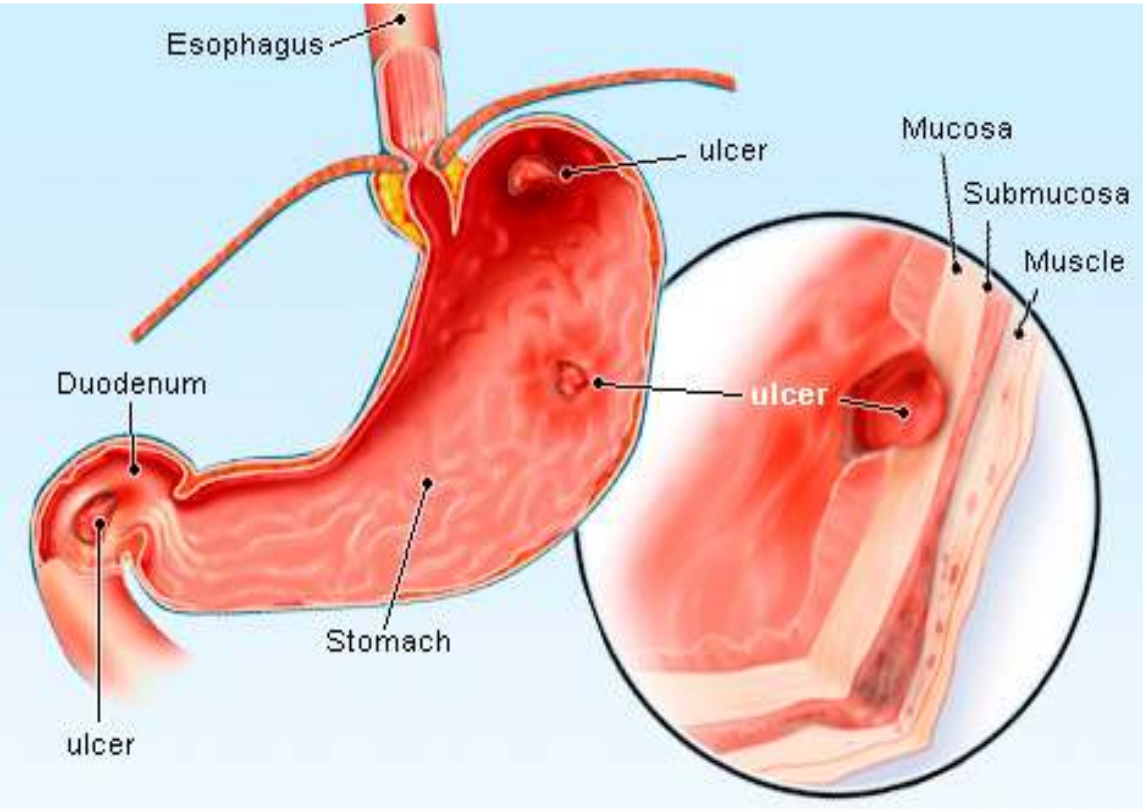

Figure 2.10: Peptic ulcers of the esophagus, stomach and duodenum

2.9.1 Etiology of peptic ulcer disease

- ***Common***
  - Hylicobacter pylori infection
  - Nonsteroidal anti inflammatory drugs (NSAIDs)
  - Stress related mucosal damage

- ***Uncommon***
  - Pathological Hypersecretory Conditions, Including Zollinger-Ellison Syndrome
  - Tumours (cancer, lymphomas)
  - Viral infections
  - Radiations/chemotherapy
- ***Rare***
  - Crohn' s disease of stomach/duodenum
  - Colonization of stomach with Helicobacter Heilmanni
  - Ideopathic **(**Malfertheiner *et al*., 2009)

- ***Clinical presentation of peptic ulcer***

Clinical presentation of peptic ulcer **(**Ramakrishnan *et al*., 2007)	
Typical symptoms	**Alarm symptoms**
• Epigastric pain • Nausea • Fullness • Bloating	• Aneamia • Malena • Heme positive stool • Blood vomiting • Anorexia or weight loss • Persisting upper abdominal pain radiating to back • Severe, spreading, upper abdominal pain

2.9.2 Treatment of acid related diseases

- ***Antacids***

  Antacids are primary treatment for acid related disorders. They act by alkalinizing the gastric acid. All antacids are available in oral preparations containing sodium bicarbonate, calcium carbonate, magnesium hydroxide and aluminum hydroxide (Mejia and Kraft, 2009).

- ***H2 -receptor antagonists***

  Gastric parietal cells contain acetylcholine, gastrin and histamine receptors, responsible for acid secretion by different mechanism. Antihistaminic drugs (H2 receptor blockers) e.g cimetidine, famotidine, nizatidine and ranitidine indicated for GERD, ulcer related with H pylori and NSAIDs, and other acid related disorders (Brittain and Jack, 1983).

- ***Proton pump inhibitors Proton***

  PPIs are antisecretary class of drugs. PPIs are indicated for the treatment of GERD, reflux esophagitis, peptic ulcers and Zollinger-Ellison syndrome. In addition, PPIs are used for gastro protection in patients using NSAIDs. In combination with two suitable antibiotics, PPIs are also used for the eradication of H. pylori infection. Most commonly used PPIs are esomeprazole, lansoprazole, omeprazole, pantoprazole and Rabeprazole (Pace *et al*., 2007).

2.10 Proton pump inhibitors

Proton pump inhibitors (PPIs) have been commenced in clinical practice for treatment of acid related disorders since 1980 as a drug of choice (Welage, 2003). The gastric H/K-ATPase enzyme is the prime board for the treatment of acid-related diseases.

Most commonly prescribed PPIs are omeprazole, lansoprazole, pantoprazole and Rabeprazole. These are potent gastric acid suppressing agents that block the last step for acid secretion by the parietal cell. They all contain a pyridylmethylsulphinyl benzimidazole moiety but vary from each other by substitutions on the pyridine or benzimidazole rings. All proton pump inhibitors act by same mechanism but differ in potency. They inhibit H+K+ ATPas at secretary surface of parietal cells. PPIs bind covalently with enzyme and inhibit irreversibly so, anti secretary activity is more potent than other anti secretary activity. The PPIs also reduce pepsin output and reducing secretory volume, which directly inhibits peptic activity. PPIs only differ from H_2 receptor antagonist by increasing gastric pH so peptic activity diminished and mucosal healing promoted (Huang and Hunt, 2001).

2.10.1 Normal acid secretion mechanism

Gastric parietal cells when exposed to stimuli e.g., histamine or acetylcholine there will be morphological transformation and become excited. The gastric H/K-ATPase, which is responsible for gastric acid secretion, becomes secretory canaliculus from cytoplasmic tubular membranes in the stimulated state of the parietal cell. Expanded secretory canaliculus produce by union of cytoplasmic vesicles with the rudimentary microvilli. The gastric H, K-ATPase shifts from tubulovesicles to apical membrane in the

canaliculus of excited state and exudes gastric acid by an electro neutral, ATP-dependent hydrogen-potassium exchange (Saches *et al*., 2007).

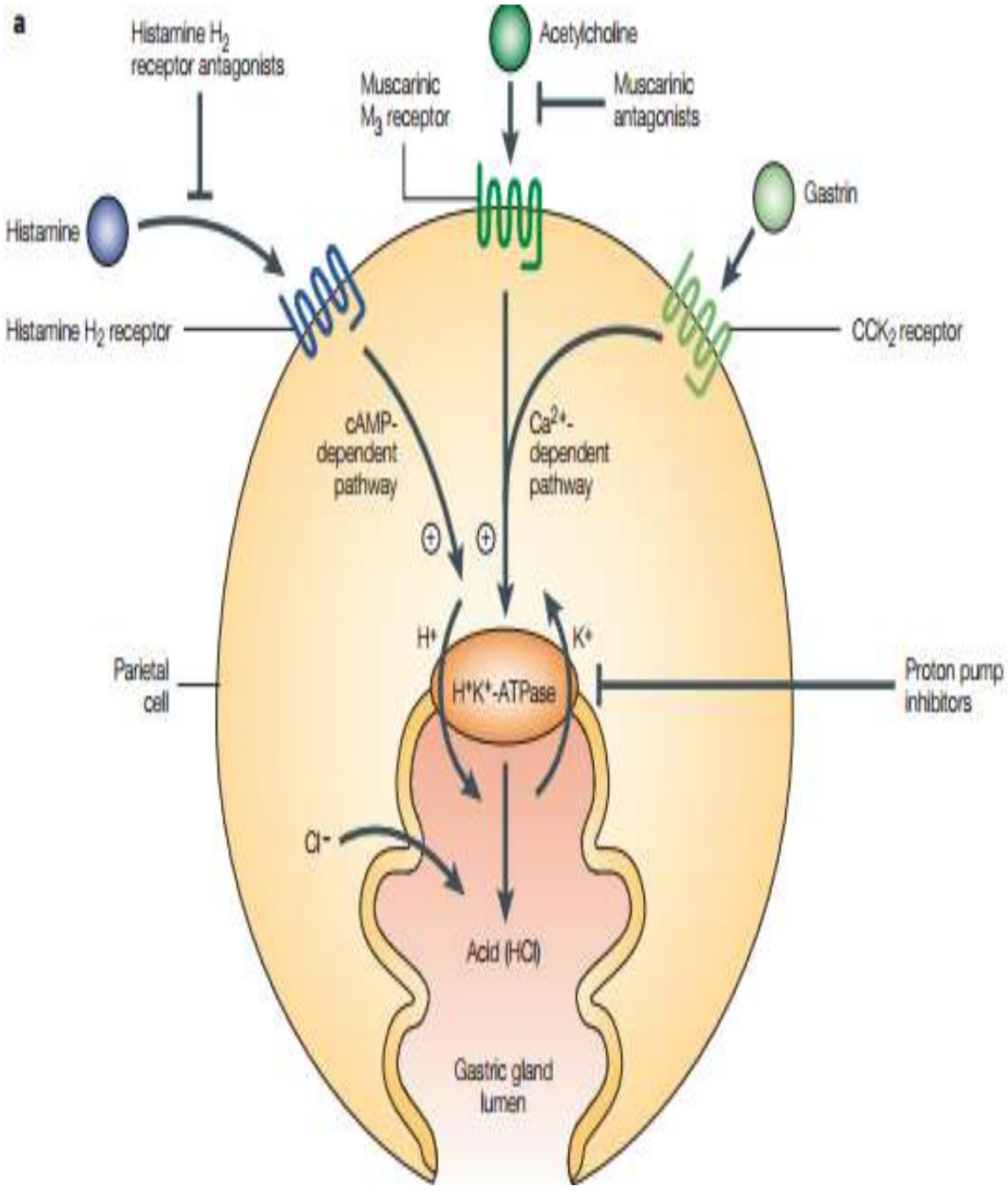

Figure 2.11: Physiological regulation of gastric acid in oxyntic/parietal cells and various targets for anti secretary drugs

2.10.2 Mechanism of action of PPIs

Pharmacological activity of PPIs is due to benzimidazoles and pyridine in their structure. They exhibit similar mechanism of action in the following steps:

a. *Activation;* All PPIs enter into acid environment of secretory canaliculus of the parietal cell. By protonation these are converted into active sulphenamide form.

b. Active sulphenamide compounds react with cysteines present at proton pump and block acid secretion. (Pace *et al*., 2007).

PPIs act by same mechanism but studies showed that a huge unevenness in their pharmacological effects (Lind *et al*., 2000; Savarino *et al*., 1998). This pharmacological variation may direct to an irregular effect of the treatment. Generally three pharmacological attributes may be responsible for such unpredictable response.

i) Pharmacogenetics

Pharmacogenetics refers to variation in genetic profile of an individual lead to unexpected response of drug. 20 years before, it was revealed that PPIs are susceptible to pharmacogenetic disparity (Andersson *et al*., 1990). PPIs are metabolized by CYP2C19 and CYP3A4. Clinical effects of PPIs directly related with genotype status of patient.CYP2C19 is the main enzyme involved in metabolism of PPIs and shows genetic variation. Several single nucleotide polymorphic variants (SNPs) of the CYP2C19 gene have been recognized that manipulate the capability to control the metabolism of PPIs. Mutations in CYP2C19 may cause toxicity in individuals because of slow metabolism of PPIs. On the contrary, some mutations may increase metabolism result in poor response of PPIs (Furuta *et al*., 1999; Li-Wan-Po *et al*., 2009; Baldwin *et al*., 2008; Sim *et al*., 2006).

ii) Pharmacokinetics

Some significant pharmacokinetic parameters, peak plasma concentration, half lives and excretion level of PPIs may vary. Oral bioavailability of omeprazole and esomeprazole and rabeprazole is low due to acid labile nature but increase with increase in dose. Pantoprazole, lansoprazole and rabeprazole have a constant bioavailability irrespective of repetitive dosing (Delhotal, 1995; Stedman, 2000; Hassan, 2000; Andersson, 1990).

iii) Pharmacodynamics

As variability in pharmacokinetic attributes modify the pharmacological effects of PPIs. pH metery technique used for studying the efficacy of acid inhibitory drugs. Intra gastric pH monitoring shows dose-effect relationship of PPIs (Geus *et al*., 1998; Hassan, 2000).

2.11 Rabeprazole Sodium

2.11.1 Introduction

Rabeprazole sodium belongs to class of substituted benzimidazole proton pump inhibitors. Stability of Rabeprazole depends on pH.

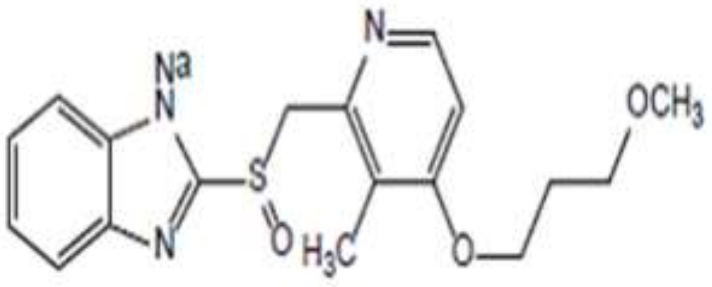

Figure 2.12: Structural formula of Rabeprazole sodium

Its molecular formula is $C_{18}H_{20}N_3NaO_3S$ with molecular weight of 381.43. Because of acid sensitive nature of Rabeprazole sodium its oral bioavailability is only 52% and half life is almost 1.5 hr. It inhibits the gastric acid secretion by blocking H^+K^+ ATPase enzyme at secretary surface of gastric parietal cells. It does not show anticholinergic and H_2 receptor blocking activity ((Mallikarjuna *et al*., 2010).

2.11.2 Pharmacokinetics

Rabeprazole sodium rapidly absorbed after oral administration. It is acid labile drug so having low bioavailability i.e., 52%. AUC and C_{max} are dose dependent, and T_{max} & half life of drug is not affected by repeated doses. Absorption of drug is not influenced by food and antacids (Swan *et al*., 1999). It shows different metabolism pathway than other PPIs. It is converted to Rabeprazole thioether by non-enzymatic pathway and other metabolites (demethylated Rabeprazole, rabeprazole-sulfone) are in very small amount by cytochrome P450 enzymes (Furuta *et al*., 2005).

2.11.3 Pharmacodynamic

- ***Mechanism of action***

  Rabeprazole sodium belongs to anti secretory class of antiulcer dugs, which do not show anticholinergic or histamine H_2- receptor blocking activity, but stifle gastric acid discharge by blocking gastric H^+,K $^+$ATPase at the secretory surface of gastric oxyntic cells. H^+,K $^+$ATPase enzyme considered as acid pump, rabeprazole has been regarde as proton pump inhibitor. Rabeprazol obstructs the last step of acid secretion. In vitro studies displayed that at pH 1.2 rabeprazole become activated by protonation, inhibit transport in gastric vesicles (Langtry and Markham, 1999).

2.11.4 Therapeutic indications

- Healing of Erosive or Ulcerative GERD (Holtman *et al*., 2002)
- Long-term Maintenance of Healing of Erosive or Ulcerative GERD (Thjodleifsson *et al*., 2000)
- Treatment of Symptomatic GERD (Langtry and Markham, 1999)
- Healing of Duodenal Ulcers (Dekkers *eta al*., 1999)
- Helicobacter pyloriEradication in Patients with Peptic Ulcer (Miwa *et al*., 1999)
- Non-Ulcer Dispypsia (Langtry and Markham 1999).
- Pathological Hypersecretory Conditions, Including Zollinger-Ellison Syndrome

2.11.5 Drug interactions

There are several mechanism involved in drug interactions of Rabeprazole sodium with other drugs.

Most common reasons include:

- Competitive inhibition of cytochrome P450 enzyme system
- Alteration in absorption of other drugs due to change in gastric pH (Gerson and Triadafilopoulos, 2001).

Table 2.3: Rabeprazole sodium interactions with other drugs

Drugs	***Mechanism of interaction***	***Reference***
Digoxin	Modulation of Gastric pH (increases in the AUC and Cmax for digoxin of 19% and 29% respectively)	Humphries, 1998
Ketoconazole	Modulation of Gastric pH (Cause 30% decrease in the bioavailability of ketoconazole)	Humphries, *et al*., 1996
Diazepam	Rabeprazole-mediated inhibition of CYP3A4	Ishizaki *et al*., 1995
Fluvoxamin	Extensive metabolisers of CYP2C19, enhanced $AUC_{0-\infty}$ and $t_{1/2}$ of rabeprazole	Uno *et al*., 2006

2.11.6 Use of rebeprazole sodium in specific populations

- ***Pregnancy***

  Animals study revealed that there are no teratogenic effects of PPIs.

- ***Category C drug***

  In animal studies drugs show risk to the fetus but for human there is no available data. Food and Drug Administration has recommended omeprazole as a category C drug in pregnancy, at high dose there are toxic effect on embryo and fetus (Ekman *et al*., 1985).

- ***Category B drugs***

  In animals studies reveal that there is no teratogenic effect but inadequate data for human. FDA has characterized PPIs except omeprazole in category B drugs.There is no adequate and well-controlled studies in pregnant women. Rabeprazole sodium should be used in pregnancy only if the potential benefit justifies the potential risk to the fetus (Richter, 2005).

- ***Pediatric Use***

  There is no adequate published data available on controlled trials of PPIs in children. It has been reported that for effective therapy of gastric acid related disorders PPIs are utilized. PPIs have a well tolerability profile in adults and children, but long-term tolerability studies are required, predominantly in children (Gibbons and Benjamin, 2003).

- ***Geriatric Use***

  No overall difference in safety and efficacy of Rabeprazole has been observed in old patients up to 75 year.

2.11.7 Adverse reactions

Rabeprazole was generally well endured during clinical trials. The practical side effects have generally been gentle or temperate and brief in nature. Only headache, diarrhoea, abdominal pain, asthenia, flatulence, rash and dry mouth have been linked with the application of rabeprazole.

The adverse events, which may or may not be causally related to rabeprazole, reported in clinical trials are listed below in downward array of rate of recurrence.

- Nervous System: headache, dizziness.
- Gastrointestinal: diarrhoea, nausea, abdominal pain, flatulence, vomiting, constipation.
- Respiratory: rhinitis, pharyngitis, coughs.
- Musculoskeletal: non-specific pain, back pain, myalgia.
- Skin: rash (Pace *et al*., 2007).

2.11.8 Dose and administration

- ***Treatment of active Gastro-Oesophageal Reflux Disease* (GERD):** The recommended oral dose for this condition is 20 mg tablet to be taken once daily for four to eight weeks.
- ***Treatment of active Duodenal Ulcer and Gastric Ulcer*: :**

  The recommended oral dose for both duodenal ulcer and gastric ulcer is 20 mg tablet to be taken once daily. This therapy may last for 4-8 weeks depending on severity of disease. Rabeprazole has also antibacterial activity against *H. pylori.* Rabeprazole sodium 20 mg with clarithromycin 500 mg and amoxycillin 1 g twice daily each for seven days. Eradication of H. pylori with this regimen has been proved most effective (Pace *et al*., 2007).

CHAPTER # 3

MATERIALS & METHODS

3. Materials &Methods

3.1 Materials

3.1.1 Chemicals

Rabeprazole sodium (*Getz Pharma-Pakistan),* Carboxy methylcellulose (CMC) (*Sigma Aldrich-Finland),* Acrylic acid (AA) (*Sigma Aldrich-Netherlands),* Potassium persulfate (*AnalaR, BDH-England),* N,N Methylene bisacrylamide (*Fluka-Switzerland),*Tris (hydroxymethyl) aminomethane (*Fluka-Switzerland),* Methanol (*Merck-Germany*), Distilled water, Potassium dihydrogen phosphate(*Merck-Germany*), Ethanol Absolute (*Merck-Germany*), Methacrylic acid (*Merck-Germany*). *Plantago ovate* (ispaghula) seed husk was purchased from local market of Pakistan. Acetic acid (*BDH laboratory-England*), Sodium hydroxide (*Sigma Aldrich-Netherlands*), Poly ethylene glycol 600 (*BDH Chemicals-England).*

3.1.2. Instrumentation and apparatus

High Performance Liquid Chromatographic[1], UV/Visible Spectrophotometer[2], Sonicator[3], Dissolution Test Apparatus[4], Centrifuge Machine[5], pH Meter[6], Ultrasonic Bath[7], Electric Balance[8], Membrane Filter[9], Magnetic Stirrer[10], B.P. Apparatus[11], Vacuum Pump[12], Distillation Plant[13], Ultra-low Freezer[14], Micropipettes[15], Filtration Assembly[16], Measuring Cylinder[17], Beakers[18] 50, 100, 250, 500 & 1000 mL, Measuring Flasks[19] 50, 100, 250, 500 & 1000 mL, Centrifuge Tubes[20], Sample Test Tubes[21], Disposable Syringes[22], Vortex Mixer[23], Incubator[24], Centrifuge[25], Fourier Transform Infrared Spectroscopy(FTIR)[26], Scanning Electron Microscopy (SEM)[27], Differential Scanning Calorimeter and Thermo Gravimetric Analyzer (DSC &TGA)[28], XRD[29],

1. Agilent 1100 Series U.S.A
2. UV-1600 Shimadzu. Germany
3. Elma, Germany
4. PTCF II Pharma Test, Germany
5. Model 4000-China

6. WTW pH 300-Germany

7. Fisher Scientific FS 28 H-Germany

8. PerciaXB120A

9. Sartorius (0.45 μm filters)-Germany

10. Gallen Kamp-England

11. Model No 500-China

12. Rotary Vane Pump ILMVAC-Germany

13. WDA/4 R & M-England

14. Sanyo-Japan

15. Softpet- Finland

16-21. Pyrex-France

22. BD-Pakistan

23. Seouline BioScirnce-Korea

24. Velp Scientifica-Italy

25. Hettich-Germany

26. Bruker, Tenser 27-Germany

27. Quanta 250, FEI

28. SDT Q-600 (TA New Castle, DE)

29. Expert pro Panalytical-Germany

3.2 Methods

3.2.1 Isolation of arabinoxylan

Arabinoxylan was isolated from the Ispaghola husk by method of Saghir *et al*. (2008). 100 g of Ispaghula seed husk was soaked in 5 liters of distilled water over night. Aqueous sodium hydroxide solution (2.5%) was added to the mixture for pH adjustment at 12 with continuous stirring for 2-3 minutes. Husk was separated from the gel by vacuum filtration. Concentrated

acetic acid was used to coagulate the sample. The gel obtained was washed with distilled water until the pH become constant and freeze dried for 1 week.

3.2.2 Carboxymethylation of arabinoxylan

The reported method was adopted after necessary modifications. Arabinoxylan (2.5 g) obtained by above procedure was suspended in ethanol. The reaction mixture was vigorously stirred at room temperature for 1 h. After addition of 25% aqueous sodium hydroxide solution, sodium monochloroacetate was added and the temperature of reaction bath was increased to 55ºC. The etherification was performed for 5 h. The product was filtered and suspended in 80% (v/v) water/methanol, neutralized with diluted acetic acid, and washed with ethanol. The product was dried under vacuum (Saghir *et al*.,2008).

3.2.3 Graft copolymer preparation

A general procedure for chemically graft copolymerization was conducted as follows.

Calculated amount given in Table 3.1 of Carboxymethyl arabinoxylan was dissolved in degassed distilled water to obtain a sticky transparent solution at 70 °C. Then potassium persulfate solution in water was added to Carboxymethyl arabinoxylan solution and stirred for 10 min at 70 °C to generate radicals. Following this, reaction mixture was cooled down to room temperature. At room temperature, solution containing monomer and cross linker was added under magnetic stirring. The final weight of solution was made by adding distilled water. Air above the solution in the test tube or any dissolved oxygen was removed by bubbling nitrogen for 15-20 min which acts as free radical scavenger. For polymerization, solution was heated in water bath at 45°C for 1 hr, 50°C for 2 hr, 55°C for 3 hr, 60°C for 4 hr and 65°C for 8 hrs (Wenbo *et al*., 2011). Hydrogels obtained were cut into 5 mm discs by blade. Washing media (0.1M Sodium hydroxide) was used to remove unreacted monomer and catalyst. These discs were thoroughly washed with water until the pH of washing media resembles distilled water. After washing, the discs were dried first at room temperature and then in oven at 45-50°C till

constant weight of hydrogels were obtained and further used for characterization and drug release study (Sadeghi *et al.*, 2012).

CMAX-g-MAA, CMC-g-MAA, CMC-g-AA, PEG-g-MAA hydrogels and PEG (HEMA-co-AA) hybrid hydrogels were also prepared in a similar fashion. Compositions of different combinations of hydrogels are given in Tables 3.1 to 3.6.

Table 3.1: Composition of 100g CMAX-g-AA Hydrogel preparation with varying monomer polymer and crosslinker concentration.

Sr.No	Formulation code	CMAX (g)	AA (g)	Crosslinker % mole ratio of monomer
1	A1	0.5	**10**	0.2
2	A2	0.5	**15**	0.2
3	A3	0.5	**20**	0.2
4	A4	**1**	15	0.2
5	A5	**1.5**	15	0.2
6	A6	**2**	15	0.2
7	A7	0.5	15	**0.4**
8	A8	0.5	15	**0.6**
9	A9	0.5	15	**0.8**

Table 3.2: Composition of 100g CMAX-g-MAA Hydrogel preparation with varying monomer polymer and crosslinker concentration.

Sr.No	Formulation code	CMAX (g)	MAA (g)	Crosslinker % mole ratio of monomer
1	M1	0.5	**20**	0.25
2	M2	0.5	**30**	0.25
3	M3	0.5	**35**	0.25
4	M4	**1**	25	0.25
5	M5	**1.5**	25	0.25
6	M6	**2**	25	0.25
7	M7	0.5	25	**0.45**
8	M8	0.5	25	**0.65**
9	M9	0.5	25	**0.85**

Table 3.3: Composition of 100g CMC-g-AA Hydrogel preparation with varying monomer polymer and crosslinker concentration.

Sr.No	Formulation code	CMC (g)	AA (g)	Crosslinker % mole ratio of monomer
1	CA1	0.5	**10**	0.2
2	CA2	0.5	**15**	0.2
3	CA3	0.5	**20**	0.2
4	CA4	**1**	15	0.2
5	CA5	**1.5**	15	0.2
6	CA6	**2**	15	0.2
7	CA7	0.5	15	**0.4**
8	CA8	0.5	15	**0.6**
9	CA9	0.5	15	**0.8**

Table 3.4: Composition of 100g CMC-g-MAA Hydrogel preparation with varying monomer polymer and crosslinker concentration.

Sr.No	Formulation code	CMC (g)	MAA (g)	Crosslinker % mole ratio of monomer
1	CMA1	0.75	**20**	0.1
2	CMA2	0.75	**30**	0.1
3	CMA3	0.75	**35**	0.1
4	CMA4	**1**	25	0.1
5	CMA5	**1.5**	25	0.1
6	CMA6	**2**	25	0.1
7	CMA7	0.75	25	**0.2**
8	CMA8	0.75	25	**0.3**
9	CMA9	0.75	25	**0.4**

Table 3.5: Composition of 100g PEG-g-MAA Hydrogel preparation with varying monomer polymer and crosslinker concentration.

Sr.No	Formulation code	PEG (%)	MAA (g)	Crosslinker % mole ratio of monomer
1	PMA1	**5**	25	0.30
2	PMA2	**10**	25	0.30
3	PMA3	**15**	25	0.30
4	PMA4	**20**	25	0.30
5	PMA5	10	**20**	0.30
6	PMA6	10	**30**	0.30
7	PMA7	10	**35**	0.30

Table 3.6: Composition of 100g PEG (HEMA-co-AA)Hydrogel preparation with varying monomer polymer and crosslinker concentration.

Sr.No	Formulation code	PEG (%)	AA (g)	HEMA (g)	Crosslinker % mole ratio of monomer
1	PHA1	10	**7.5**	2.5	0.25
2	PHA2	10	**10**	2.5	0.25
3	PHA3	10	**12.5**	2.5	0.25
4	PHA4	10	**15**	2.5	0.25
5	PHA5	10	15	**1**	0.25
6	PHA6	10	15	**1.5**	0.25
7	PHA7	10	15	**2**	0.25
8	PHA8	10	15	**3**	0.25

3.2.4 Swelling Studies

3.2.4.1 Preparation of buffer (British Pharmacopoeia Volume V) solutions of different pH for swelling studies

a) Buffer of pH 1.2

250 mL solution of 0.2M sodium chloride was mixed with 425 mL of 0.2M hydrochloric acid. The final volume was made up to 1000 mL with distilled water.

b) Buffer of pH 7.4

250 mL solution of 0.2M potassium dihydrogen phosphate (KH_2PO_4) was mixed with 195.5 mL of sodium hydroxide solution 0.2M. The final solution was diluted up to 1000 mL with distilled water.

3.2.4.2 Swelling analysis

Smart swelling behavior of hydrogels was investigated in buffer solutions at different pH values. Dried hydrogels with a 0.45 g were immersed in 100 mL USP phosphate buffer solution of pH 1.2 and pH 7.4 at 37°C. Swollen samples were weighed at 0.5, 1, 1.5, 2, 3, 4, 6, 8, 10, 12, 14, 18, 24, 48, 72 hours and excess media were removed by blotting with a piece of filter paper. Studies were performed in triplicate and average values were taken for data analysis. Swelling of various samples was continued until they attained constant

weight (Raghavendra *et al.,* 2011). Dynamic swelling ratio (q) was calculated using following as given in equation 1(Bumsang *et al.,* 2003).

$$q = W_s/W_d \qquad (1)$$

Where q is dynamic swelling ratio, W_s is the weight of swollen gel at time t and W_d is the initial weight of dry hydrogel.

3.2.5 pH responsive/Pulsatile behavior

For controlled delivery of drug from graft copolymer, the swelling process must be reversible to ensure that the release of drug could be initiated and stopped promptly upon change in pH. To investigate reversibility of swelling/deswelling process of polymer networks with respect to environmental pH change, selected hydrogel samples were swollen in a buffer solution of pH 7.4, placed them in a buffer solution of pH 1.2, returned them to a buffer solution of pH 7.4, and finally collapsed them in a buffer solution of pH 1.2. The consecutive time interval for each cycle was 45 min (Sadeghi, 2011).

3.2.6 Drug loading

Samples showed maximum swelling were selected for drug loading and release study. Drug was loaded by incubation after polymerization. Incubation after polymerization removed all non reacted monomers and decomposed products of the catalyst.

Selected hydrogels were soaked in 0.1M sodium hydroxide solution containing 1% Rabeprazole sodium for time period until swelling equilibrium achieved. Loaded hydrogels were washed after swelling with water to remove surface adhered drug on disc. For drug loading, 0.1 M sodium hydroxide solution was selected due to maximum swelling ratio of hydrogels and drug stability in that solution. The drug loaded hydrogels were freeze dried because drug has thermal stability issues (Oprea *et al.,* 2010).

3.2.7 Determination of drug loading

Two methods were used for determining drug loading in hydrogels. The first method used to calculate the amount of drug loaded in hydrogel was determined by following equation as given in equation 2:

$$\text{Amount of drug} = W_L - W_o \qquad (2)$$

W_o and W_L are the weight of dried hydrogels before and after immersion in drug solution, respectively.

In 2nd method, amount of drug entrapped in hydrogels was calculated by repeatedly extracting the weighed quantity of powdered loaded gels by using 0.1M sodium hydroxide solution. Each time fresh 0.1M sodium hydroxide solution was replaced after specific interval until there was no drug in the solution. Drug concentration was determined spectrophotometrically at λ_{max} 284 nm. Amount of drug present in all portions was considered as total amount of drug loaded into hydrogel (Kuldeep and Nath, 2012). Amount of drug loaded in hydrogel was determined by following as given in equation 3:

$$\text{Total drug loaded} = \frac{WL - Wo}{Wo} \times 100 \qquad (3)$$

W_o and W_L are the weight of dried hydrogels before and after immersion in drug solution, respectively.

3.2.8 Sol-gel fraction.

The hydrogels prepared by free radical polymerization were dried to measure the gelation. Hydrogels were cut into 4-5 mm thickness and oven dried at 50 °C until constant weight was obtained. Then few dried hydrogels were extracted with water at room temperature in order to extract the insoluble parts of hydrogel until the weight became constant. The gel fraction was calculated as given in equation 4 and 5 (Ranjha *et al*., 2014):

$$\text{Sol fraction } \% = \frac{W_o - W_1}{W_o} \times 100 \qquad (4)$$

$$\text{Gel fraction } (\%) = 100 - \text{Sol fraction} \qquad (5)$$

Where W_o is weight of hydrogel before extraction and $W_1$is weight of hydrogel after extraction.

3.2.9 Determination of the equilibrium water content

Dried hydrogel samples were soaked in buffer of pH 1.2 and pH 7.4 at 37 $^{\circ}$C to measure water uptake of hydrogel in a thermostatically controlled chamber to the equilibrium state. Fully swollen samples were removed and weighed after removal of excess of solvent with absorbent paper. The equilibrium water content in swollen samples (W_{eq}) was calculated as given in equation 6 (Jagadish *et al*., 2012).

$$W_{eq}\% = \frac{W_s - W_d}{W_s} \times 100 \qquad (6)$$

Where W_s is the weight of swollen sample at equilibrium state and W_d is weight of the dry sample.

3.2.10 Release studies

i) ***Preparation of standard stock solution***

Rabeprazole sodium (100 mg) was accurately weighed and transferred to a 100 mL volumetric flask. It was first dissolved in 25 mL of 0.1N NaOH and sonicated for about 10-15 min, then finally made up to the volume with 0.1N NaOH (1000 µg/mL) (Mallikarjuna *et al*., 2010).

ii) ***In vitro release/dissolution studies***

The selected *in vitro* dissolution conditions were in accordance with US Food and Drug Administration, CDER (Center for Drug Evaluation and Research) recommended for rabeprazole sodium. Drug release studies were carried out using a USP type II dissolution test apparatus (PTCF II Pharma Test, Germany) at 100 rpm for 24hrs in 0.1M HCl (900mL) maintained at 37±0.5°C. 5 mL of sample was collected at 0, 0.5, 1, 1.5, 2, 4, 6, 8, 10, 12 and 24 hour with an automated sample collector (PT-DT7Pharma Test, Germany) after filtering through sinter filters (10 µm) and same volume of fresh dissolution media was added after each sample collection. The collected samples were diluted up to 50 mL and analyzed at 284

nm using a UV-spectrophotometer (UV-1600 Shimadzu. Germany)**.**Same studies were conducted with 0.6M tris buffer, pH 8.0 (900mL) and tested for drug release for 24hrs at same temperature and rotation speed. Samples were taken out and volume of fresh tris buffer pH 8.0 was added to kept volume of dissolution medium constant and samples were analyzed using UV spectrophotometer at 284 nm. *In-vitro* cumulative drug release study was conducted in triplicate (Rakesh *et al*., 2011).

iii) Release kinetics

Dissolution profile can be described by different mathematical functions. To obtain a more quantitative understanding of the transport kinetics in hydrogel, the drug release data was analyzed as a function of time. The release models with major application and best describing drug release phenomena are, in general, the Higuchi model, zero order model, first order model and Korsemeyer-Peppas model (Suvakanta *et al.*,2010). Release models are explained in Tables 3.7.

Table 3.7: Release models

Sr.No	Release Models	Equation	Description
1	Zero order model	$Q = Q_0 + K_0 t$	Where Q is the amount of drug released or dissolved, Q_0 is the initial amount of drug in solution (it is usually zero), and K_0 is the zero order release constant. Plot made: cumulative % drug release vs. time
2.	First order	$logQ = logQ_0 - k_t/2.303$	Where, Q_0 is the initial concentration of drug and K is first order constant. Plot made: log cumulative of % drug remaining vs. time
3.	Higuchi Model	$Q_{t=K_H\sqrt{t}}$	Where, Q_t is the amount of drug released in time t and K_H is Higuchi release rate constant. Plot made: cumulative % drug release vs. square root of time
4.	Korsmeyer-Peppas Model	$\frac{M_t}{M_\infty} = Kt^n$	Where M_t / M_∞ is fraction of drug released at time t, k is the rate constant and n is the release exponent. The n value is used to characterize different release mechanisms. Plot made: log cumulative % drug release vs. log time

3.2.11 FTIR analysis

Grafting were confirmed by FTIR spectroscopy. IR spectra for individual components and prepared hydrogel were recorded in a Fourier transform infrared (FTIR) spectrophotometer (Bruker, Tensor-27, Germany). For FTIR analysis hydrogel samples were ground to powder. A small quantity of sample was placed in crystal area and pressure arm was locked. Bands were in the region from 4000 to 600 cm^{-1} (Lim and Lee, 2005).

3.2.12 SEM analysis

Surface morphology of crosslinked hydrogel was evaluated by Quanta 250 SEM (FEI), operating at 10 kV with secondary electrons, in low vacuum mode. For a better observation of the pores, swollen hydrogels were previously freeze-dried in freeze dryer (Christ Alpha 1-4 Germany), for 24 hrs at -55 °C. The sample was prepared by cutting the dry hydrogels with a sharp razor blade, in order to expose the internal structures (Lim and Lee, 2005).

3.2.13 Thermal analysis

Thermal behavior of the prepared graft copolymers were studied by Thermogravimetric Analyzer model SDT Q 600 series Thermal Analysis System (TA instruments, New Castle DE, UK) from room temperature to 600 ºC. The hydrogel samples were ground and passed through mesh 40. Sample dry weight was 5-10 mg placed in an open pan (platinum 100 µl) attached to a microbalance. Heating rate of 10 ºC/min was used under nitrogen atmosphere at a flow rate of 20 mL/min. All the measurements were made in triplicate. Thermograms were recorded by software (Guirguis & Moselhey, 2012)

3.2.14 X-ray Diffraction

X-ray diffraction patterns were recorded, in reflection, with a Xpert pro Panalytical instrument, at room temperature, using nickel filtered CuKα radiation (λ= 1·54050 Å) and operating at 30 kV and 10 mA. Powdered samples were filled onto sample holder and smoothing the surface with a glass slide. Samples were scanned over range 5-50° 2θ at a rate of 1º 2θ/min (Siddhi *et al*., 2011).

3.2.15 Acute oral toxicity of prepared hydrogels

The purified prepared dried hydrogels were grinded into powder and suspended in water for acute oral toxicity test. Swiss albino mice (29–35 g) of either sex were used. Animals were divided into five groups (n=3), group scheme was given in Table 3.8. OECD guidelines for testing of chemicals recommended that minimum number of animals (n=3) must be used (OECD, 2001). Animals were kept in clean cages in a 12 h light/dark cycle. They were fed with standard laboratory diet and ordinary tap water. Acute oral toxicity

studies of CMAX-g-AA, CMAX-g-MAA, CMC-g-AA, CMC-g-MAA hydrogels were executed in Swiss albino mice using an MTD (Maximal Tolerance Dose) method ensuing the OECD (organization for economic cooperation and development) guidelines for analysis of chemicals toxicity. At the instigation of the study the weight variation of animals involved in study must be minimal and not go beyond ±20 % of the mean weight. Mice were orally administered 1-10 g/Kg/day of hydrogel dispersion. The dose was designated as the maximum potential dose that can be administered orally owing to high viscosity of the swollen hydrogels at the extreme capacity of oral gavage. Clinical manifestations for general conditions (weight, diet, activity, mortality, and signs of illness) were carried out twice daily for 2 weeks. On day 15 blood biochemistry and necropsies were performed to observe the gross pathological changes. To analyze microscopically obtained tissue samples were fixed by conserving in 10 % buffered formaldehyde solution for 48 hrs, and then fixed in paraffin, sectioned at 5 μm, and imagined by hematoxylin and eosin staining. Primary dermal and eye irritation were also observed (Chen *et al*., 2008).

Table 3.8: Group scheme for acute oral toxicity study of hydrogels in mice

Group I	Group II	Group III	Group IV	Group V
Control	Treated with CA hydrogel	Treated with CMA hydrogel	Treated with A hydrogel	Treated with M hydrogel

3.2.16 In Vivo analysis

3.2.16.1 Experimental Design

Healthy rabbits having weight greater than 2.5 ± 0.61 Kg were used for *in vivo* study. Rabbits were divided into three groups randomly, each group consisting of 10 rabbits. The study protocol was approved by Pharmacy Research Ethics Committee, The Islamia University of Bahawalpur, Punjab Pakistan. All rabbits were fasted for 12 hours before dose administration except free excess to drinking water. Each rabbit was administered hydrogel disc containing Rabeprazole sodium equivalent to (5 mg/kg/day) with the help of silicone rubber gastric intubation tube with gavage (Amitava *et al*., 2008).

3.2.16.2 Sample Collection

The rabbit was fixed in rabbit holder with its head protruding outside. Blood samples were collected from jugular vein of rabbit in heparinized centrifuge tubes. One sample was collected at zero time and then at 0.50, 1, 2, 3, 4, 6, 8, 12, 24 hours after dosing Rabeprazole sodium. A 3 mL blood sample was collected each time. Blood samples were centrifuged at 5000 rpm for 10 minutes and the separated plasma was stored frozen at -70 $^{\circ}$C until analysis.

3.2.16.3 HPLC Conditions

The HPLC parameters and their conditions are given in Table 3.9.

Table 3.9: Conditions for HPLC analysis

Sr. No	Parameter	Condition
1.	Mobile Phase	0.1M Ammonium acetate Buffer (60 %): Acetonitrile (40 %)
2.	Flow Rate	1.0 mL/min
3.	Retention Time	5.4 min
4.	HPLC Detector	UV Detector
5.	HPLC Column	C18
6.	Column Dimension	4.6 x 250 mm
7.	Injection Volume	20 µl
8.	Run Time	10 min
9.	λ_{max}	284 nm

3.2.16.4 Preparation of mobile phase

The mobile phase consisted of 60% of 100 mM Ammonium acetate buffer & 40% Acetonitrile and eluted at a flow rate of 1.0 mL/min. Acetonitrile and Ammonium acetate buffer were measured separately and then mixed. After mixing, it was filtered through 0.45 µm membrane filter. Mobile phase was degassed by sonication before running in HPLC.

3.2.16.5 Method for Sample Analysis

a) Preparation of stock solution

Initial stock solution of Rabeprazole sodium was prepared by dissolving 1 gram of Rabeprazole sodium in 100 mL of 0.1N sodium hydroxide. Standard solutions were obtained by serial dilution of this stock solution to give concentrations over the range of 4000-31.25 ng/mL according to plasma spiking. Stock solution was prepared on daily basis.

b) Preparation of sample

Prior to injection, rabeprazole sodium was extracted from the plasma samples according to the following procedure:

Chloroform was added into 500 µl plasma sample containing Rabeprazole as an extraction solvent. Mixture was then vortexed for 1 min by using a vortex mixer (Seouline BioScience-Korea), and centrifuged at 5,000 rpm for 5 min by centrifuge machine. After centrifugation, organic layer was withdrawn by using micropipette and solvent was dried under a gentle stream of nitrogen at 45^{o}C. The residue was reconstituted with 100 µl of mobile phase and 20 µl injected into column.

c) Preparation of Standard Curve

Standard curve was constructed to predict the anticipated range of Rabeprazole sodium plasma concentration found in healthy rabbits. Blank plasma was spiked with Rabeprazole sodium solutions to give concentrations of 4000, 2000, 1000, 500.250, 125, 62.5, 31.25 ng/mL. Extraction procedure was same as described above. Injections of 20µl were injected and spectra were taken of each concentration. The peak areas were noted for each concentration.

d) High Performance Liquid Chromatography

Analysis was performed by using Agilent Liquid Chromatography, with a pump series 1100, Agilent UV detector at wavelength of 284 nm. Column was used consisting of Silica C18 column (250 mm x 5 µm particle size x 4.6 mm

I.D.). The mobile phase was pumped at a rate of 1.0 mL/minute. Sample of 20 µl were injected, with a run time of 10 minutes.

e) Pharmacokinetic analysis

The pharmacokinetic parameters of Rabeprazole sodium analyzed from the plasma levels in rabbits by noncompartmental pharmacokinetic analysis using the software package kinetic v 4.4. The peak plasma concentration (C_{max}) and time to reach peak plasma concentration (T_{max}) was obtained from the visual inspection of the plasma concentration-time curves. The area under the plasma concentration curve (AUC_{0-t}) was determined using the trapezoidal rule.

f) Statistical analysis

Software Kinitica version 4.4 was used for evaluation of pharmacokinetic parameters of rabeprazole sodium. Pharmacokinetic parameters of rabeprazole sodium was statistically analyzed by One way ANOVA.

g) Precision and accuracy

Percent coefficient of variation (% CV) was calculated to find out intra-day and inter-day precision and accuracy of present method for rabeprazole sodium in rabbit plasma. The validation run was consisted of calibration curve and three replicates of each low and high quantification concentrations. For inter-day, analysis of three batches of drug rabeprazole sodium was performed on three different days.

h) Quantification and detection limits

Limit of detection (LOD) and Limit of quantification (LOQ) of rabeprazole sodium as mean ± SD were 8.0 ± 0.227 ng/mL and 12.0 ± 0.528 ng/mL. Lower quantification limits showed the higher sensitivity of present method.

CHAPTER # 4

RESULTS

4. Results

4.1 Characterization of CMAX-g-AA hydrogels

4.1.1 Swelling studies at pH1.2 and pH 7.4

To investigate the time and pH dependent swelling pattern of CMAX-g-AA hydrogels, we executed swelling analysis of discs CMAX-g-AA with various AA and CMAX compositions in 0.1N HCl (pH 1.2) and phosphate buffer (pH 7.4) solutions. Formulations were assigned codes (A1-A3), (A4-A6) and (A7-A9) for varying concentration of acrylic acid, CMAX and crosslinker respectively. Table 4.1.1 presents the (q) values of series of hydrogels with varying concentration of acrylic acid A1 (1 to 7.773), A2 (1 to 5.268) and A3 (1 to 2.742) in pH 1.2 and A1 (1 to 47.295), A2 (1 to 53.459) and A3 (1 to 58.181) in 7.4 buffer solutions at 37 ºC. Table 4.1.2 represented comparative swelling ratio of CMAX-g-AA with different contents of CMAX, A4 (1 to 4.777), A5 (1 to 4.181) and A6 (1 to3.533) at pH 1.2 and A4 (1 to 59.322), A5 (1 to 62.788) and A6 (1 to 64.191) at pH7.4. Table 4.1.3 showed effect of crosslinker contents on swelling ratio of hydrogels A7 (1 to 3.965), A8 (1 to 3.458) and A9 (1 to 3.141) at pH 1.2 and A7 (1 to 48.373), A8 (1 to 43.626) and A9 (1 to 31.629) at pH 7.4.

Table 4.1.1: Comparative swelling ratios of CMAX-g-AA (A) hydrogels using different concentrations of acrylic acid (n=3)

Time (Hrs)	**Swelling ratio (q) at pH 1.2**			**Swelling ratio (q) at pH 7.4**		
	A1	A2	A3	A1	A2	A3
0	1±0	1±0	1±0	1±0	1±0	1±0
0.5	1.45±0.19	1.3±0.23	1.03±0.22	4.3±0.21	4.71±0.22	5.02±0.21
1	1.94±0.22	1.61±0.29	1.06±0.24	7.6±0.24	8.46±0.23	9.04±0.24
1.5	2.43±0.32	1.91±0.31	1.09±0.19	10.91±0.33	12.21±0.34	13.06±0.33
2	2.92±0.27	2.21±0.3	1.15±0.22	14.21±0.34	15.96±0.38	17.08±0.45
3	3.41±0.3	2.51±0.28	1.2±0.32	17.51±0.38	19.71±0.41	21.09±4.21
4	3.9±0.31	2.82±0.32	1.26±0.33	20.81±0.42	23.46±0.43	25.11±4.76
6	4.4±0.33	3.12±0.31	1.33±0.35	24.11±0.46	27.21±0.45	29.13±6.73
8	4.89±0.32	3.42±0.33	1.43±0.35	27.42±0.53	30.96±4.21	33.15±0.53
10	5.38±0.31	3.72±0.35	1.49±0.36	30.72±0.63	34.7±4.76	37.17±0.63
12	5.87±0.32	4.03±0.35	1.57±0.34	34.02±0.74	38.45±6.73	41.19±0.74
14	6.35±0.35	4.33±0.36	1.64±0.34	37.32±0.75	42.2±0.74	45.21±0.75
18	6.85±0.36	4.63±0.34	1.78±0.33	40.62±0.81	45.95±0.75	49.22±0.81
24	7.34±0.34	4.93±0.34	2.01±0.33	43.93±0.82	49.7±0.81	53.24±0.82
48	7.77±0.34	5.24±0.35	2.74±0.34	47.23±0.84	53.45±0.82	58.06±0.84
72	7.77±0.35	5.27±0.35	2.74±0.34	47.3±0.89	53.46±0.88	58.18±0.89

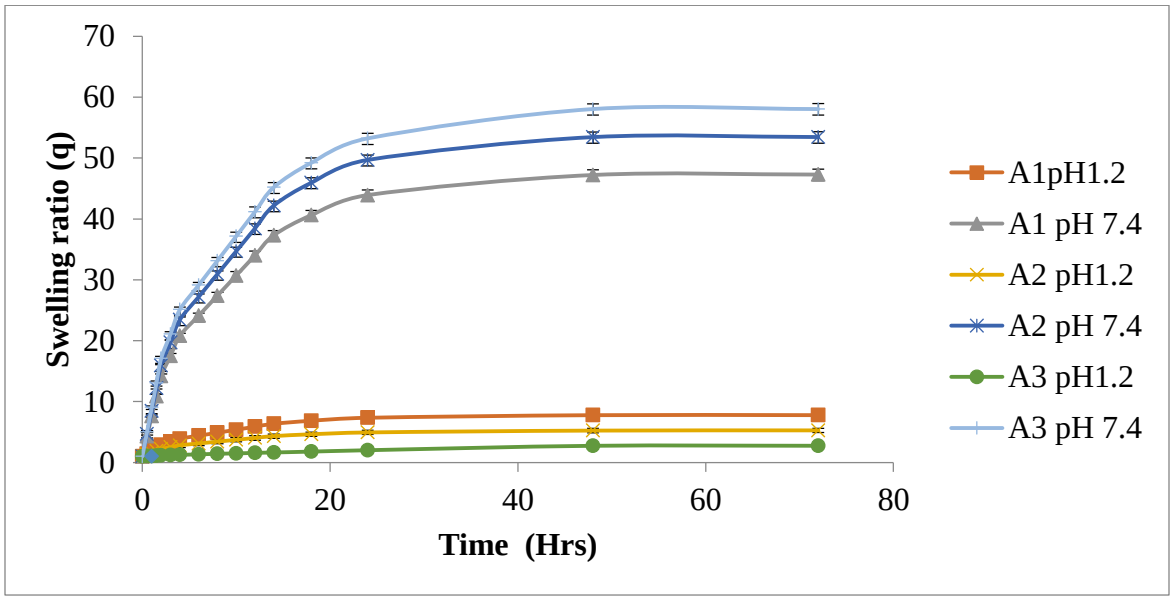

Figure 4.1.1: Comparative swelling of CMAX-g-AA (A) hydrogels using different concentrations of monomer

Table 4.1.2: Comparative swelling ratios of CMAX-g-AA (A) hydrogels using different concentrations of CMAX (n=3)

Time (Hrs)	**Swelling ratio (q) at pH 1.2**			**Swelling ratio (q) at pH 7.4**		
	A4	A5	A6	A4	A5	A6
0	1±0	1±0	1±0	1	1	1
0.5	1.27±0.23	1.23±0.19	1.18±0.22	5.16±0.24	5.41±0.21	5.47±0.2
1	1.54±0.21	1.45±0.22	1.36±0.24	9.32±0.33	9.81±0.24	9.93±0.22
1.5	1.81±0.29	1.68±0.32	1.54±0.33	13.47±0.34	14.22±0.33	14.39±0.31
2	2.08±0.43	1.9±0.33	1.72±0.51	17.63±0.68	18.63±0.63	18.86±0.62
3	2.35±0.32	2.13±0.35	1.9±0.62	21.79±0.77	23.03±0.74	23.32±0.73
4	2.62±0.22	2.35±0.35	2.08±0.73	25.95±0.79	27.44±0.75	27.79±0.77
6	2.89±0.32	2.58±0.36	2.26±0.77	30.11±0.81	31.85±0.81	32.25±0.8
8	3.16±0.33	2.81±0.54	2.44±0.65	34.26±0.83	36.26±0.82	36.72±0.83
10	3.43±0.35	3.03±0.68	2.62±0.74	38.42±0.86	40.66±0.84	41.18±0.85
12	3.7±0.35	3.26±0.77	2.8±0.79	42.58±0.88	45.07±0.89	45.65±0.87
14	3.97±0.36	3.48±0.79	2.98±0.85	46.74±0.79	49.48±0.75	50.11±0.77
18	4.24±0.34	3.71±0.68	3.16±0.77	50.9±0.85	53.88±0.81	54.58±0.8
24	4.5±0.34	3.93±0.81	3.34±0.8	55.06±0.92	58.29±0.82	59.04±1.17
48	4.77±0.35	4.16±0.82	3.52±0.83	59.21±1.01	62.75±1.17	64.18±1.34
72	4.78±0.35	4.18±0.84	3.53±0.85	59.32±1.44	62.79±1.44	64.19±1.52

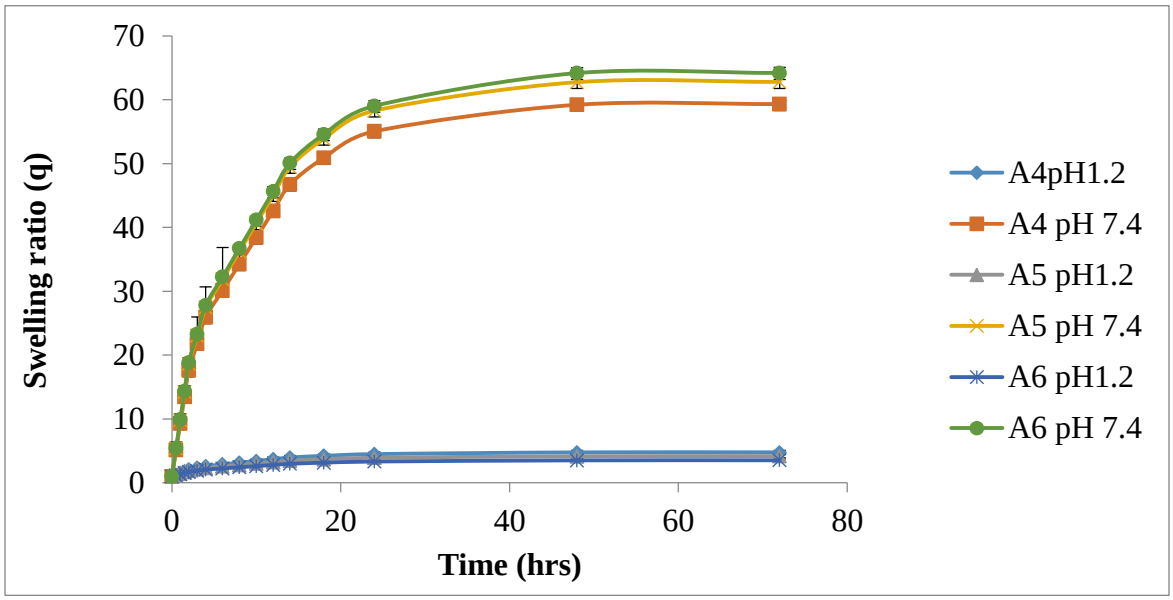

Figure 4.1.2: Comparative swelling of CMAX-g-AA hydrogels using different concentrations of CMAX

Table 4.1.3: Comparative swelling ratios of CMAX-g-AA (A) hydrogels using different concentrations of crosslinker (n=3)

Time (Hrs)	**Swelling ratio (q) at pH 1.2**			**Swelling ratio (q) at pH 7.4**		
	A7	A8	A9	A7	A8	A9
0	1±0	1±0	1±0	1±0	1±0	1±0
0.5	1.21±0.23	1.18±0.19	1.15±0.22	4.38±0.24	4.05±0.21	3.19±0.2
1	1.42±0.22	1.35±0.22	1.3±0.24	7.77±0.33	7.09±0.31	5.38±0.22
1.5	1.63±0.32	1.53±0.32	1.46±0.32	11.15±0.34	10.13±0.62	7.56±0.31
2	1.84±0.43	1.7±0.33	1.61±0.33	14.53±0.68	13.18±0.73	9.75±0.62
3	2.05±0.32	1.88±0.35	1.76±0.35	17.92±0.77	16.22±0.77	11.94±0.73
4	2.26±0.22	2.05±0.35	1.91±0.35	21.3±0.79	19.27±0.75	14.13±0.77
6	2.47±0.32	2.23±0.36	2.06±0.68	24.68±0.81	22.31±0.81	16.31±0.75
8	2.68±0.33	2.4±0.54	2.22±0.77	28.07±0.83	25.36±0.82	18.5±0.81
10	2.89±0.35	2.58±0.85	2.37±0.74	31.45±0.86	28.4±0.84	20.69±0.82
12	3.1±0.35	2.75±0.77	2.52±0.79	34.83±0.88	31.45±0.89	22.88±0.84
14	3.31±0.36	2.93±0.8	2.67±0.85	38.22±0.79	34.49±0.75	25.06±0.77
18	3.52±0.34	3.11±0.83	2.82±0.77	41.6±0.85	37.54±0.8	27.25±0.83
24	3.73±0.34	3.28±0.81	2.97±0.8	44.98±0.92	40.58±1.17	29.44±1.19
48	3.94±0.35	3.46±0.82	3.13±0.83	48.37±1.01	43.62±1.34	31.63±1.44
72	3.97±0.35	3.46±0.84	3.14±0.85	48.37±1.44	43.63±1.52	31.63±1.48

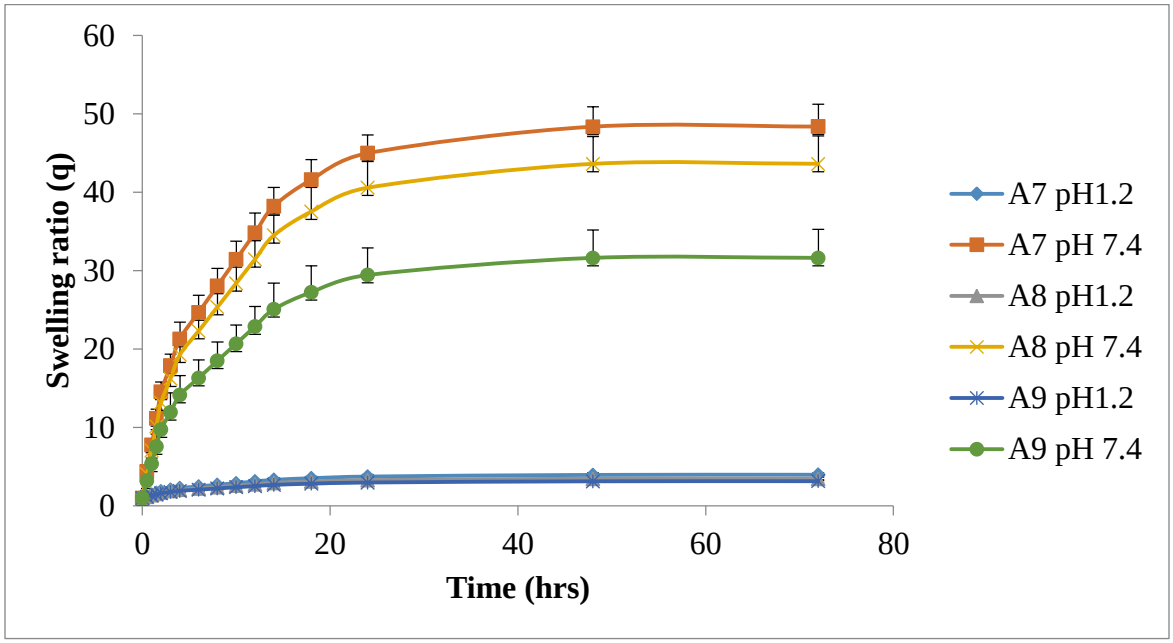

Figure 4.1.3: Comparative swelling of CMAX-g-AA hydrogels using different concentrations of crosslinker

4.1.2 Pulsatile behavior of hydrogel

Since the hydrogels swelling analysis illustrate diverse swelling pattern at acidic and basic pH, so we investigated their pH-reversibility in pH 1.2 and pH 7.4 buffer solution (Figure 4.1.4). A stepwise reproducible swelling variation of the hydrogel at 37ºC with alternating acidic and basic pH was observed. At pH 7.4, the hydrogel expanded up to 64.19 g (in 72 Hrs) due to revolting electrostatic forces, whereas, at pH 1.2, it shriveled in less than 25 minutes due to protonation of carboxylate groups of acrylic acid.

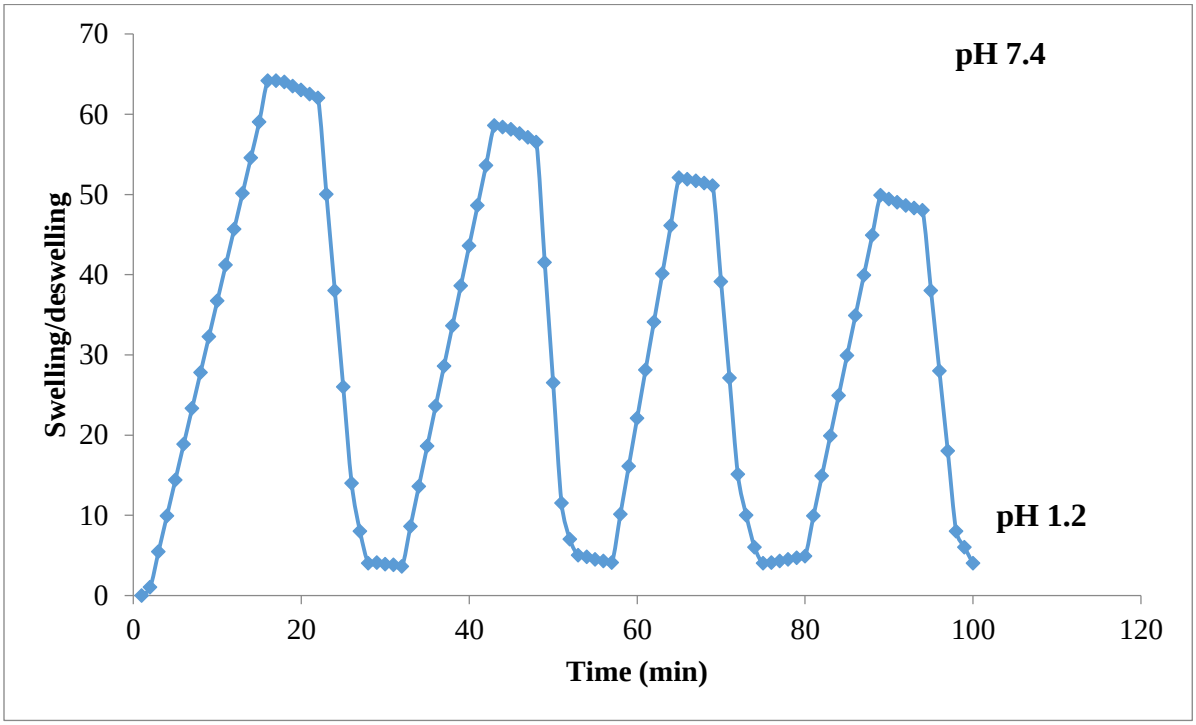

Figure 4.1.4:On-off switching behavior as reversible pulsatile swelling (pH 7.4) and de-swelling (pH 1.2) of CMAX-g-AA (A) hydrogel

4.1.3 Equilibrium water contents (EWC) and gel fraction

To evaluate the water content, preweighed dry hydrogels were immersed in deionized water at 37ºC to achieve equilibrium swelling. Table 4.1.4 indicated the effect of varying composition of hydrogels on equilibrium water contents and gel fraction. Figure 4.1.5 showed the gelation content as a function of AA, CMAX and N, N MBA contents in the hydrogels.

Table 4.1.4: Equilibrium water contents and gel fraction of CMAX-g-AA (A) hydrogels using different concentrations of AA, CMAX and crosslinker

Formulation code	Contents w/w%	EWC	Gel fraction (%)	Amount of Rabeprazole sodium loaded (mg per 0.4 g of dry disc)	
				By extraction	By weight
A1	AA 10	0.96	68.15	99	100
A 2	AA 15	0.97	81.01	114	114.8
A 3	AA 20	0.98	84.11	119	120
A 4	CMAX 1	0.97	77.67	113	113.8
A 5	CMAX 1.5	0.97	83.07	123	123.6
A 6	CMAX 2	0.98	83.22	128	128.9
A 7	MBA 0.4	0.93	86.84	102	102
A 8	MBA 0.6	0.91	90.02	91	91.7
A 9	MBA 0.8	0.85	96.40	83	83.3

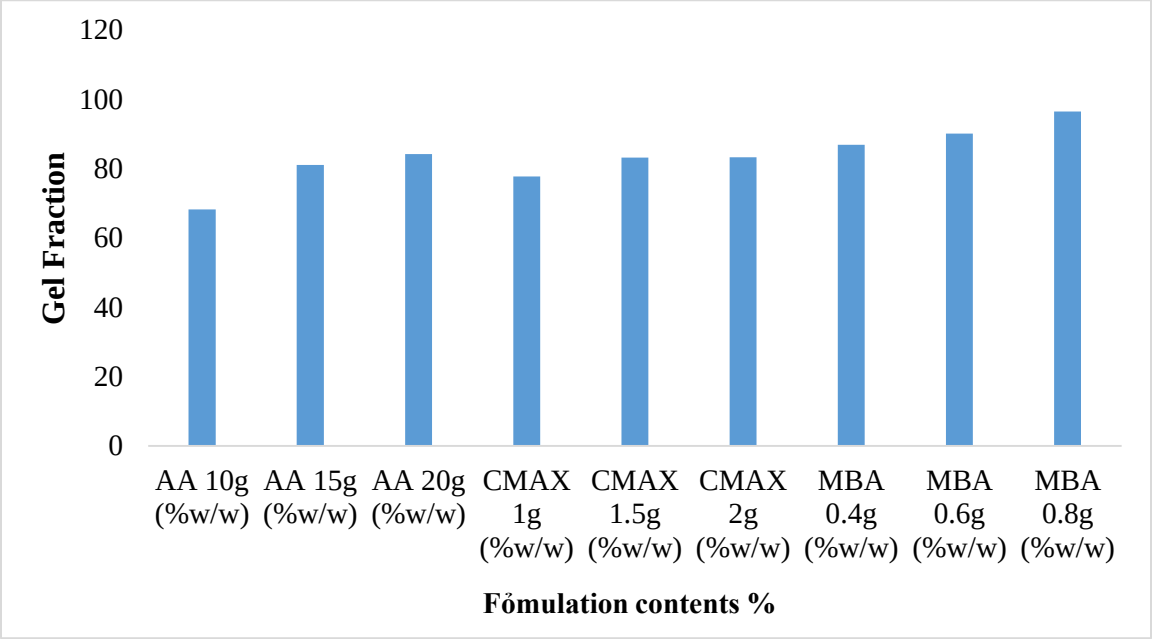

Figure 4.1.5: Gel fraction of CMAX-g-AA (A) hydrogel with different concentrations of AA, CMAX and crosslinker

4.1.4 Instrumental analysis

a) Scanning electron microscopy

To evaluate the surface morphology of CMAX-g-AA hydrogels scanning electron microscopy was employed. Figure 4.1.6 depicted the surface morphology and inner porous structure of lyophilized hydrogels at magnification of 100 X and 200 X and 10 µ, 30 µ, 300 µ, and 500 µ scale bar respectively**.**

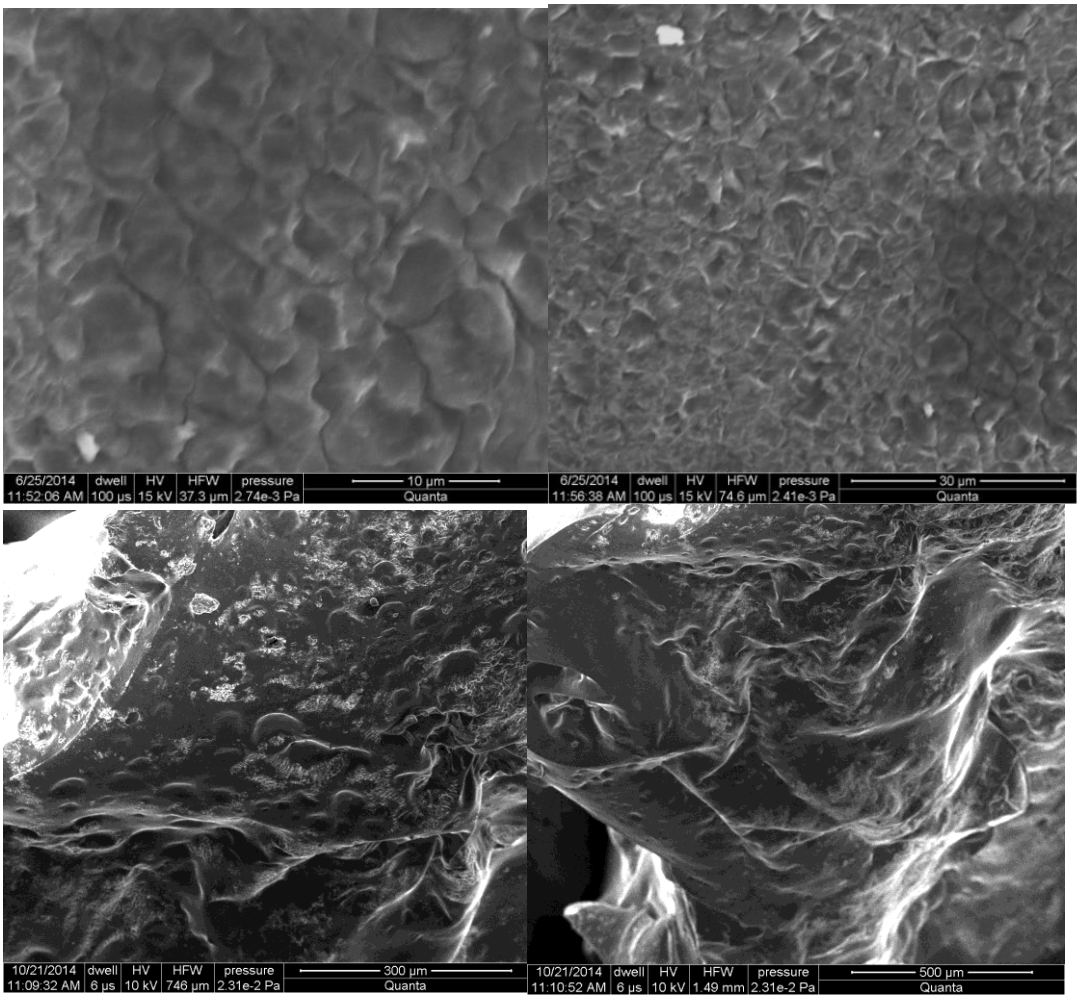

Figure 4.1.6: SEM images of lyophilized hydrogels (CMAX-g-AA) at magnification of 100 X and 200 X and 10µ, 30µ, 300µ, and 500µ scale bar respectively

b) FTIR spectral analysis

FTIR spectra of polymerized hydrogel and individual components were recorded on a Fourier transform infrared (FTIR) spectrophotometer (Bruker, Tensor-27, Germany) using a single reflectance ATR cell. Figure 4.1.7 represented FTIR spectra of CMAX (polymer), acrylic acid (monomer), and CMAX-g-AA (A) (prepared hydrogel). All data were recorded at room temperature, in the spectral range of 600–4000cm^{-1}.

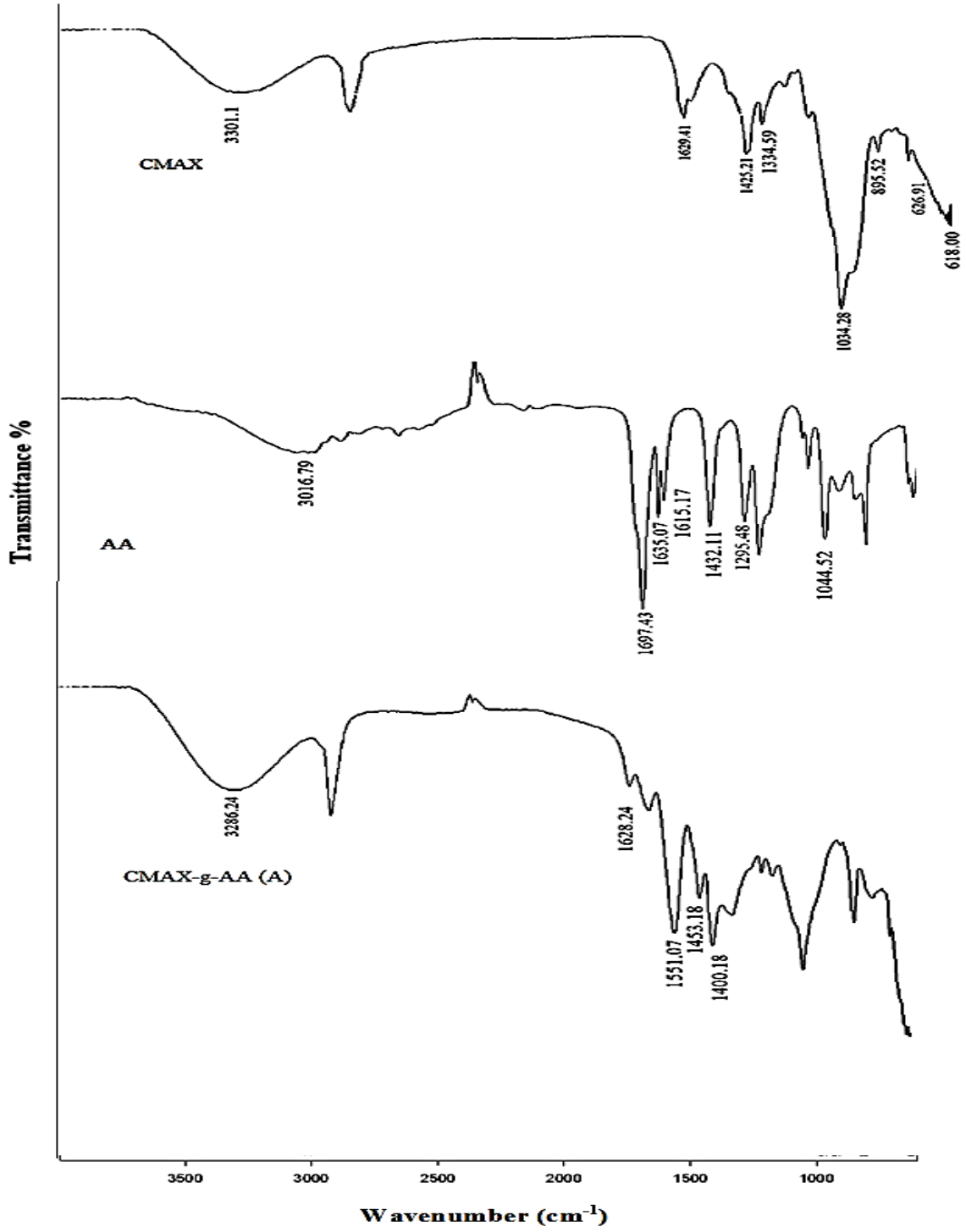

Figure 4.1.7: FTIR spectra of AA, CMAX, and CMAX-g-AA (A)

c) Thermal analysis

The thermal properties of CMAX-g-AA copolymers were studied by means of TGA and DSC analyses. The thermogravimetric analysis was conducted in air from 20–1000°C.

DTG data summarized in Table 4.1.5 representing Tdi (initial thermal degradation temperature), Tdm (medium degradation temperature), Tdf (final decomposition temperature) and percent weight loss at Tdf of polymer, monomer and prepared hydrogel. Figure 4.1.8 show TGA curve representing percent weight loss with temperature elevation of individual constituents (CMAX and AA) and prepared hydrogel. DSC curve displayed in Figure 4.1.9.

Table 4.1.5: DTG data of acrylic acid (AA), CMAX and CMAX-g-AA (A)

Sample	Step	Tdi (°C)	Tdm (°C)	Tdf (°C)	Weight loss % at Tdf
A	1	443	461	515	21.51
	II	610	614	616	1.17
AA	I	83	93	100	54.24
	II	101	112	122	22.22
CMAX	I	266	332	382	44.8
	II	431	503	562	25

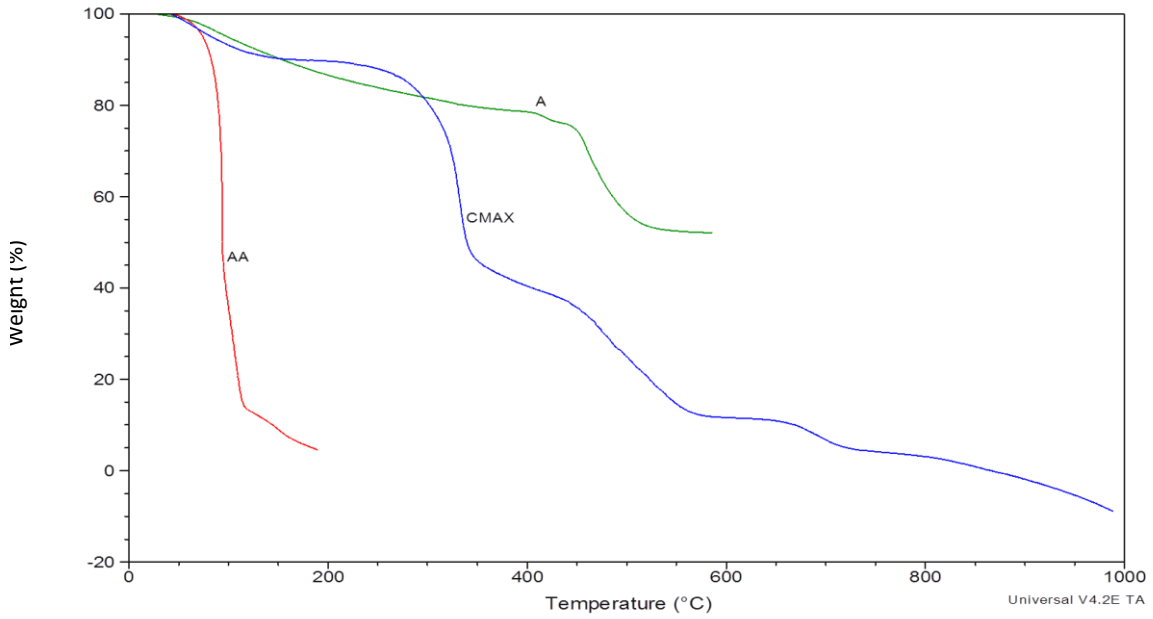

Figure 4.1.8: TGA curves of acrylic acid (AA), CMAX and CMAX-g-AA (A)

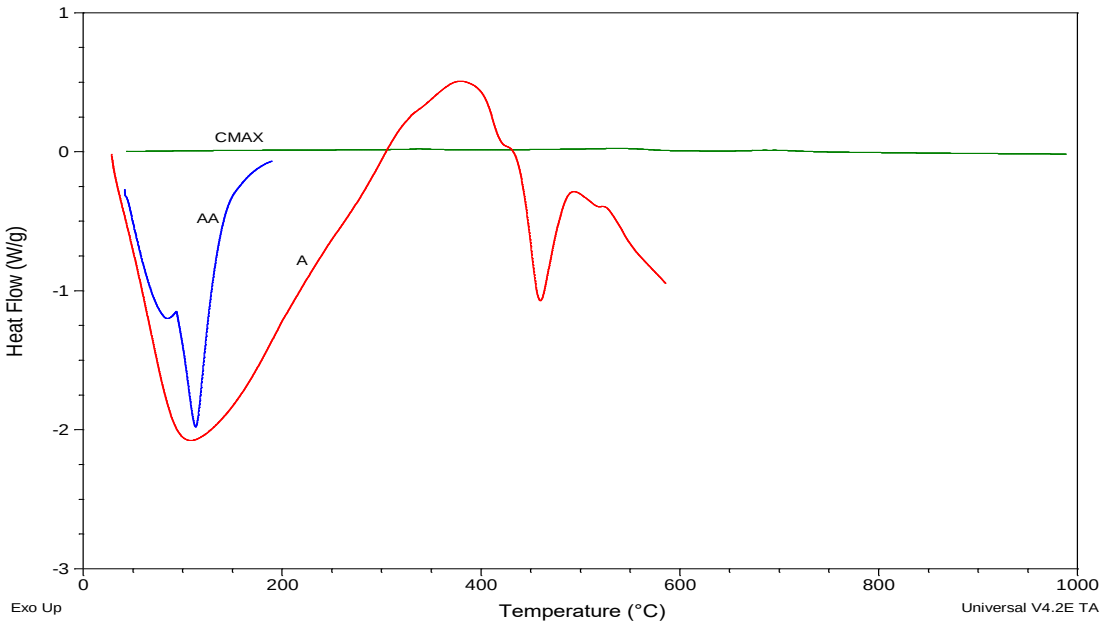

Figure 4.1.9: DSC curve of acrylic acid (AA), CMAX and CMAX-g-AA (A)

d) X-ray Diffraction

For X-ray diffraction samples was scanned over range5-50° 2θ at a rate of 1º 2θ/min. XRD spectrum of unloaded, drug loaded and pure drug are presented in Figure 4.1.10.X-ray diffraction spectra of hydrogel produced no peaks.

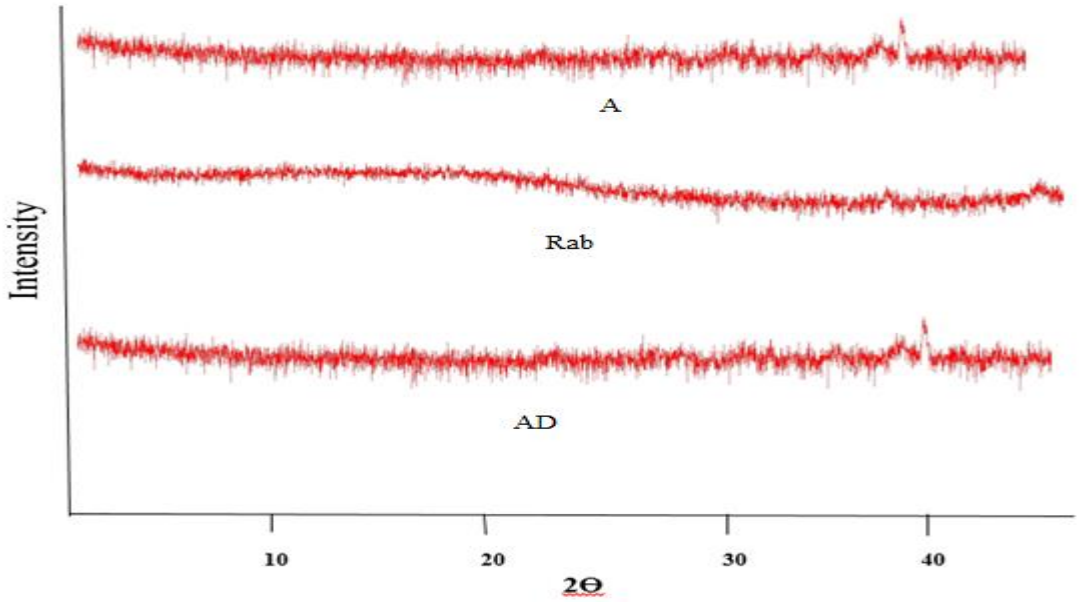

Figure 4.1.10: X-ray diffraction patterns of CMAX-g-AA hydrogel.

4.1.5:In vitro release kinetics of Rabeprazole sodium from CMAX-g-AA hydrogel

To evaluate the pH sensitive release of rabeprazole sodium from CMAX-g-AA hydrogel, *in vitro* release studies were conducted in0.1N HCl (pH 1.2) and Tris buffer(pH 8) (recommended by US FDA for rabeprazole sodium dissolution study) at 37ºC. Figure 4.1.11 exhibited effect of concentration of acrylic acid on percent cumulative percent drug release. Effect of different concentrations of CMAX on percent cumulative release of rabeprazole sodium was summarized in Table 4.1.7 and graphically presented in Figure 4.1.12. Crosslinking density may also alter release percent and pattern of drug from hydrogels. Table 4.1.8 illustrated effect of crosslinker (N, N MBA) concentration on cumulative percent drug release. To determine the release mechanism, *in vitro* release data was fitted in various mathematical models and results were presented in Table 4.1.9. Log plot of the cumulative percent drug release versus the time provides the value of n, which determined the nature of the dissolution medium diffusion process.

Table 4.1.6: Effect of acrylic acid concentration on cumulative percent drug release of Rabeprazole sodium

Time (hr)	A1 pH 1.2	A2 pH 1.2	A3 pH 1.2	A1 pH 8	A2 pH 8	A3 pH 8
0.5	1.49±0.21	1.08±0.22	0.49±0.23	6.29±1.21	8.85±1.112	9.68±1.23
1	2.52±0.32	1.71±0.23	0.82±0.21	8.55±1.48	10.19±1.78	13.49±1.45
1.5	3.44±0.33	2.32±0.34	1.15±0.29	11.95±2.13	11.82±2.08	16.83±1.54
2	4.36±0.67	2.94±0.45	1.47±0.43	13.28±2.11	13.77±2.23	18.51±1.78
3	5.26±0.77	3.54±0.54	1.78±0.32	16.86±2.46	16.36±2.48	20.64±1.99
4	6.16±0.79	4.14±0.78	2.1±0.22	20.75±2.46	19.31±2.50	24.24±2.11
6	7.04±0.79	4.73±0.87	2.41±0.32	27.53±2.18	22.56±2.38	32.05±2.33
8	7.92±0.57	5.32±0.90	2.72±0.43	35.6±2.56	29.75±2.56	38.92±2.77
12	8.79±0.35	5.9±0.56	3.02±0.45	46.53±3.23	42.89±3.33	53.51±3.00
16	9.64±0.87	6.47±0.33	3.32±0.45	60.06±3.24	57.96±3.34	65.9±2.99
20	10.54±0.83	7.08±0.35	3.62±0.56	70.31±3.36	71.39±3.46	79.47±3.99
24	11.52±0.65	7.64±0.65	3.91±0.34	79.77±3.43	85.51±3.54	93.18±4.11

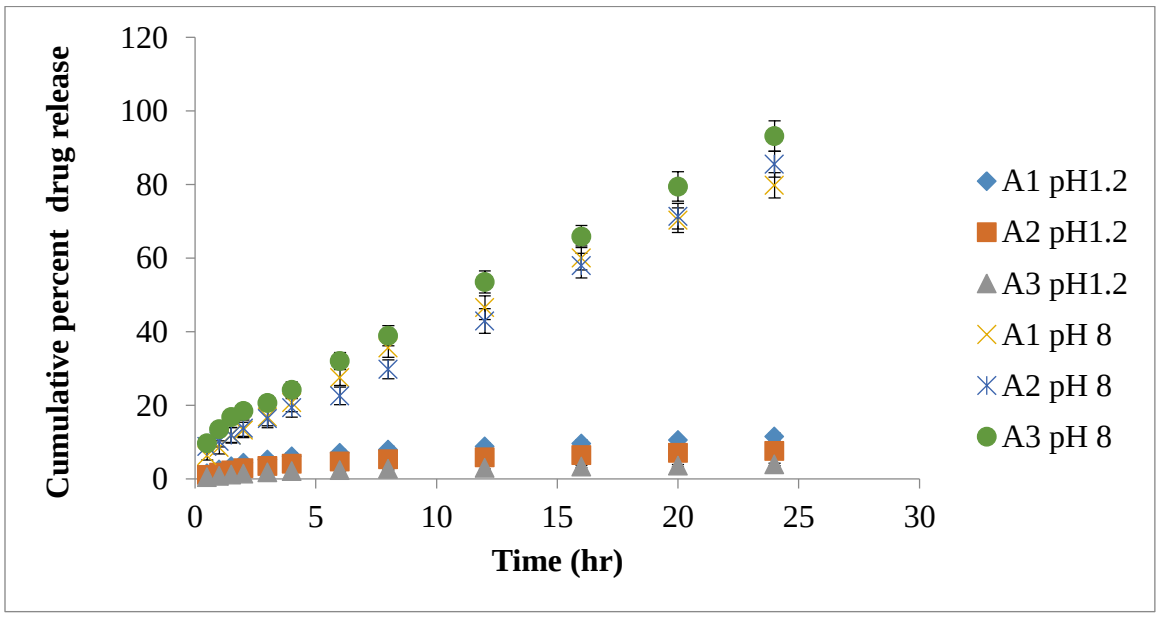

Figure 4.1.11: Effect of acrylic acid concentration on cumulative percent drug release of Rabeprazole sodium from hydrogel formulations (A1-A3)

Table 4.1.7: Effect of CMAX concentration on cumulative percent drug release of Rabeprazole sodium

Time (hr)	A4 pH 1.2	A5 pH 1.2	A6 pH 1.2	A4 pH 8	A5 pH 8	A6 pH 8
0.5	1.62±0.11	1.04±0.21	1±0.24	7.59±1.22	12.47±1.18	16.12±1.26
1	2.15±0.32	1.51±0.23	1.57±0.21	11.78±1.78	16.32±1.48	19.29±1.30
1.5	2.68±0.33	2.02±0.34	2.17±0.29	16.46±2.08	20.95±2.13	23.72±1.78
2	3.2±0.67	2.48±0.45	2.73±0.43	18.24±1.23	23.03±2.23	25.32±2.08
3	3.72±0.77	2.9±0.54	3.24±0.77	20.5±3.33	25.19±2.48	27.75±3.24
4	4.22±0.79	3.28±0.78	3.71±0.79	24.3±3.34	30.2±2.50	30.91±3.36
6	4.73±0.79	3.69±0.87	4.22±0.79	32.52±3.46	36.57±2.38	37.97±3.43
8	5.23±0.57	4.1±0.90	4.72±0.43	39.35±2.56	41.65±2.56	45.98±2.77
12	5.72±0.45	4.5±0.65	5.21±0.45	54.01±3.23	55.46±3.33	58.22±3.00
16	6.21±0.45	4.89±0.33	5.7±0.45	68.6±3.24	68.45±3.34	72.02±2.23
20	6.74±0.56	5.33±0.35	6.21±0.56	82.49±3.36	81.19±3.46	84.24±2.48
24	7.22±0.45	5.75±0.65	6.73±0.34	92.83±3.43	96.76±3.54	98.44±2.50

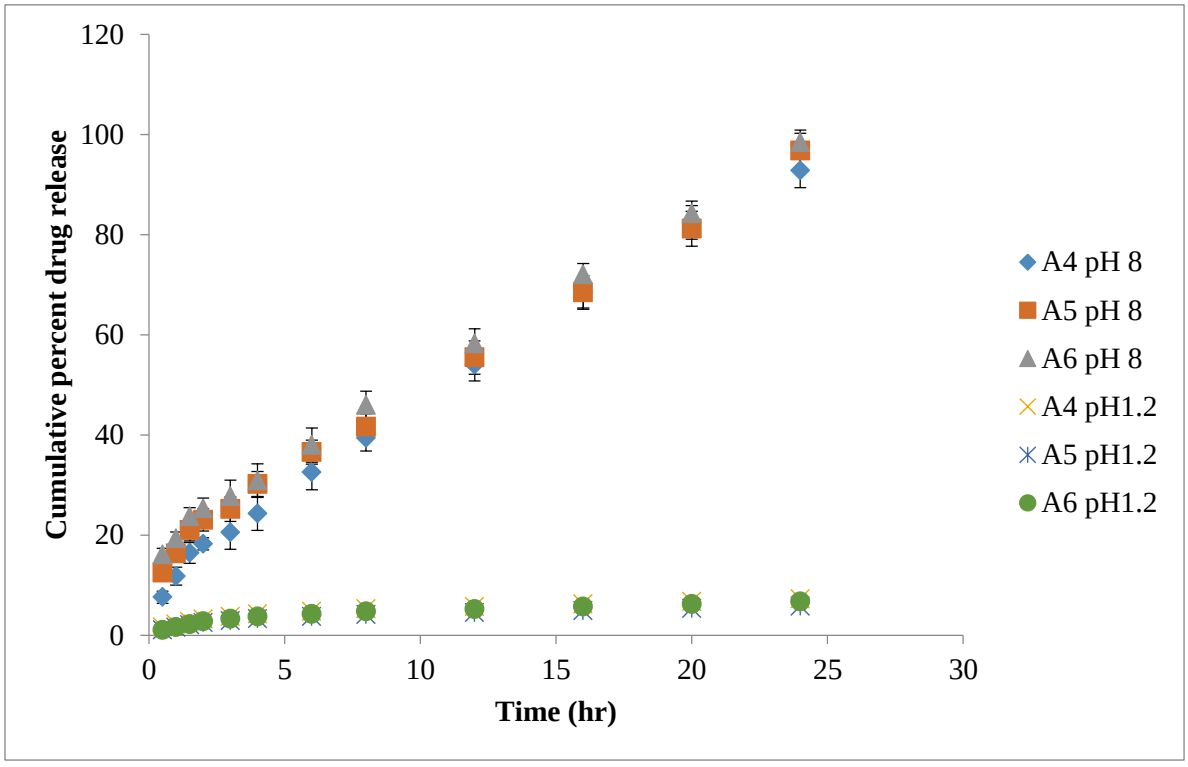

Figure 4.1.12: Effect of CMAX concentration on cumulative percent drug release of Rabeprazole sodium from hydrogel formulations (A4-A6)

Table 4.1.8: Effect of MBA concentration on cumulative percent drug release of Rabeprazole sodium

Time (hr)	A7 pH1.2	A8 pH1.2	A9 pH1.2	A7 pH 8	A8 pH 8	A9 pH 8
0.5	0.62±0.11	0.86±0.20	0.59±0.27	6.49±1.24	5.06±1.17	3.54±1.23
1	1.2±0.21	1.29±0.23	0.94±0.24	10.46±2.11	8.98±1.44	5.66±1.28
1.5	1.81±0.23	1.87±0.34	1.35±0.29	14.61±2.23	12.04±2.13	7.86±1.75
2	2.38±0.34	2.4±0.79	1.69±0.43	16.69±2.48	14.39±2.23	10.45±3.33
3	2.88±0.29	2.86±0.57	1.98±0.77	19.82±3.33	16.86±2.48	12.61±3.34
4	3.34±0.43	3.27±0.45	2.2±0.79	22.64±3.34	20.04±2.50	15.55±3.46
6	3.84±0.79	3.73±0.45	2.47±0.79	29.86±3.46	25.55±2.38	20.62±2.56
8	4.33±0.57	4.18±0.90	2.75±0.43	34.98±2.56	31.48±2.56	25.3±3.24
12	4.82±0.45	4.62±0.56	3.02±0.45	48.03±3.23	40.81±3.33	34.43±3.36
16	5.3±0.56	5.07±0.33	3.29±0.21	59.13±3.24	50.73±3.34	43.66±3.43
20	5.83±0.45	5.55±0.35	3.61±0.23	70.21±3.36	61.16±3.46	52.91±2.48
24	6.34±0.45	6.04±0.64	3.93±0.34	82.34±3.42	74.85±3.57	63.51±3.90

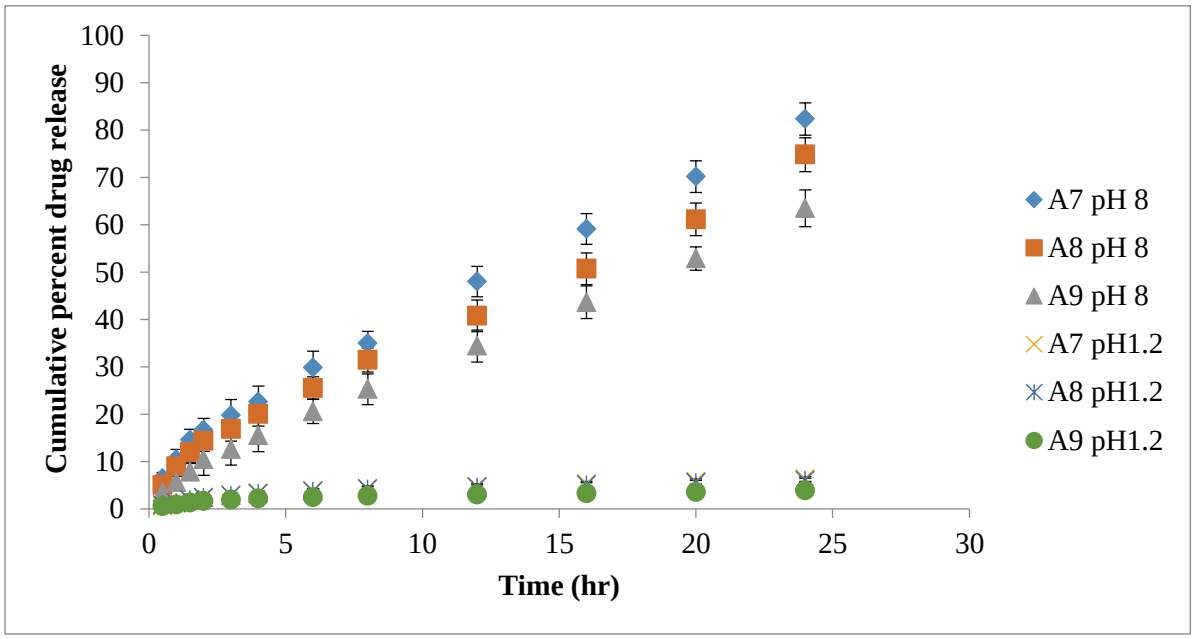

Figure 4.1.13: Effect of crosslinker concentration on cumulative percent drug release of Rabeprazole sodium from hydrogel formulations (A7-A9)

Table 4.1.9: Kinetic parameters of Rabeprazole sodium release from CMAX-g-AA hydrogel

Formulation code	***Higuchi***	***First order***	***Zero order***	***Korsmayer-peppas***	
	R^2	R^2	R^2	R^2	***n***
A1	0.971	0.557	0.998	0.997	0.855
A2	0.941	0.639	0.996	0.982	0.961
A3	0.983	0.617	0.994	0.999	0.699
A4	0.977	0.570	0.995	0.998	0.737
A5	0.972	0.492	0.996	0.989	0.863
A6	0.972	0.463	0.997	0.991	0.778
A7	0.981	0.567	0.994	0.995	0.821
A8	0.975	0.594	0.994	0.994	0.972
A9	0.976	0.670	0.996	0.997	0.931

4.2 Characterization of CMAX-g-MAA hydrogels

4.2.1 Swelling studies at pH1.2 and pH 7.4

To evaluate the pH sensitivity, swelling of prepared hydrogels was carried out in acidic (1.2) and basic (7.4) pH buffer solution. Formulations were assigned codes (M1-M3), (M4-M6) and (M7-M9) for varying concentration of methacrylic acid, CMAX and crosslinker respectively. Effect of varying concentration of methacrylic acid on swelling ratio (q), M1 (1 to 5.032), M2 (1 to 4.095) and M3 (1 to 3.140) in pH 1.2 and M1 (1 to 20.855), M2 (1 to 16.693) and M3 (1 to 14.285) in 7.4 buffer solutions at 37 ºC has been given in Table 4.2.1 and graphically presented in Figure 4.2.1. Comparative swelling ratio (q) of hydrogels by using different concentrations of CMAX, M4 (1 to 4.658), M5 (1 to 3.462) and M6 (1 to 2.770) at pH 1.2 and M4 (1 to 18.808), M5 (1 to 22.122) and M6 (1 to 24.638) at pH 7.4 were given in Table 4.2.2. Table 4.2.3 showed effect of crosslinker contents on swelling ratio of hydrogels M7 (1 to 4.005), M8 (1 to 3.342) and M9 (1 to 2.696) at pH 1.2 and M7 (1 to 15.371), M8 (1 to 12.131) and M9 (1 to 8.972) at pH 7.4.

Table4.2.1: Comparative swelling ratios of CMAX-g-MAA hydrogels using different concentrations of MAA (n=3)

Time (Hrs)	**Swelling ratio (q) at pH 1.2**			**Swelling ratio (q) at pH 7.4**		
	M1	M2	M3	M1	M2	M3
0	1	1	1	1	1	1
0.5	1.29±0.23	1.22±0.19	1.15±0.22	2.42±0.24	2.11±0.21	1.94±0.2
1	1.57±0.22	1.44±0.22	1.3±0.24	3.84±0.33	3.21±0.31	2.88±0.22
1.5	1.86±0.32	1.66±0.32	1.46±0.32	5.25±0.34	4.32±0.62	3.83±0.31
2	2.14±0.43	1.88±0.22	1.61±0.33	6.67±0.68	5.43±0.73	4.77±0.62
3	2.43±0.32	2.1±0.32	1.76±0.35	8.09±0.77	6.53±0.31	5.71±0.73
4	2.72±0.22	2.33±0.33	1.91±0.35	9.51±0.79	7.64±0.62	6.65±0.77
6	3±0.32	2.55±0.36	2.06±0.68	10.92±0.81	8.75±0.73	7.6±0.75
8	3.29±0.33	2.77±0.54	2.21±0.77	12.34±0.83	9.86±0.77	8.54±0.81
10	3.57±0.35	2.99±0.85	2.37±0.74	13.76±0.86	10.96±0.84	9.48±0.81
12	3.86±0.35	3.21±0.77	2.52±0.79	15.18±0.88	12.07±0.89	10.42±0.83
14	4.15±0.77	3.43±0.8	2.67±0.85	16.59±0.89	13.18±0.75	11.37±0.86
18	4.43±0.8	3.65±0.83	2.82±0.77	18.01±0.75	14.28±0.8	12.31±0.83
24	4.72±0.83	3.87±0.81	2.97±0.8	19.43±0.8	15.39±1.17	13.25±1.19
48	5.01±0.81	4.09±0.82	3.13±0.83	20.85±1.17	16.68±1.24	14.19±1.33
72	5.03±0.81	4.1±0.84	3.14±0.85	20.86±1.34	16.69±1.42	14.29±1.38

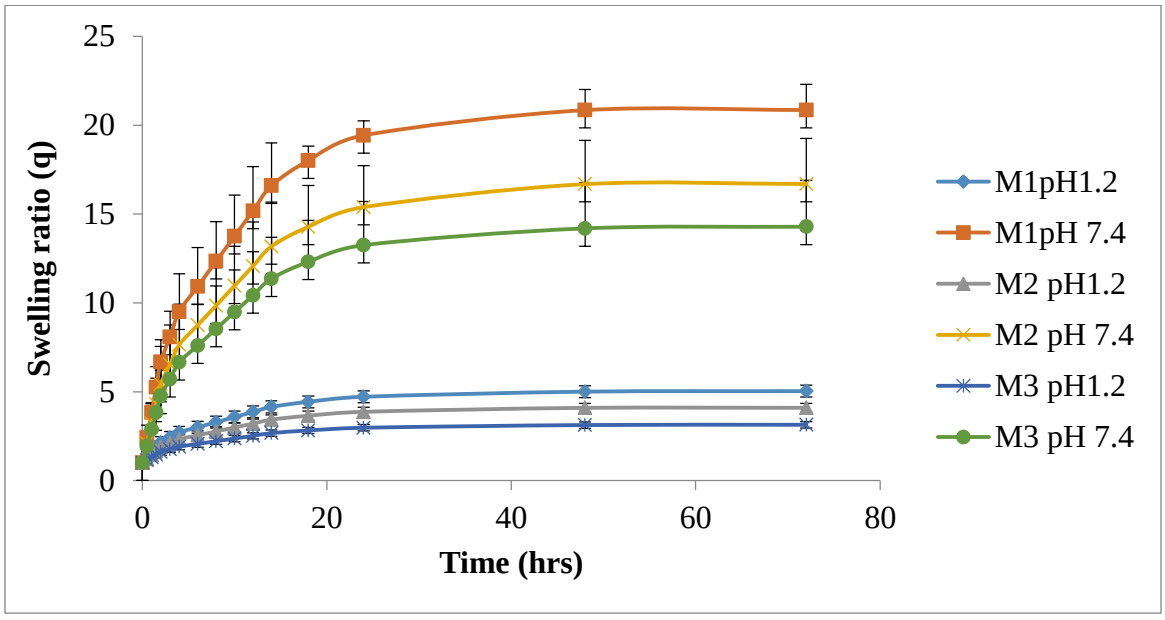

Figure 4.2.1: Comparative swelling ratios of CMAX-g-MAA hydrogels using different concentrations of MAA

Table 4.2.2: Comparative swelling ratios of CMAX-g-MAA (M) hydrogels using different concentrations of CMAX (n=3)

Time (Hrs)	**Swelling ratio (q) at pH 1.2**			**Swelling ratio (q) at pH 7.4**		
	M4	M5	M6	M4	M5	M6
0	1	1	1	1	1	1
0.5	1.26±0.23	1.18±0.19	1.13±0.22	2.27±0.24	2.51±0.21	2.69±0.2
1	1.52±0.22	1.35±0.22	1.25±0.24	3.54±0.33	4.02±0.31	4.37±0.22
1.5	1.78±0.32	1.53±0.32	1.38±0.32	4.81±0.34	5.52±0.62	6.06±0.31
2	2.04±0.43	1.7±0.33	1.5±0.33	6.08±0.68	7.03±0.73	7.75±0.62
3	2.3±0.32	1.88±0.35	1.63±0.35	7.35±0.77	8.54±0.77	9.43±0.73
4	2.56±0.22	2.05±0.35	1.75±0.35	8.62±0.79	10.05±0.75	11.12±0.77
6	2.83±0.32	2.23±0.36	1.88±0.68	9.89±0.81	11.56±0.73	12.81±0.75
8	3.09±0.33	2.4±0.54	2.01±0.77	11.16±0.83	13.06±0.77	14.49±0.81
10	3.35±0.35	2.58±0.85	2.13±0.77	12.43±0.86	14.57±0.75	16.18±0.82
12	3.61±0.35	2.75±0.77	2.26±0.68	13.7±0.88	16.08±0.89	17.87±0.84
14	3.87±0.36	2.93±0.68	2.38±0.65	14.97±0.79	17.59±0.75	19.55±0.77
18	4.13±0.34	3.1±0.77	2.51±0.77	16.24±0.85	19.09±0.8	21.24±0.89
24	4.39±0.34	3.28±0.74	2.64±0.8	17.51±0.92	20.6±1.17	22.93±0.75
48	4.65±0.35	3.46±0.79	2.76±0.73	18.78±1.01	22.11±1.34	24.61±0.8
72	4.66±0.35	3.46±0.75	2.77±0.75	18.81±1.44	22.12±1.32	24.64±1.18

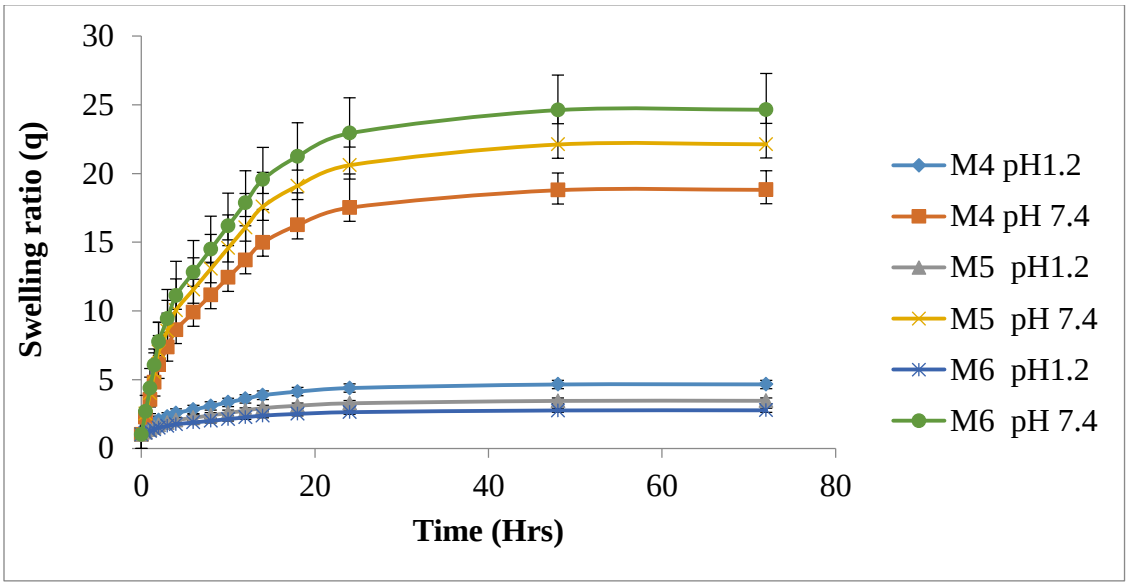

Figure 4.2.2: Comparative swelling ratios of CMAX-g-MAA hydrogels using different concentrations of CMAX

Table 4.2.3: Comparative swelling ratios of CMAX-g-MAA hydrogels using different concentrations of crosslinker

Time (Hrs)	**Swelling ratio (q) at pH 1.2**			**Swelling ratio (q) at pH 7.4**		
	M7	M8	M9	M7	M8	M9
0	1	1	1±0	1	1	1
0.5	1.2±0.19	1.17±0.23	1.04±0.22	2.03±0.21	1.79±0.22	1.57±0.21
1	1.4±0.22	1.33±0.29	1.16±0.24	3.05±0.24	2.59±0.23	2.14±0.24
1.5	1.6±0.32	1.49±0.31	1.29±0.19	4.07±0.33	3.38±0.34	2.72±0.33
2	1.8±0.27	1.66±0.3	1.41±0.22	5.1±0.34	4.18±0.42	3.29±0.45
3	2±0.3	1.82±0.28	1.54±0.32	6.12±0.38	4.97±0.46	3.86±0.21
4	2.19±0.31	1.99±0.32	1.66±0.33	7.15±0.42	5.77±0.53	4.43±0.76
6	2.39±0.33	2.15±0.31	1.79±0.35	8.17±0.46	6.56±0.45	5±0.73
8	2.59±0.32	2.32±0.32	1.92±0.35	9.2±0.53	7.36±0.21	5.57±0.53
10	2.79±0.31	2.48±0.35	2.04±0.36	10.22±0.63	8.15±0.76	6.15±0.63
12	2.99±0.32	2.65±0.36	2.17±0.34	11.25±0.74	8.95±0.73	6.72±0.74
14	3.19±0.35	2.81±0.36	2.29±0.34	12.27±0.75	9.74±0.74	7.29±0.75
18	3.39±0.36	2.98±0.34	2.42±0.33	13.3±0.81	10.54±0.75	7.86±0.81
24	3.59±0.34	3.14±0.34	2.54±0.33	14.32±0.82	11.33±0.81	8.43±0.82
48	3.79±0.34	3.31±0.35	2.67±0.34	15.34±0.84	12.13±0.82	9±0.84
72	4.01±0.35	3.34±0.35	2.7±0.34	15.37±0.89	12.13±0.88	8.97±0.89

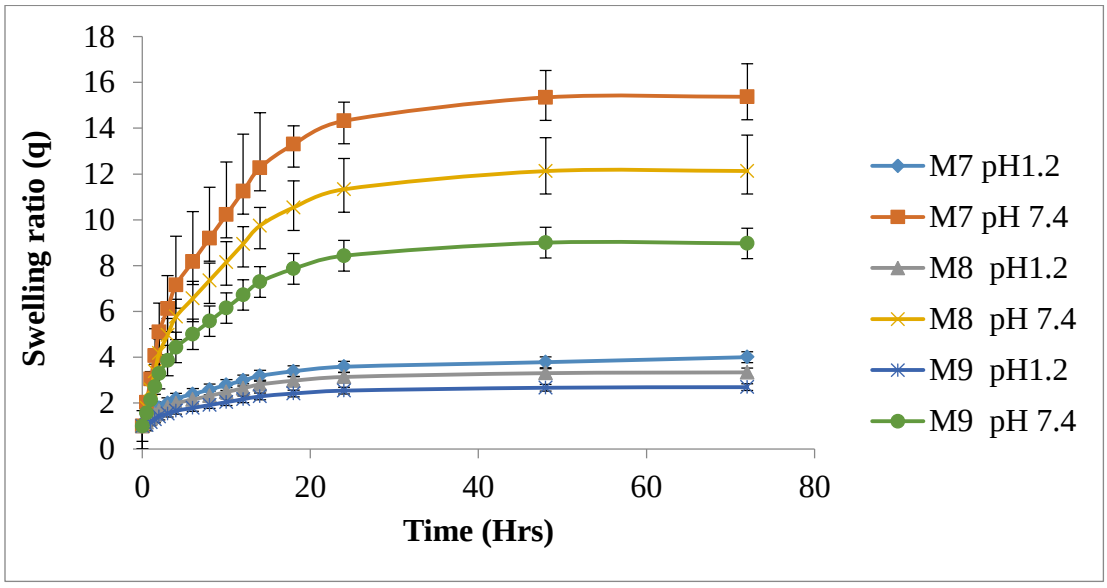

Figure 4.2.3: Comparative swelling ratios of CMAX-g-MAA hydrogels using different concentrations of MBA (crosslinker)

4.2.2: Pulsatile behavior of hydrogel

Effect of copolymer composition on the swelling behavior was examined in (pH 1.2) and(pH 7.4) buffer solutions. Mechanism of water transport through the gel was significantly affected by pH modulation. Reversible pH responsive swelling behavior is key element for controlled delivery of drug through hydrogels. So, to evaluate the reversible swelling behavior, hydrogels samples (M6)swelled in buffer solution of pH 7.4, until equilibrium swelling was attained (almost 72 Hrs). Afterwards swollen hydrogels were placed in a buffer solution of pH 1.2 the hydrogels collapsed within few minute (less than 25 mins).Again they were returned to a buffer solution of pH 7.4, and finally collapsed in a buffer solution of pH 1.2. Figure 4.2.4 showed that swollen networks relapsed to comparatively shrunken networks whenever the pH decreased.

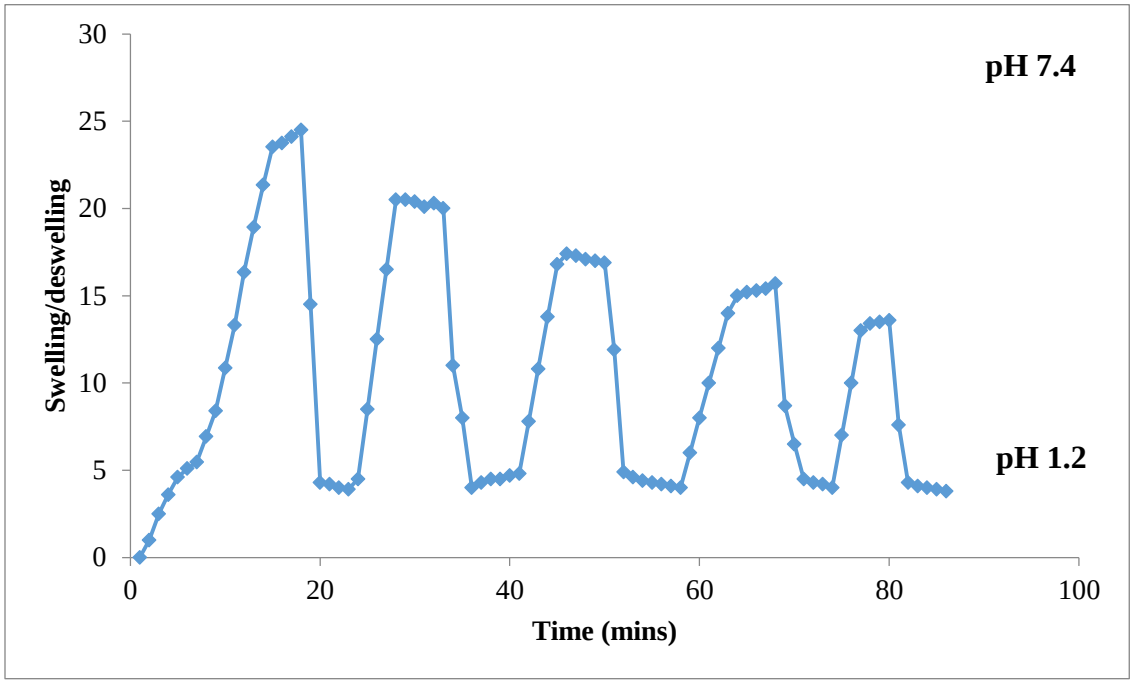

Figure 4.2.4: On-off switching behavior as reversible pulsatile swelling (pH 7.4) and deswelling (pH 1.2) of CMAX-g-MAA hydrogel

4.2.3: Equilibrium water contents and gel fraction of CMAX-g-MAA hydrogels

Uses of hydrogels are centered on their water absorption property, the water content of a hydrogel was one of utmost fundamentals, affecting its worth and functionality.

Equilibrium water content was evaluated by immersing hydrogels in deionized water and results were presented in Table 4.2.4, exhibiting water absorption modulation by varying composition of hydrogels. Gel fraction was also affected by hydrogel composition as shown in Figure 4.2.5.

Table 4.2.4: Equilibrium water contents, gel fraction and drug loaded of CMAX -g-MAA hydrogels using different concentrations of MAA, CMAX and crosslinker

Formulation code	**Contents w/w%**	**EWC**	**Gel fraction (%)**	**Amount of Rabeprazole sodium loaded** (mg per 0.4 g of dry disc)	
				By extraction	By weight
M1	MAA 20	0.95	59.67	89	90
M2	MAA 30	0.93	88.45	87	87.9
M3	MAA 35	0.91	90.32	83	83.7
M4	CMAX 1	0.95	87.17	90	91.3
M5	CMAX 1.5	0.95	74.83	94	95
M6	CMAX 2	0.95	90.35	97	98.4
M7	MBA 0.45	0.92	86.84	81	81.8
M8	MBA 0.65	0.85	91.83	77	78
M9	MBA 0.85	0.81	95.64	71	71.9

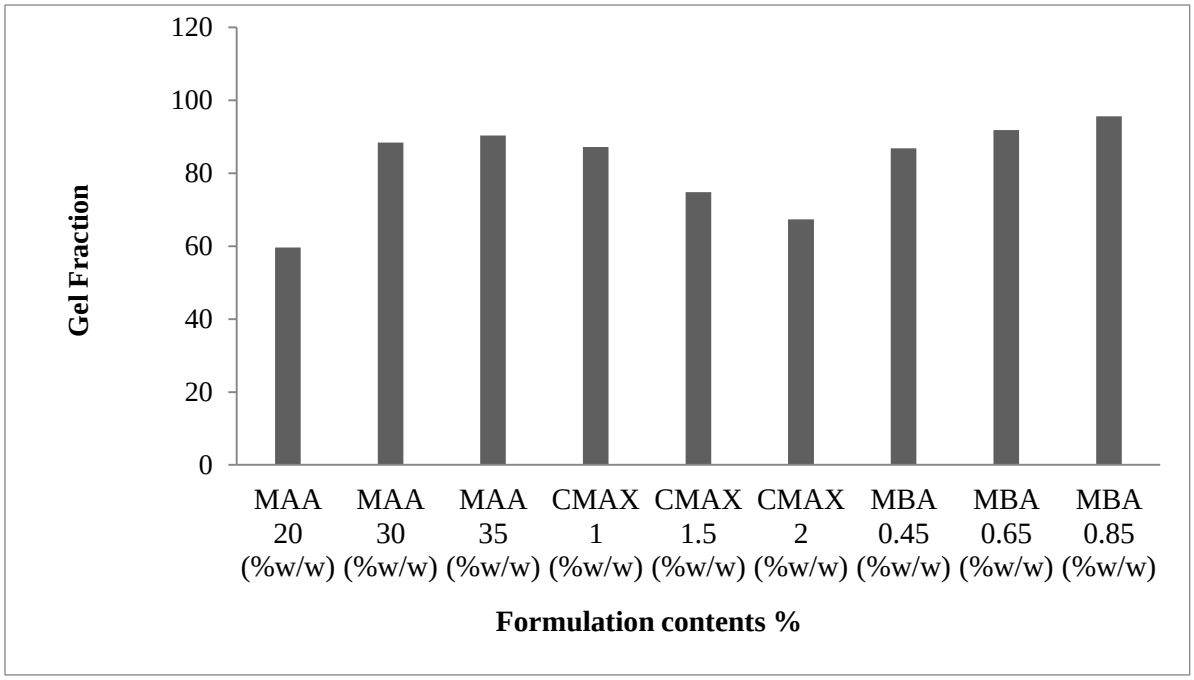

Figure 4.2.5: Gel fraction of CMAX-co-MAA hydrogel with different concentrations of MAA, CMAX and crosslinker

4.2.4: *Instrumental analysis*

a) Scanning electron microscopy

Surface morphology of hydrogel was examined by scanning electron microscopy of lyophilized hydrogels to evaluate the porous structure. SEM images were summarized in Figure 4.2.6.

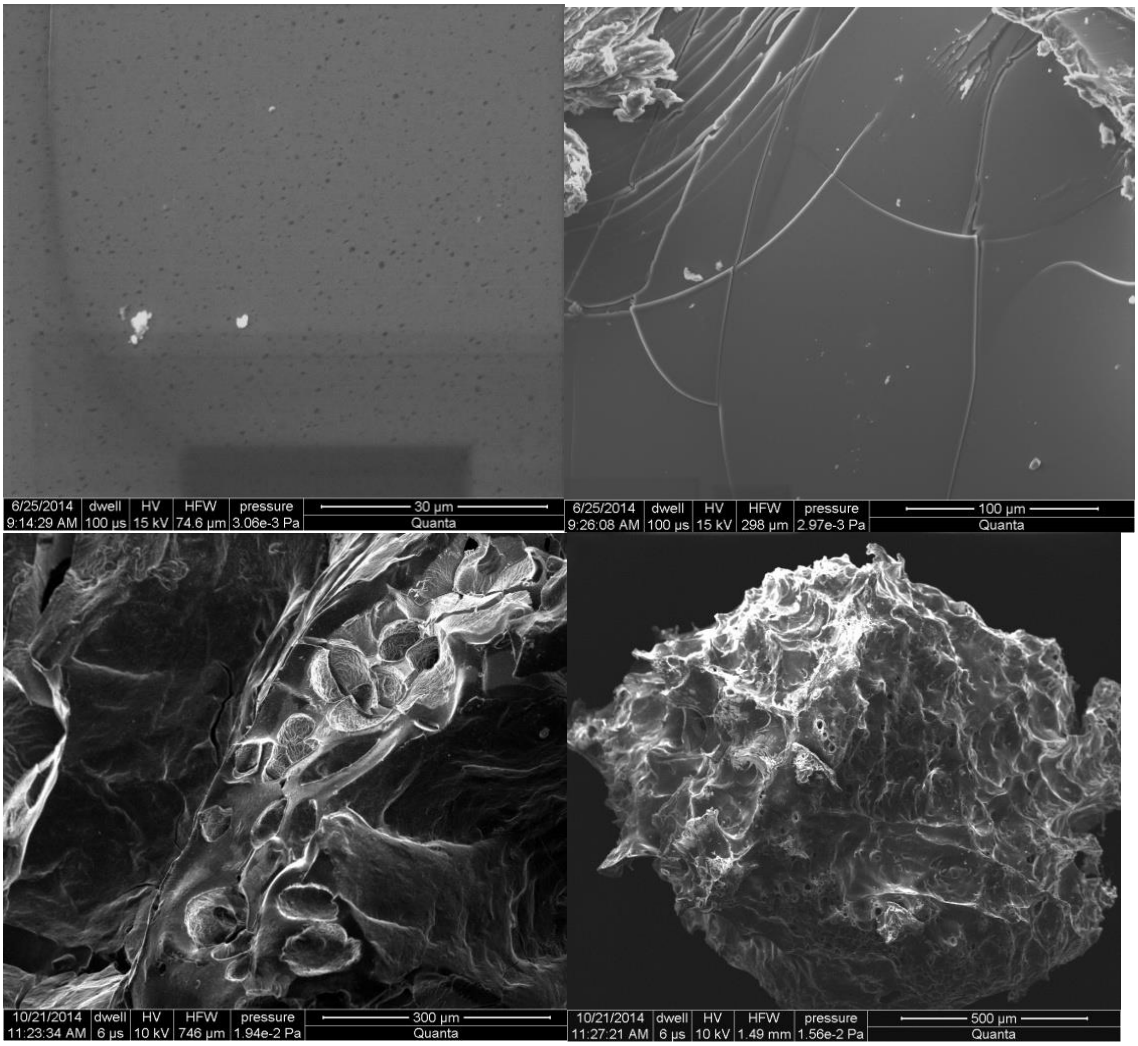

Figure 4.2.6: SEM images of lyophilized hydrogels (CMAX-g-MAA) at magnification of 100 X and 200 X and 30µ, 100µ, 300µ, and 500µ scale bar respectively

b) FTIR spectrum analysis

Fourier transform infrared spectroscopy (FTIR) was used to characterize the presence of specific chemical groups added in the copolymeric matrix. Figure 4.2.7 showed FTIR

spectra of polymer (CMAX), monomer (methacrylic acid) and prepared hydrogel formulation (M). All spectra were recorded in 4000-600cm^{-1} range.

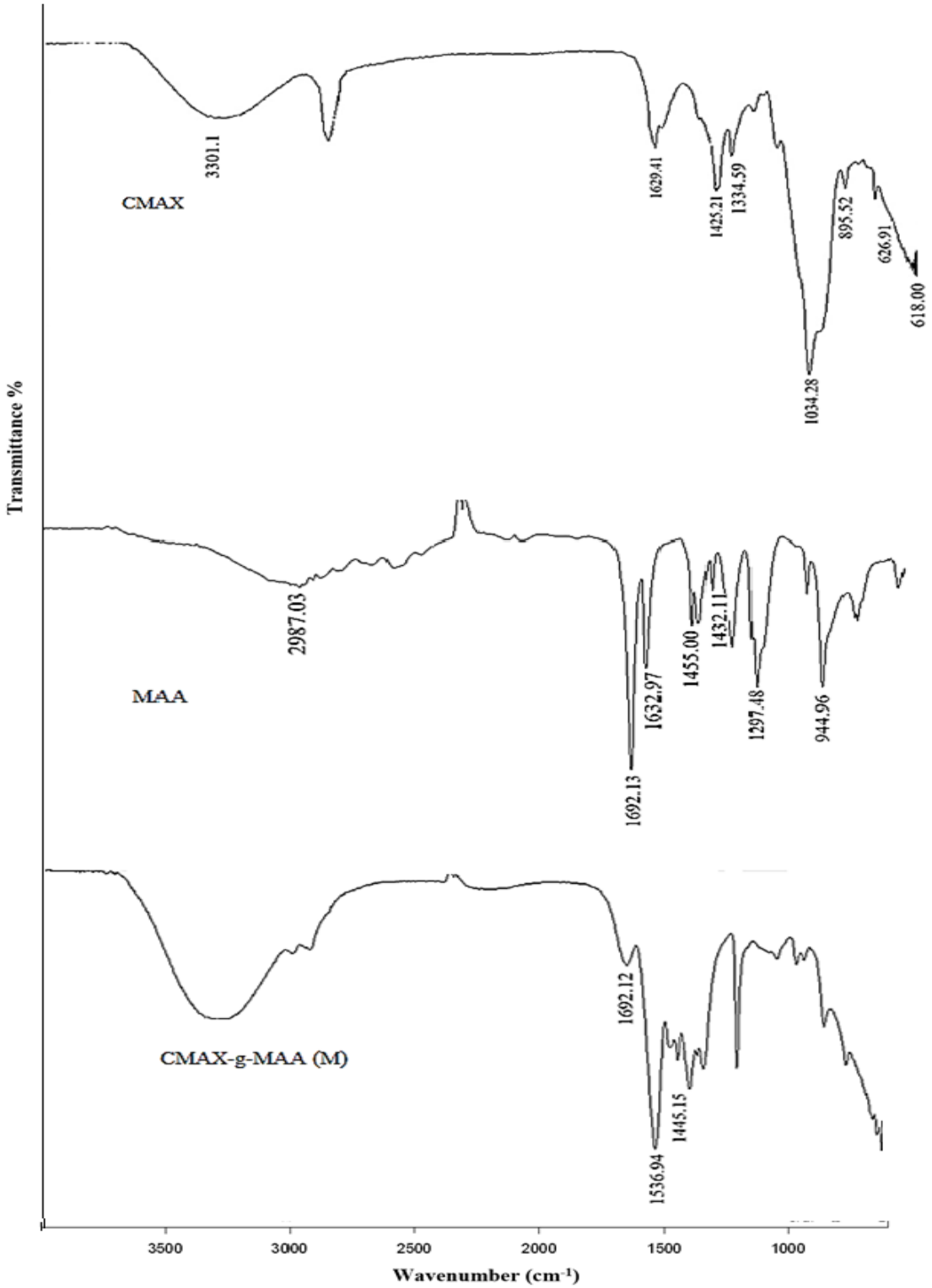

Figure 4.2.7: FTIR spectrum of CMAX, MAA, and prepared hydrogel (M)

c) Thermal analysis

The thermal properties of CMAX-g-MAA copolymer and CMAX (polymer), and monomer (MAA) were studied by means of DSC and TG analyses. The thermogravimetric analysis was conducted in nitrogen flow from 20–1000°C. TGA curve exhibited percent weight loss as a result of elevation of temperature of CMAX,MAA and prepared hydrogel M shown in Figure 4.2.8. DSC curve exhibited percent heat flow with subsequent increase in temperature displayed in Figure 4.2.9. DTG data was presented in Table 4.2.5.

Table 4.2.5: DTG data of acrylic acid (AA), CMAX and CMAX-g-AA hydrogel (A)

Sample	Step	Tdi (°C)	Tdm (°C)	Tdf (°C)	Weight loss %at Tdf
M	1	66	94	152	21.51
	II	435	462	536	31.05
MAA	I	48	130	144	97.02
CMAX	I	266	332	382	44.8
	II	431	503	562	25

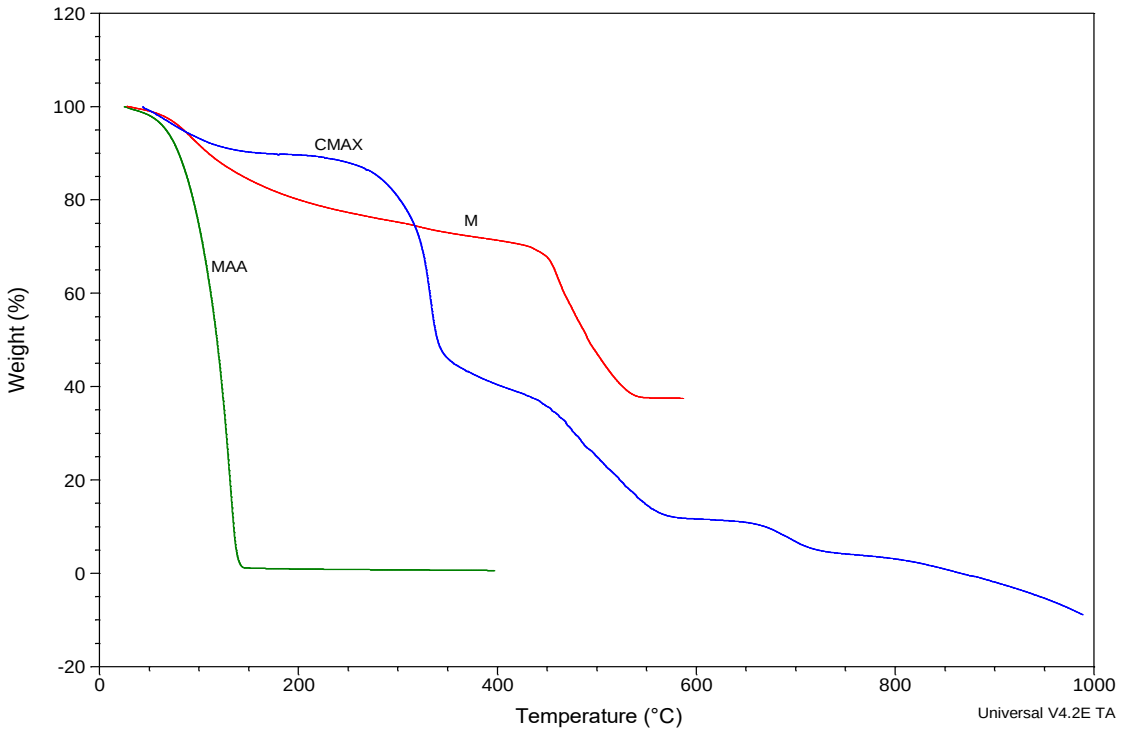

Figure 4.2.8:TGA curves of methacrylic acid (MAA), CMAX and CMAX-g-AA

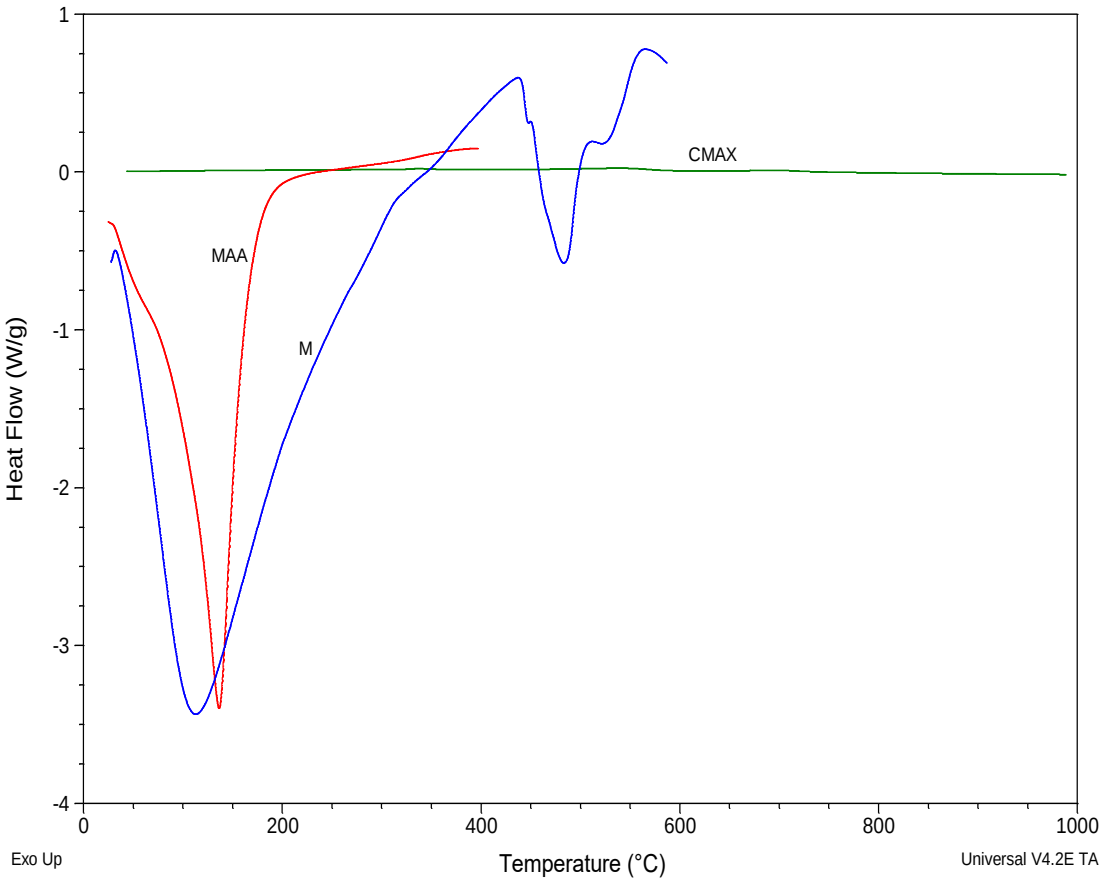

Figure 4.2.9:DSC curves of methacrylic acid (MAA), CMAX and CMAX-g-AA

d) X-ray Diffraction

The XRD pattern of prepared hydrogel (M), rabeprazole sodium (Rab) and drug loaded formulation (MD) depicted in Figure 4.2.10 revealed that there was no peak observed, which shows amorphous nature of prepared hydrogel.

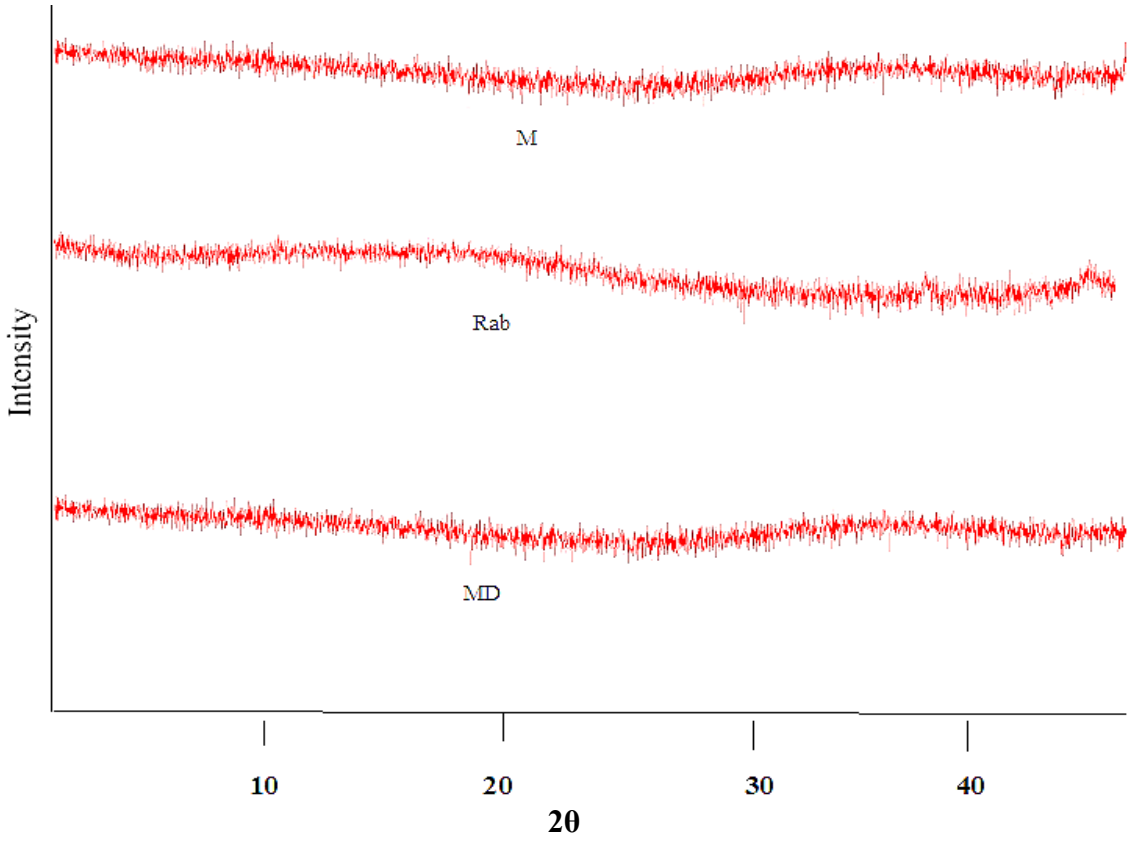

Figure 4.2.10: X-ray diffraction patterns of CMAX, Rab, and drug loaded formulation (CMAX-g-MAA) hydrogel

4.2.5: In vitro release kinetics of Rabeprazole sodium from CMAX-g-MAA hydrogel

In vitro drug release from the CMAX-g-MAA hydrogels was conducted out in triplicate in acidic (0.1N HCl) and basic (0.6M Tris buffer) medium. Cumulative percent drug release was determined and effect of various graft copolymer component on rabeprazole sodium was observed. Effect of methacrylic acid, CMAX and N,N MBA concentration on percent cumulative percent drug release was examined and data was summarized in Tables 4.2.6,4.2.7 and 4.2.8 respectively. Drug release kinetics was determined by fitting data into mathematical release models and release mechanism was proposed by calculating diffusion exponent, findings were given in Table 4.2.9.

Table 4.2.6: Effect of methacrylic acid concentration on cumulative percent drug release of Rabeprazole sodium

Time (hr)	M1 pH 1.2	M2 pH 1.2	M3 pH 1.2	M1 pH 8	M2 pH 8	M3 pH 8
0.5	1.49±0.45	0.85±0.24	0.77±0.21	14.6±1.23	8.85±1.11	6.91±1.31
1	2.04±0.56	1.24±0.45	1±0.21	16.79±1.98	10.19±1.87	8.97±1.45
1.5	2.9±0.34	1.74±0.33	1.35±0.11	18.9±1.76	11.82±1.67	10.98±1.76
2	3.76±0.21	2.23±0.34	1.69±0.19	20.49±2.34	13.77±1.98	12.8±2.00
3	4.61±0.11	2.94±0.92	2.03±0.56	24.72±3.46	16.36±2.01	15.52±1.78
4	5.45±0.09	3.64±0.13	2.37±0.98	28.53±3.76	19.31±2.47	18.62±2.56
6	6.28±0.87	4.34±0.35	2.88±0.76	33.64±2.98	22.56±3.91	23.25±3.09
8	7.1±0.98	5.02±0.35	3.38±0.23	38.6±2.65	29.75±2.98	29.07±2.88
12	7.92±0.88	5.71±0.49	3.87±0.12	50.17±3.23	41.8±3.01	40.58±2.66
16	8.72±0.34	6.38±0.13	4.36±0.36	60.17±3.24	54.73±3.41	49.79±2.76
20	9.52±0.12	7.05±0.28	4.85±0.23	73.72±1.99	64.95±2.99	62.65±3.02
24	10.3±0.23	7.7±0.99	5.33±0.76	84.19±3.98	75.9±3.11	71.26±3.41

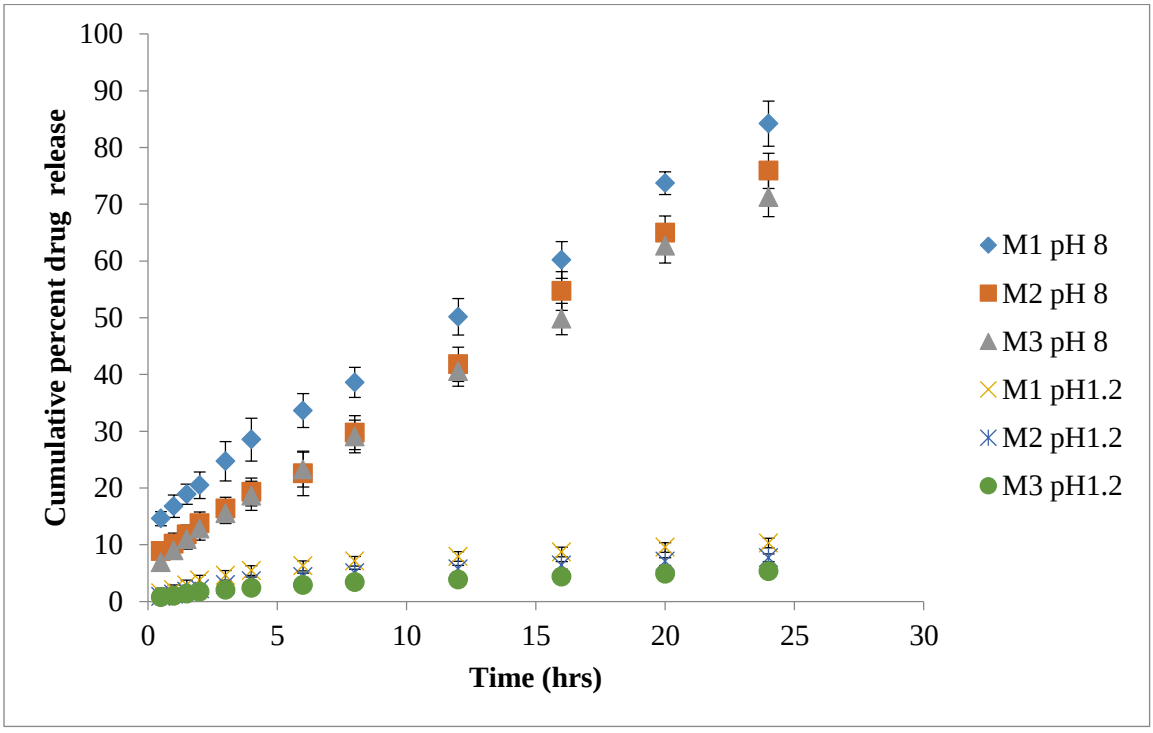

Figure 4.2.11: Effect of methacrylic acid concentration on cumulative percent drug release of Rabeprazole sodium

Table 4.2.7: Effect of CMAX concentration on cumulative percent drug release of Rabeprazole sodium

Time (hr)	M4 pH1.2	M5pH1.2	M6 pH1.2	M4 pH 8	M5 pH 8	M6 pH 8
0.5	0.71±0.35	0.68±0.27	0.51±0.09	12.69±1.43	13.19±1.35	20.11±1.46
1	0.92±0.23	0.83±0.39	0.66±0.29	17.41±1.49	17.97±1.67	22.53±1.25
1.5	1.24±0.21	0.99±0.33	0.8±0.34	20.04±1.66	20.48±1.98	24.93±1.76
2	1.56±0.19	1.14±0.41	0.95±0.36	22.47±2.64	22.81±2.91	27.15±2.52
3	1.88±0.34	1.28±0.77	1.09±0.48	24.93±3.26	25.92±2.91	30.15±2.78
4	2.19±0.11	1.43±0.29	1.24±0.76	27.74±3.86	29.37±2.67	33.46±2.56
6	2.65±0.38	1.73±0.34	1.53±0.23	31.95±2.88	34.4±3.12	38.31±3.09
8	3.11±0.68	2.02±0.36	1.81±0.12	37.27±2.85	41.49±2.68	45.16±2.88
12	3.57±0.76	2.31±0.48	2.1±0.73	47.83±3.53	53.08±3.12	56.36±2.66
16	4.02±0.41	2.6±0.26	2.38±0.21	56.79±3.24	64.12±1.67	67.04±2.76
20	4.47±0.23	2.89±0.76	2.65±0.19	68.44±1.69	78.21±3.21	80.67±3.02
24	4.91±0.31	3.17±0.87	2.93±0.34	79.78±3.48	87.93±3.51	90.06±3.41

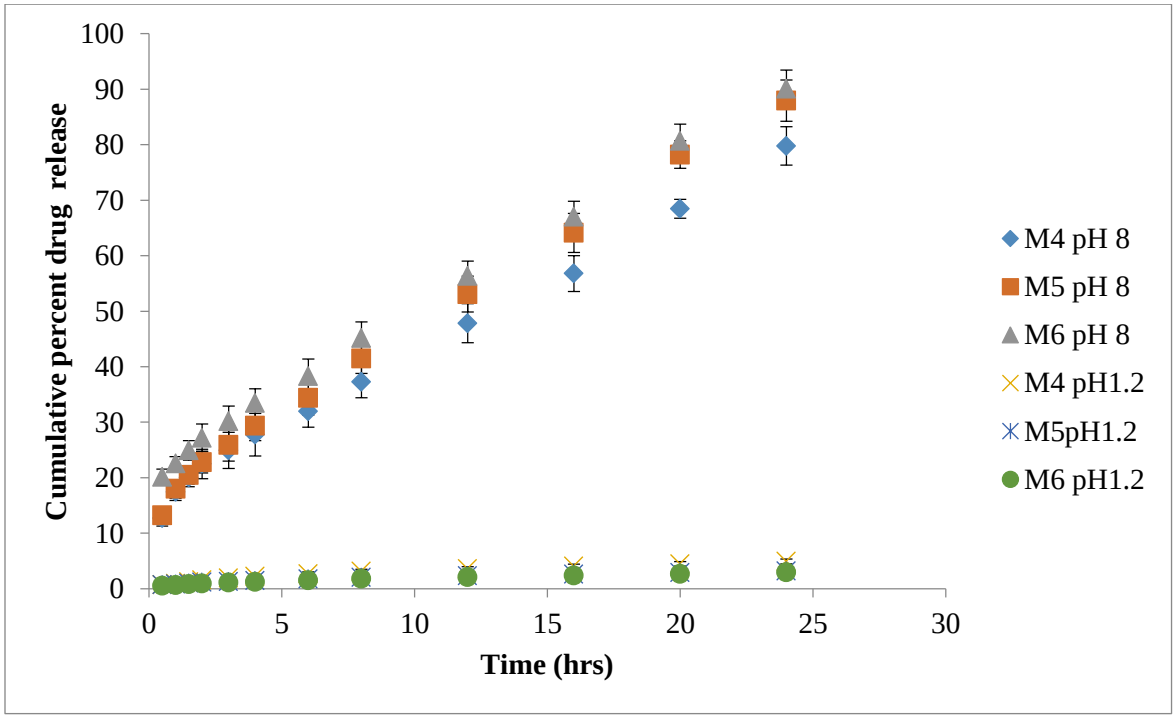

Figure 4.2.12: Effect of CMAX concentration on cumulative percent drug release of Rabeprazole sodium

Table 4.2.8: Effect of crosslinker concentration on cumulative percent drug release of Rabeprazole sodium

Time (hr)	M7 pH 1.2	M8 pH1.2	M9 pH 1.2	M7 pH 8	M8 pH 8	M9 pH 8
0.5	0.61±0.34	0.7±0.37	0.76±0.07	7.56±1.43	5.79±1.95	2.49±1.56
1	0.79±0.69	0.95±0.36	0.97±0.29	10.82±1.49	8.2±1.67	4.82±1.55
1.5	0.96±0.24	1.2±0.69	1.17±0.36	13.77±1.66	10.31±1.47	7.13±1.84
2	1.14±0.62	1.45±0.41	1.37±0.36	16.94±2.64	12.06±1.98	9.43±2.78
3	1.31±0.34	1.69±0.77	1.56±0.48	19.18±3.26	13.17±2.78	12.02±2.78
4	1.48±0.34	1.93±0.45	1.76±0.76	21.58±3.86	15.15±2.67	14.06±2.98
6	1.83±0.83	2.17±0.37	1.95±0.23	26.24±3.88	19.55±3.62	17.49±3.09
8	2.17±0.68	2.41±0.43	2.14±0.54	30.27±3.85	23.81±2.94	20.74±2.88
12	2.51±0.76	2.64±0.48	2.33±0.73	37.7±3.93	32.21±3.21	28.94±2.88
16	2.84±0.47	2.87±0.43	2.52±0.26	47.35±3.28	41.87±3.81	36.02±3.76
20	3.18±0.46	3.1±0.76	2.7±0.67	56.93±2.69	51.99±2.89	46.95±3.02
24	3.51±0.91	3.33±0.83	2.88±0.78	69.5±3.89	62.84±3.91	55.51±3.91

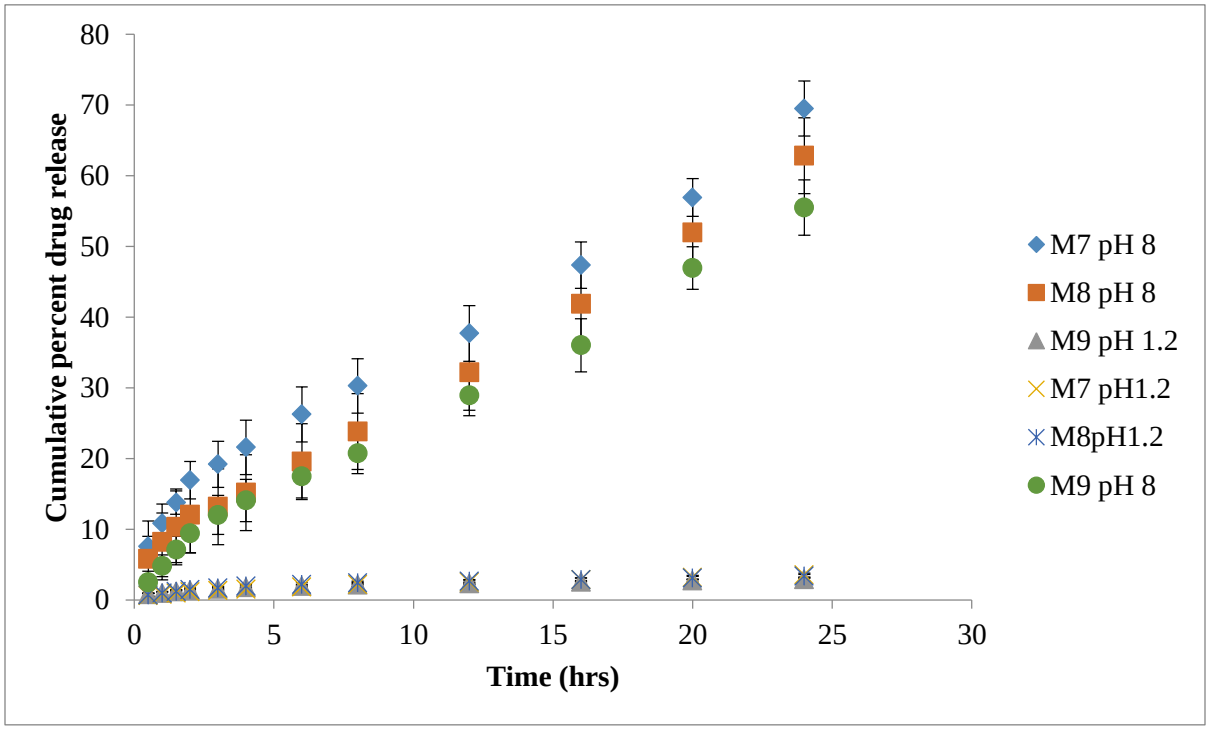

Figure 4.2.13: Effect of crosslinker concentration on cumulative percent drug release of Rabeprazole sodium

Table 4.2.9: Kinetic parameters of Rabeprazole sodium release from CMAX-g-MAA hydrogels

Formulation code	***Higuchi***	***First order***	***Zero order***	***Korsmayer-peppas***	
	R^2	R^2	R^2	R^2	***n***
M1	0.972	0.480	0.997	0.985	0.819
M2	0.958	0.614	0.999	0.987	0.810
M3	0.970	0.620	0.998	0.994	0.867
M4	0.972	0.461	0.995	0.980	0.846
M5	0.976	0.471	0.996	0.976	0.766
M6	0.972	0.414	0.998	0.984	0.716
M7	0.970	0.531	0.990	0.979	0.960
M8	0.954	0.633	0.997	0.989	1.004
M9	0.968	0.681	0.993	0.984	1.053

4.3 Characterization of CMC-g-AA hydrogels

4.3.1 Swelling studies at pH1.2 and pH 7.4

The effect of acrylic acid, carboxymethyl cellulose and crosslinker on the swelling curve of prepared hydrogels was evaluated by immersing hydrogels disc at pH 1.2 and 7.4 at temperature 37 ºC. Formulations were assigned codes (CA1-CA3), (CA4-CA6) and (CA7-CA9) for varying concentration of acrylic acid, CMC and crosslinker respectively. Effect of varying concentration of acrylic acid on swelling ratio (q), CA1 (1 to 5.19), CA2 (1 to 3.58) and CA3 (1 to 4.23) in pH 1.2 and CA1 (1 to 26.82), CA2 (1 to 35.32) and CA3 (1 to 40.69) in 7.4 buffer solutions at 37 ºC has been given in Table 4.3.1 and graphically presented in Figure 4.3.1.Comparative swelling ratio (q) of hydrogels by using different concentrations of CMC, CA4 (1 to 4.84), CA5 (1 to 6.43) and CA6 (1 to 5.95) at pH 1.2 and CA4 (1 to 37.81), CA5 (1 to 43.36) and CA6 (1 to 31.61) at pH 7.4 were given in Table 4.3.2.

Table 4.3.3 showed effect of crosslinker contents on swelling ratio of hydrogels CA7 (1 to5.79), CA8 (1 to 4.86) and CA9 (1 to 3.49) at pH 1.2 and CA7 (1 to 32.35), CA8 (1 to 28.61) and CA9 (1 to 23.74) at pH 7.4.

Table 4.3.1: Comparative swelling ratios of CMC-g-AA hydrogels using different concentrations of acrylic acid (n=3)

Time (Hrs)	**Swelling ratio (q) at pH 1.2**			**Swelling ratio (q) at pH 7.4**		
	CA1	CA2	CA3	CA1	CA2	CA3
0	1	1	1	1	1	1
0.5	1.12±0.19	1.17±0.23	1.19±0.22	2.16±0.21	2.62±0.22	2.82±0.21
1	1.25±0.22	1.34±0.29	1.38±0.24	3.32±0.24	4.24±0.23	4.65±0.24
1.5	1.37±0.32	1.51±0.31	1.57±0.19	4.48±0.33	5.86±0.34	6.47±0.33
2	1.5±0.27	1.68±0.3	1.76±0.22	5.64±0.34	7.48±0.38	8.3±0.45
3	1.62±0.3	1.85±0.28	1.95±0.32	6.8±0.38	9.1±0.41	10.12±4.21
4	1.75±0.31	2.02±0.32	2.14±0.33	7.96±0.42	10.72±0.43	11.95±4.76
6	1.87±0.33	2.194±0.31	2.33±0.35	9.13±0.46	12.34±0.45	13.77±6.73
8	2±0.32	2.36±0.33	2.52±0.35	10.29±0.53	13.96±4.21	15.6±0.53
10	2.13±0.31	2.53±0.35	2.71±0.36	11.45±0.63	15.58±4.76	17.42±0.63
12	2.25±0.32	2.7±0.35	2.9±0.34	12.61±0.74	17.2±6.73	19.25±0.74
14	2.38±0.35	2.87±0.36	3.09±0.34	13.77±0.75	18.82±0.74	21.07±0.75
18	2.5±0.36	3.04±0.34	3.28±0.33	14.93±0.81	20.44±0.75	22.9±0.81
24	2.63±0.34	3.21±0.34	3.59±0.33	16.07±0.82	22.06±0.81	27.1±0.82
48	3.69±0.34	3.3±0.35	3.91±0.34	21.22±0.84	29.02±0.82	33.32±0.84
72	5.19±0.35	3.58±0.35	4.23±0.34	26.82±0.89	35.32±0.88	40.69±0.89

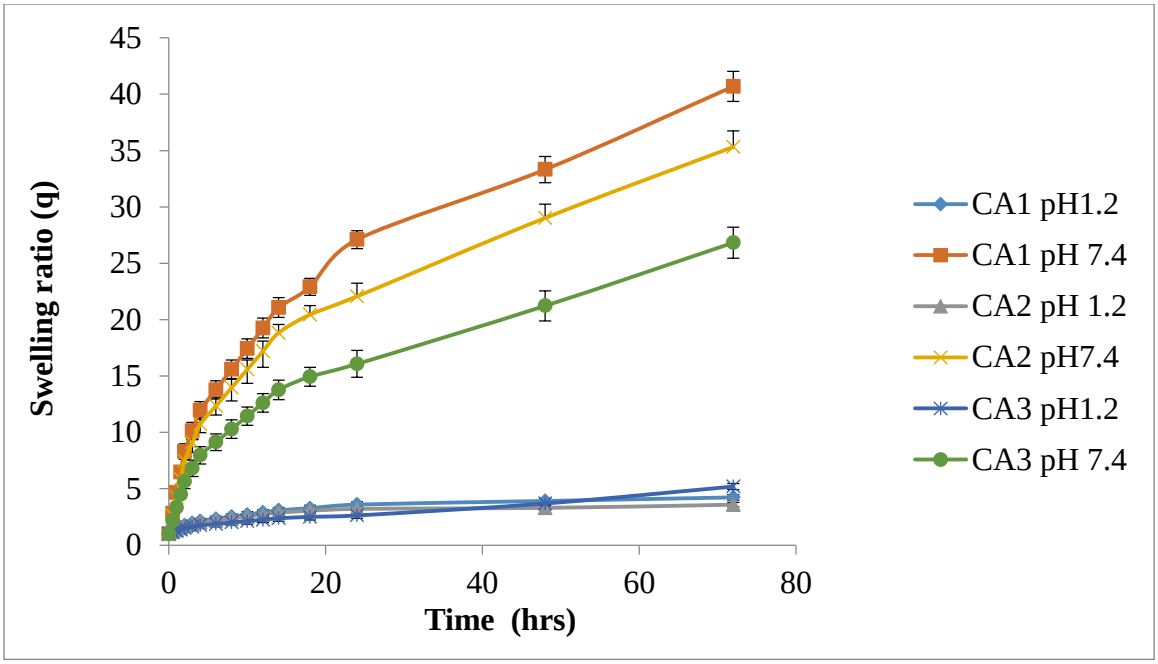

Figure 4.3.1: Comparative swelling ratios of CMC-g-AA hydrogels using different concentrations of monomer

Table 4.3.2: Comparative swelling ratios of CMC-g-AA (CA) hydrogels using different concentrations of polymer (n=3)

Time (Hrs)	Swelling ratio (q) at pH 1.2			Swelling ratio (q) at pH7.4		
	CA4	CA5	CA6	CA4	CA5	CA6
0	1	1	1	1	1	1
0.5	1.62±0.23	1.38±0.19	1.2±0.22	3.79±0.24	3.97±0.21	2.82±0.2
1	1.74±0.22	1.57±0.22	1.41±0.32	6.59±0.33	6.94±0.31	4.65±0.22
1.5	1.78±0.32	1.76±0.32	1.62±0.43	9.38±0.34	9.91±0.62	6.47±0.34
2	1.85±0.43	1.95±0.22	1.83±0.32	11.07±0.68	11.72±0.73	8.3±0.68
3	2.03±0.32	2.14±0.32	2.04±0.35	12.32±0.77	13.83±0.31	10.13±0.77
4	2.12±0.22	2.33±0.33	2.25±0.35	14.67±0.79	15.24±0.62	11.95±0.77
6	2.28±0.32	2.52±0.36	2.46±0.68	16.36±0.81	17.38±0.73	13.78±0.75
8	2.37±0.33	2.71±0.35	2.66±0.77	17.17±0.83	18.57±0.77	15.6±0.81
10	2.45±0.35	3.09±0.68	2.87±0.74	18.33±0.86	20.06±0.84	17.43±0.81
12	2.7±0.35	3.47±0.77	3.08±0.79	19.27±0.88	21.87±0.89	19.26±0.83
14	2.99±0.35	3.86±0.74	3.29±0.85	20.32±0.89	24.27±0.75	21.08±0.86
18	3.31±0.68	4.24±0.79	3.5±0.77	23.4±0.75	26.66±0.8	22.91±0.83
24	3.56±0.77	4.62±0.81	3.71±0.8	26.96±0.8	29.63±1.17	24.73±0.86
48	4.15±0.74	5.38±0.82	4.63±0.83	32.86±1.17	36.73±1.24	28.28±0.88
72	4.84±0.79	6.43±0.84	5.95±0.85	37.81±1.34	43.36±1.42	31.61±1.38

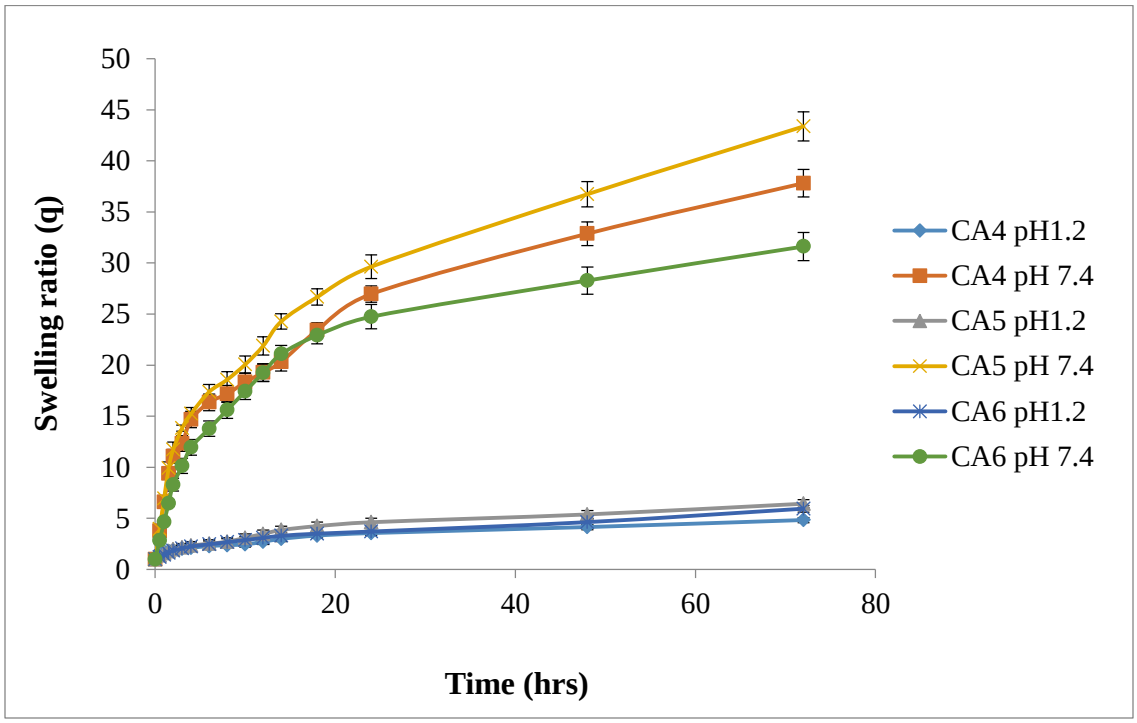

Figure 4.3.2: Comparative swelling ratios of CMC-g-AA hydrogels using different concentrations of polymer

Table 4.3.3: Comparative swelling ratios of CMC-g-AA (CA) hydrogels using different concentrations of crosslinker (n=3)

Time (Hrs)	**Swelling ratio (q) at pH 1.2**			**Swelling ratio (q) at pH7.4**		
	CA7	CA8	CA9	CA7	CA8	CA9
0	1	1	1	1	1	1
0.5	1.32±0.23	1.25±0.22	1.17±0.22	4.1±0.24	4.07±0.21	2.52±0.2
1	1.64±0.22	1.51±0.32	1.35±0.24	5.28±0.33	5.25±0.31	4.04±0.22
1.5	1.96±0.32	1.77±0.43	1.53±0.32	6.15±0.34	5.96±0.62	5.56±0.31
2	2.12±0.43	1.9±0.32	1.71±0.33	7.38±0.68	7.29±0.73	7.08±0.62
3	2.27±0.32	2.03±0.35	1.96±0.35	9.92±0.77	9.52±0.31	7.83±0.73
4	2.43±0.22	2.16±0.35	1.99±0.35	11.15±0.79	10.69±0.62	8.59±0.62
6	2.59±0.32	2.29±0.68	2.14±0.68	13.13±0.81	12.36±0.73	9.35±0.73
8	2.75±0.33	2.55±0.77	2.23±0.77	16.02±0.83	13.62±0.77	10.87±0.75
10	3.07±0.35	2.81±0.74	2.41±0.74	17.77±0.86	15.42±0.84	12.39±0.75
12	3.39±0.35	3.06±0.83	2.59±0.79	19.8±0.88	16.9±0.89	13.91±0.8
14	3.71±0.77	3.32±0.86	2.77±0.85	21.59±0.89	18.67±0.75	15.43±1.17
18	4.03±0.8	3.58±0.88	2.95±0.77	23.65±0.75	21.39±0.8	16.95±0.83
24	4.35±0.83	4.09±0.8	3.13±0.8	25.77±0.8	23.49±1.17	18.47±1.19
48	5±0.81	4.84±0.83	3.31±0.83	29.44±1.17	26.52±1.24	21.51±1.33
72	5.79±0.81	4.86±0.85	3.49±0.85	32.35±1.34	28.61±1.42	23.74±1.38

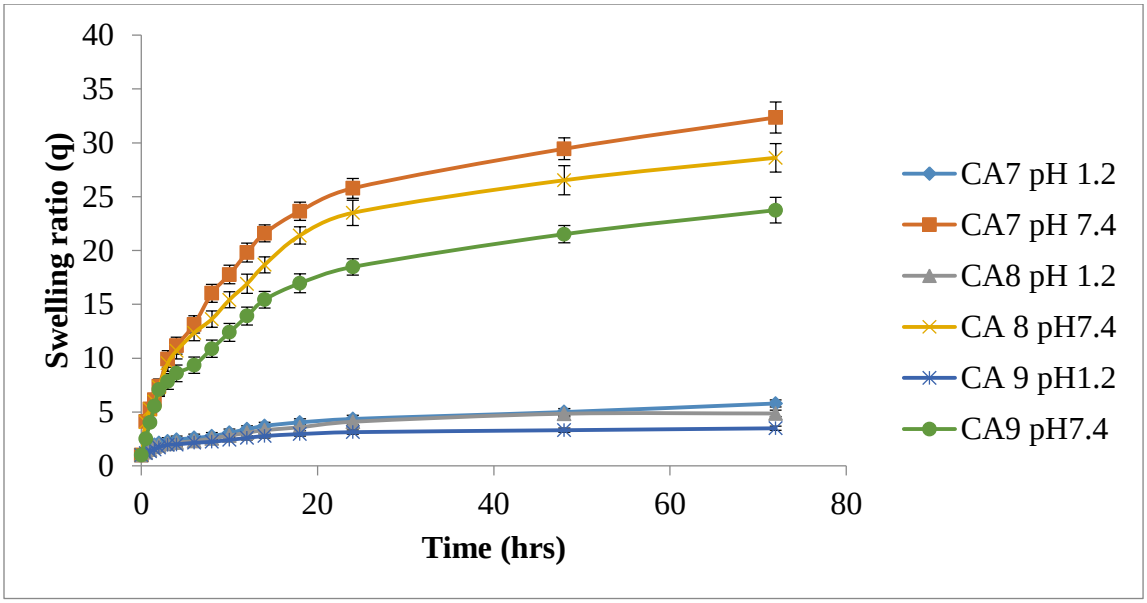

Figure 4.3.3: Comparative swelling ratios of CMC-g-AA hydrogels using different concentrations of crosslinker

4.3.2 Pulsatile behavior of hydrogels

The pH-reliant swelling reversibility of CMC-g-AA hydrogel was scrutinized in buffered solutions. A distinctive result of the pulsatile reversible swelling of CMC-g-AA was shown in Figure 4.3.4, proved the hydrogel swelling reversibility upon alteration in pH.

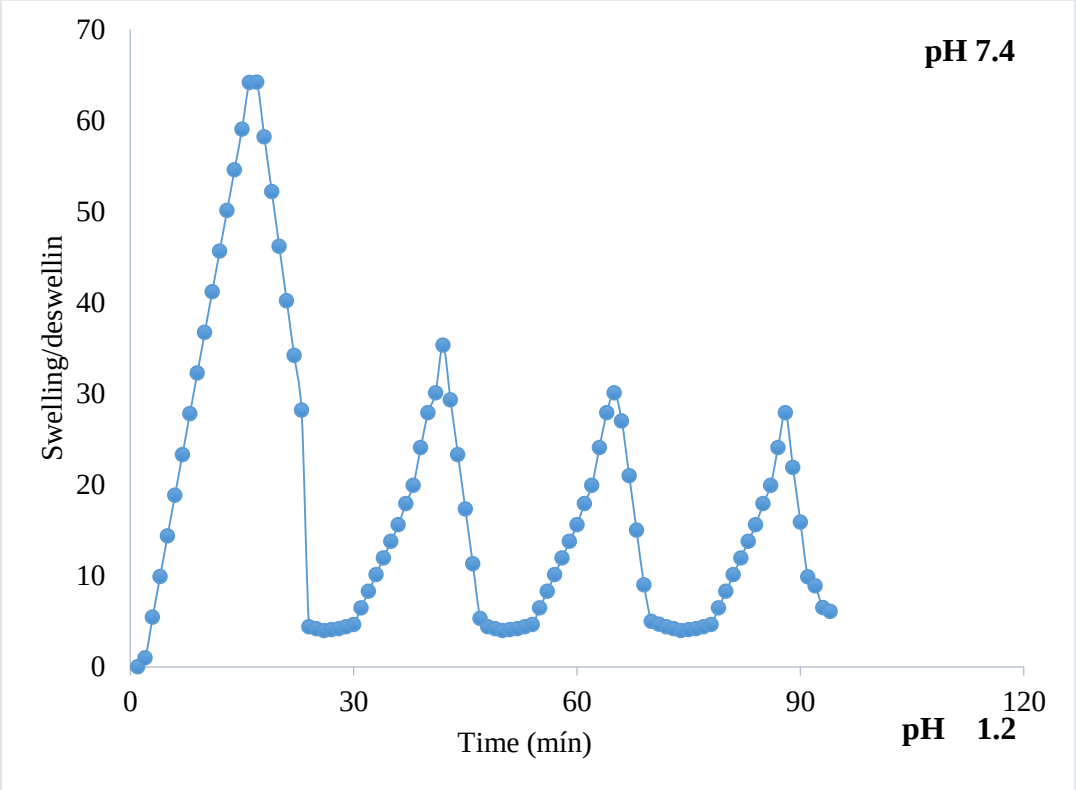

Figure 4.3.4: On-off switching behavior as reversible pulsatile swelling (pH 7.4) and deswelling (pH 1.2) of CMC-g-AA hydrogel

4.3.3: Equilibrium water contents (EWC) and gel fraction

To evaluate the equilibrium water content, dry hydrogels were immersed in deionized water at 37 ºC to achieve equilibrium swelling (72 Hrs). Table 4.3.4 indicated the effect of varying composition of hydrogels on equilibrium water contents and gel fraction. Figure 4.3.5 showed the gel fraction as a function of AA, CMC and N, N MBA contents in the hydrogels.

Table 4.3.4: Equilibrium water contents and gel fraction of CMC-g-AA hydrogels using different concentrations of AA, CMC and crosslinker

Formulation code	Contents w/w%	EWC	Gel fraction (%)	Amount of Rabeprazole sodium loaded (mg per 0.4 g of dry hydrogel disc)	
				By extraction	By weight
CA1	AA 10	0.96	80.24	74	75
CA2	AA 15	0.97	92.92	90	91
CA3	AA 20	0.98	93.07	98	99
CA4	CMC 1	0.99	87.17	99	99
CA5	CMC 1.5	0.98	94.87	102	100
CA6	CMC 2	0.97	74.149	82	83
CA7	MBA 0.4	0.97	86.84	85	86
CA8	MBA 0.6	0.96	93.64	72	73
CA9	MBA 0.8	0.96	96.78	59	60

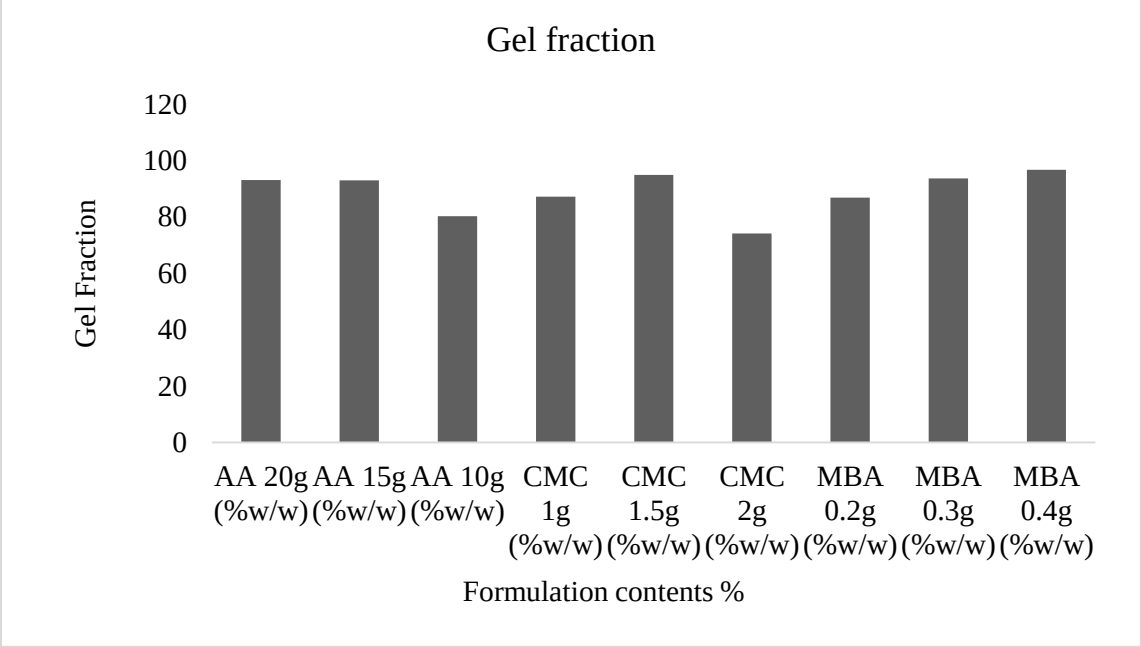

Figure 4.3.5: Gel fraction of CMC-g-AA hydrogel with different concentrations of AA, CMC and crosslinker

4.3.4 Instrumental analysis

a) Scanning electron microscopy

Scanning electron micrographs were attained from freeze-dried hydrogels depicted in Figure 4.3.6.

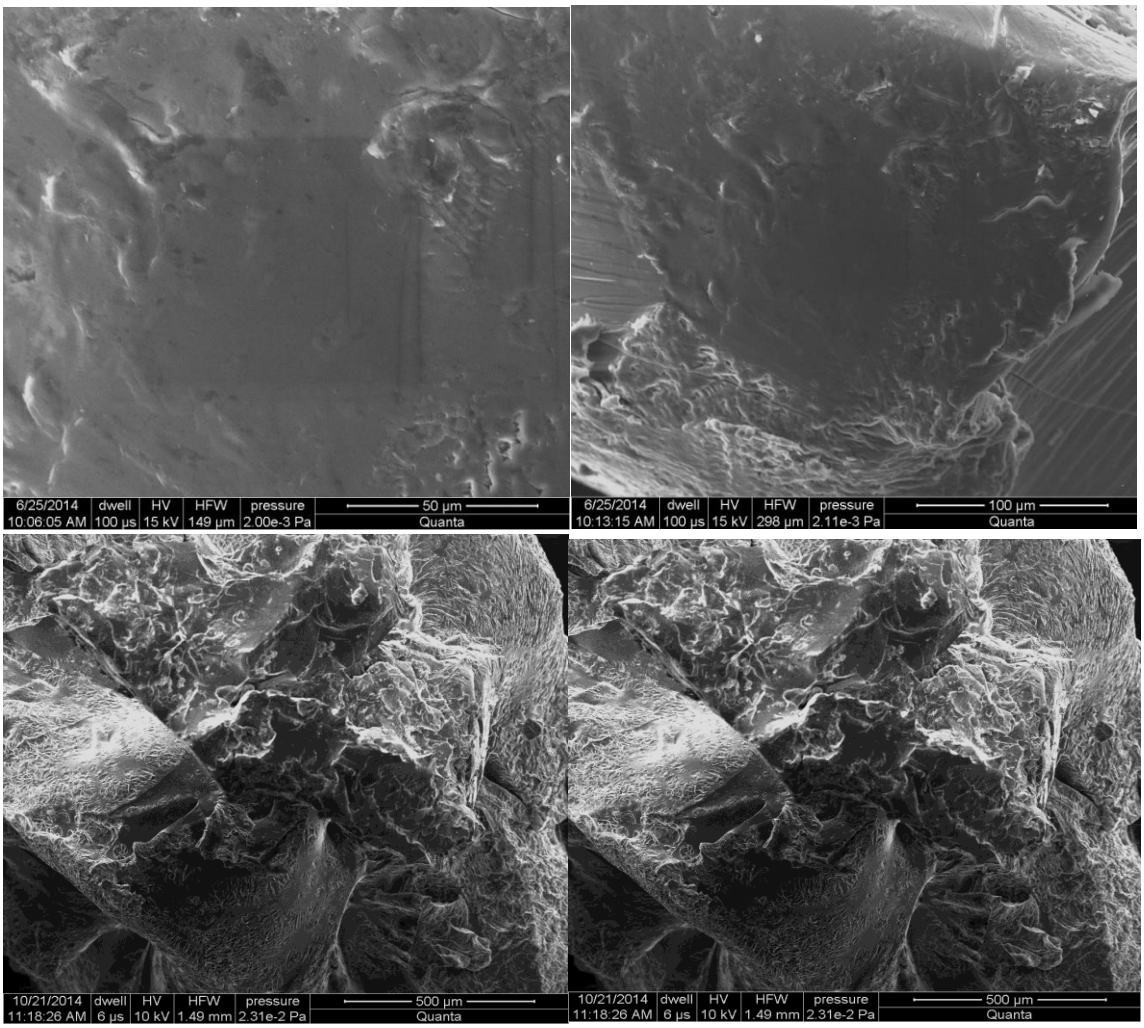

Figure 4.3.6: SEM images of lyophilized hydrogels (CMAX-g-MAA) at magnification of 100 X and 200 X and 50µ, 100µ, 300µ, and 500µ scale bar respectively

b) FTIR Analysis

In this study, attenuated total reflectance (ATR) technology along with OPUS data collection software was employed to compute Fourier transform infrared (FTIR) spectra of all samples using Bruker FTIR (Tensor 27 series, Germany).FTIR spectrum of pure components (AA and CMC) and prepared formulations (CA) were recorded at 600 to 4000 $cm^{-1}$are shown in Figure 4.3.7.

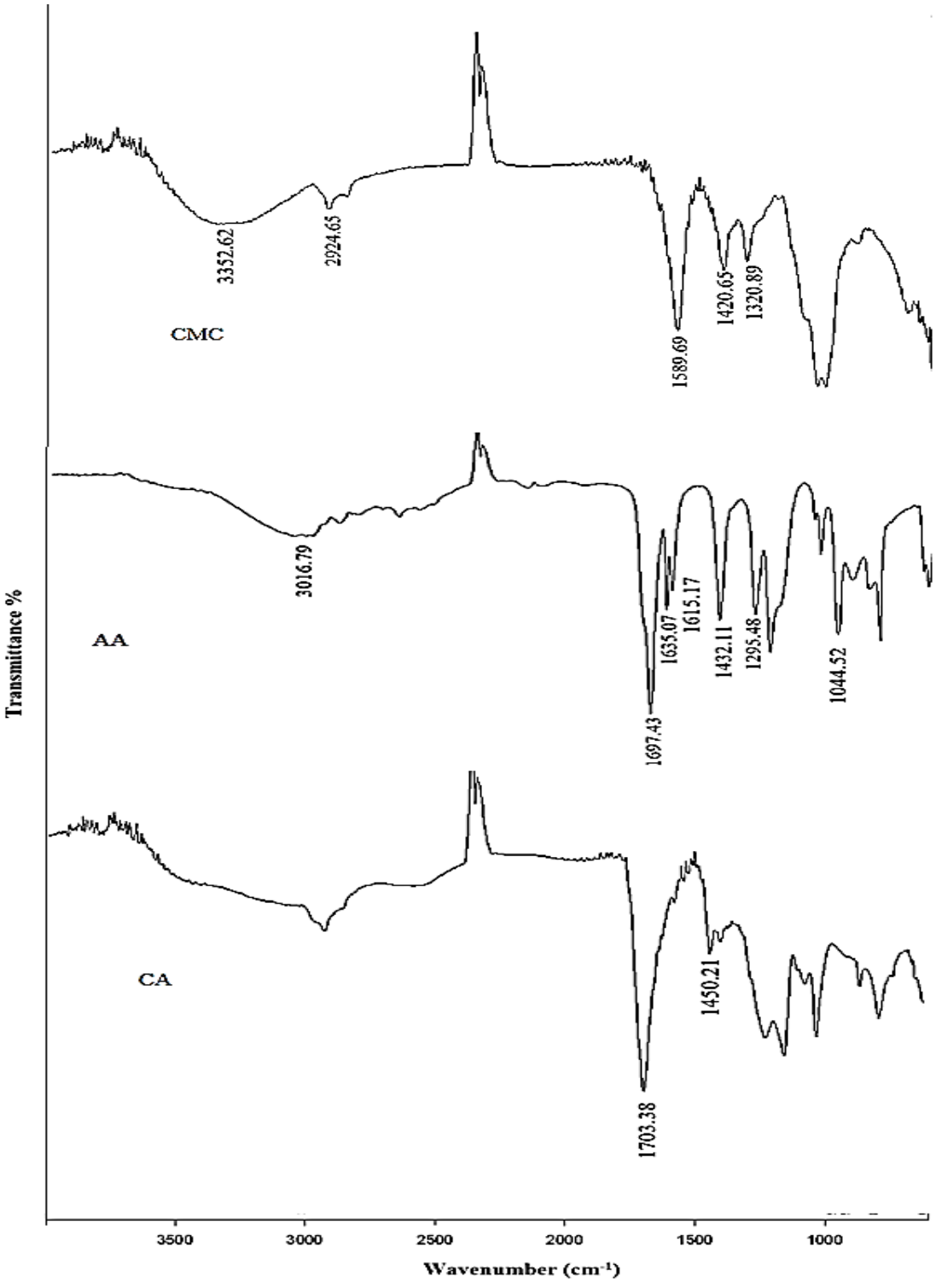

Figure 4.3.7: FTIR spectra of CMC, acrylic acid (AA) and prepared hydrogel (CA)

c) Thermal analysis

Thermal stability of the hydrogel (CA) and separate components(CMC and acrylic acid)were studied by TGA analyzer in the temperature range from 0 ºC to 600 ºC under inert nitrogen atmosphere. TGA curve of CMC (carboxymethyl cellulose), AA (acrylic acid) and CA (CMC-g-AA) hydrogel formulation depicted in Figure 4.3.8. DSC curves of CMC, AA and CA hydrogel formulation are described in Figure 4.3.9.

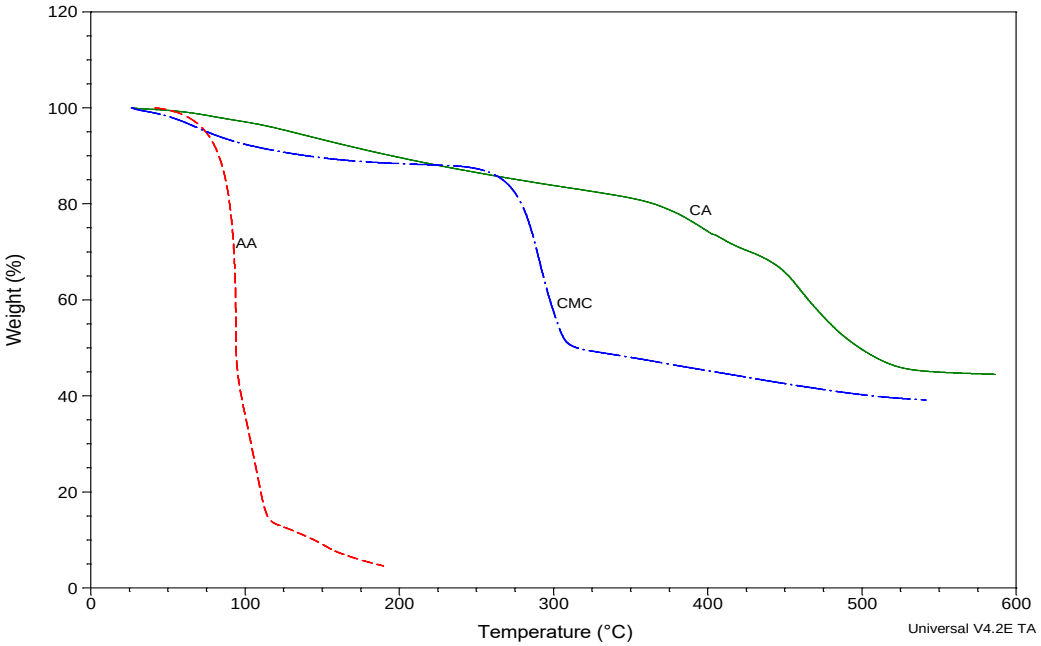

Figure 4.3.8: TGA curves of AA, CMC and hydrogel formulation (CA)

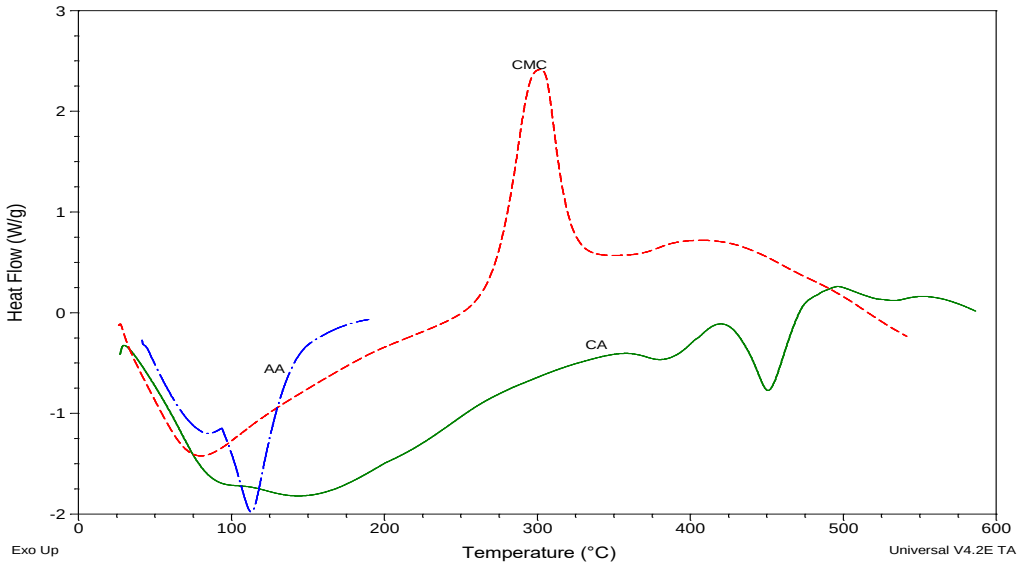

Figure 4.3.9: DSC curves of AA, CMC and hydrogel formulation (CA)

4.3.5: In vitro release kinetics of Rabeprazole sodium from CMC-g-AA hydrogel

Cumulative percent drug release of CMC-g-AA has been evaluated at acidic and basic pH to estimate pH dependent release of rabeprazole sodium. Drug release was also influenced by individual constituents of hydrogels and cross linking density of hydrogels. Drug release from CMC-g-AA by using different concentrations of acrylic acid, CMC and MBA has been expressed in Table 4.3.5, 4.3.6 and 4.3.7 respectively.

Table 4.3.5: Effect of acrylic acid concentration on cumulative percent drug release of Rabeprazole sodium

Time (hr)	CA1 pH 1.2	CA2 pH 1.2	CA3 pH 1.2	CA1 pH8	CA2 pH 8	CA3 pH 8
0.5	1.84±0.03	0.89±0.05	1±0.08	8.78±1.12	11.33±1.19	12.25±1.28
1	3.05±0.21	1.4±0.31	1.55±0.21	13.51±1.34	16.67±1.28	17.83±1.39
1.5	3.85±0.34	1.77±0.26	2.09±0.34	17.97±1.56	21.93±1.56	22.92±1.68
2	5.24±0.45	2.14±0.28	2.57±0.39	22.2±1.78	27.13±2.98	26.82±1.68
3	5.83±0.34	2.51±0.29	3.05±0.43	28±1.98	32.28±2.78	31.61±1.99
4	6.59±0.27	2.87±0.51	3.53±0.53	31.55±1.87	37.38±2.66	36.01±1.67
6	7.16±0.56	3.23±0.42	4±0.20	35.89±1.67	42.42±2.33	41.57±1.78
8	7.72±0.45	3.58±0.76	4.46±0.52	41.4±1.59	47.41±2.77	46.02±2.56
12	8.46±0.43	3.93±0.45	4.97±0.61	44.07±1.87	51.98±2.76	52.63±3.32
16	9.2±0.09	4.28±0.56	5.42±0.41	48.08±1.67	56.86±2.34	61.18±3.24
20	9.93±0.45	4.62±0.45	5.87±0.43	51.3±1.59	61.87±2.76	67.56±3.07
24	10.66±0.41	4.96±0.56	6.27±0.09	57.72±1.89	70.19±2.34	77.69±3.87

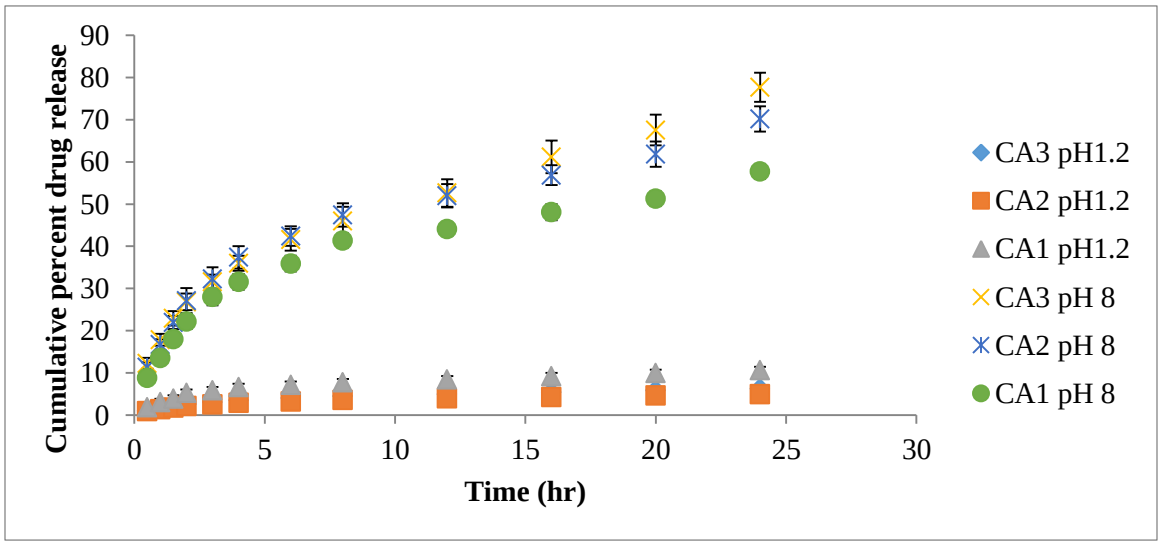

Figure 4.3.10: Effect of acrylic acid concentration on cumulative percent drug release of Rabeprazole sodium

Table 4.3.6: Effect of CMC concentration on cumulative percent drug release of Rabeprazole sodium

Time (hr)	CA4 pH 1.2	CA5 pH 1.2	CA6 pH 1.2	CA4 pH8	CA5 pH 8	CA6 pH 8
0.5	1.68±0.18	1.72±0.15	0.31±0.13	12.92±1.08	14.42±1.21	8.82±1.14
1	2.29±0.21	2.74±0.31	1.15±0.21	16.66±1.34	18.45±1.28	14.18±1.34
1.5	2.84±0.34	3.8±0.26	1.63±0.34	19.53±1.89	23.37±1.56	17.41±1.67
2	3.43±0.39	4.22±0.28	2.1±0.28	23.25±1.67	28.16±2.98	20.67±1.78
3	3.91±0.34	4.68±0.29	2.57±0.29	27.42±1.78	33.26±3.32	24.35±2.56
4	4.39±0.45	5.14±0.51	3.03±0.51	32.75±1.78	37.99±3.24	27.76±1.78
6	4.87±0.28	5.97±0.42	3.49±0.42	37.89±2.56	43.83±3.87	30.85±2.56
8	5.34±0.29	6.66±0.76	3.9±0.45	43.84±2.77	48.18±2.77	35.74±1.87
12	5.8±0.51	7.28±0.45	4.31±0.43	54.71±2.76	56.27±2.76	41.15±1.87
16	6.26±0.42	7.91±0.56	4.75±0.45	61.43±2.34	62.25±2.34	49.33±1.78
20	6.72±0.53	8.57±0.78	5.24±0.56	69.23±3.46	70.19±3.01	55.41±2.56
24	7.26±0.64	9.22±0.67	5.71±0.78	78.36±3.54	80.75±2.99	59.01±2.77

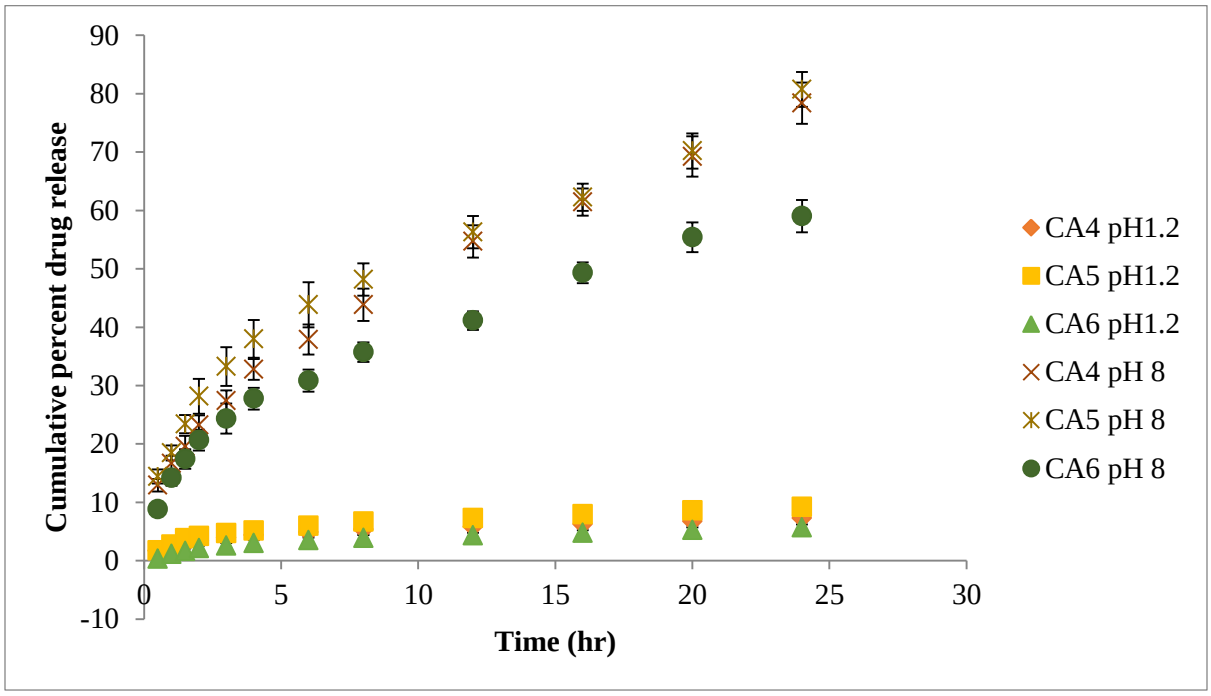

Figure 4.3.11: Effect of CMC concentration on cumulative percent drug release of Rabeprazole sodium

Table 4.3.7: Effect of crosslinker concentration on cumulative percent drug release of Rabeprazole sodium

Time (hr)	CA7 pH 1.2	CA8 pH 1.2	CA9 pH 1.2	CA7 pH8	CA8 pH 8	CA9 pH 8
0.5	1.11±0.28	1.11±0.21	0.49±0.19	8.27±1.11	7.7±1.28	7.15±1.02
1	1.48±0.21	1.53±0.31	0.82±0.21	13.32±1.34	13.15±1.18	11.16±1.24
1.5	1.32±0.34	1.73±0.26	1.14±0.34	18.31±1.29	18.39±1.46	15.12±1.47
2	2.09±0.39	2±0.28	1.3±0.28	23.15±1.72	23.19±2.38	19.03±1.68
3	2.71±0.21	2.26±0.29	1.54±0.29	28.19±1.55	27.53±3.32	23.95±2.36
4	3.01±0.31	2.52±0.51	1.77±0.51	32.98±1.78	31.96±3.14	27.78±1.27
6	3.35±0.26	2.78±0.42	2±0.42	37.47±2.56	36.15±3.37	32.52±1.57
8	3.64±0.28	3.17±0.76	2.23±0.21	42.01±2.57	40.42±2.47	35.56±1.97
12	3.93±0.51	3.42±0.19	2.46±0.31	46.5±2.86	44.64±2.86	39.41±1.93
16	4.21±0.42	3.61±0.21	2.68±0.26	51.04±2.84	48.95±2.74	44.34±1.58
20	4.54±0.67	3.79±0.34	2.9±0.28	55.53±2.94	53.85±3.11	47.26±2.65
24	4.82±0.24	3.97±0.28	3.12±0.48	63.17±3.04	58.01±2.69	50.68±2.45

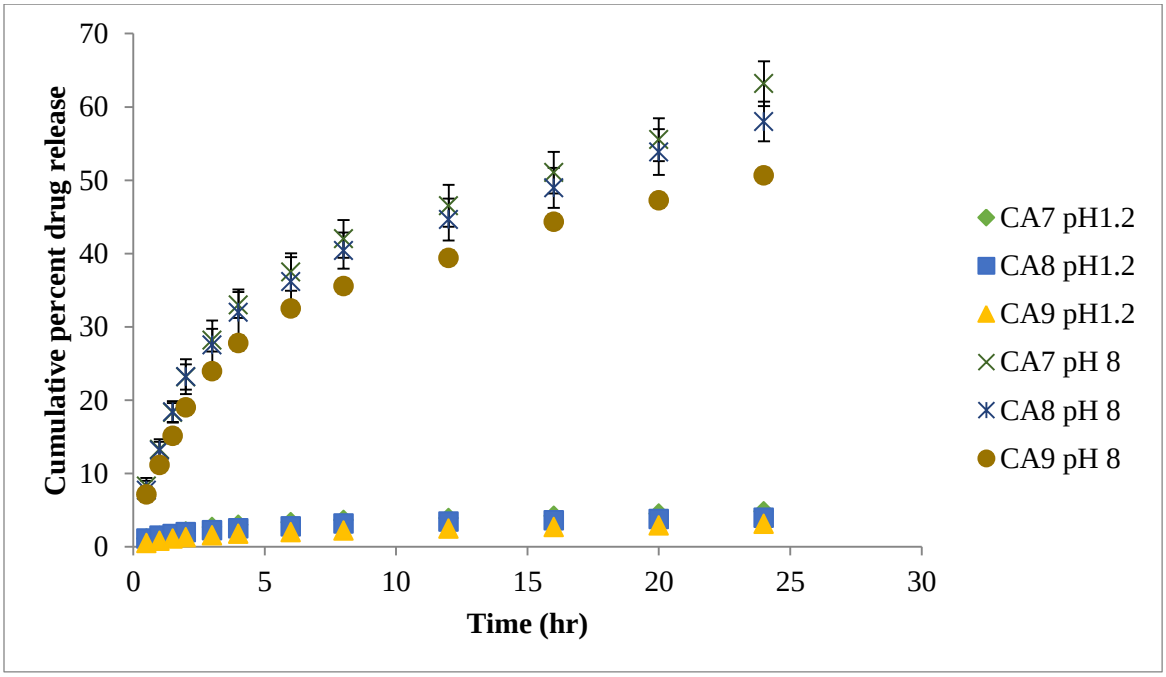

Figure 4.3.12: Effect of crosslinker concentration on cumulative percent drug release of Rabeprazole sodium

Table 4.3.8: Kinetic parameters of Rabeprazole sodium release

Formulation code	*Higuchi*	*First order*	*Zero order*	*Korsmayer-peppas*	
	R^2	R^2	R^2	R^2	*n*
CA1	0.991	0.381	0.945	0.990	0.60
CA2	0.971	0.354	0.887	0.988	0.53
CA3	0.959	0.365	0.860	0.986	0.46
CA4	0.999	0.432	0.964	0.997	0.54
CA5	0.988	0.373	0.929	0.990	0.55
CA6	0.994	0.412	0.947	0.991	0.58
CA7	0.970	0.382	0.884	0.989	0.54
CA8	0.963	0.370	0.867	0.994	0.41
CA9	0.965	0.394	0.865	0.993	0.33

4.4 Characterization of CMC-g-MAA hydrogels

4.4.1 Swelling studies at pH1.2 and pH 7.4

Equilibrium swelling of CMC-g-MAA graft copolymer was determined by swelling the dried hydrogels discs in acidic and basic pH buffer solution at 37ºC.Formulations were assigned codes (CMA1-CMA3), (CMA4-CMA6) and (CMA7-CMA9) for varying concentration of methacrylic acid, CMC and crosslinker respectively. Effect of varying concentration of methacrylic acid on swelling ratio (q), CMA1 (1 to 6.684), CMA2 (1 to 4.182) and CMA3 (1 to 3.667) in pH 1.2 and CMA1 (1 to 30.040), CMA2 (1 to 23.516) and CMA3 (1 to 20.387) in 7.4 buffer solutions at 37 ºC has been given in Table 4.4.1 and graphically presented in Figure 4.4.1. Comparative swelling ratio (q) of hydrogels by using different concentrations of CMC, CMA4 (1 to 6.204), CMA5 (1 to 7.659) and CMA6 (1 to 10.813) at pH 1.2 and CMA4 (1 to 26.451), CMA5 (1 to 24.890) and CMA6 (1 to 24.493) at pH 7.4 were given in Table 4.4.2. Table 4.4.3 showed effect of crosslinker contents on swelling ratio of hydrogels CMA7 (1 to 5.386), CMA8 (1 to 3.089) and CMA9 (1 to 2.898) at pH 1.2 and CMA7 (1 to 18.960), CMA8 (1 to 13.664) and CMA9 (1 to 10.993) at pH 7.4.

Table 4.4.1: Comparative swelling ratios of CMC-g-MAA (CMA) hydrogels using different concentrations of MAA (n=3)

Time (Hrs)	**Swelling ratio (q) at pH 1.2**			**Swelling ratio (q) at pH 7.4**		
	CMA_1	CMA_2	CMA_3	CMA_1	CMA_2	CMA_3
0	1	1	1	1	1	1
0.5	1.37±0.23	1.21±0.19	1.19±0.22	3.07±0.24	2.61±0.21	2.38±0.2
1	1.73±0.22	1.42±0.22	1.38±0.24	5.14±0.33	4.21±0.31	3.77±0.22
1.5	2.1±0.32	1.64±0.32	1.57±0.32	7.22±0.34	5.82±0.62	5.15±0.31
2	2.46±0.43	1.85±0.33	1.76±0.33	9.29±0.68	7.43±0.73	6.53±0.62
3	2.83±0.32	2.06±0.35	1.95±0.35	11.36±0.77	9.03±0.77	7.91±0.73
4	3.19±0.22	2.27±0.35	2.14±0.35	13.43±0.79	10.64±0.75	9.3±0.77
6	3.56±0.32	2.49±0.36	2.33±0.68	15.51±0.81	12.25±0.81	10.68±0.75
8	3.92±0.33	2.7±0.54	2.52±0.77	17.58±0.83	13.85±0.82	12.06±0.81
10	4.29±0.35	2.91±0.85	2.7±0.74	19.65±0.86	15.46±0.84	13.44±0.82
12	4.65±0.35	3.12±0.77	2.89±0.79	21.72±0.88	17.06±0.89	14.83±0.84
14	5.02±0.36	3.33±0.8	3.08±0.85	23.79±0.79	18.67±0.75	16.21±0.77
18	5.38±0.34	3.55±0.83	3.27±0.77	25.87±0.85	20.28±0.8	17.59±0.83
24	5.75±0.34	3.76±0.81	3.46±0.8	27.94±0.92	21.88±1.17	18.97±1.19
48	6.11±0.35	3.97±0.82	3.65±0.83	30.01±1.01	23.49±1.34	20.36±1.44
72	6.68±0.35	4.18±0.84	3.67±0.85	30.04±1.44	23.52±1.52	20.39±1.48

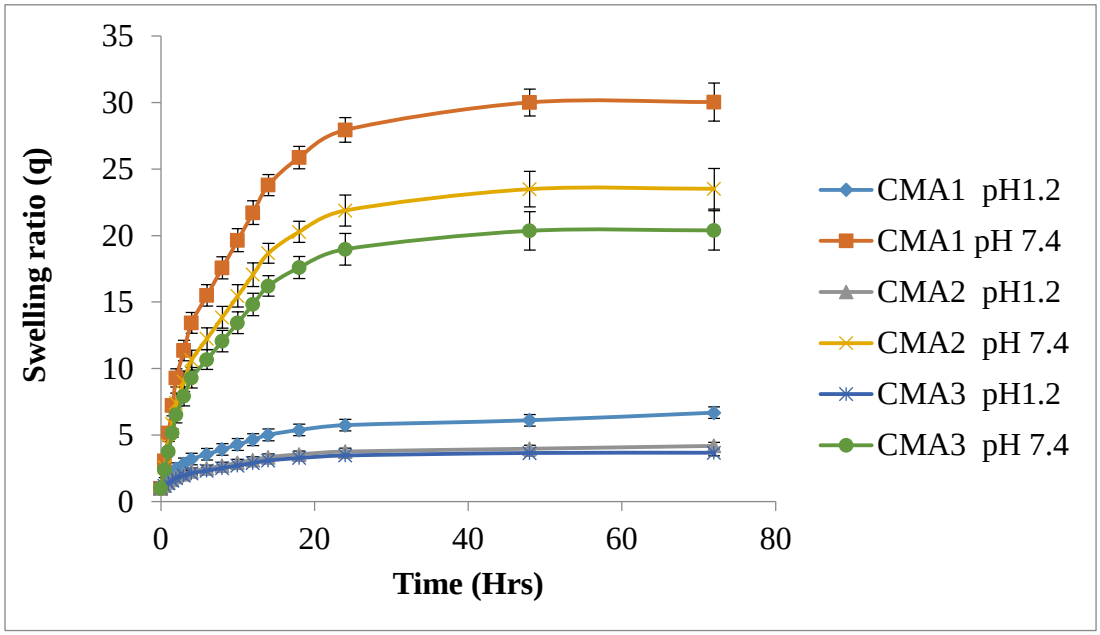

Figure 4.4.1: Comparative swelling ratios of CMC-g-MAA hydrogels using different concentrations of MAA

Table 4.4.2: Comparative swelling ratios of CMC-g-MAA hydrogels using different concentrations of CMC

Time (Hrs)	**Swelling ratio (q) at pH 1.2**			**Swelling ratio (q) at pH 7.4**		
	CMA4	CMA 5	CMA 6	CMA 4	CMA 5	CMA 6
0	1	1	1	1	1	1
0.5	1.37±0.23	1.37±0.19	1.65±0.22	2.78±0.24	2.71±0.21	2.68±0.2
1	1.74±0.22	1.74±0.22	2.31±0.24	4.6±0.33	4.41±0.31	4.35±0.22
1.5	2.11±0.32	2.11±0.32	2.96±0.32	6.42±0.34	6.12±0.62	6.03±0.31
2	2.48±0.43	2.47±0.22	3.62±0.33	8.24±0.68	7.82±0.73	7.7±0.62
3	2.85±0.32	2.84±0.32	4.27±0.35	10.06±0.77	9.53±0.31	9.38±0.73
4	3.22±0.22	3.21±0.33	4.93±0.35	11.88±0.79	11.24±0.62	11.05±0.77
6	3.59±0.32	3.58±0.36	5.58±0.68	13.7±0.81	12.94±0.73	12.73±0.75
8	3.96±0.33	3.95±0.54	6.23±0.77	15.52±0.83	14.65±0.77	14.4±0.81
10	4.32±0.35	4.32±0.85	6.89±0.74	17.34±0.86	16.35±0.84	16.08±0.81
12	4.69±0.35	4.68±0.77	7.54±0.79	19.16±0.88	18.06±0.89	17.76±0.83
14	5.06±0.77	5.05±0.8	8.2±0.85	20.98±0.89	19.77±0.75	19.43±0.86
18	5.43±0.8	5.42±0.83	8.85±0.77	22.79±0.75	21.47±0.8	21.11±0.83
24	5.8±0.83	5.79±0.81	9.51±0.8	24.61±0.8	23.18±1.17	22.78±1.19
48	6.17±0.81	7.46±0.82	10.16±0.83	26.43±1.17	24.88±1.24	24.46±1.33
72	6.2±0.81	7.66±0.84	10.81±0.85	26.45±1.34	24.89±1.42	24.49±1.38

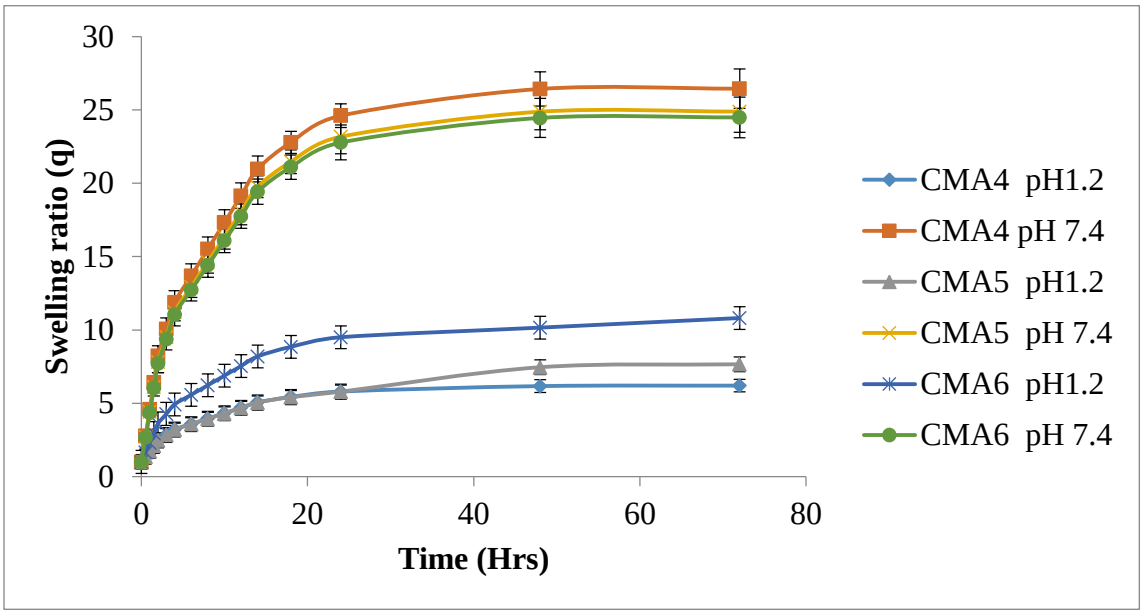

Figure 4.4.2: Comparative swelling ratios of CMC-g-MAA hydrogels using different concentrations of CMC

Table 4.4.3: Comparative swelling ratios of CMC-g-MAA hydrogels using different concentrations of crosslinker (n=3)

Time (Hrs)	**Swelling ratio (q) at pH 1.2**			**Swelling ratio (q) at pH 7.4**		
	CMA7	CMA 8	CMA 9	CMA 7	CMA 8	CMA 9
0	1	1	1	1	1	1
0.5	1.31±0.23	1.15±0.19	1.2±0.22	3.25±0.24	1.93±0.21	1.73±0.2
1	1.63±0.22	1.3±0.22	1.33±0.24	4.46±0.33	2.82±0.31	2.44±0.22
1.5	1.94±0.32	1.44±0.32	1.46±0.32	5.66±0.34	3.71±0.62	3.15±0.31
2	2.25±0.43	1.59±0.33	1.59±0.33	6.87±0.68	4.6±0.73	3.86±0.62
3	2.57±0.32	1.74±0.35	1.72±0.35	8.07±0.77	5.49±0.77	4.57±0.73
4	2.88±0.22	1.89±0.35	1.85±0.35	9.28±0.79	6.38±0.75	5.28±0.77
6	3.19±0.32	2.04±0.36	1.97±0.68	10.48±0.81	7.27±0.73	6±0.75
8	3.51±0.33	2.18±0.54	2.1±0.77	11.69±0.83	8.16±0.77	6.71±0.81
10	3.82±0.35	2.33±0.85	2.23±0.77	12.9±0.86	9.05±0.75	7.42±0.82
12	4.13±0.35	2.48±0.77	2.36±0.68	14.1±0.88	9.94±0.89	8.13±0.84
14	4.45±0.36	2.63±0.68	2.49±0.65	15.31±0.79	10.83±0.75	8.84±0.77
18	4.76±0.34	2.78±0.77	2.62±0.77	16.51±0.85	11.72±0.8	9.55±0.89
24	5.07±0.34	2.92±0.74	2.75±0.8	17.72±0.92	12.61±1.17	10.26±0.75
48	5.39±0.35	3.07±0.79	2.87±0.73	18.92±1.01	13.5±1.34	10.97±0.8
72	5.39±0.35	3.09±0.75	2.9±0.75	18.96±1.44	13.66±1.32	10.99±1.18

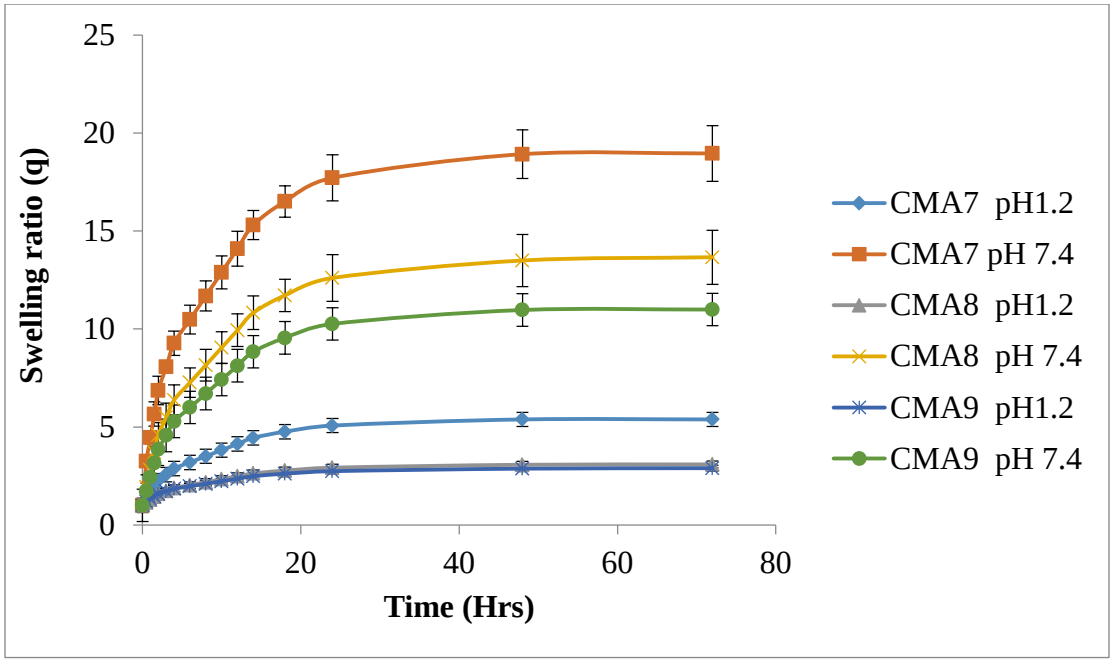

Figure 4.4.3: Comparative swelling ratios of CMC-g-MAA hydrogels using different concentrations of MBA (crosslinker)

4.4.3: Pulsatile behavior of hydrogel

Transition of the swelling/de-swelling behavior was proved by recurrently cycling the CMC-g-MAA hydrogel (CMA6) between buffers at pH 1.2 and pH 7.4. As shown in Figure 4.4.4, the hydrogel quickly constricted when placed in a pH 1.2 buffer but slowly resumed to nearly the original swollen size at pH 7.4.

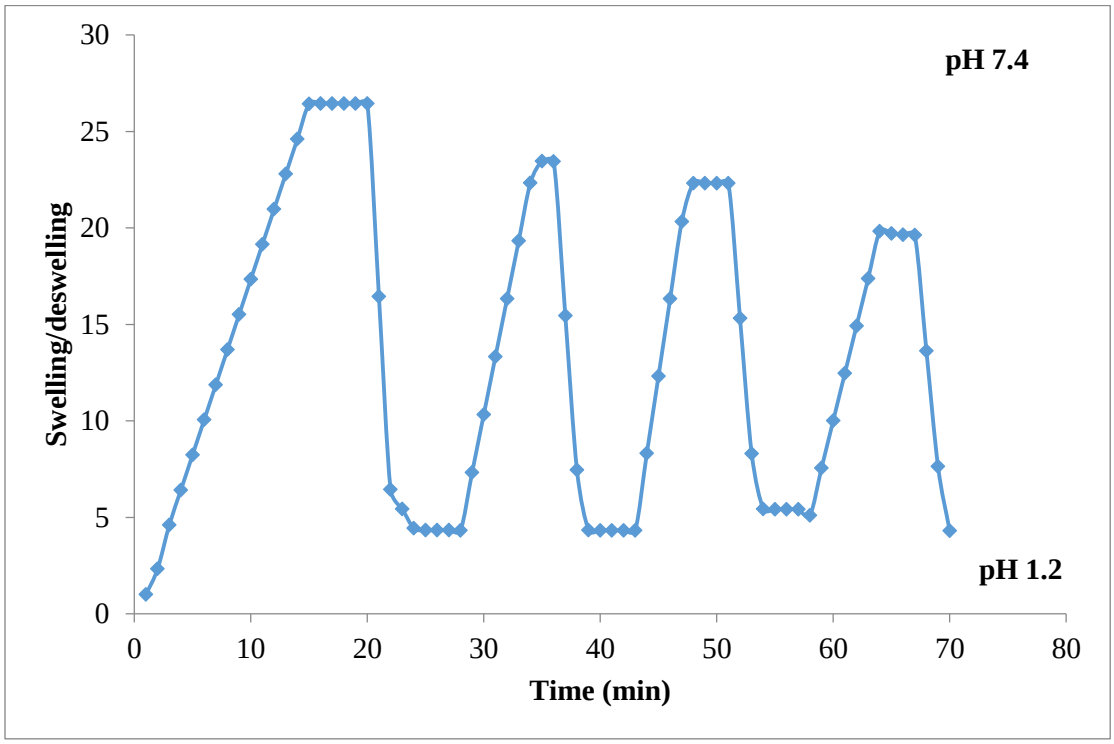

Figure 4.4.4: On-off switching behavior as reversible pulsatile swelling (pH 7.4) and deswelling (pH 1.2) of CMC-g-MAA hydrogel

4.4.3: Equilibrium water contents and gel fraction

Water absorbed by CMC-g-MAA copolymeric hydrogels was quantitatively signified by the equilibrium water content (EWC). EWC values of the hydrogels were calculated and tabulated in Table 4.4.4. By extraction of prepared hydrogels insoluble part (gelled part) was collected and washed with water to remove unreacted contents. Calculated gel fraction of hydrogel was summarized in Table 4.4.4.

Table 4.4.4: Equilibrium water contents and gel fraction of CMC-g-MAA hydrogels using different concentrations of MAA, CMC and crosslinker

Formulation code	Contents w/w %	EWC	Gel fraction (%)	Amount of Rabeprazole sodium loaded (mg per 0.4 g of dry disk)	
				By extraction	By weight
CMA1	MAA 20	0.96	67.41	48	49.3
CMA 2	MAA 30	0.93	88.45	45	45.9
CMA 3	MAA 35	0.90	92.33	41	41.7
CMA 4	CMC 1	0.95	89.54	52	52.8
CMA 5	CMC 1.5	0.96	92.65	59	60.2
CMA 6	CMC 2	0.97	74.14	66	67.3
CMA 7	MBA 0.45	0.89	84.64	39	39.4
CMA 8	MBA 0.65	0.86	86.38	37	38
CMA 9	MBA 0.85	0.66	93.75	34	35

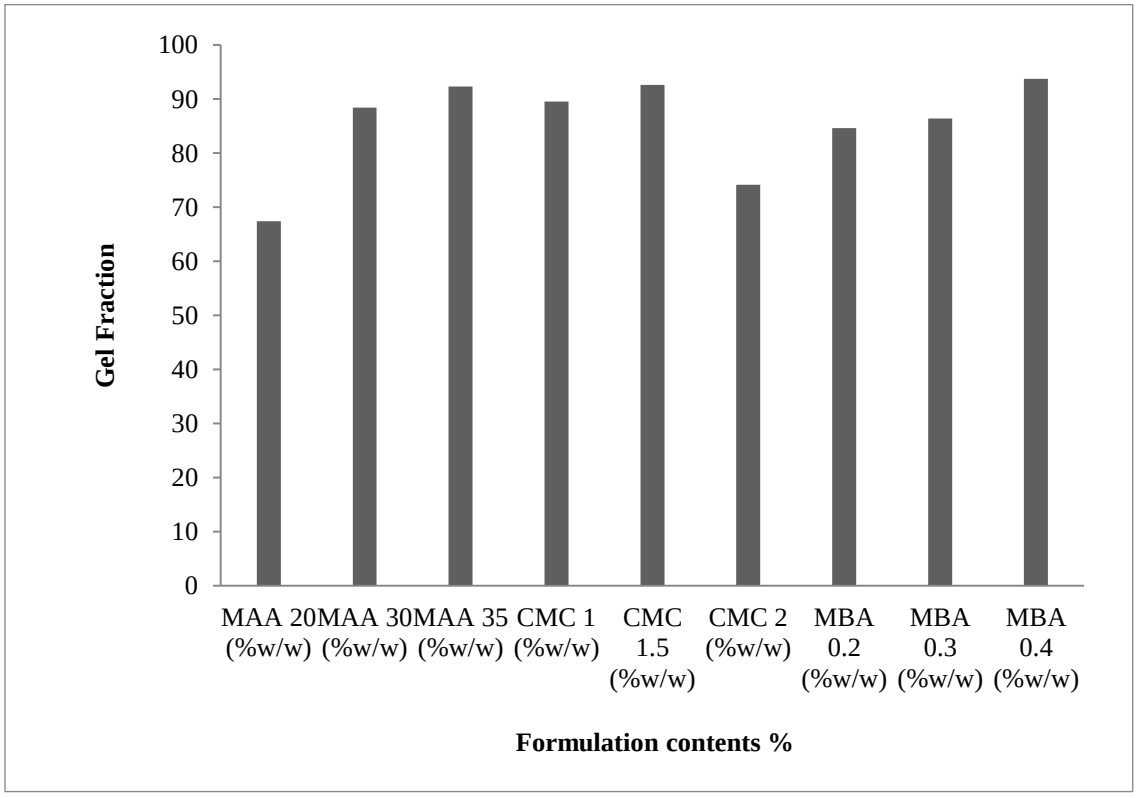

Figure 4.4.5: Gel fraction of CMC-g-MAA hydrogel with different concentrations of MAA, CMC and crosslinker

4.4.4: *Instrumental analysis*

a) Scanning electron microscopy

SEM images deliver evidence about pore size and geometry and homogeneity/heterogeneity of graft copolymeric network. SEM images of CMC-g-MAA hydrogels were presented in Figure 4.4.6.

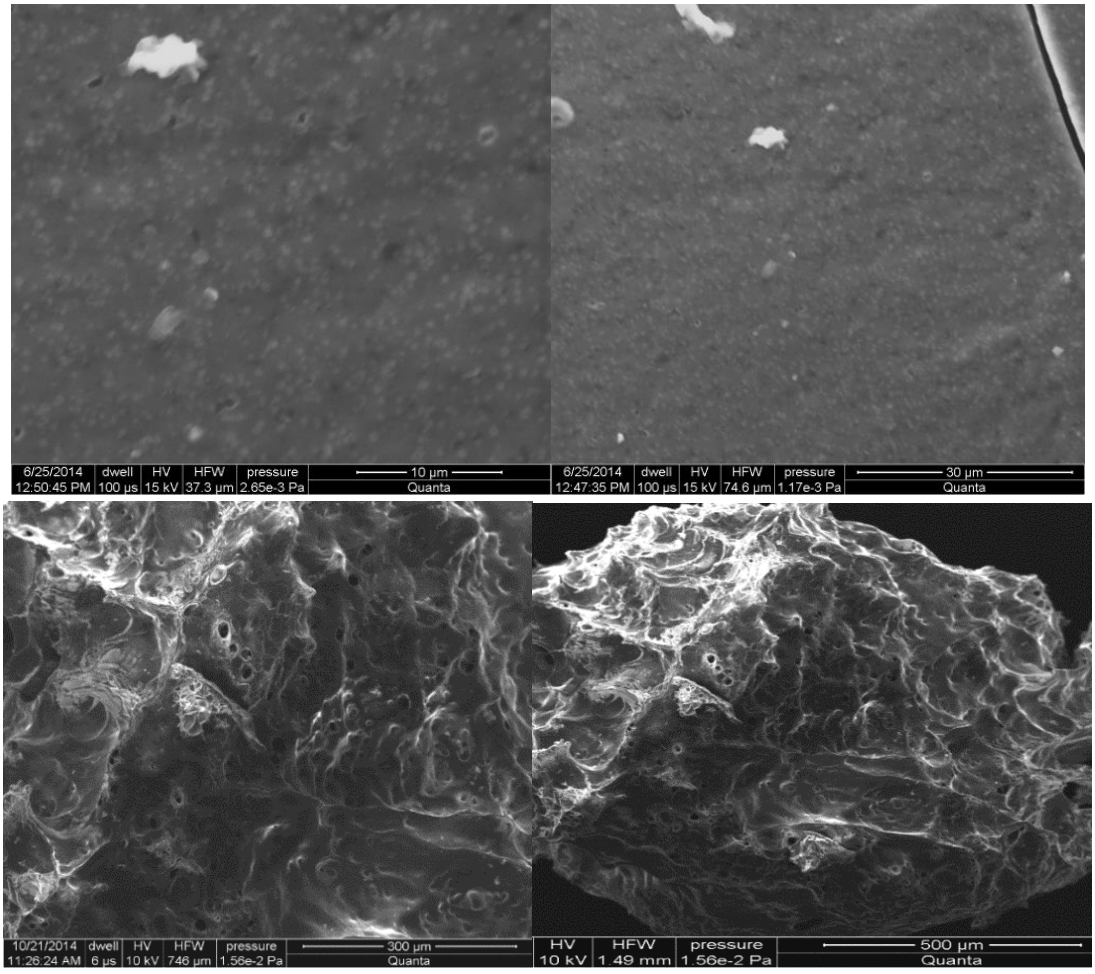

Figure 4.4.6: SEM images of lyophilized hydrogels (CMC-g-MAA) at magnification of 100 X and 200 X and 10µ, 30µ, 300µ, and 500µ scale bar respectively

b) FTIR analysis

The chemical structures for new CMC-g-MAA hydrogels and their individual components were confirmed by FTIR analysis. FTIR spectra of CMC (carboxymethyle cellulose), MAA (methacrylic acid) and CMA (formulation) shown in Figure 4.4.7 confirmed that modifications of CMC with methacrylic acid by grafting.

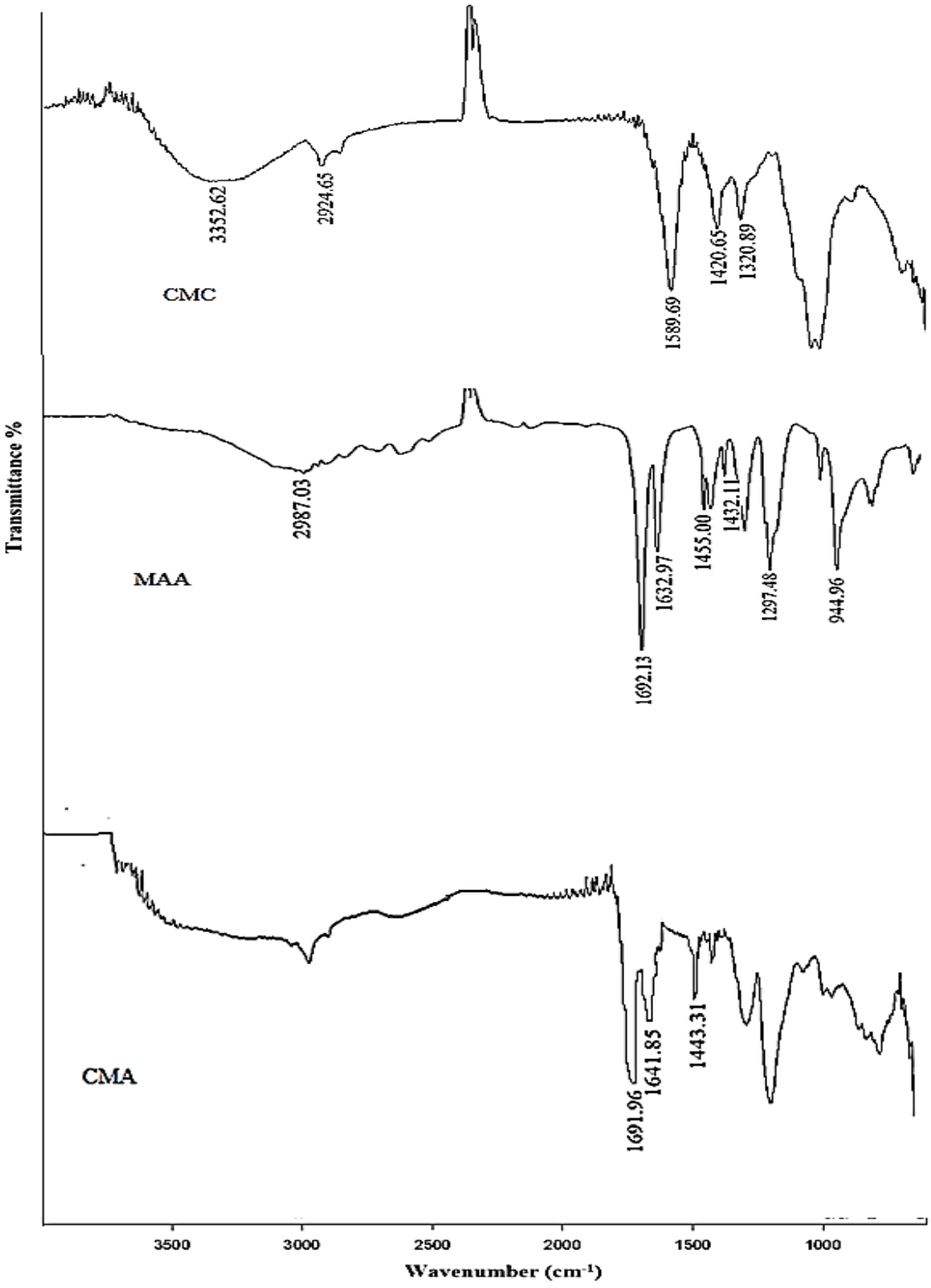

Figure 4.4.7: FTIR spectra of CMC, MAA, and prepared hydrogel (CMA)

c) Thermal analysis

Thermal stability of the copolymer (CMA) and individual constituents CMC and methacrylic acid were studied by TGA analyzer in the temperature range from 0 ºC to 600 ºC under inert nitrogen atmosphere. DTG data was summarized in Table 4.4.5. TGA curve of CMC (carboxymethyl cellulose), MAA (methacrylic acid) and CMA (CMC-g-MAA) hydrogel formulation depicted in Figure 4.4.8. DSC curve of CMC, MAA and CMA hydrogel formulation described in Figure 4.4.9.

Table 4.4.5: DTG data of methacrylic acid (MAA), CMC and CMC-g-MAA hydrogel (CMA)

Sample	Step	Tdi (°C)	Tdm (°C)	Tdf (°C)	Weight loss % at Tdf
CMA	1	67	91	130	8.8
	II	447	460	531	21.79
MAA	I	48	130	144	97.02
CMC	I	51	67	89	4.76
	II	255	290	314	36.08

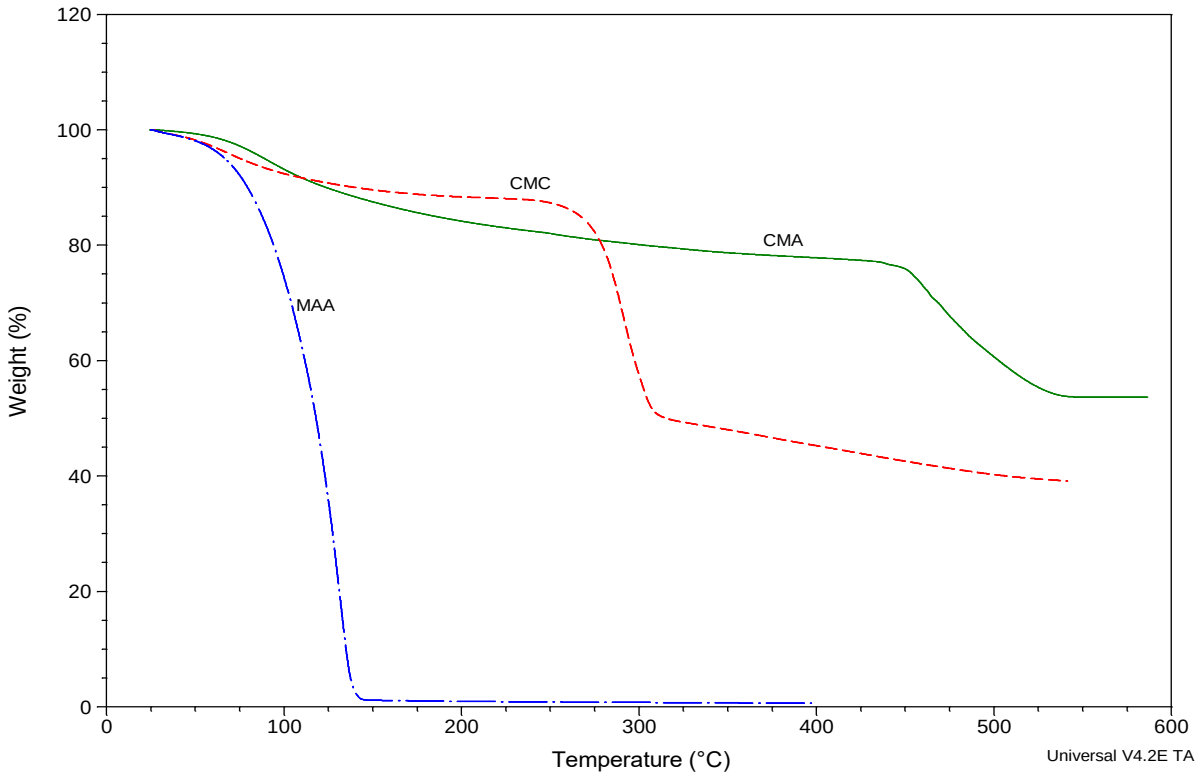

Figure 4.4.8:TGA curves of methacrylic acid (MAA), CMC and CMC-g-MAA(CMA)

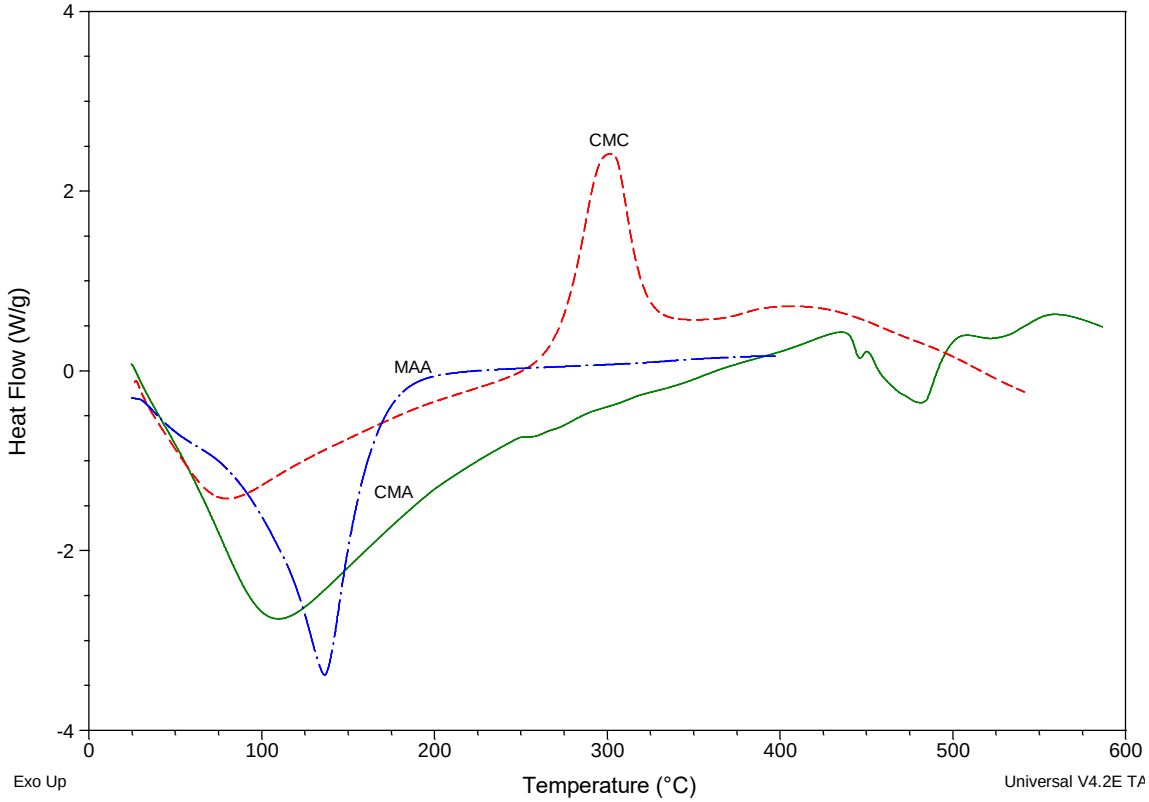

Figure 4.4.9: DSC curves of methacrylic acid (MAA), CMC and CMC-g-MAA

4.4.5:In vitro release kinetics of Rabeprazole sodium from CMC-g-MAA hydrogel

Release of rabeprazole sodium from CMC-g-MAA was carried out at acidic and basic pH to evaluate the pH sensitive release. Effect of methacrylic acid on cumulative release of rabeprazole sodium was described in Table 4.4.6. Effect of CMC and crosslinker (MBA) on drug release was demonstrated in Table 4.4.7 and 4.4.8 respectively. Release kinetics of drug can be determined by fitting *in vitro* release data into mathematical release models and calculate diffusion exponent 'n' to find out the release pattern of drug from hydrogel given in Table 4.4.9.

Table 4.4.6: Effect of methacrylic acid concentration on cumulative percent drug release of Rabeprazole sodium from CMA hydrogel

Time (hr)	CMA1 pH1.2	CMA2 pH1.2	CMA3 pH1.2	CMA1 pH 8	CMA2 pH 8	CMA3 pH 8
0.5	1.67±0.43	0.93±0.24	1.26±0.76	4.66±1.23	4.24±1.11	4.68±1.31
1	2.15±0.56	1.32±0.45	1.68±0.54	7.87±1.98	5.56±1.87	6.64±1.45
1.5	2.61±0.34	1.71±0.33	2.09±0.76	10.93±1.31	8.03±1.67	10.71±1.76
2	3.08±0.21	2.10±0.34	2.49±0.56	14.89±1.45	10.48±1.98	13.68±2.00
3	4.12±0.11	2.74±0.92	2.89±0.98	18.82±1.76	14.08±2.01	20.46±1.78
4	5.15±0.76	3.37±0.13	3.29±0.45	24.23±2.00	18.54±2.47	24.96±2.56
6	6.06±0.54	4.13±0.35	3.68±0.56	31.67±2.98	26.44±3.91	31.30±3.09
8	6.95±0.76	4.88±0.49	4.07±0.34	36.62±2.65	32.23±2.98	37.69±2.88
12	8.07±0.88	5.62±0.13	4.46±0.21	44.49±3.23	39.59±3.01	45.06±2.66
16	9.29±0.34	6.36±0.28	4.84±0.23	56.18±2.88	48.66±3.41	52.56±2.76
20	10.27±0.12	7.08±0.99	5.21±0.76	64.01±2.66	57.65±2.99	59.47±3.02
24	11.69±0.23	7.80±0.23	5.59±0.23	71.85±2.76	66.78±3.11	63.11±3.41

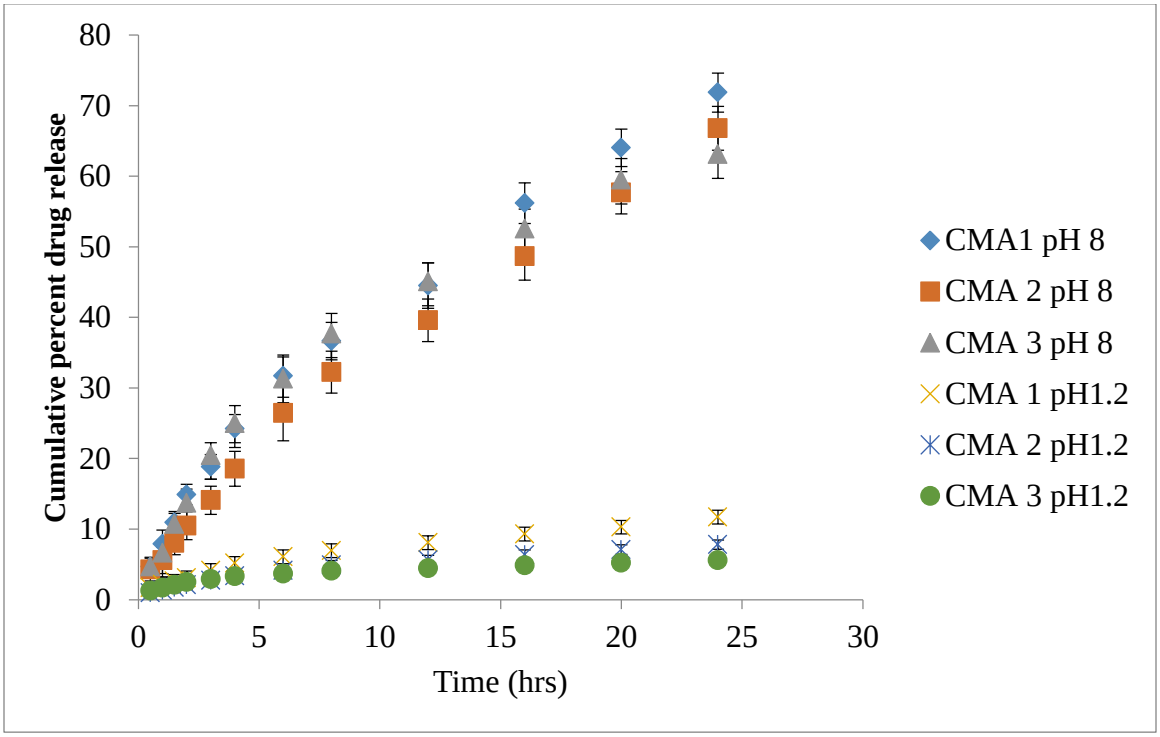

Figure 4.4.10: Effect of methacrylic acid concentration on cumulative percent drug release of Rabeprazole sodium

Table 4.4.7: Effect of CMC concentration on cumulative percent drug release of Rabeprazole sodium from hydrogel CMA

Time (hr)	CMA 4 pH1.2	CMA5 pH1.2	CMA 6 pH1.2	CMA4 pH 8	CMA5 pH 8	CMA6 pH 8
0.5	1.84±0.35	1.91±0.27	1.41±0.67	5.31±1.43	5.48±1.35	5.42±1.46
1	2.14±0.73	2.24±0.39	1.93±0.29	7.24±1.49	7.47±1.67	8.01±1.25
1.5	2.44±0.21	2.73±0.33	2.58±0.35	10.05±1.66	9.66±1.67	9.97±1.76
2	2.73±0.19	3.21±0.41	3.09±0.73	12.83±2.64	11.83±2.88	11.90±2.52
3	3.52±0.34	3.92±0.77	3.65±0.21	19.18±3.26	17.16±2.85	16.44±2.78
4	4.60±0.11	4.80±0.29	4.51±0.19	26.38±3.86	21.23±1.35	20.72±2.56
6	5.67±0.83	5.91±0.34	5.21±0.23	33.32±2.88	30.81±3.12	29.86±3.09
8	6.73±0.68	7.170.73	5.9±0.12	40.77±2.85	37.92±2.68	39.00±2.88
12	7.78±0.76	8.49±0.21	6.59±0.73	50.11±1.35	47.33±3.21	46.90±2.66
16	8.82±0.41	9.80±0.19	7.27±0.21	57.90±1.67	56.66±3.51	55.14±2.88
20	9.94±0.23	11.50±0.76	8.08±0.19	65.21±1.67	66.83±2.49	63.36±2.85
24	11.34±0.31	13.80±0.87	9.03±0.34	73.59±1.98	75.88±3.71	75.01±1.35

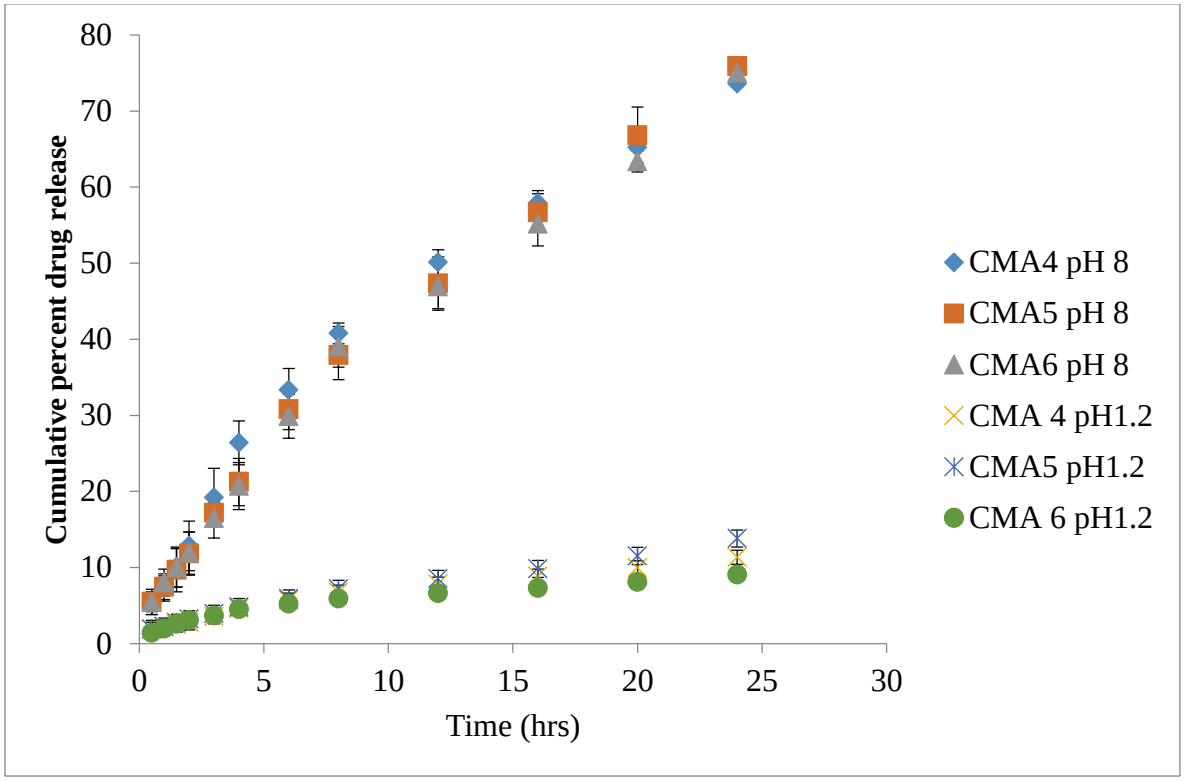

Figure 4.4.11: Effect of CMC concentration on cumulative percent drug release of Rabeprazole sodium

Table 4.4.8: Effect of crosslinker concentration on cumulative percent drug release of Rabeprazole sodium

Time (hr)	CMA7 pH1.2	CMA8pH1.2	CMA9 pH1.2	CMA7 pH 8	CMA8 pH 8	CMA9 pH 8
0.5	1.51±0.67	1.06±0.37	0.87±0.34	5.40±1.56	3.46±1.25	3.75±1.43
1	1.88±0.29	1.32±0.36	0.87±0.69	10.16±1.55	8.05±1.37	7.91±1.49
1.5	2.25±0.36	1.71±0.69	1.29±0.24	12.49±1.84	11.03±1.47	10.46±1.66
2	2.61±0.36	2.10±0.68	1.71±0.36	14.67±2.78	13.97±1.98	12.98±2.64
3	3.34±0.34	2.61±0.76	2.13±0.48	18.18±2.78	18.01±2.78	16.88±3.26
4	4.06±0.34	3.11±0.47	2.54±0.76	22.76±3.86	21.74±2.67	20.47±2.98
6	4.78±0.83	3.61±0.46	2.95±0.23	28.52±3.88	26.96±3.62	25.42±3.09
8	5.73±0.41	4.11±0.43	3.35±0.54	36.66±3.85	36.73±2.94	31.19±2.88
12	6.55±0.77	4.60±0.48	3.75±0.34	43.51±3.93	42.68±3.21	40.87±2.88
16	7.48±0.45	5.08±0.43	4.15±0.69	50.76±3.28	49.51±3.71	47.44±3.76
20	8.28±0.37	5.69±0.76	4.54±0.24	57.93±2.69	58.19±2.79	55.58±3.02
24	8.83±0.91	6.29±0.83	4.93±0.78	67.41±3.89	64.75±3.91	61.47±3.91

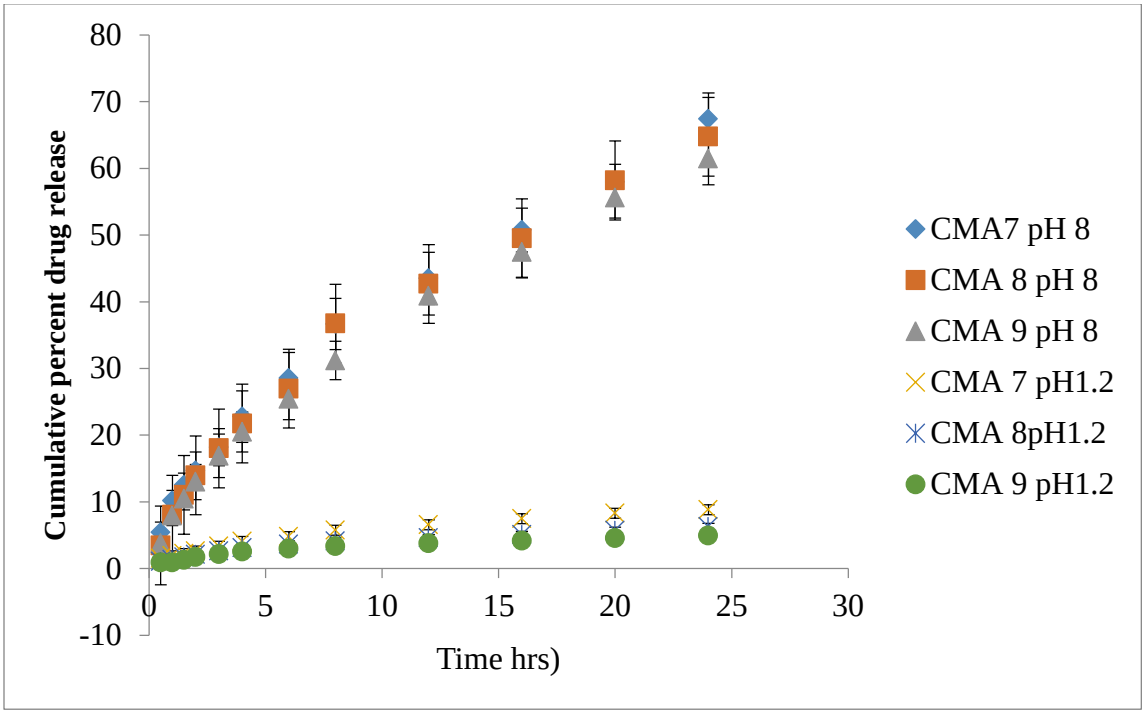

Figure 4.4.12: Effect of crosslinker concentration on cumulative percent drug release of Rabeprazole sodium

Table 4.4.9: Release kinetic parameters of Rabeprazole sodium from hydrogel CMA

Formulation code	***Higuchi***	***First order***	***Zero order***	***Korsmayer-peppas***	
	R^2	R^2	R^2	R^2	***n***
CMA1	0.997	0.567	0.971	0.995	0.604
CMA 2	0.992	0.639	0.982	0.993	0.783
CMA 3	0.994	0.541	0.936	0.996	0.439
CMA 4	0.996	0.572	0.954	0.988	0.598
CMA 5	0.993	0.613	0.980	0.994	0.718
CMA 6	0.990	0.618	0.987	0.997	0.774
CMA 7	0.996	0.540	0.971	0.994	0.711
CMA 8	0.997	0.560	0.962	0.992	0.654
CMA 9	0.998	0.575	0.974	0.992	0.631

4.5 Characterization of PEG-g-MAA hydrogels

4.5.1 Swelling studies at pH1.2 and pH 7.4

The reliance of the swelling aptitude of PEG-g-MAA hydrogels on PEG and methacrylic acid concentration was evaluated by preparation of hydrogels with varying contents of PEG and methacrylic acid at physiological temperature. Formulations were assigned codes (PMA1-PMA4) and (PMA5-PMA7) for varying concentration of PEG and methacrylic acid respectively. Effect of varying concentration of PEG on swelling ratio (q), PMA1 (1 to 4.854), PMA2 (1 to 4.438) and PMA3 (1 to 3.038) and PMA4 (1 to 2.692) in pH 1.2 and PMA1 (1 to 11.464), PMA2 (1 to 13.766), PMA3 (1 to 16.422) and PMA4 (1 to17.443) in 7.4 buffer solutions at 37 ºC has been given in Table 4.5.1 and graphically presented in Figure 4.5.1. Comparative swelling ratio (q) of hydrogels by using different concentrations of methacrylic acid, PMA5 (1 to 4.867), PMA6 (1 to 3.515) and PMA7 (1 to 2.212) at pH 1.2 and PMA5 (1 to 17.039), PMA6 (1 to 12.468) and PMA7 (1 to 10.765) at pH 7.4 were given in Table 4.5.2.

Table 4.5.1: Comparative swelling ratios of PEG-g-MAA hydrogels using different concentrations of PEG

Time (Hrs)	Swelling ratio (q) at pH 1.2				Swelling ratio (q) at pH 7.4			
	PMA1	PMA 2	PMA 3	PMA4	PMA 1	PMA 2	PMA 3	PMA4
0	1	1	1	1	1	1	1	1
0.5	1.23±0.23	1.2±0.19	1.12±0.22	1.1±0.24	1.62±0.21	1.75±0.2	1.91±0.21	1.97±0.23
1	1.45±0.22	1.4±0.22	1.24±0.32	1.2±0.33	2.23±0.31	2.5±0.22	2.81±0.32	2.93±0.83
1.5	1.68±0.32	1.61±0.32	1.36±0.43	1.3±0.34	2.85±0.62	3.25±0.34	3.72±0.86	3.9±0.86
2	1.91±0.43	1.81±0.22	1.48±0.32	1.4±0.68	3.46±0.73	4±0.68	4.63±0.83	4.87±0.88
3	2.13±0.32	2.01±0.32	1.6±0.35	1.5±0.77	4.08±0.31	4.76±0.77	5.54±0.86	5.84±1.38
4	2.36±0.22	2.21±0.33	1.72±0.35	1.6±0.79	4.69±0.62	5.51±0.77	6.44±0.88	6.8±1.44
6	2.59±0.32	2.42±0.36	1.84±0.68	1.7±0.81	5.31±0.73	6.26±0.75	7.35±1.38	7.77±1.17
8	2.81±0.33	2.62±0.35	1.96±0.77	1.8±0.83	5.92±0.77	7.01±0.81	8.26±1.17	8.74±1.44
10	3.04±0.35	2.82±0.68	2.08±0.74	1.9±0.86	6.54±0.84	7.76±0.81	9.16±1.24	9.71±1.41
12	3.27±0.35	3.02±0.77	2.2±0.79	2±0.88	7.16±0.89	8.51±0.83	10.07±1.42	10.67±1.48
14	3.49±0.35	3.22±0.74	2.32±0.85	2.1±0.89	7.77±0.75	9.26±0.86	10.98±1.41	11.64±0.8
18	3.72±0.68	3.43±0.79	2.44±0.77	2.19±0.75	8.39±0.8	10.01±0.83	11.89±1.34	12.61±1.17
24	3.95±0.77	3.63±0.81	2.56±0.8	2.29±0.8	9±1.17	10.76±0.86	12.79±1.46	13.57±1.24
48	4.4±0.74	4.03±0.82	2.8±0.83	2.49±1.17	10.23±1.24	12.26±0.88	14.61±1.26	15.51±1.42
72	4.85±0.79	4.44±0.84	3.04±0.85	2.69±1.34	11.46±1.42	13.77±1.38	16.42±1.39	17.44±2.17

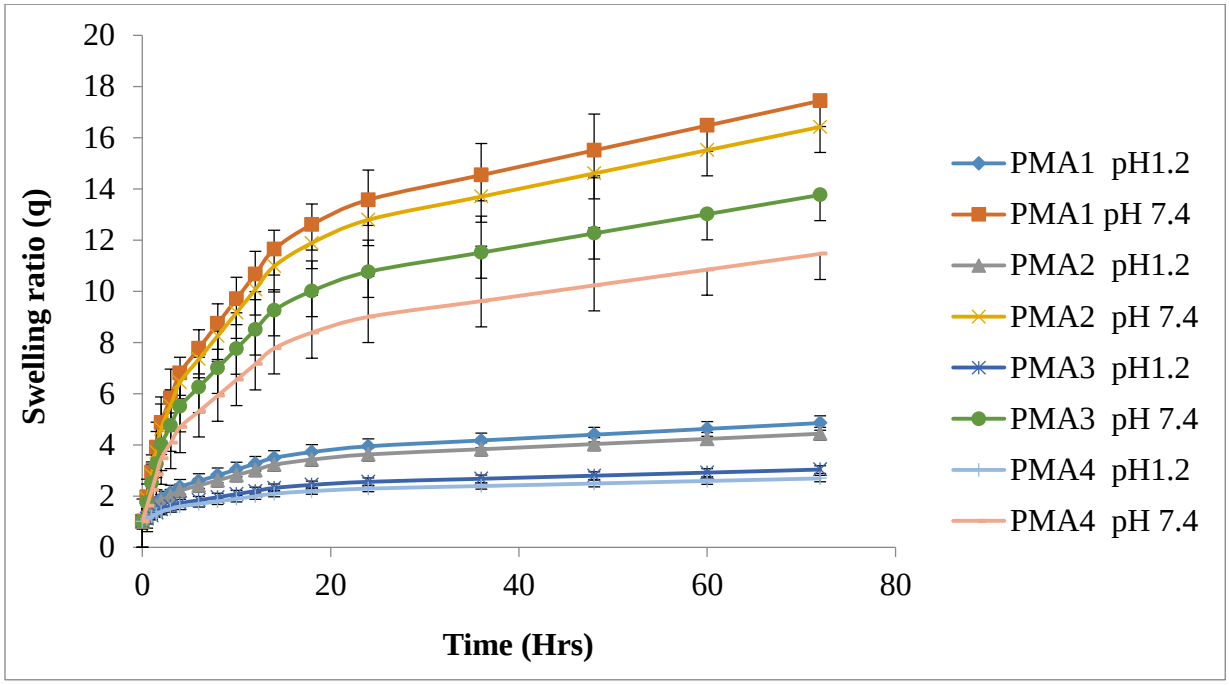

Figure 4.5.1: Comparative swelling ratio of PEG-g-MAA hydrogels using different concentrations of PEG

Table 4.5.2: Comparative swelling ratios of PEG-g-MAA (PMA) hydrogels using different concentrations of MAA

Time (Hrs)	**Swelling ratio (q) at pH 1.2**			**Swelling ratio (q) at pH 7.4**		
	PMA5	PMA6	PMA7	PMA5	PMA6	PMA7
0	1	1	1	1	1	1
0.5	1.23±0.23	1.15±0.22	1.07±0.22	1.94±0.24	1.68±0.21	1.57±0.2
1	1.46±0.22	1.3±0.32	1.14±0.24	2.89±0.33	2.35±0.31	2.15±0.22
1.5	1.68±0.32	1.44±0.43	1.21±0.32	3.83±0.34	3.02±0.62	2.72±0.31
2	1.91±0.43	1.59±0.32	1.29±0.33	4.77±0.68	3.7±0.73	3.3±0.62
3	2.14±0.32	1.74±0.35	1.36±0.35	5.72±0.77	4.37±0.31	3.87±0.73
4	2.37±0.22	1.89±0.35	1.43±0.35	6.66±0.79	5.05±0.62	4.45±0.62
6	2.59±0.32	2.04±0.68	1.5±0.68	7.6±0.81	5.72±0.73	5.02±0.73
8	2.82±0.33	2.18±0.77	1.57±0.77	8.55±0.83	6.4±0.77	5.6±0.75
10	3.05±0.35	2.33±0.74	1.64±0.74	9.49±0.86	7.07±0.84	6.17±0.75
12	3.28±0.35	2.48±0.83	1.71±0.79	10.44±0.88	7.75±0.89	6.74±0.8
14	3.5±0.77	2.63±0.86	1.78±0.85	11.38±0.89	8.42±0.75	7.32±1.17
18	3.73±0.8	2.78±0.88	1.86±0.77	12.32±0.75	9.1±0.8	7.89±0.83
24	3.96±0.83	2.92±0.8	1.93±0.8	13.27±0.8	9.77±1.17	8.47±1.19
48	4.41±0.81	3.22±0.83	2.07±0.83	15.15±1.17	11.12±1.24	9.62±1.33
72	4.87±0.81	3.52±0.85	2.21±0.85	17.04±1.34	12.47±1.42	10.77±1.38

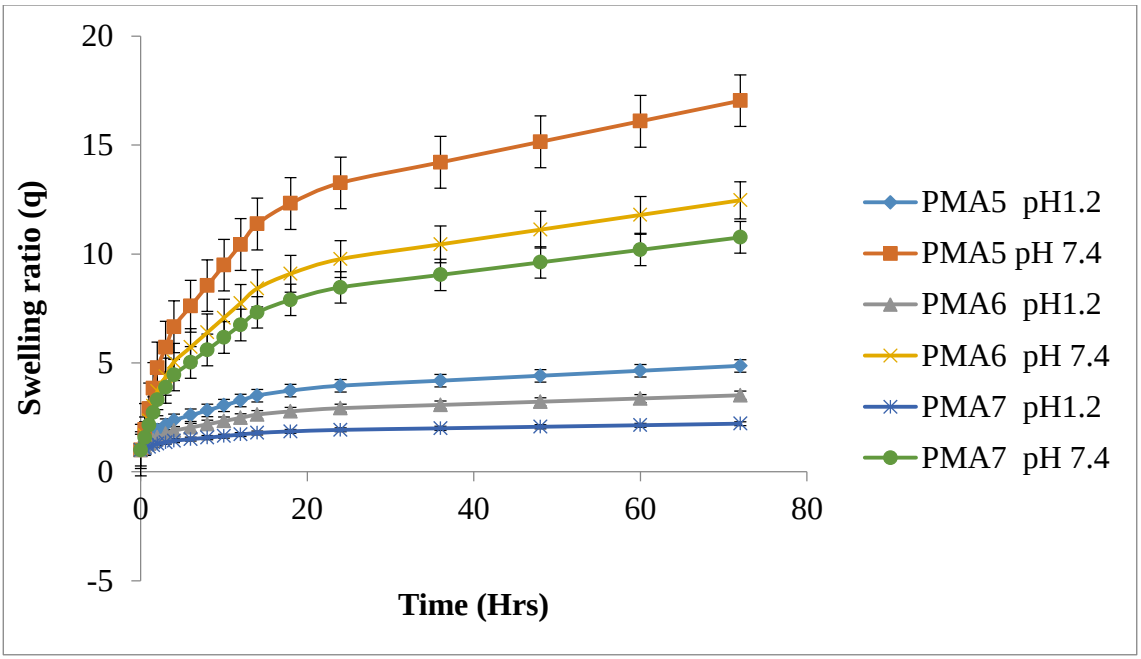

Figure 4.5.2: Comparative swelling ratios of PMA-g-MAA hydrogels using different concentrations of MAA

4.5.2: Pulsatile behavior of hydrogel

PEG-g-MAA hydrogels also showed reproducible swelling-deswelling cycles at pH levels of 1.2 and 7.4, as demonstrated in Figure 4.5.3. At pH 7.4, the hydrogel swelled due to anion-anion repulsive electrostatic forces, while, at pH 1.2, it shrank within a few minutes due to the protonation of the carboxylate groups of methacrylic acid. Hydrogel formulation exhibited maximum swelling ratio (q) was selected for evaluation of reproducible swelling behavior.

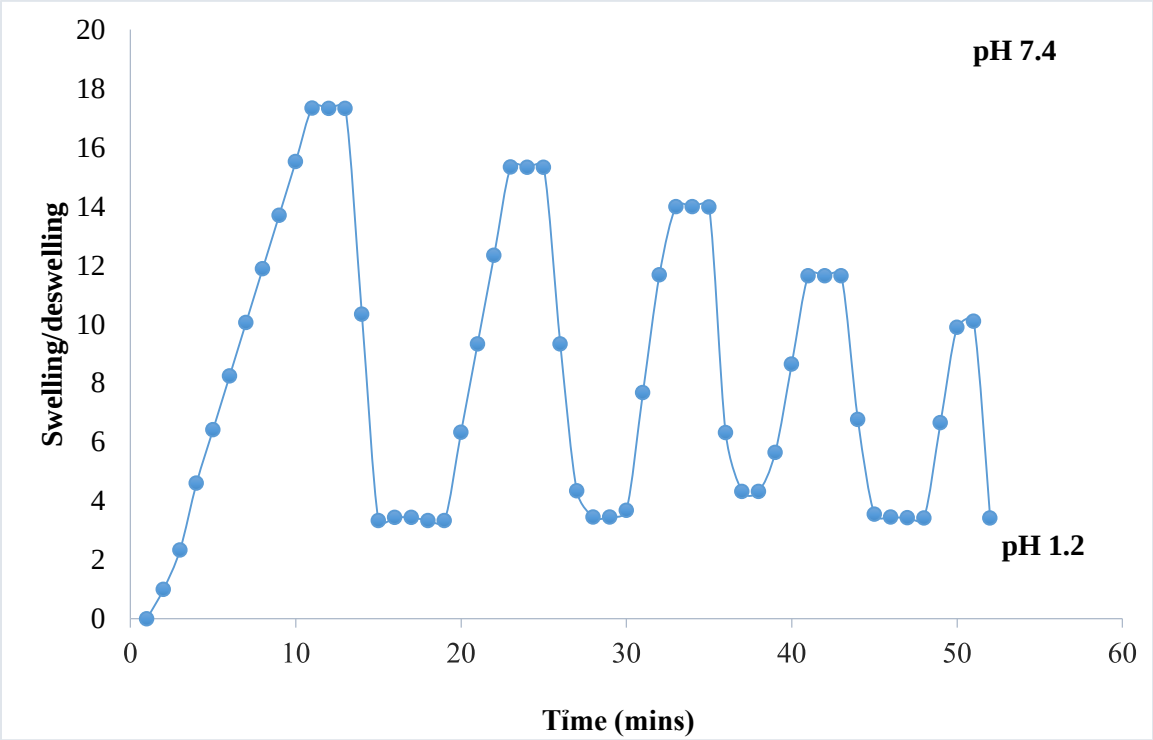

Figure 4.5.3: On-off switching behavior as reversible pulsatile swelling (pH 7.4) and deswelling (pH 1.2) of PEG-g-MAA hydrogel

4.5.3: Equilibrium water contents and gel fraction of hydrogels

Hydrogels were prepared in water and swollen to equilibrium in deionized water. Equilibrium water contents values were used for the determination of diffusional behavior of water. It was found that swelling of hydrogels dwindled with increasing methacrylic acid, and it increased with the increasing content of PEG in hydrogels as expressed in Table 4.5.3.

Table 4.5.3: Equilibrium water contents gel fraction and amount of drug loaded of PEG-g-MAA hydrogels using different concentrations of PEG and MAA

Formulation code	Contents w/w %	EWC	Gel fraction (%)	Amount of Rabeprazole sodium loaded (mg per 0.4 g of dry disk)	
				By extraction	By weight
PMA1	PEG 5	0.89	51.63	80	80
PMA2	PEG10	0.93	63.07	94.6	95
PMA3	PEG15	0.94	80.24	94	94.8
PMA4	PEG20	0.95	87.17	97	98
PMA5	MAA 20	0.95	63.88	75	76
PMA6	MAA 30	0.93	76.42	55	55.9
PMA7	MAA 35	0.91	82.68	47	47

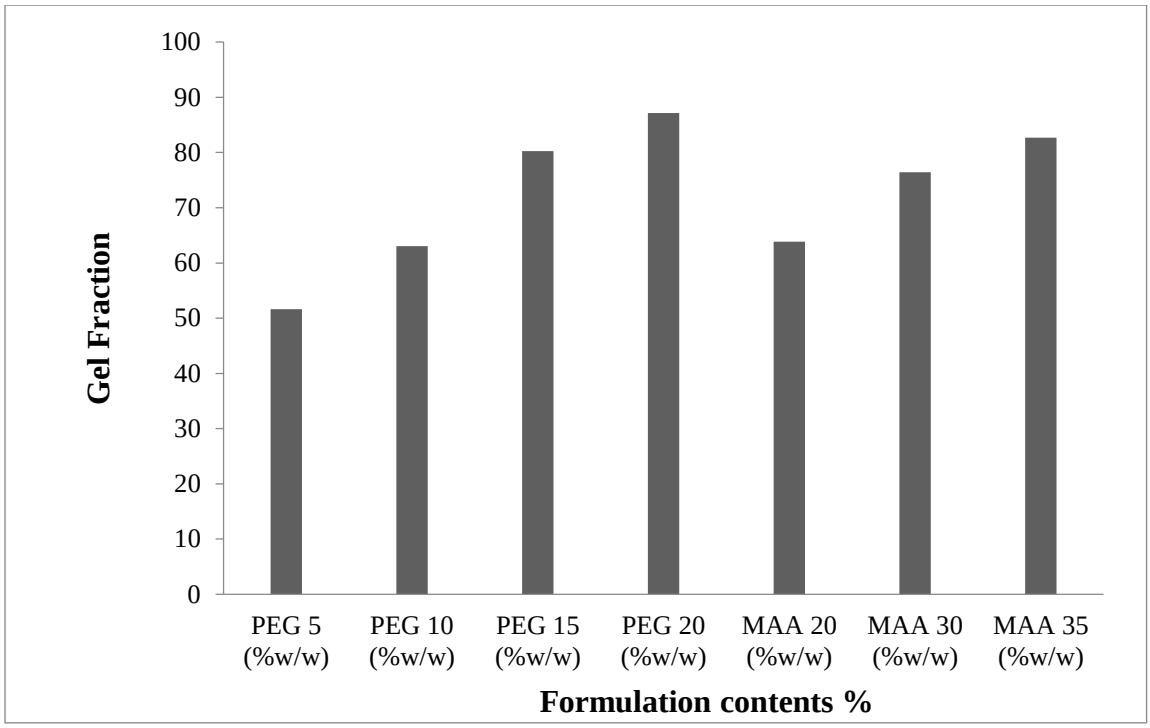

Figure 4.5.4: Gel fraction of PEG-g-MAA hydrogel with different concentrations of methacrylic acid and PEG

4.5.4 Instrumental analysis

a) *Scanning electron microscopy*

Micro porous structure of hydrogel dictate the drug release pattern. Surface morphology of hydrogel was examined by scanning electron microscopy. Microphotographs were presented in Figure 4.5.5.

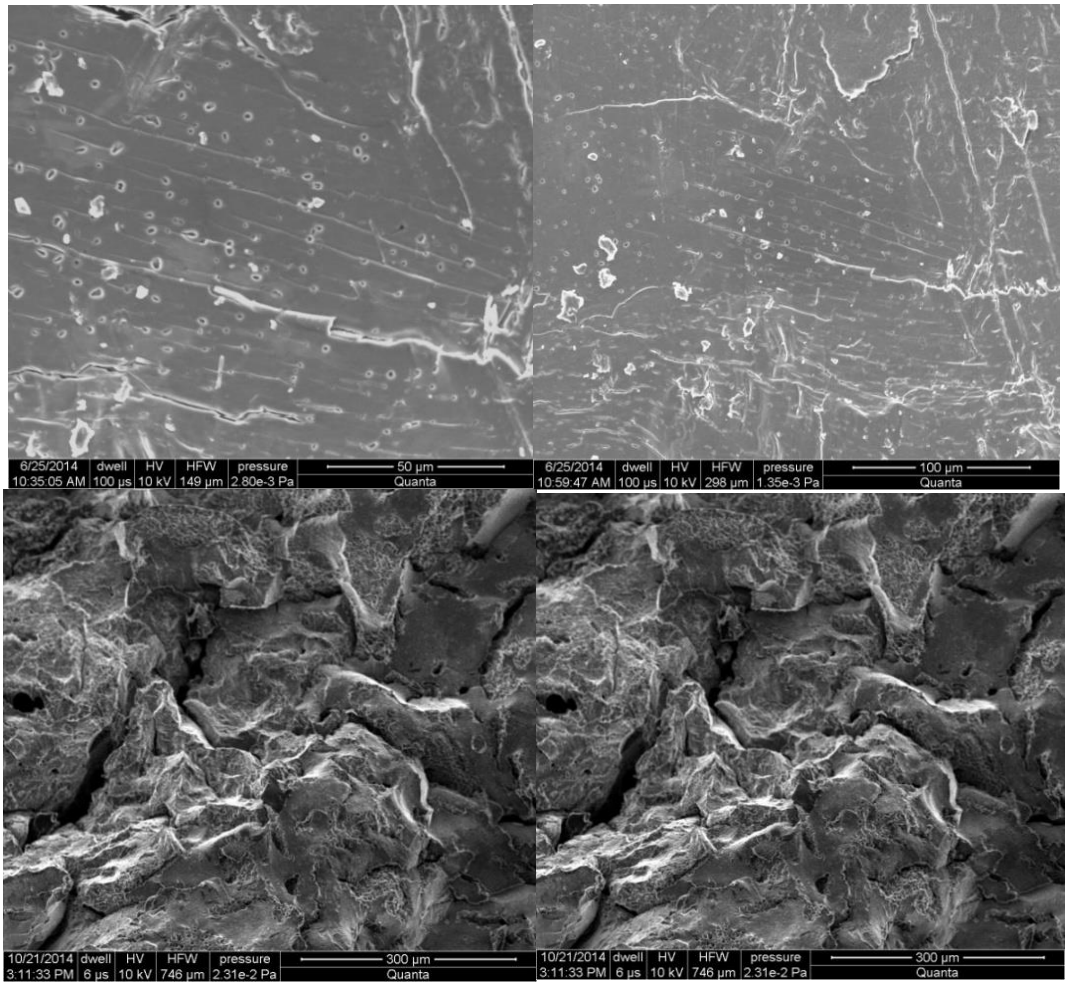

Figure 4.5.5: SEM images of lyophilized hydrogels (PEG-g-MAA) at magnification of 100 X and 200 X and 50µ, 100µ, 300µ, and 500µ scale bar respectively

b)FTIR spectrum analysis

FTIR spectrum analysis technique was used to evaluate the chemical structural changes in graft copolymer. Figure 4.5.5 exhibited the FTIR spectra of methacrylic acid(MAA), PEG (polyethylene glycol 600) and PMA hydrogel formulation.

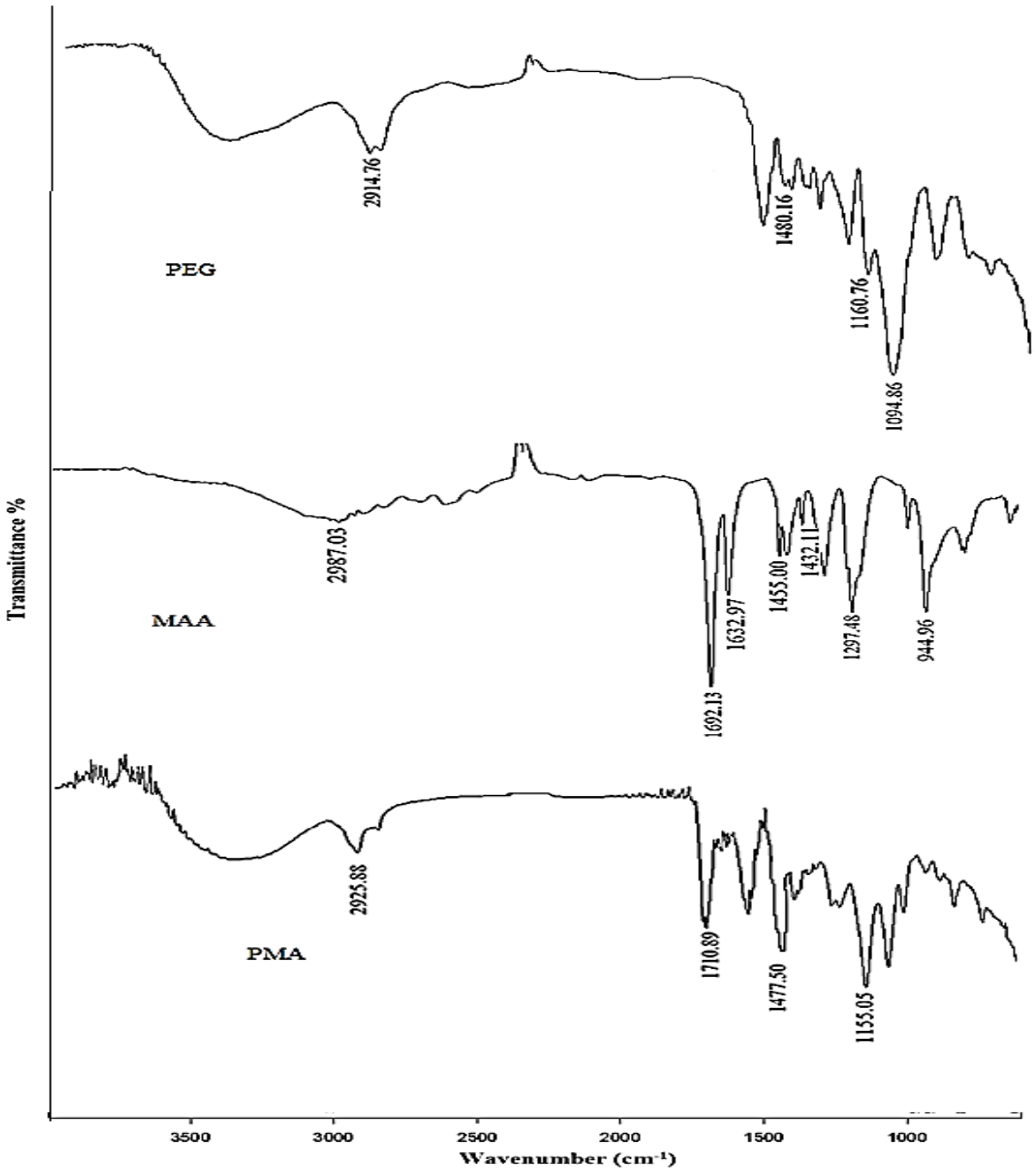

Figure 4.5.6:FTIR spectra of PEG, methacrylic acid (MAA) and prepared formulation (PMA)

c) Thermal analysis

The thermal properties of prepared hydrogel (PMA), and individual components (PEG and MAA) were studied by means of TGA and DSC analysis shown in Figure 4.5.6 and 4.5.7.

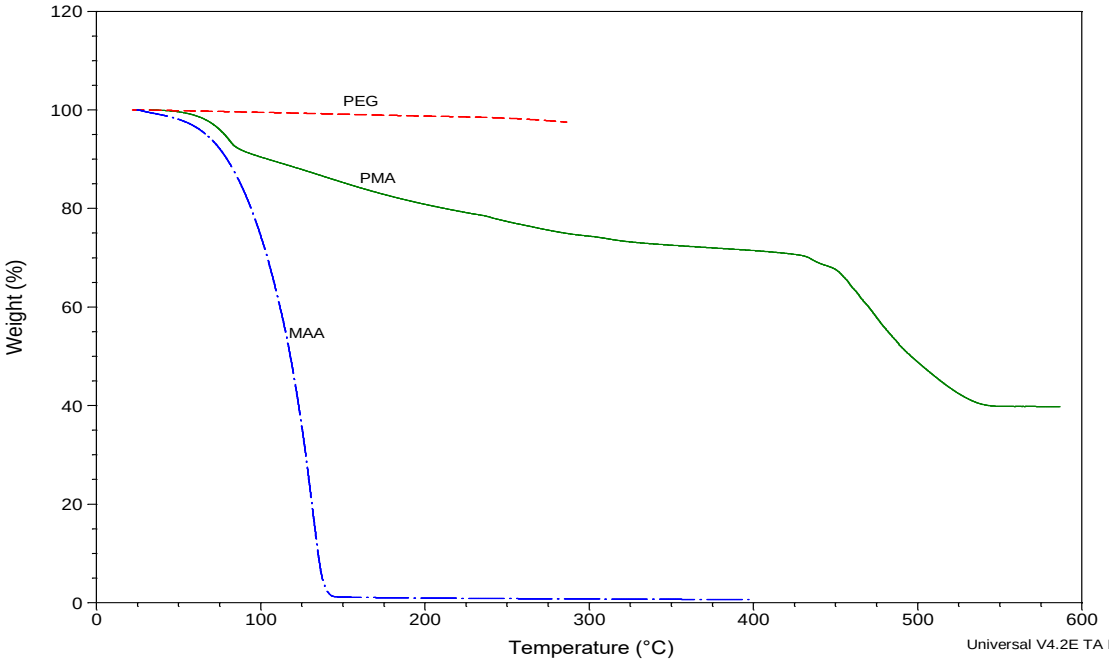

Figure 4.5.7: TGA curves of PEG, MAA, and PMA (PEG-g-MAA) hydrogel formulation

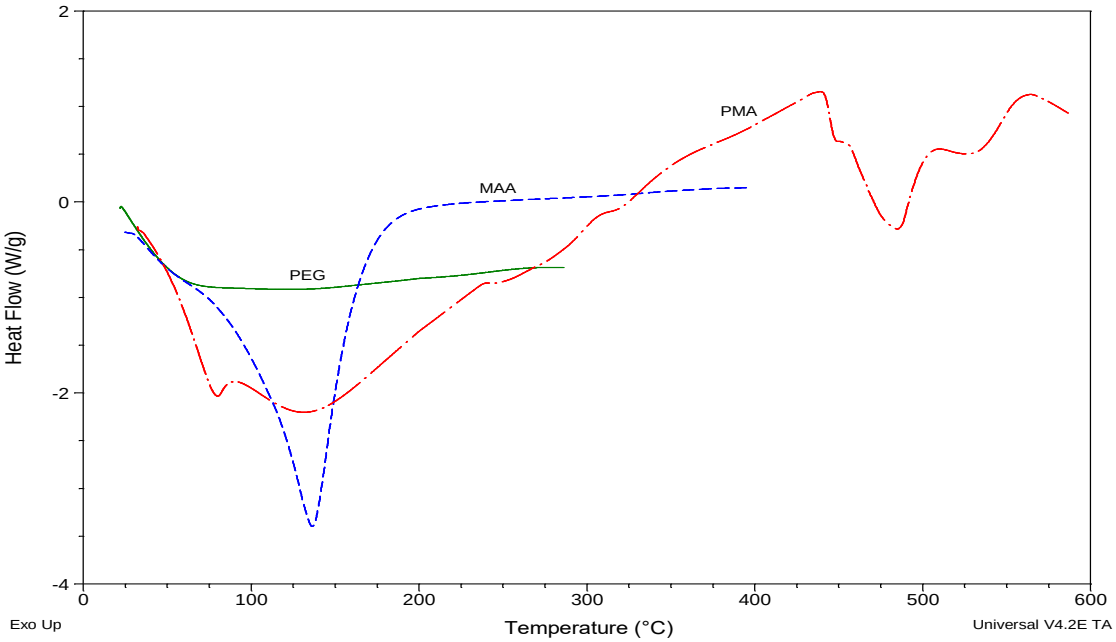

Figure 4.5.8: DSC curves of PEG, MAA, and PMA (PEG-g-MAA) hydrogel formulation

4.5.5: In vitro release kinetics of Rabeprazole sodium from PEG-g-MAA hydrogel

To evaluate the pH sensitive rabeprazole sodium release for controlled drug delivery from PEG-g-MAA hydrogel, *in vitro* drug release was estimated at acidic and basic pH at 37 ºC. Effect of hydrogel composition on cumulative percent drug release was examined and summarized in Table 4.5.4 and 4.5.5.

Table 4.5.4: Effect of PEG concentration on cumulative percent drug release of Rabeprazole sodium from hydrogel

Time (hr)	PMA1 pH 1.2	PMA2 pH 1.2	PMA3 pH 1.2	PMA4 pH 1.2	PMA1 pH 8	PMA2 pH 8	PMA3 pH 8	PMA4 pH 8
0.5	1.43±0.23	1.55±0.32	1.79±0.37	1.79±0.67	8.03±1.43	12.55±1.95	12.93±1.56	12.68±1.28
1	2.27±0.45	2.27±0.43	2.27±0.36	2.39±0.29	12.78±1.49	16.65±1.67	20.04±1.55	23.04±1.18
1.5	2.73±0.26	2.73±0.43	2.73±0.69	2.97±0.36	18.69±1.66	20.08±1.47	25.76±1.84	28.58±1.46
2	3.19±0.25	3.19±0.53	3.19±0.41	3.55±0.36	24.6±2.64	23.47±1.98	31.41±2.78	34.04±2.38
3	4.12±0.55	4.12±0.65	4.12±0.77	4.59±0.48	30.33±3.26	29.37±2.78	38.03±2.78	37.44±3.32
4	5.03±0.63	5.03±0.78	5.27±0.45	5.62±0.76	34.86±3.86	34.27±2.67	43.56±2.98	42.78±3.14
6	5.94±0.64	5.94±0.91	6.29±0.37	6.76±0.23	39.11±3.88	39.31±3.62	48.73±3.09	48.77±3.37
8	6.84±0.26	6.95±0.84	7.19±0.43	7.76±0.54	43.78±3.85	44.43±2.94	54±2.88	53.85±2.47
12	7.84±0.27	8.19±0.36	8.53±0.48	8.99±0.73	48.76±3.93	52.7±3.21	61.81±2.88	63.41±2.86
16	9.06±0.27	9.52±0.94	9.86±0.43	10.44±0.26	56.38±3.28	62.44±3.81	71.19±3.76	74.48±2.74
20	10.16±0.34	10.61±0.65	10.96±0.76	11.3±0.67	63.8±2.69	71.9±2.89	80.28±3.02	84.27±3.11
24	11.8±0.87	12.26±0.56	12.37±0.83	13.28±0.78	73.76±3.89	83.16±3.91	91.29±3.91	93.84±2.69

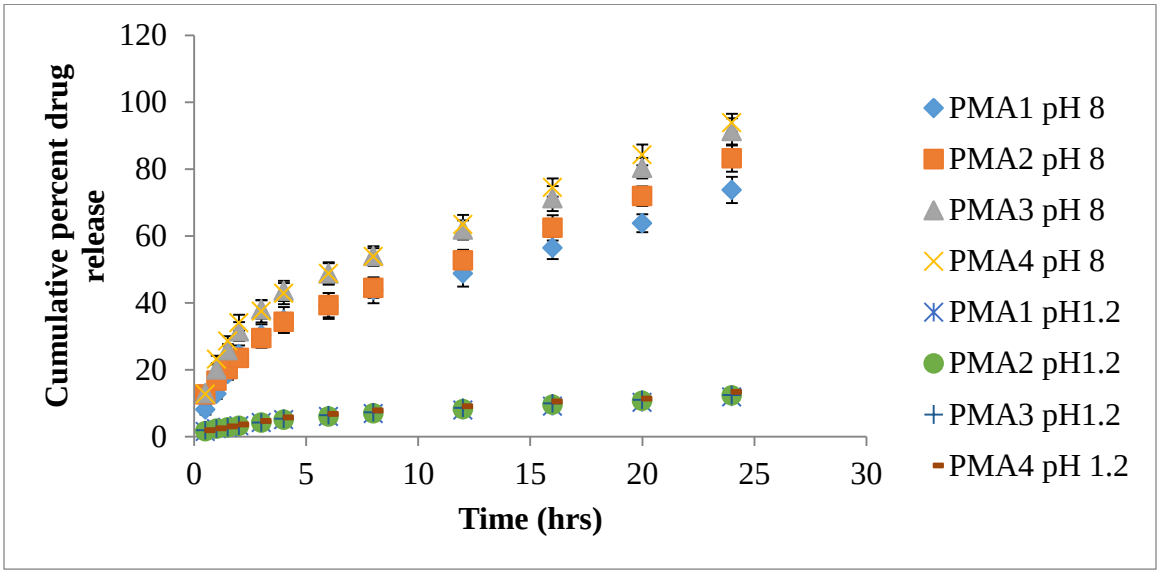

Figure 4.5.9: Effect of PEG concentration on cumulative percent drug release of Rabeprazole sodium from hydrogel PMA

Table 4.5.5: Effect of MAA concentration on cumulative percent drug release of Rabeprazole sodium from hydrogel PMA

Time (hr)	PMA5 pH1.2	PMA6 pH1.2	PMA7 pH1.2	PMA5 pH 8	PMA6 pH 8	PMA7 pH 8
0.5	1.6±0.11	1.6±0.21	1.88±0.24	7.75±1.22	10.16±1.18	6.57±1.26
1	2.67±0.32	2.49±0.23	2.6±0.21	16.09±1.78	15.04±1.48	9.59±1.30
1.5	3.19±0.33	2.84±0.34	2.9±0.29	18.79±2.08	18.6±2.13	12.86±1.78
2	3.97±0.67	1.86±0.45	1.56±0.43	21.87±1.23	22.13±2.23	15.63±2.08
3	4.47±0.77	3.94±0.54	12.27±0.77	25.19±3.33	27.19±2.48	19.86±3.24
4	4.98±0.79	4.28±0.78	4.33±0.79	28.51±3.34	31.16±2.50	24.67±3.36
6	5.47±0.79	4.6±0.87	4.47±0.79	33.66±3.46	35.69±2.38	29.4±3.43
8	5.96±0.57	4.93±0.90	4.85±0.43	36.99±2.56	41.22±2.56	34.55±2.77
12	6.45±0.45	5.24±0.56	5.13±0.45	44.43±3.23	47.01±3.33	42.37±3.00
16	6.93±0.45	5.56±0.33	5.41±0.45	54.45±3.24	51.74±3.34	49.74±2.23
20	7.4±0.56	5.87±0.35	5.68±0.56	64.8±3.36	58.78±3.46	54.94±2.48
24	7.87±0.45	6.18±0.65	5.94±0.34	71.68±3.43	64.66±3.54	60.12±2.50

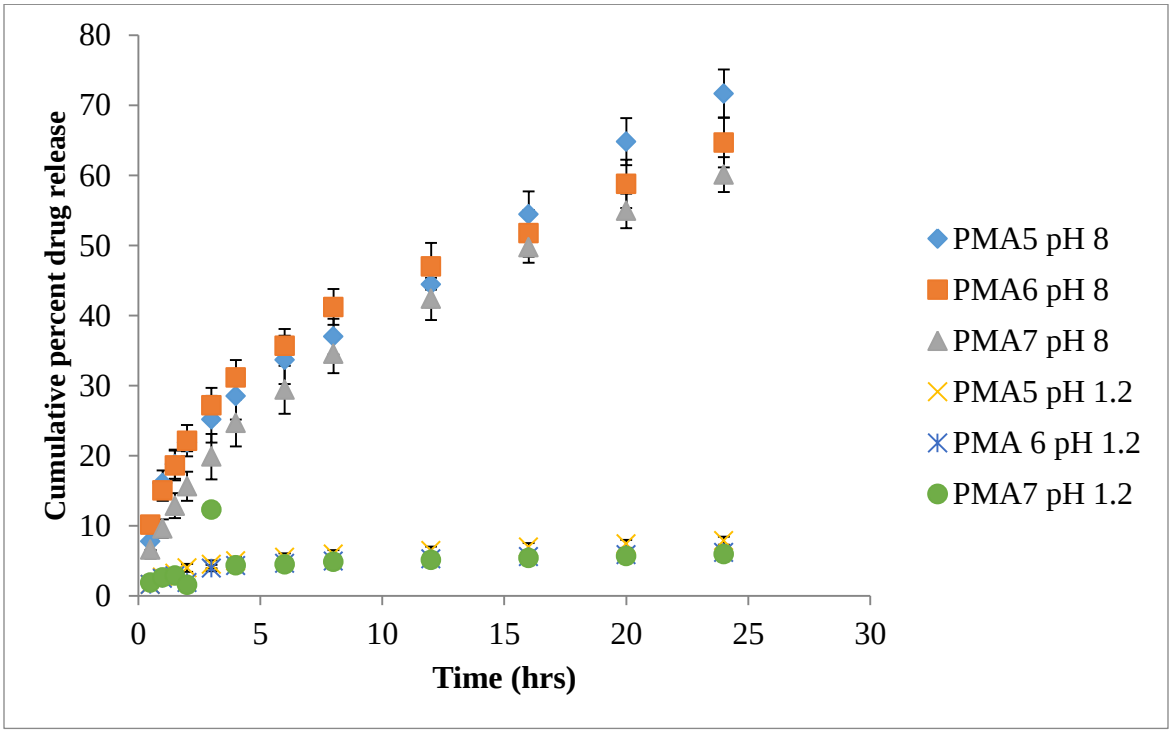

Figure 4.5.10: Effect of MAA concentration on cumulative percent drug release of Rabeprazole sodium from hydrogel PMA

Table 4.5.6: Release kinetíc of rabeprazole sodium from PMA hydrogel

Formulation code	***Higuchi***	***First order***	***Zero order***	***Korsmeyer-peppas***	
	R^2	R^2	R^2	R^2	***n***
PMA1	0.979	0.409	0.919	0.980	0.674
PMA 2	0.993	0.432	0.973	0.987	0.715
PMA 3	0.988	0.372	0.936	0.985	0.621
PMA 4	0.990	0.364	0.950	0.989	0.571
PMA 5	0.991	0.436	0.971	0.992	0.666
PMA 6	0.991	0.397	0.930	0.995	0.547
PMA 7	0.994	0.496	0.952	0.992	0.507

4.6: Characterization of PEG (HEMA-co-AA) hydrogels

4.6.1 Swelling studies at pH1.2 and pH 7.4

Swelling behavior of PEG(HEMA-co-AA) have been observed in acidic and basic pH. Effect of hydrogels components on swelling behavior has also been studied. Formulations were assigned codes (PHA1-PHA4) and (PHA5-PHA8) for varying concentration of acrylic acid and HEMA respectively. Effect of varying concentration of acrylic acid on swelling ratio (q), PHA1 (1 to 3.587), PHA2 (1 to 3.304) and PHA3 (1 to 2.662) and PHA4 (1 to 2.249) in pH 1.2 and PHA1 (1 to 12.895), PHA2 (1 to 14.070), PHA3 (1 to 16.134) and PHA4 (1 to 19.723) in 7.4 buffer solutions at 37 ºC has been given in Table 4.6.1 and graphically presented in Figure 4.6.1. Comparative swelling ratio (q) of hydrogels by using different concentrations of HEMA, PHA5 (1 to 4.043), PHA6 (1 to 3.346), PHA7 (1 to 3.164) and PHA8 (1 to 2.249)at pH 1.2 and PHA5 (1 to 26.945), PHA6 (1 to 24.659), PHA7 (1 to 21.429) and PHA8 (1to 16.354) at pH 7.4 were given in Table 4.6.2.

Table 4.6.1: Comparative swelling ratios of PEG (HEMA-co-AA) (PHA) hydrogels using different concentrations of AA

Time (Hrs)	**Swelling ratio (q) at pH 1.2**				**Swelling ratio (q) at pH 7.4**			
	PHA1	PHA2	PHA3	PHA4	PHA1	PHA2	PHA3	PHA4
0	1	1	1	1	1	1	1	1
0.5	1.15±0.19	1.14±0.23	1.1±0.22	1.07±0.21	1.7±0.22	1.77±0.21	1.89±0.23	2.1±0.24
1	1.3±0.22	1.27±0.29	1.2±0.24	1.15±0.24	2.4±0.23	2.54±0.24	2.78±0.32	3.2±0.28
1.5	1.46±0.32	1.41±0.31	1.29±0.19	1.22±0.33	3.1±0.34	3.31±0.33	3.67±0.33	4.3±0.31
2	1.61±0.27	1.54±0.3	1.39±0.22	1.29±0.34	3.8±0.42	4.08±0.45	4.56±0.61	5.41±0.42
3	1.76±0.3	1.68±0.28	1.49±0.32	1.37±0.38	4.5±0.46	4.84±0.21	5.45±0.73	6.51±0.47
4	1.91±0.31	1.81±0.32	1.59±0.33	1.44±0.42	5.2±0.53	5.61±0.76	6.34±0.77	7.61±0.77
6	2.07±0.33	1.95±0.31	1.69±0.35	1.51±0.46	5.9±0.45	6.38±0.73	7.23±0.75	8.71±0.75
8	2.22±0.32	2.08±0.32	1.78±0.35	1.59±0.53	6.6±0.21	7.15±0.53	8.12±0.67	9.81±0.67
10	2.37±0.31	2.22±0.35	1.88±0.36	1.66±0.63	7.3±0.76	7.92±0.63	9.01±0.75	10.91±0.87
12	2.52±0.32	2.36±0.36	1.98±0.34	1.74±0.74	8±0.73	8.69±0.74	9.9±0.67	12.01±0.83
14	2.67±0.35	2.49±0.36	2.08±0.34	1.81±0.75	8.7±0.74	9.46±0.75	10.79±0.77	13.12±0.65
18	2.83±0.36	2.63±0.34	2.17±0.33	1.88±0.81	9.4±0.75	10.23±0.81	11.68±0.71	14.22±0.74
24	2.98±0.34	2.76±0.34	2.27±0.33	1.96±0.82	10.1±0.81	11±0.82	12.57±0.75	15.32±0.79
48	3.28±0.34	3.03±0.35	2.47±0.34	2.1±0.84	11.5±0.82	12.53±0.84	14.35±0.78	17.52±0.84
72	3.59±0.35	3.3±0.35	2.66±0.34	2.25±0.89	12.9±0.88	14.07±0.89	16.13±0.81	19.72±0.85

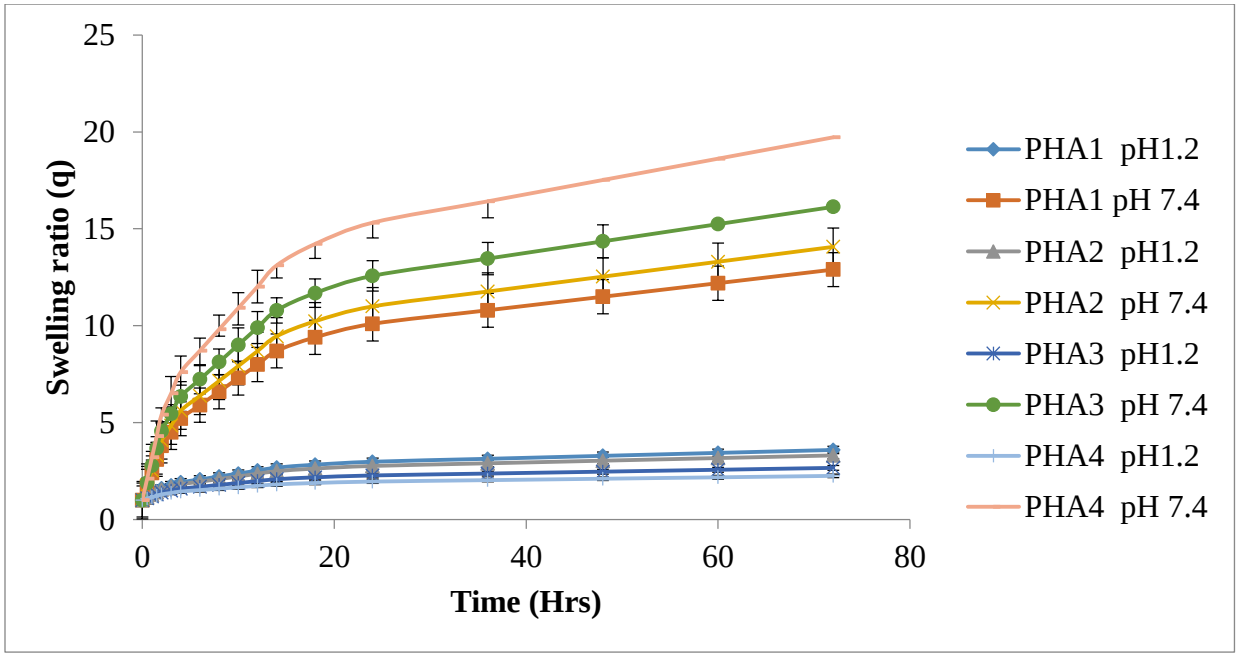

Figure 4.6.1: Comparative swelling ratios of PEG (HEMA-co-AA) hydrogels using different concentrations of AA

Table 4.6.2: Comparative swelling ratios of PEG(HEMA-co-AA) hydrogels using different concentrations of HEMA

Time (Hrs)	**Swelling ratio (q) at pH 1.2**				**Swelling ratio (q) at pH 7.4**			
	PHA5	PHA6	PHA7	PHA8	PHA5	PHA6	PHA7	PHA8
0	1	1	1	1	1	1	1	1
0.5	1.18±0.19	1.14±0.23	1.13±0.22	1.07±0.23	2.53±0.21	2.39±0.23	2.17±1.17	1.9±0.21
1	1.36±0.22	1.28±0.29	1.26±0.24	1.15±0.21	4.05±0.32	3.78±1.17	3.37±1.44	2.81±0.32
1.5	1.54±0.32	1.41±0.31	1.38±0.19	1.22±0.29	5.58±1.44	5.18±1.44	4.58±1.17	3.71±1.17
2	1.72±0.27	1.55±0.3	1.51±0.22	1.29±0.43	7.11±2.13	6.57±2.13	5.78±1.44	4.61±1.26
3	1.9±0.3	1.69±0.28	1.64±0.32	1.37±0.32	8.63±2.5	7.96±2.23	6.98±2.13	5.52±1.44
4	2.07±0.31	1.83±0.32	1.76±0.33	1.44±0.22	10.16±2.31	9.35±2.29	8.19±2.5	6.42±2.13
6	2.25±0.33	1.97±0.31	1.89±0.35	1.51±0.32	11.68±2.41	10.74±2.31	9.39±2.31	7.32±2.19
8	2.43±0.32	2.1±0.33	2.02±0.35	1.59±0.33	13.21±2.38	12.13±2.5	10.59±2.41	8.23±2.23
10	2.61±0.31	2.24±0.35	2.15±0.36	1.66±0.35	14.74±2.31	13.53±2.41	11.8±2.38	9.13±2.31
12	2.79±0.32	2.38±0.35	2.27±0.34	1.74±0.35	16.26±2.5	14.92±2.48	13±2.33	10.03±2.5
14	2.97±0.35	2.52±0.36	2.4±0.34	1.81±0.36	17.79±2.41	16.31±2.5	14.21±2.34	10.94±2.41
18	3.15±0.36	2.66±0.34	2.53±0.33	1.88±0.34	19.31±2.34	17.7±2.33	15.41±2.46	11.84±0.81
24	3.33±0.34	2.79±0.34	2.66±0.33	1.96±0.34	20.84±2.46	19.09±2.34	16.61±2.59	12.74±0.82
48	3.69±0.34	3.07±0.35	2.91±0.34	2.1±0.35	23.89±1.26	21.88±2.36	19.02±2.55	14.55±1.17
72	4.04±0.35	3.35±0.35	3.16±0.34	2.25±0.35	26.95±1.39	24.66±2.47	21.43±2.65	16.35±1.44

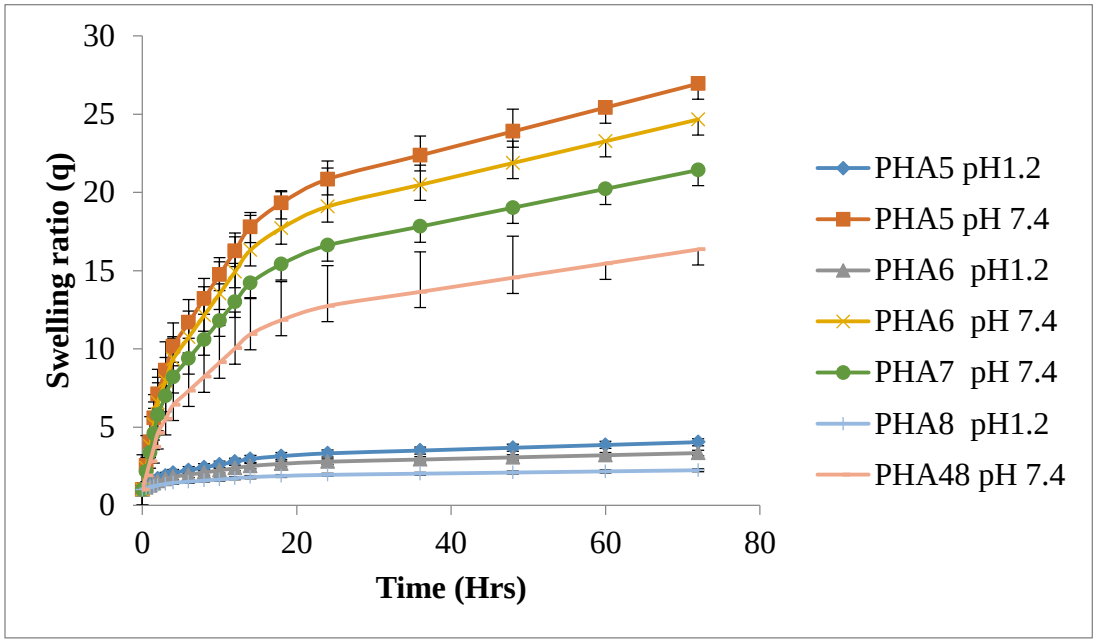

Figure 4.6.2: Comparative swelling ratios of PEG (HEMA-co-AA) hydrogels using different concentrations of HEMA

5.6.2: Pulsatile behavior of hydrogels

Reversible swelling behavior of PEG(HEMA-co-AA) has been evaluated at pH 1.2 and pH 7.4. Figure 4.6.3 represented on off swelling behavior of hydrogels at pH 7.4 and pH 1.2.

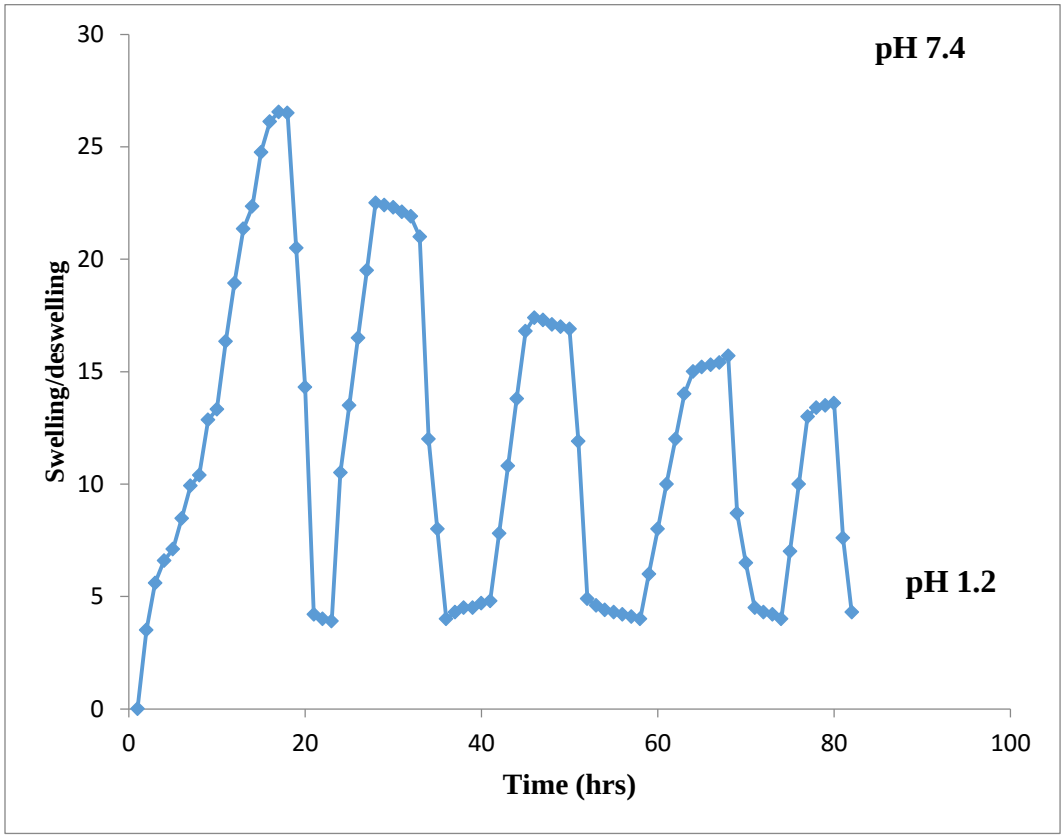

Figure 4.6.3: On-off switching behavior as reversible pulsatile swelling (pH 7.4) and deswelling (pH 1.2) of PEG(HEMA-co-AA hydrogel

4.6.3: Equilibrium water contents and gel fraction

Water absorbed by PEG (HEMA-co-AA) copolymeric hydrogels was quantitatively symbolized by the equilibrium water content (EWC). The EWC values of the hydrogels were calculated and tabulated in Table 4.6.3. Calculated gel fraction of hydrogel was summarized in Table 4.6.3.

Table 4.6.3: Equilibrium water contents, gel fraction and amount of drug loaded of PEG (HEMA-co-AA) hydrogels using different concentrations of AA and HEMA

Formulation code	Contents w/w %	EWC	Gel fraction (%)	Amount of Rabeprazole sodium loaded (mg per 0.4 g of dry disk)	
				By extraction	By weight
PHA1	7.5	0.84	74.74	41	42
PHA2	10	0.88	79.51	46	46.9
PHA3	12.5	0.93	87.29	56	57.2
PHA4	15	0.94	94.77	60	61
PHA5	1	0.92	70.37	67	67.8
PHA6	1.5	0.88	82.53	67	68
PHA7	2	0.81	91.88	67	68.4
PHA8	3	0.53	94.55	40	40.3

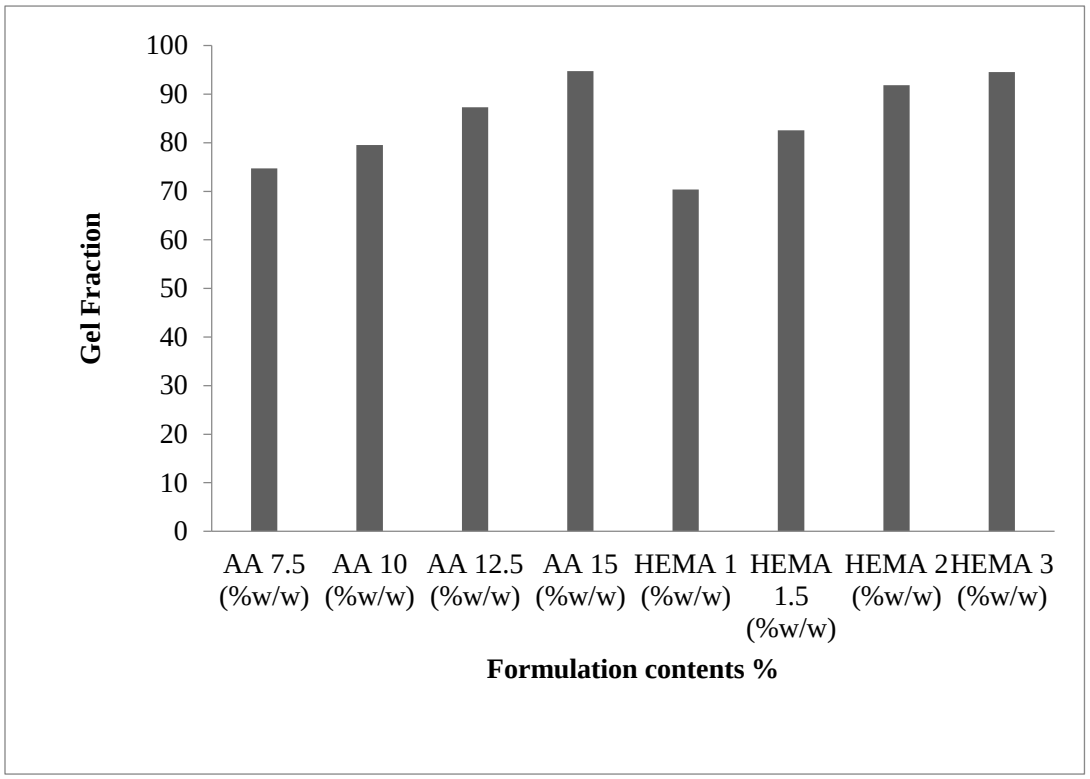

Figure 4.6.4: Gel fraction of PEG (HEMA-co-AA) hydrogel with different concentrations of AA and HEMA

4.6.4: Instrumental analysis

a) Scanning electron microscopy

SEM analysis was executed to analyze the morphological manners of swollen hydrogels. The SEM photomicrographs of lyophilized hydrogels were shown in Figures 4.6.5.

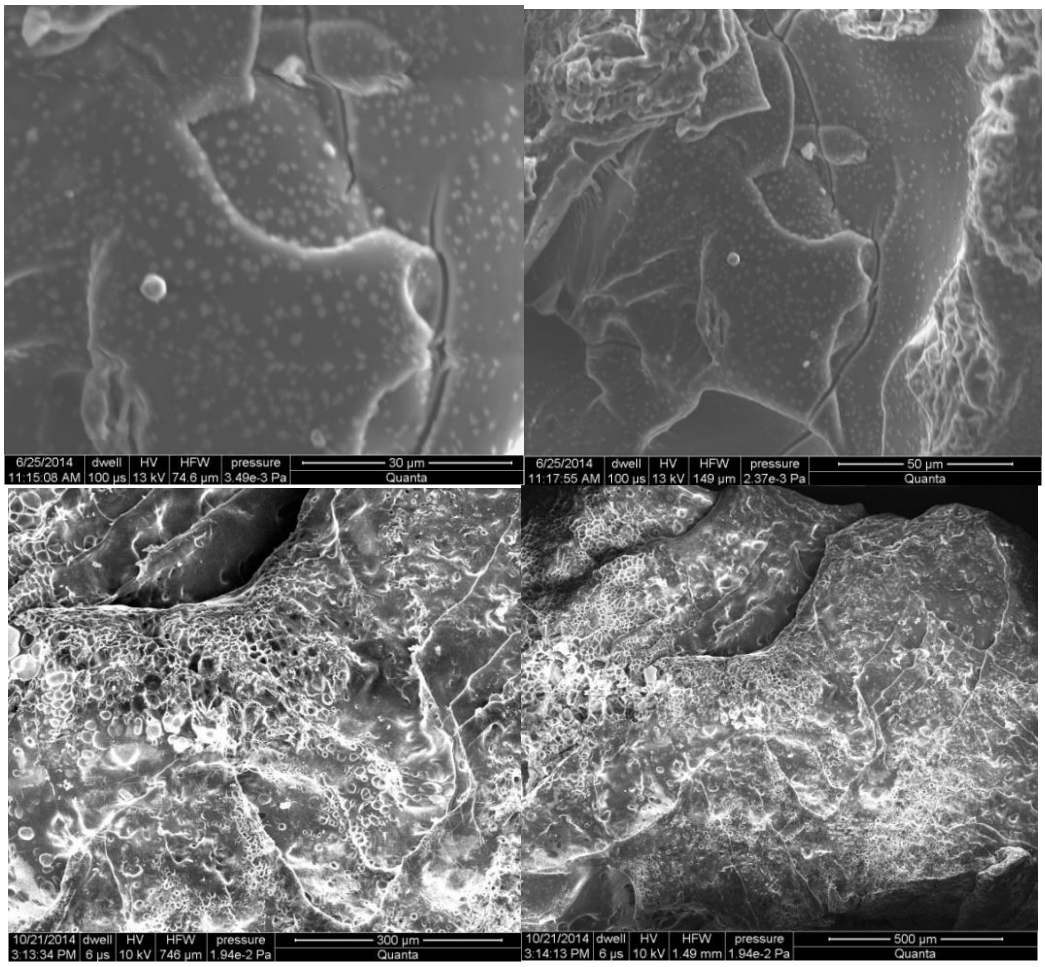

Figure 4.6.5: SEM images freeze dried PEG(HEMA-co-AA)at magnification of 100 X and 200 X and 30µ, 50µ, 300 µ, and 500 µ scale bar respectively

b) FTIR spectrum analysis

FTIR spectrum over the wavelength range 600–4000 $cm^{-1}$was recorded. FTIR spectrum of PHA hydrogel and its separate components have been depicted in Figure 4.6.6 with main peaks assignment.

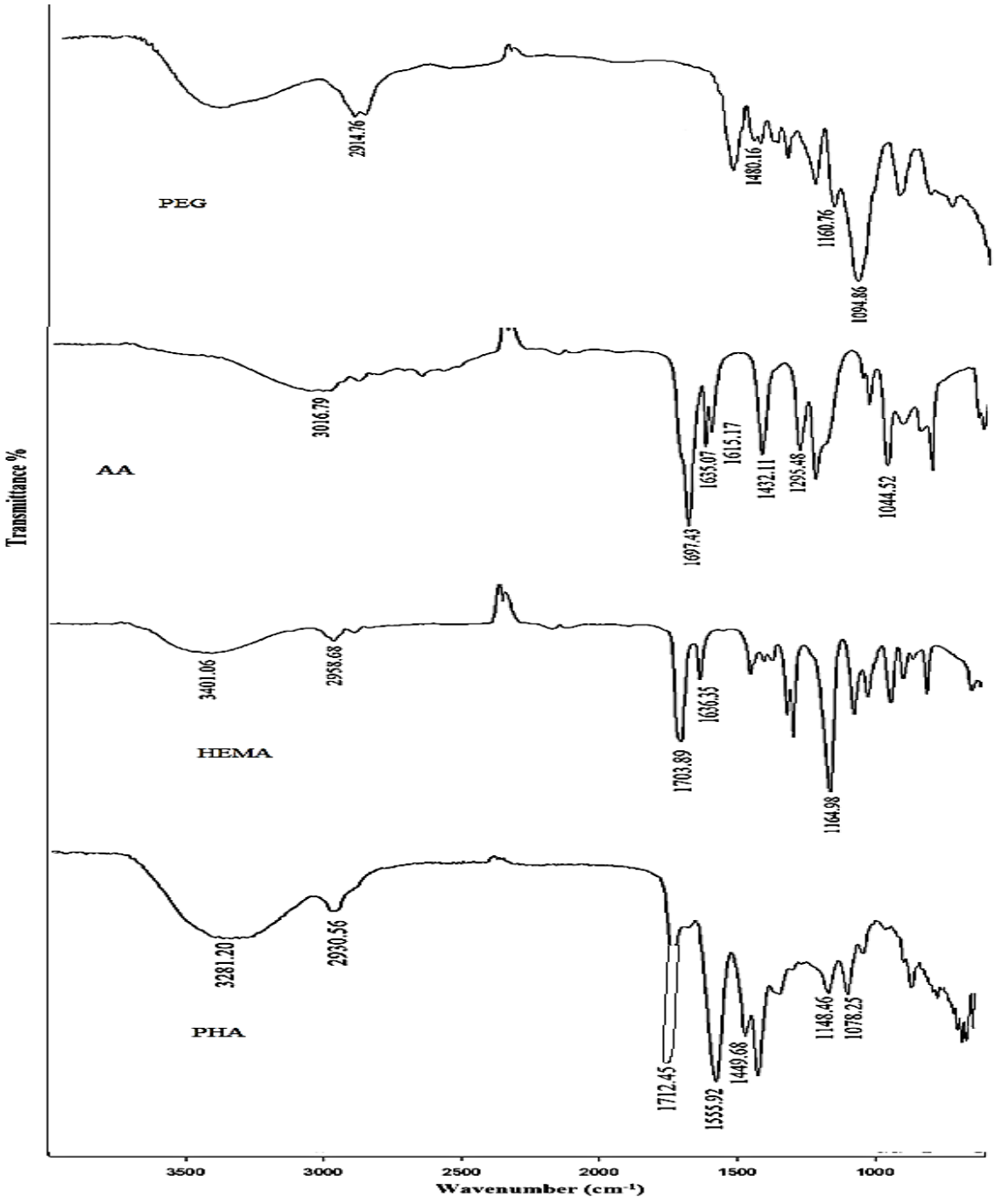

Figure 4.6.6:FTIR spectra of PEG, AA, HEMA and prepared hydrogel (PHA)

c) Thermal analysis

Thermal stability of prepared hydrogels and its formulation constituents was examined by analyzing TGA and DSC curves. The thermal analysis of hydrogel by TGA demonstrated

stability of the polymeric network upto 600 ºC shown in Figure 4.6.7 and DSC curve in Figure 4.6.8.

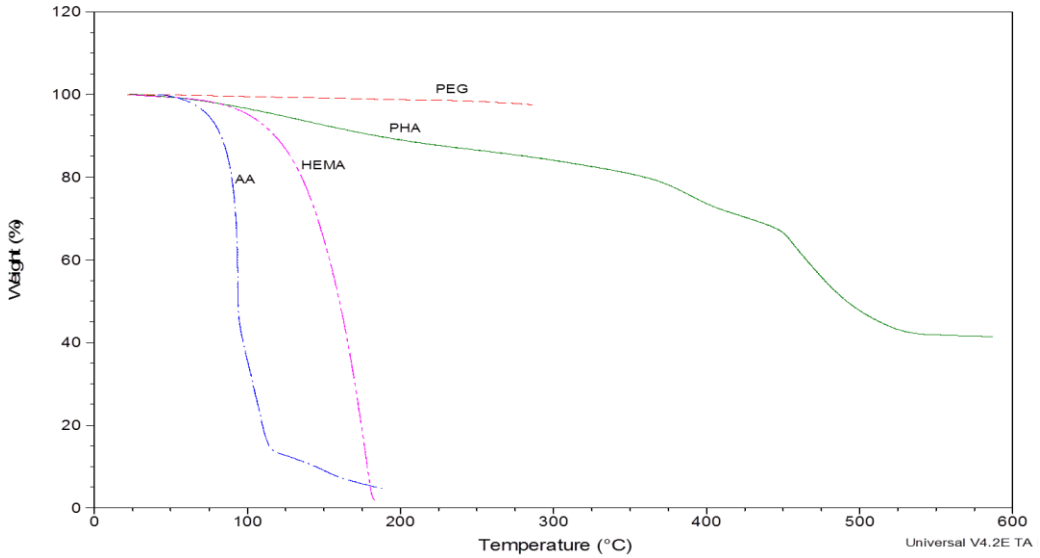

Figure 4.6.7: TGA curves of PEG, HEMA, AA PHA (hydrogel formulation

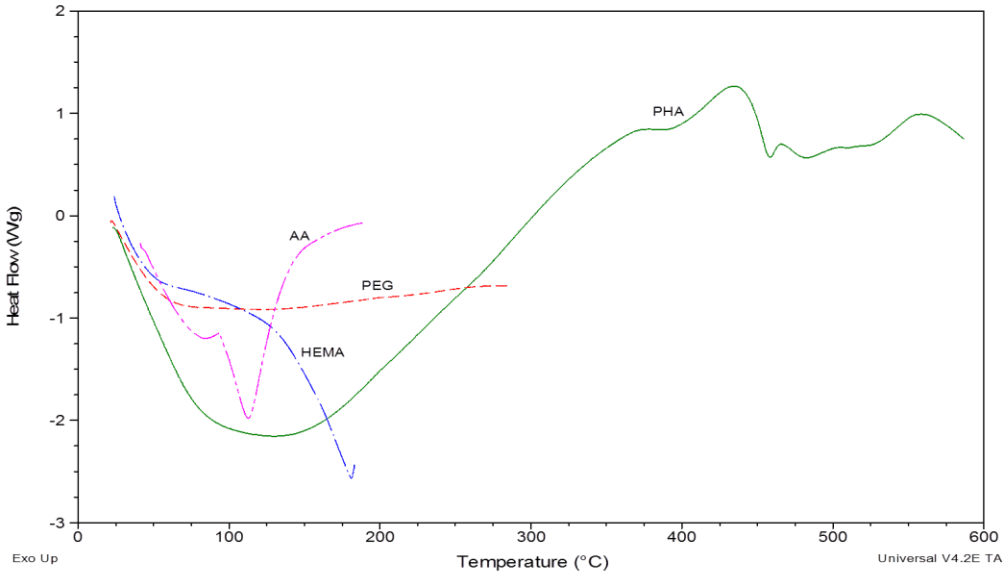

Figure 4.6.8: DSC curves of PEG, HEMA, AA PHA (hydrogel formulation)

4.6.5: In vitro release kinetics of Rabeprazole sodium from PEG (HEMA-co-AA) hydrogel

To evaluate the pH sensitive and controlled release of rabeprazole sodium from PEG (HEMA-co-AA) hydrogel, *in vitro* release studies were conducted in 0.1N HCl (pH 1.2) and Tris buffer (pH 8) at 37 ºC. Figure 4.6.9 exhibited effect of concentration of acrylic

acid on cumulative percent drug release. Effect of different concentration of HEMA on percent cumulative release of rabeprazole sodium has been summarized in Table 4.6.5.

Table 4.6.4: Effect of AA concentration on cumulative percent drug release of Rabeprazole sodium from hydrogel PHA

Time (hr)	PHA1 pH 1.2	PHA2 pH 1.2	PHA3 pH 1.2	PHA4 pH 1.2	PHA1 pH 8	PHA2 pH 8	PHA3 pH 8	PHA4 pH 8
0.5	1.2±0.3	1.07±0.4	0.88±0.7	0.82±0.2	9.92±1.4	5.33±2.0	7.44±1.6	13.15±1.0
1	1.55±0.7	1.38±0.4	1.14±0.3	1.06±0.2	13.85±1.5	6.49±1.7	9.53±1.6	15.43±
1.5	1.9±0.2	1.69±0.7	1.39±0.4	1.3±0.3	16.52±1.7	9.11±1.5	13.31±1.8	19.25±1.5
2	2.25±0.6	2±0.4	1.65±0.4	1.54±0.4	19.16±2.6	11.7±2.0	16.28±2.8	24.24±1.7
3	2.82±0.3	2.52±0.8	2.07±0.5	1.93±0.8	25.64±3.3	17.92±2.8	18.61±2.8	29.83±2.4
4	3.39±0.3	3.03±0.5	2.49±0.8	2.32±0.8	30.91±3.9	23.05±2.7	24.93±3.0	33.05±1.3
6	3.96±0.8	3.53±0.4	2.9±0.2	2.71±0.8	39.59±3.9	30.2±3.6	31.37±3.1	38.84±1.6
8	4.52±0.7	4.03±0.4	3.31±0.5	3.09±0.4	44.74±3.9	37.28±2.9	41.13±2.9	47.58±1.9
12	5.19±0.8	4.62±0.5	3.8±0.7	3.55±0.4	50.5±3.9	50.42±3.2	52.4±2.9	58.13±2.0
16	5.85±0.5	5.21±0.4	4.28±0.3	4±0.4	60.78±3.9	60.41±3.8	64.22±3.8	70.6±1.6
20	6.39±0.5	5.7±0.8	4.68±0.7	4.37±0.6	68.69±2.7	68.45±2.9	74.01±3.0	81.4±2.7
24	7.04	6.27±0.8	5.15±0.8	4.81±0.3	71.99±3.9	77.09±3.9	82.61±3.9	90.6±2.5

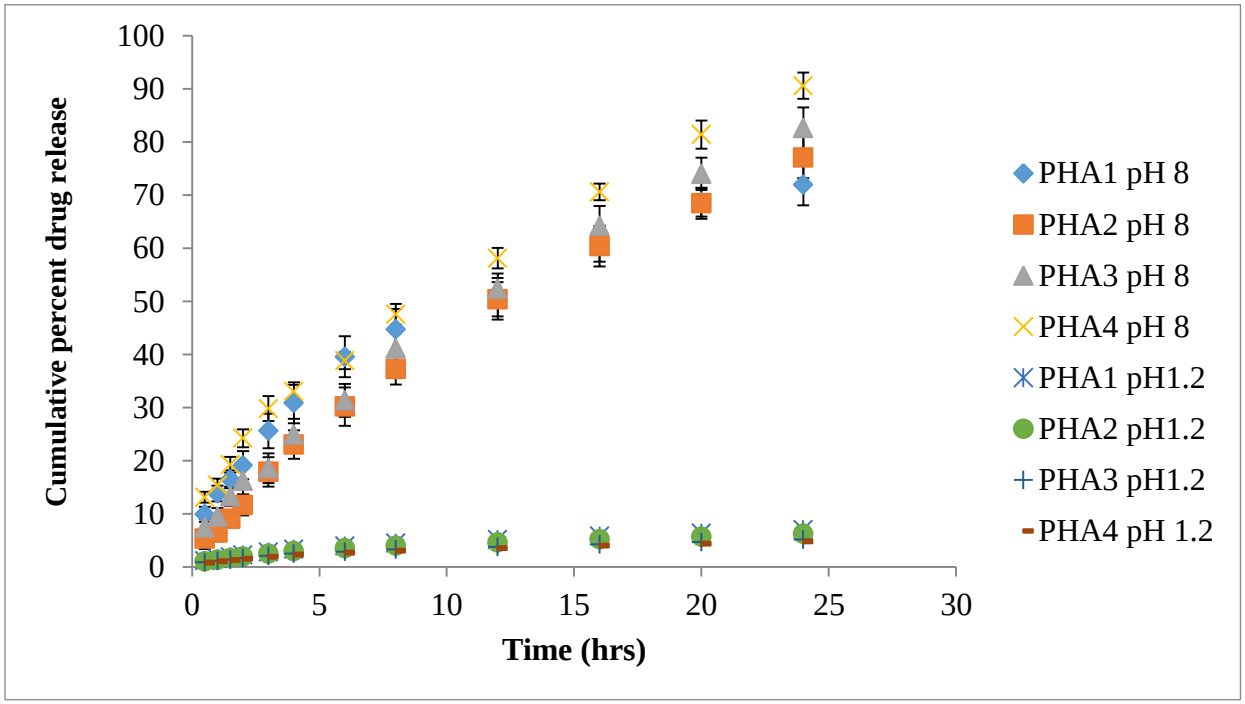

Figure 4.6.9: Effect of AA concentration on cumulative percent drug release of Rabeprazole sodium from hydrogel PHA

Table 4.6.5: Effect of HEMA concentration on cumulative percent drug release of Rabeprazole sodium from hydrogel PHA

Time (hr)	PHA5 pH 1.2	PHA6 pH 1.2	PHA7 pH 1.2	PHA8 pH 1.2	PHA5 pH 8	PHA6 pH 8	PHA7 pH 8	PHA8 pH 8
0.5	0.77±0.2	0.73±0.3	0.7±0.4	1.1±0.7	6.97±1.4	8.56±2.0	7.97±1.6	6.25±1.3
1	0.99±0.5	0.95±0.4	0.91±0.4	1.47±0.3	9.03±1.5	10.31±1.7	9.36±1.6	8.69±1.2
1.5	1.22±0.3	1.16±0.4	1.11±0.3	1.83±0.4	13.24±1.7	13.38±1.5	12.65±1.8	12.05±1.5
2	1.44±0.3	1.38±0.4	1.32±0.4	2.18±0.4	17.04±2.6	17±2.0	16.28±2.8	15.39±2.4
3	1.81±0.6	1.73±0.7	1.65±0.8	2.53±0.5	21.85±3.3	21.6±2.8	20.88±2.8	21.82±3.3
4	2.17±0.6	2.08±	1.99±0.4	2.88±0.8	29.01±3.9	28.43±2.7	27.71±3.0	30.46±3.1
6	2.54±0.3	2.42±0.8	2.32±0.4	3.22±0.2	36.4±3.9	35.49±3.6	34.77±3.1	37.6±3.4
8	2.9±0.3	2.77±0.4	2.65±0.5	3.56±0.7	48.16±3.9	46.71±2.9	46±2.9	47.73±2.5
12	3.32±0.3	3.17±0.9	3.04±0.4	3.9±0.3	60.32±3.9	61.84±3.2	57.62±2.9	56.6±2.9
16	3.75±0.3	3.58±0.7	3.43±0.3	4.23±0.7	73.97±3.3	71.38±3.8	70.66±3.8	64.78±2.7
20	4.09±0.3	3.91±	3.74±0.8	4.56±0.7	82.17±2.7	79.19±2.9	78.49±3.0	73.1±3.1
24	4.51±0.9	4.31±0.6	4.12±0.8	4.89±0.8	90.54±3.9	87.19±3.9	85.8±3.9	78.9±2.7

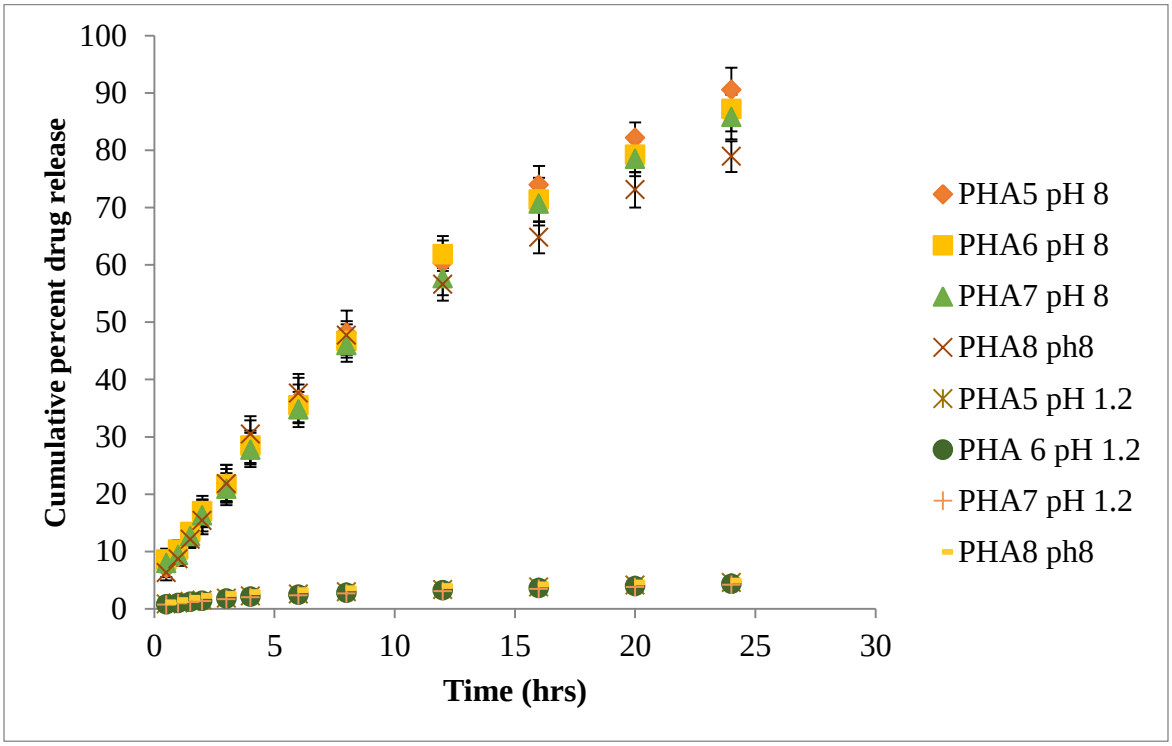

Figure 4.6.11: Effect of HEMA concentration on cumulative percent drug release of Rabeprazole sodium from hydrogel PHA

Table 4.6.6: Release kinetics of rabeprazole sodium from hydrogel PHA

Formulation code	***Higuchi***	***First order***	***Zero order***	***Korsmeyer-peppas***	
	R^2	R^2	R^2	R^2	***n***
PHA1	0.994	0.457	0.941	0.991	0.402
PHA 2	0.995	0.619	0.979	0.998	0.606
PHA 3	0.991	0.576	0.984	0.996	0.619
PHA 4	0.993	0.468	0.982	0.992	0.612
PHA 5	0.996	0.567	0.970	0.993	0.501
PHA 6	0.993	0.557	0.967	0.991	0.501
PHA 7	0.993	0.568	0.967	0.990	0.505
PHA 8	0.992	0.536	0.939	0.977	0.501

4.7 Acute oral toxicity study of prepared hydrogels

General conditions of all groups were observed. Body weights, water and food intake, common signs of illness, dermal and ocular irritation and mortality of both the control and treatment groups were recorded accordingly during the whole treatment period mentioned in Table 4.7.1.

Table 4.7.1: Clinical observations of acute oral toxicity test for hydrogels formulations

Observations	**Group I** (Control)	**Group II** (CA hydrogel treated) 10 g/kg/b.w	**Group III** (CMA hydrogel Treated) 10g/kg/b.w	**Group IV** (A hydrogel treated) 10g/kg/b.w	**Group V** (M hydrogel treated) 10g/kg/b.w
Signs of illness	Nil	Nil	Nil	Nil	Nil
Body weight (g)					
Pretreatment	29.8±2.4	28.3±4.5	31.8±1.0	20.8±1.0	27.2±3.5
Day1	29.8±3.4	28.5±3.2	33.3±2.2	21.1±1.1	27.5±2.2
Day7	30.6±2.3	33.5 ±1.2	34.6±1.2	22.6±1.6	29.5 ±3.2
Day14	31.4±3.2	34.5±2.1	36.1±1.8	22.8±1.9	30.4±1.2
Water intake(mL)					
Pretreatment	8 ±1	10 ±1.5	10 ±1.4	9 ±1.2	9.5 ±2.5
Day1	10 ±1.5	8 ±1.8	12±1.2	11 ±1.7	12 ±3.5
Day7	9 ±1.3	12 ±1.3	10 ±1.5	9 ±2.8	13 ±2.5
Day14	10 ±1.4	9 ±1.6	8.5 ±1.4	10 ±2.6	12 ±1.5
Food Intake (g)					
Pretreatment	5 ±0.7	5.5 ±1.5	8.5 ±0.3	6.6 ±1.0	5.6 ±1.0
Day1	7 ±0.8	7.5 ±0.8	7.4 ±0.4	5.6 ±1.0	7.6 ±1.0
Day7	5 ±1.0	6.5 ±1.0	8.5 ±0.2	6.6 ±0.8	6.8 ±0.8
Day14	7.5±1.0	6.5 ±1.2	8.0 ±0.6	5.8±0.4	5.8±0.4
Dermal toxicity Dermal irritation	Nil	Nil	Nil	Nil	Nil
Ocular toxicity Simple Irritation or corrosion	Nil	Nil	Nil	Nil	Nil
Mortality	Nil	Nil	Nil	Nil	Nil

4.7.1 Biochemical blood analysis

Purpose of biochemical blood analysis was to investigate whether hydrogel prepared by free radical polymerization could result in to the blood system's defect. Whole blood samples from rat were collected for biochemical blood analysis which was determined by a hematology Analyzer. Biochemical blood analysis in our study included the following variables: white blood cell count (WBC), red blood cell count (RBC), hemoglobin (HB), platelet count, mean corpuscular volume (MCV), mean corpuscular hemoglobin (MCH), mean corpuscular hemoglobin concentration (MCHC) summarized in Table 4.7.2 and liver function test, lipid profile and kidney function test has been shown in Table 4.7.3.

Table 4.7.2: Biochemical blood analysis

Haematology	**Group I** (Control)	**Group II** (CA hydrogel treated) 1-10 g/kg	**Group III** (CMA hydrogel treated) 1-10g/kg	**Group IV** (A hydrogel treated) 1-10g/kg	**Group V** (M hydrogel treated) 1-10g/kg
Hb g/dL	14.1±1	14.3±2.5	14.5±2	13.2 ±1.5	11.2±1.5
WBCs x 10^3 / µl	4.9±0.51	5.1±0.48	4.9±0.83	4.1±0.76	6.6±0.34
RBCs x 10^6 / µl	8.46±1.1	8.85±0.4	8.52±1.5	8.30±0.40	8.26±0.37
Platelets x 10^3/µl	1398±1.3	1089±1.5	1584±1.5	1319±4	1081±3
Monocytes%	2±0.34	1±0.45	1±0.87	2±0.78	2±.54
Neutrophils%	24±3.95	21±2.43	23±4.87	25±3.45	27±3.21
Lymphocytes%	94±0.95	95±1.87	96±3	87±5.23	94±3.45
MCV	54±1.55	54.5±2.47	53.5±3.37	52.4±2.23	52.3±3.12
MCH	16.3±0.12	16.2±0.50	17±0.51	15.9±0.57	16.8±0.95
MCHC g/dl	30±0.47	31.8±0.57	30.3±0.54	32.1±1.2	28.6±2.50

Table 4.7.3: Liver, kidney and lipid profile of mice treated with hydrogel formulations

Biochemical analysis	**Group I** (Control)	**Group II** (CA hydrogel treated) 1-10 g/kg	**Group III** (CMA hydrogel treated) 1-10g/kg	**Group IV** (A hydrogel treated) 1-10g/kg	**Group V** (M hydrogel treated) 1-10g/kg
ALT(IU/l)	54	53	66	63	55
AST (IU/l)	246	144	184	185	213
Creatinine (mg/dl)	0.42	0.39	0.37	0.44	0.46
Urea(mg/dl)	72	59	39	29	38
Uric acid(mg/dl)	3.5	2.9	3.4	4.8	5.7
Cholesterol(mg/dl)	82	116	130	64	137
Triglyceride(mg/dl)	110	90	115	97	85

4.7.2 Histopathological study

To evaluate acute toxicity caused by hydrogel formulations accurately, histopathological modifications of major organs were tested**.** Observed organ weight of mice was given in Table 4.7.4.Histological examination of stomach, heart, liver, spleen, kidney and intestine of mice of control group (a), after hydrogel treatment. (b) of group II, (c) of group III, (d) of group IV, and (e) of group V have been depicted in Figures 4.7.1, 4.7.2, 4.7.3, 4.7.4, 4.7.5 and 4.7.6 respectively.

Table 4.7.4: Effect of oral administration of hydrogel on the organ weight (gms) of mice

Treatment groups	**Heart**	**Liver**	**Lung**	**Kidney**	**Stomach**	**Spleen**
Control	0.54 ± 0.12	6.10 ±0.20	0.74 ± 0.07	0.813 ±0.05	1.78 ± 0.1	0.57 ± 0.01
Group I	0.60 ± 0.71	6.48 ±0.27	0.64±0.22	0.96 ± 0.07	1.05 ±0.18	0.61 ± 0.02
Group II	0.56 ± 0.01	6.11 ±0.12	0.62 ± 0.21	1.20 ± 0.07	1.79 ± 0.1	0.52 ± 0.11
Group III	0.54 ± 0.02	5.62 ±0.24	0.68 ± 0.03	0.87 ± 0.05	1.38 ± 0.4	0.56 ± 0.04
Group IV	0.53 ± 0.01	5.70 ±0.22	0.49 ± 0.01	1.62 ± 0.12	1.6 ± 0.20	0.57±0.20
Group V	0.58± 0.32	5.89± 0.61	0.54± 0.21	1.37± 0.06	1.99± 0.19	0.89± 0.11

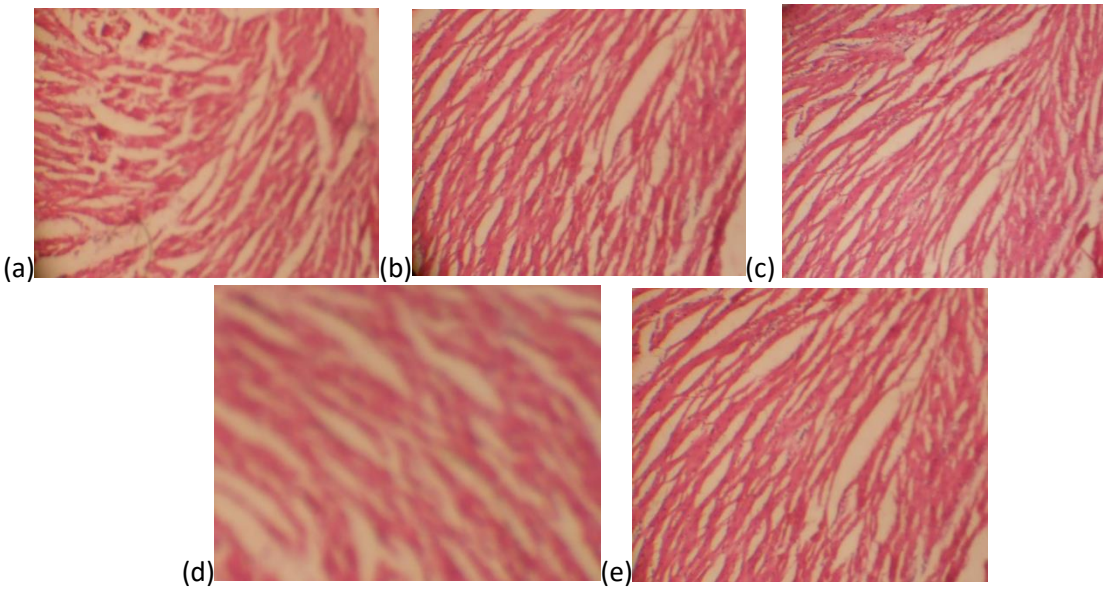

Figure 4.7.1. Histological examination of stomach of mice of control group (a), after hydrogel treatment. (b) of group II, (c) of group III, (d) of group IV, and (e) of group V.

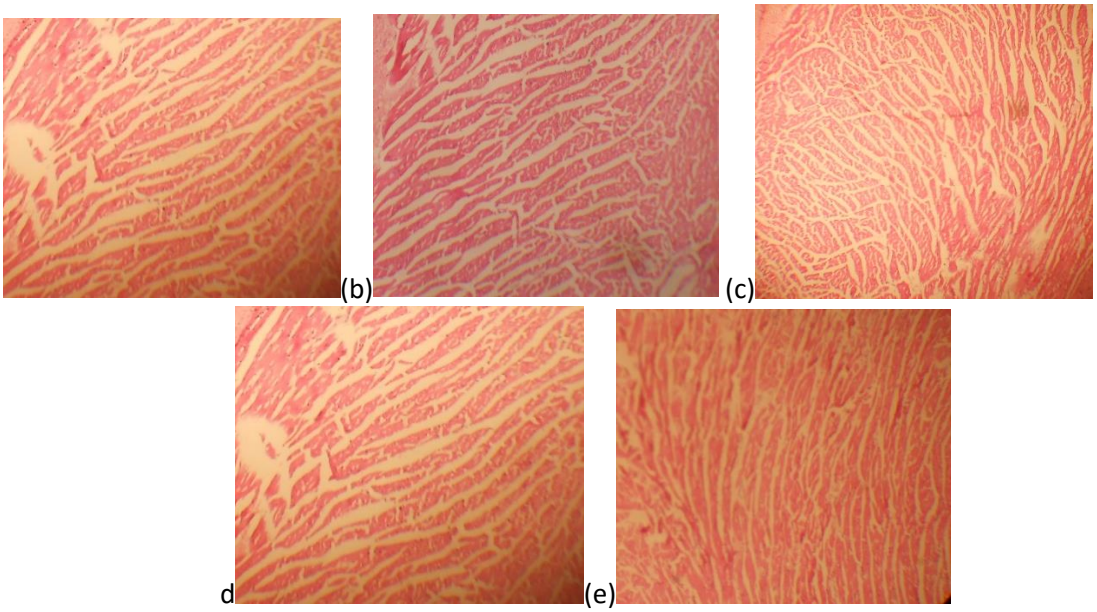

Figure 4.7.2. Histological examination of heart of mice of control group (a), after hydrogel treatment. (b) of group II, (c) of group III, (d) of group IV, and (e) of group V.

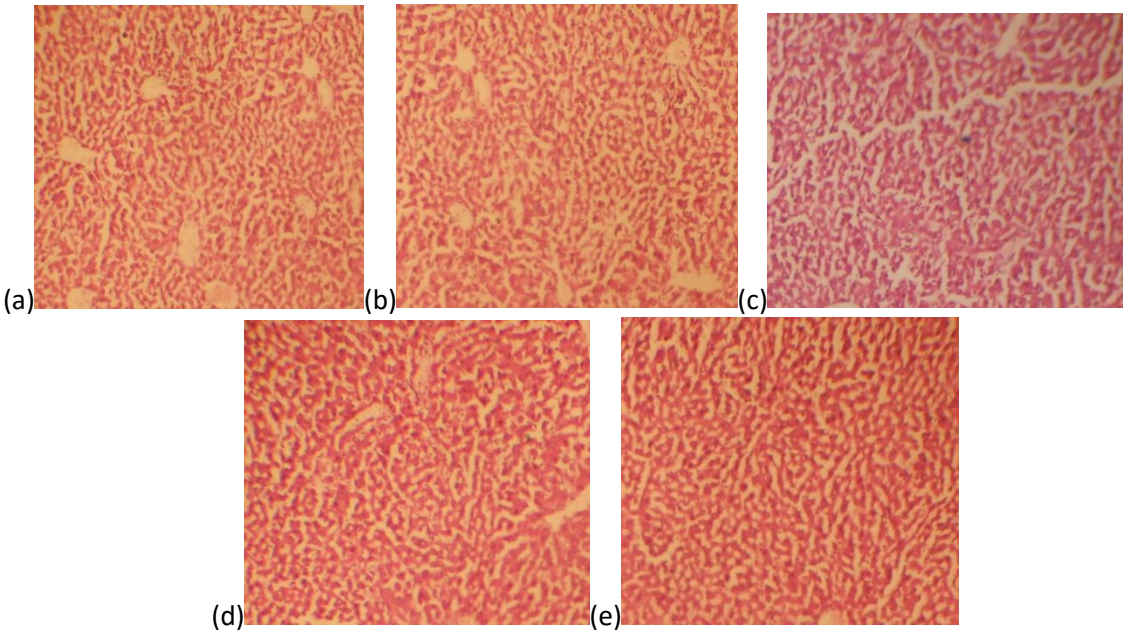

Figure 4.7.3. Histological examination of liver of mice of control group (a), after hydrogel treatment, (b) of group II, (c) of group III, (d) of group IV, and (e) of group V.

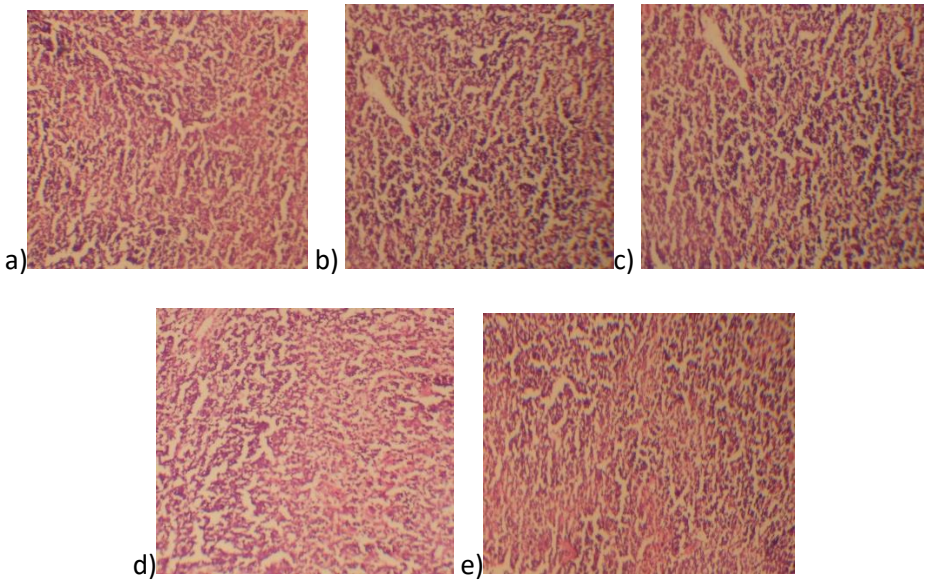

Figure 4.7.4. Histological examination of spleen of mice of control group (a), after hydrogel treatment, (b) of group II, (c) of group III, (d) of group IV, and (e) of group V

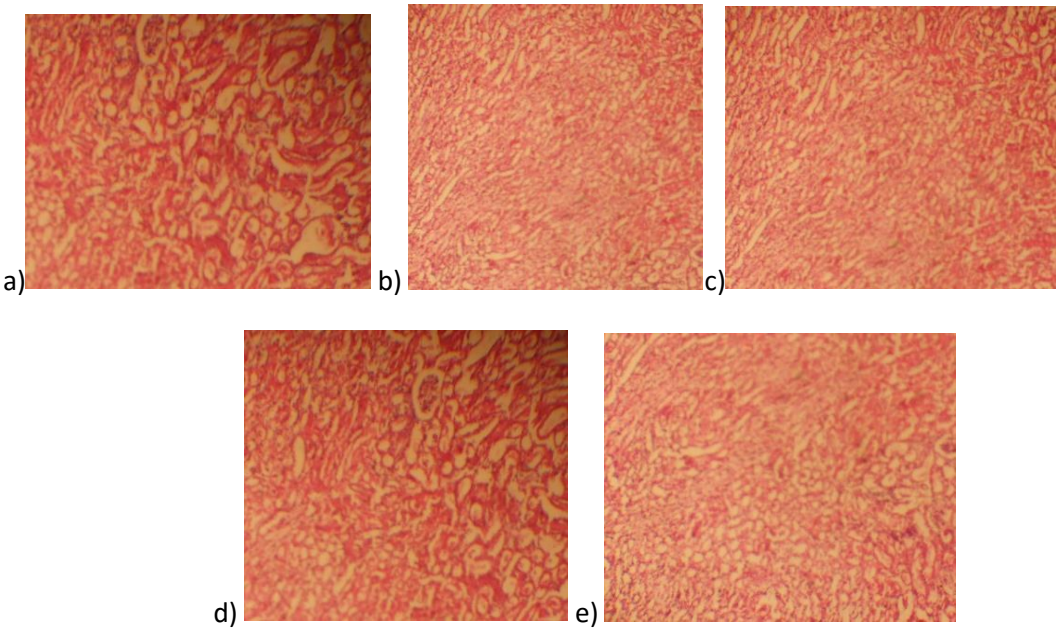

Figure 4.7.5. Histological examination of kidney of mice of control group (a), after hydrogel treatment. (b) of group II, (c) of group III, (d) of group IV, and (e) of group V

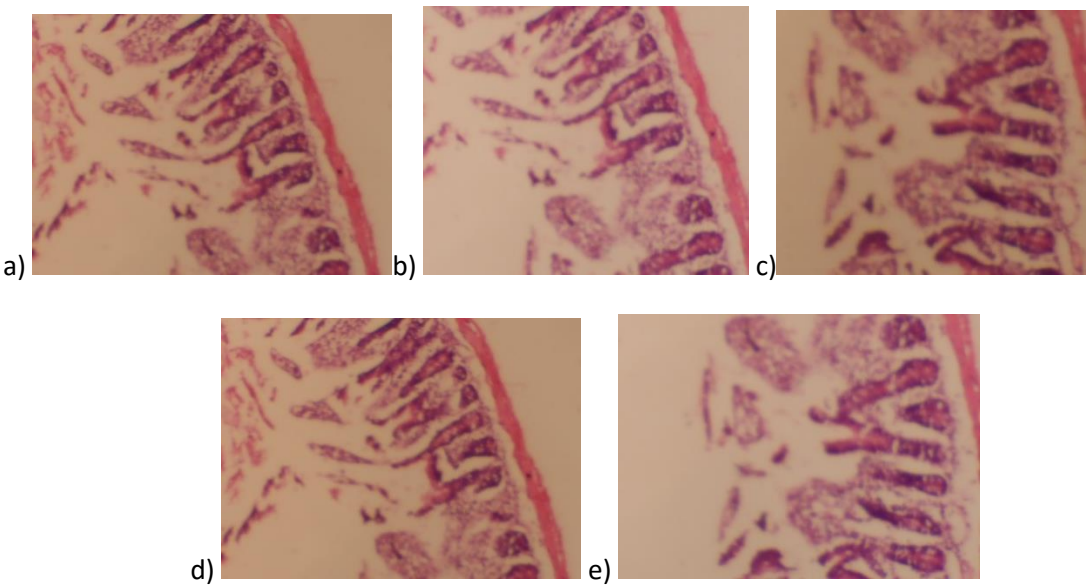

Figure 4.7.6. Histological examination of intestine of mice of control group(a), after hydrogel treatment. (b) of group II, (c) of group III, (d) of group IV, and (e) of group V

4.8 Pharmacokinetic evaluation of rabeprazole sodium

4.8.1: Standard curve

The standard curve of Rabeprazole sodium was constructed using known plasma drug concentrations within ranges of 31.25 ng/mL to 1000 ng/mL and linear regression was applied to fit straight line. Mean R^2 values was also determined 0.999.

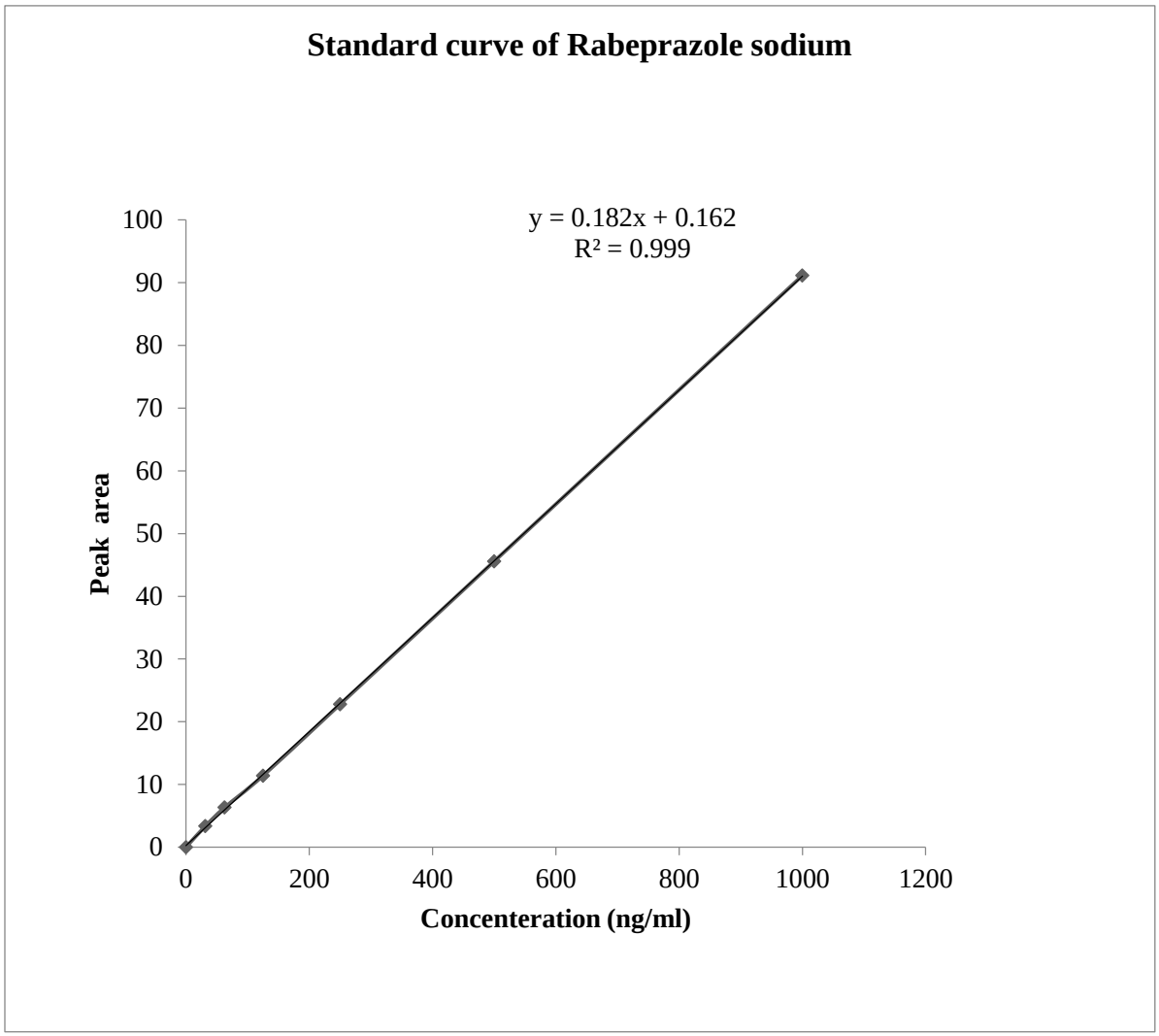

Figure 4.8.1: Standard curve of rabeprazole sodium in rabbit plasma

Rabbits were divided into three groups having 10 rabbits in each group. CA (CMC-g-AA), A (CMAX-g-AA), and drug solution of same strength(5 mg/kg/day) as that of hydrogels disc were administered to Group A, Group B and Group C respectively. Mean plasma concentration of CA (CMC-g-AA), A (CMAX-g-AA), and drug solution were summarized in Table 4.8.1, 4.8.2 and 4.8.3 respectively. Representative chromatograms in Figure 4.8.2 showed that retention time of rabeprazole sodium was 5.4 min in simple solution analysis. Figure 4.8.3 depicted the retention time of rabeprazole sodium in spiked plasma analysis was also 5.4 min.

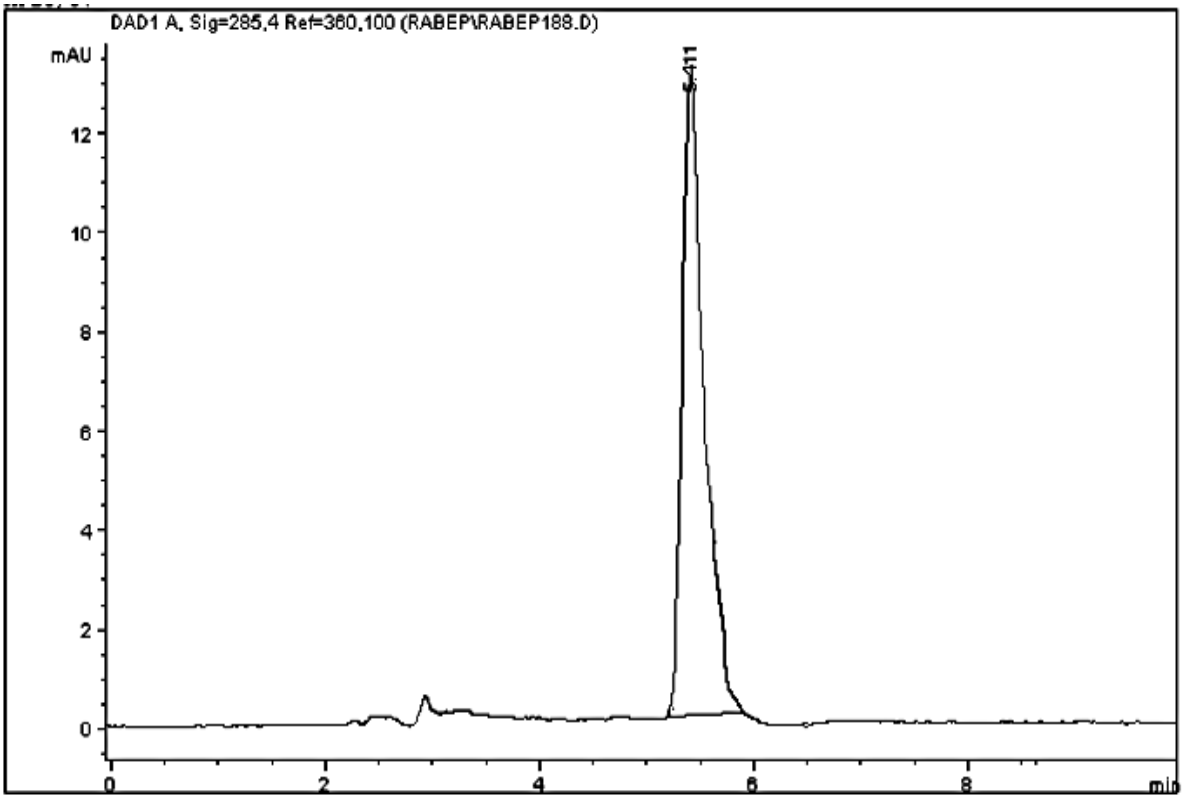

Figure 4.8.2: Chromatogram of rabeprazole sodium

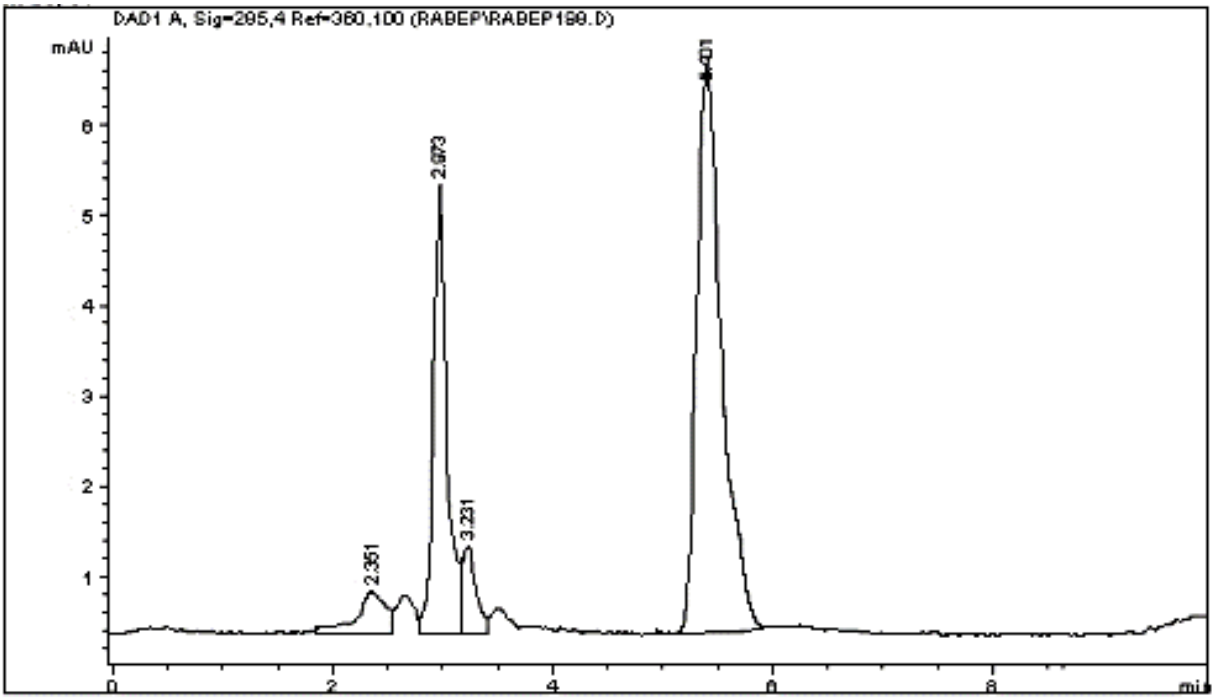

Figure 4.8.3: Chromatogram of spiked plasma with rabeprazole sodium

Table 4.8.1: Intra-day and Inter-day precision and accuracy of Rabeprazole sodium in rabbit plasma

Rabeprazole		
Intra day		
Parameter	LQC (ng/mL)	HQC (ng/mL)
Nominal Conc.	15	1000
Mean	13.07	995.27
S.D.	0.11	0.82
Precision CV (%)	0.4	0.1
Accuracy (%)	97.2	99.5
Inter day		
Parameter	LQC (ng/mL)	HQC (ng/mL)
Nominal Conc.	15	1000
Mean	13.39	992.60
S.D.	0.28	1.28
Precision CV (%)	0.9	0.1
Accuracy (%)	95.1	99.3

Table 4.8.2: Mean plasma concentration of Rabeprazole sodium after administration of CA (CMC-g-AA) hydrogel in rabbits (n=10)

Group A	
Time (hr)	Mean Conc. (ng/mL)±SEM
0	0
0.5	0
1	0
2	0
3	30.727±6.907
4	85.299±3.926
5	86.333±4.006
6	85.602±4.079
8	63.349±4.957
12	31.140±2.252

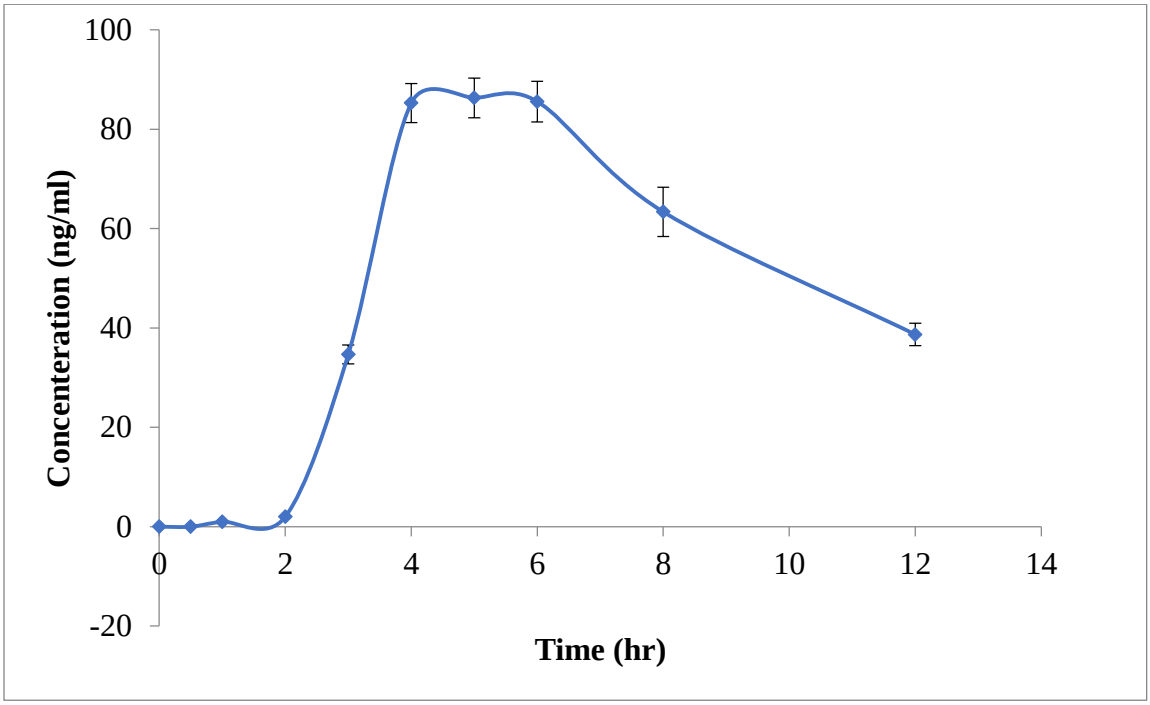

Figure 4.8.4: Plasma profile of Rabeprazole sodium after administration of CA (CMC-g-AA) hydrogel formulation

Table 4.8.3: Mean plasma concentration of Rabeprazole sodium after administration of A (CMAX-g-AA) hydrogel in rabbits (n=10)

Group B	
Time (hr)	Mean Conc. (ng/mL) ±SEM
0	0
0.5	0
1	0
2	0
3	38.152±6.773
4	103.717±4.588
5	103.717±4.588
6	103.717±4.588
8	86.625±3.455
12	39.209±4.622

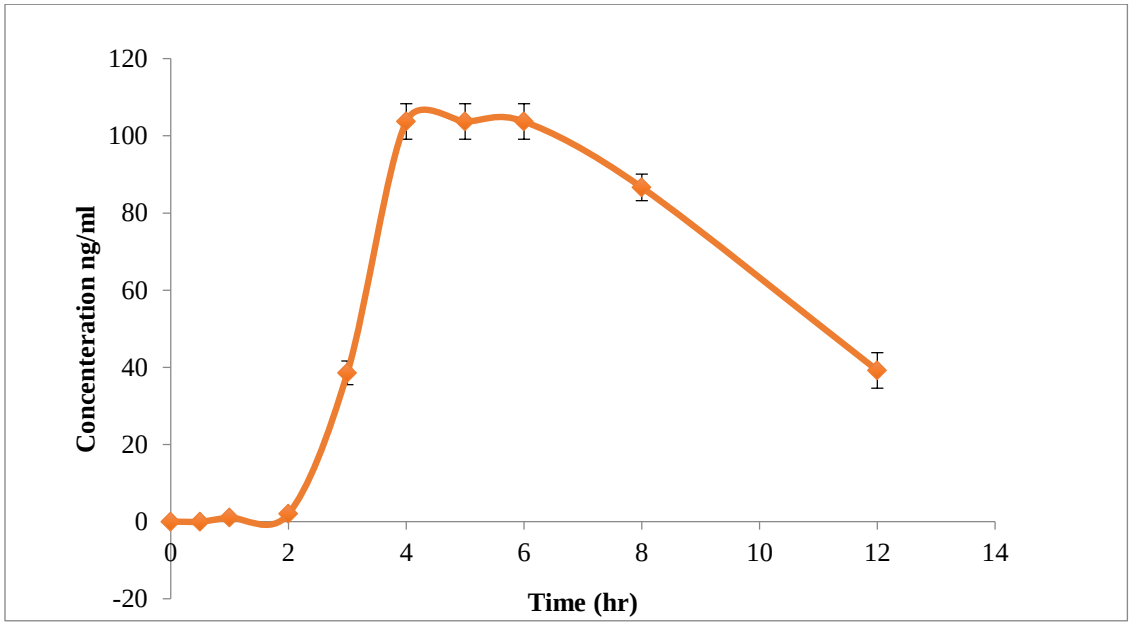

Figure 4.8.5: Plasma profile of Rabeprazole sodium after administration of A (CMAX-g-AA) hydrogel formulation

Table 4.8.4: Mean plasma concentration of Rabeprazole sodium after administration of oral drug solution in rabbits (n=10)

Group C	
Time (Hrs)	**Mean conc.(ng/mL) ±SEM**
0	0
0.25	6.128±0.65
0.5	20.133±1.44
0.75	43.289±1.38
1	61.263±1.70
1.5	39.320±1.44
2	18.148±0.95
3	8.003±0.30
4	0.946±0.35

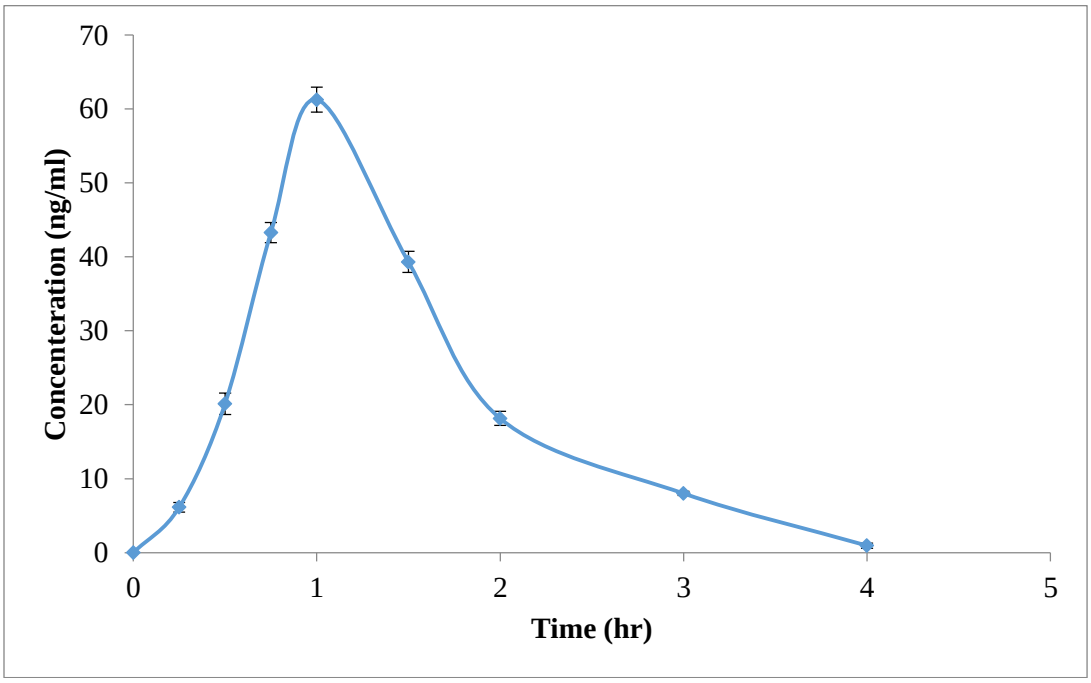

Figure 4.8.6: Plasma profile of Rabeprazole sodium after administration of oral drug solution

Pharmacokinetic parameters of Rabeprazole sodium following administration of CMC-g-AA, CMAX-g-AA hydrogel formulations and oral drug solution were described in Table 4.8.4. Pharmacokinetic parameters of Rabeprazole sodium were statistically analyzed by one way ANOVA, results were summarized in Table 4.8.5.

Table 4.8.5: Mean values of pharmacokinetic parameters of Rabeprazole sodium following administration of two different formulations (hydrogel) and oral drug solution.

Sr No.	Parameters	CA (Hydrogel)	A (Hydrogel)	Drug solution
1	C_{max}(ng/mL)	87.287	103.717	61.263
2	T_{max}(Hrs)	4.3	4	1
3	AUC_{o-t}(ng/mL.h)	952.2552	1084.576	83.672
4	MRT (Hrs)	10.605	9.700	1.481
5	C_{last}(ng/mL)	38.256	42.962	2.192
6	T_{last}(Hrs)	12	12	4
7	$t_{1/2}$(Hrs)	5.367	4.536	0.553

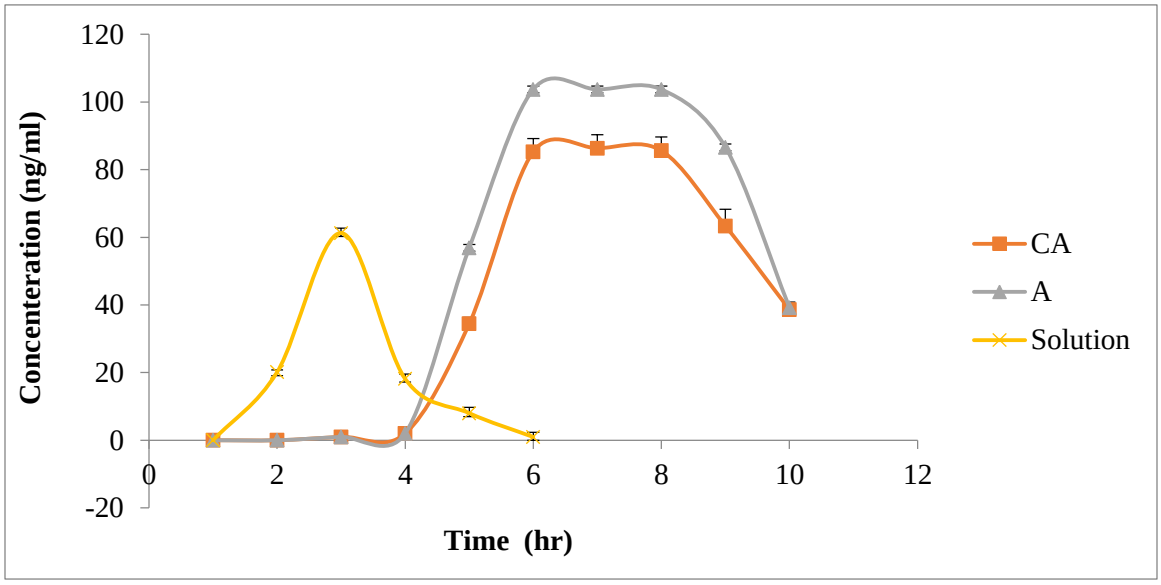

Figure 4.8.7: Combined plasma profile of Rabeprazole sodium after administration of oral drug solution, CA (CMC-g-AA) and A (CMAX-g-AA) hydrogel formulations

Table 4.8.6: ANOVA table for pharmacokinetic parameters of hydrogels (formulation codes A &CA) and drug solution

source	df	Sum of squares	Mean square	F	P-value
C_{max}	2	9470	4735	28.1611	0.0000 P < 0.05
AUC_{0-t}	2	5912508	2956254	151.1963	0.0000 P < 0.05
MRT	2	505	252	354.9876	-0.0000 P < 0.05
T_{max}	2	66.600	33.300	428.1429	-0.0000 P < 0.05

df=Degree of freedom

CHAPTER # 5

DISCUSSION

5. Discussion

5.1 Characterization of CMAX-g-AA hydrogels

5.1.1 Effect of variation of pH, monomer, polymer and cross-linker on swelling behavior of CMAX-g-AA hydrogel

5.1.1.1 Effect of monomer concentration on swelling

The swelling ratio depends upon the accessible free spaces of the expanded polymer matrix, polymer chain relaxation, and accessibility of ionizable functional groups i.e., carboxylic group. Dynamic swelling behavior of the hydrogels with varying concentrations (10%w/w, 15%w/w and 20%w/w) of acrylic acid was studied as a function of pH. Swelling profiles of the samples are given in Table 4.1.1. Initially swelling rate was slow but increased gradually at pH 7.4. CMAX-g-AA exhibit obviously pH dependent behavior, because of carboxylic acid side group. At higher pH carboxylic acid group on the acrylic acid became progressively more ionized, hydrogels swelled more rapidly. Rate of fluid uptake was considerably higher for the polymeric network in solutions with pH>5 than for the network in lower pH. Since pKa value of acrylic acid is 4.5-5.0, acrylic acid hydrogels swell extensively at higher pH. pH of surrounding medium is an important feature to evaluate swelling capacity in CMAX-g-AA hydrogel. Acrylic acid impart pH responsive behavior to CMAX-g-AA hydrogel. Swelling profile of formulations A1, A2 and A3 given in Table 4.1.1 indicated that swelling ratio (q) at alkaline pH (47.295, 54.37and 60.28 of A1, A2 and A3 respectively) increased with increase concentration of acrylic acid and (7.36, 5.49and 2.74 of A1, A2 and A3 respectively) decreased swelling at acidic pH. The effect of acrylic acid on swelling behavior has been studied by many researchers, enhanced acrylic acid contents in hydrogels increase hydrophilicity and pH sensitivity. As the contents of acrylic acid increased more carboxyl groups for ionization available, resulted in chain relaxation of coiled molecule due to electrostatic repulsion of carboxyl group, hydrogels exhibited high swelling rate at alkaline pH and low at acidic pH (Hossein, 2010; Huang *et al*., 2007; Jafari and Hamid, 2005).

5.1.1.2 Effect of polymer concentration on swelling

Effect of varying concentrations of CMAX also has been investigated on swelling capacity and pH responsive behavior of CMAX-g-AA hydrogel. It has been observed that as the contents of CMAX enhanced in formulations, there was increased swelling at alkaline pH. Swelling ratio of CMAX-g-AA hydrogel given in Table 4.1.2 has shown the swelling fashion at pH 1.2 (4.777, 4.181, and 3.533) and at pH 7.4 (59.322, 62.788 and 64.191) by raising CMAX contents from 1 %w/w, 1.5 %w/w and 2 %w/w respectively. Degree of swelling was highly pH dependent and increased by increasing concentration of CMAX. It may be assumed that increased contents of CMAX impart hydrophilicity to hydrogel. As it has been reported that carboxymethylation of Arabinoxylan modified its fundamental properties like hydrophilicity and anionic nature depending on degree of substitution (Saghir *et al*., 2008). Same behavior was depicted with carboxymethyl cellulose, but at high concentration above 2% w/w polymer ratio (high viscosity of medium) reduced crosslinking density of hydrogel. In contrast to CMC (carboxymethyl cellulose), CMAX reduce solution viscosity (Meenakshi and Munish,2015).

5.1.1.3 Effect of crosslinker concentration on swelling

Degree of swelling depends on crosslinked monomer concentration, polymer concentration and also on crosslinking density of hydrogels. Effect of crosslinker concentration on swelling phenomenon has been studied by keeping the monomer and polymer contents constant. Table 4.1.3 and Figure 4.1.3 depicts the degree of swelling with varying concentration of N, N methylene bisacrylamide used as crosslinker. Over all swelling was reduced with increasing contents of N, N MBA (0.2% w/w to 0.8% w/w), imparted hydrophobicity to hydrogels by reducing porosity (dense network) of hydrogels. With high contents of crosslinker swelling ratio decreased upto 50% (31.629) as that of high contents of (20 %w/w) acrylic acid, (60.28) and at 2 %w/w contents of CMAX (64.19) at pH 7.4.

Relationship between degree of swelling and crosslinker concentration has been explained by Flory equation

$$S = KC_c^{-n} \qquad (1)$$

Here K and n are constant values for individual hydrogels.

It has been reported that crosslinker concentration and swelling have inverse relation. By increasing N, N MBA concentration swelling was reduced. Concentration of crosslinker determines the crosslinking density of hydrogel. High contents of crosslinker fabricated harder and dense network, obstruct water absorption hence negative effect on swelling capacity and enhanced mechanical strength of hydrogel (Elliott *et al*., 2004; Pourjavadi and Mahdavinia, 2006).

5.1.2 Pulsatile behavior of hydrogel

The oscillatory swelling studies were also performed to scrutinize whether the response to the environmental pH was reversible and to check how rapid graft copolymer could retorted to the stimuli. Synthesized CMAX-g-AA hydrogels showed inverse reproducible behavior of swelling in acidic and alkaline medium. At pH 7.4, the hydrogel sample (A6) swelled up to 64 g/g due to anion-anion repulsive electrostatic forces, while at pH 1.2, it shrank within a few minutes due to protonation of the carboxyl groups. Equilibrium swelling was observed in long duration (in 72 hours) as compared to deswelling (25-35 minutes). The hydrogels experienced a number of swelling-deswelling cycles without representing any distortion in their shapes. This quick swelling deswelling manner of the hydrogels renders them appropriate nominee for controlled drug delivery systems. Since the presence of counter ions in the buffer solutions, the swelling capacity of hydrogel was significantly depleted. The maximum swelling capacity in the second cycle of the pH-reversibility curve of Figure 4.1.4 was lower than that of the first cycle due to enhancement tendency of the polymer network to mix with the solution. Such on-off switching behavior via reversible swelling and deswelling has been reported for other ionic hydrogels (Pourjavadi *et al*., 2006; Sadeghi & Hosseinzadeh, 2008).

5.1.3 Equilibrium water contents and gel fraction of CMAX-g-AA copolymer

For all the prepared hydrogels (series A1-A9) with varying concentrations of acrylic acid, CMAX and N, N MBA equilibrium water contents was determined as shown in Table 4.1.4. EWC have been evaluated for comparison of EWC at equilibrium

swelling state (0.85-0.98) with the EWC of the human body cells (0.6). For biomedical utility of hydrogel EWC determination is an essential parameter (Maryam *et al*., 2014).

EWC of hydrogels (A1-A9) ranging from 0.85 to 0.98 with different concentrations of acrylic acid, CMAX and crosslinker depend on the factors which favor the hydrophilicity. So high water contents of the gel at equilibrium state can be elucidated by hydrophilicity/hydrophobicity ratio of hydrogel. Thus, CMAX-g-AA copolymeric hydrogels revealed fluid contents analogous to those of living tissues. Malana and Zohra, 2013, have been prepared terpolymers of methacrylate, vinyl acetate and acrylic acid cross linked with ethylene glycol dimethacrylate (EGDMA) described analogous conclusion. They recommended that high crosslinker contents in the gel obstruct hydrophilicity and consequently lower EWC and AA contents exhibit reverse behavior in the hydrogel.

Gel fraction of prepared hydrogels has been investigated to evaluate the degree of grafting and cross linking density. Figure 4.1.5 illustrates the consequences of AA, CMAX and crosslinking agent concentrations on the gel fraction of different formulations (A1-A9) of CMAX-g-AA hydrogel. Table 4.1.4 was shown that by raising the concentration, of AA (10-20%w/w), gel fraction increased (68.15 to 84.11) CMAX (1 to 2%w/w) gel fraction increased (77.67 to 83.22) but above 1.5 %w/w there was no significant increment in gel fraction and MBA (0.4 to 0.8%w/w) gel fraction increased up to 96.40. Amin *et al.*,(2014) have also reported that as the acrylic acid and crosslinker contents increased in hydrogel formulation gel fraction increased because of increased degree of grafting.(Amin *et al.,* 2014)

5.1.4 Instrumental analysis

a) Scanning electron microscopy

One of the most important features is microstructure of hydrogel for swelling and drug release. Because crosslinking ratio and hydrogels composition direct the morphology of hydrogels and consequently affect hydrogel swelling behavior and drug release characteristics. Scanning electron microscopy was brought about to analyze surface

morphology and porosity of hydrogels. SEM analysis was performed to study the morphological behaviors of hydrogels presented in photomicrographs (Figure 4.1.6) exhibited porous surface. Porous structure of hydrogels allows water permeation and provides interaction sites to external stimuli with hydrophilic group of graft copolymer (Nihar and Patel, 2014).

It was also observed that porous structure of hydrogel swelled in pH 7.4 buffer and lyophilized become more prominent by increasing contents of acrylic acid in the hydrogels. This fact also has been explained that hydrogels with high acrylic acid concentration demonstrated a more open and porous structure as a result of electrostatic repulsion of the (carboxyl group) ionic charges of its complex in basic buffer (Thakur *et al*., 2011).

b) FTIR spectral analysis

FTIR spectral analysis was used to verify the graft copolymerization of monomer on natural polymer. The FTIR spectrum of pure Carboxymethylarabinoxylan (Figure 4.1.7) showed the characteristic peak at 3301 cm^{-1} due to –OH stretching, –C=O of –COOH at 1629 cm^{-1} and ether linkage at 1425 cm^{-1}. This can be related to the absorption of carboxymethyl groups in arabinoxylan and peaks at 1334, 1034, 895, 626, 618 cm^{-1} are due to polymer backbone. FTIR spectrum of CMAX-g-AA (Figure 4.1.7) showed characteristic peaks of –OH at 3286$cm^{-1,}$ –C=O of –COOH at 1628 $cm^{-1}$and ether linkage at 1453 and 1400 cm^{-1}, and the new bands at 1551 cm^{-1}(C=O stretching vibration of -COOH groups), showed that AA monomers were grafted onto CMAX chains. Psyllium (Psy) is a natural plant polysaccharide obtained from *plantago ovata* and psyllium mucilage contain arabinoxylan (arabinose 22.6%, xylose 74.6%) (Fischer *et al*., 2004). Cross-linked Psy-g-poly (AA) showed peaks at 2857 cm^{-1} (O-H stretching of carboxylic acid), 2361 cm^{-1} (N-H stretching), 1737 cm^{-1} (C=O stretching in carboxylic acid), 1636 cm^{-1} (strong C…O asymmetric stretching vibration) and1400 cm^{-1} (weak C…O asymmetric stretching vibration) these peaks confirmed grafting of acrylic acid on to psyllium backbone (Kaith *et al*., 2007).

c) Thermal analysis

The proof of grafting can also be verified by thermal (TGA/DSC) analysis. Thermal behavior of polymers was peculiar, so each polymer was prophesied to demonstrate a distinctive thermogram of both the parent polymer and crosslinked polymer. TGA studies were performed as a function of percent weight loss verses temperature. Decomposition of CMAX has been observed in two stages given in Table 4.1.5. Primary decomposition started at 266 °C and continued upto 382°C with 44.8 % weight loss. Second stage decomposition started at 431 °C and continues upto 562 °C with 25 % weight loss. While CMAX-g-AA (A) also showed decomposition in two stages, initial decomposition temperature (Tdi) at 443 °C and final decomposition temperature (Tdf) at 515 °C with 21.1 % weight loss. Second decomposition started from 610 °C and ended at 616 °C with 1.17% weight loss. Second stage of decomposition may contribute to the decomposition of different structure of the graft copolymer. Tdi of CMAX was lower than that of grafted polymer because CMAX-g-AA underwent morphological changes during grafting which modified its structure and properties as well, whereas Tdf of grafted polymer is slightly higher than that of CMAX, which showed more thermal stability as compared to the raw back bone. Similar results have been observed that cannabis indica-g-poly (AAc) fibers are thermally more stable than the raw fibers (Singha and Ashvinder, 2011).

DSC curve of CMAX and CMAX-g-AA given in Figure 4.1.9 show that in the CMAX has no endothermic and exothermic peak. CMAX-g-AA exhibit endothermic peak at 387 °C and exothermic peak at 467°C. DSC curve showed that grafting preceded to modifications in the thermal characteristics. It has been reported that pure polymer has no glass transition temperature (Tg) and melting temperature (Tm) due to strong inter- and intra molecular hydrogen bonding (Hatakeyama and Nakamura, 1982). Above mentioned justification, described that slight deviation in DSC curve of graft copolymer is a smashing symbol for both the presence of a Tg due to the graft side chains on the carboxymethyl arabinoxylan backbone and for the proof of grafting. These results are in good agreement with Zhe *et al* work. They demonstrated that CMC does not display any transition between -40 °C and 60 °C, while poly

(methylacrylate)-grafted CMC and poly(methyl acrylate) have glass transition temperatures at 19.2 ºC and 13.75 ºC, respectively (Zhe *et al*., 2011).

d) X-ray diffraction

Prepared hydrogel CMAX-g-MAA was investigated for amorphous or crystalline nature by X-ray diffraction as shown in figure 4.1.10. In general at low intensities diffraction decreased and peaks become broader when angle was increased depicting partial crystallinity of substance. Diffractogram ofXRD of formulations proved that graft copolymerization enlarges amorphous regions resulting in decreased value of percentage crystallinity. Grafting was thought to be basic reason behind amorphous nature of hydrogels as grafting of monomer side chain on basic polymer back bone imparts amorphous regions to copolymer. Chandra also reported that hydrogel formulations did not have any peak on x-ray difractogram giving justification on its highly amorphous nature (Chandra *et al.*, 2013). With the purpose to approve the physical state of the Rabeprazole in hydrogel, X-ray diffraction studies of unloaded formulation, drug and drug loaded formulation were conceded out. X-ray diffractograms were shown in Figure 4.1.10 exhibited that rabeprazole was still present in its amorphous state. As both polymeric network with or without drug showed analogous diffraction patterns. Furthermore, these results demonstrated that hydrogel and Rabeprazole did not interfere with each other in the formulation (Kazimiera, 2001).

5.1.5: In vitro release kinetics of Rabeprazole sodium CMAX-g-AA hydrogel

One of the most imperative function of hydrogels is controlled release systems, drug release to definite areas of the body. When close contact is ascertained to the target site, the rate and duration of drug release depends on the swelling manners of the hydrogel (Edith *et al*., 1999; Blancofuente *et al*., 1996; Donini *et al*., 2002).

Mechanism of drug release from polymeric network depends upon the composition of network, structural design of polymer network, medium to which it exposed and drug concentration in the polymer. In the following study the consequences of diverse factors on the drug release has been illustrated. Percent cumulative release of drug

from the polymeric carriers as a function of time and different pH values (1.2 & 7.4) were conducted as shown in Tables (4.1.6-4.1.8). The factors that control swelling fashion of hydrogel directly influenced release of drug as concentration of acrylic acid (formulation A1-A3), CMAX (A4-A5) and cross linker (A7-A9) given in Figures (4.1.11- 4.1.13) and pH of drug release medium. At acidic pH cumulative drug release from CMAX-g-AA hydrogels decreased (11.52 %, 7.64%, and 3.91 %) with progressive increase of acrylic acid (10 %, 15 % and 20 %) contents, because electrostatic repulsion between the carboxylic groups of backbone was low and decline gel swelling and reduces release of drug (Figure 4.1.11). However, at basic pH OH– group raises the electrostatic repulsion between carboxylate groups, thus enhance the gels swelling degree and so the release of drug amplified. Swelling studies divulged that pH and cross-linking density control polymer swelling. Polymer swelling take places at a pH above the pKa of the carboxyl group of acrylic acids. Swelling amplifies as the COO^- concentration increases, while by enhancing the cross-linking density swelling was declined. As acrylic acid impart hydrophilicity and pH sensitivity, so drug release accordingly. These results were supported by previous studies that drug release enhanced by increasing concentration of acrylic acid. High contents of acrylic acid causes the expansion of the coiled chains and consequences in better swelling of the gels (Ranjha and Mudassir 2008; Michel *et al*., 2011).

Furthermore, Carboxymethyl arabinoxylan has a hydrophilic nature, when the CMAX concentration was increased, the hydrophilic character of the hydrogel was increased. As swelling of hydrogels increased by increasing concentration of CMAX, swelling was directly proportional to drug release (92.83%, 96.76%, and 98.44% at CMAX concentration 1%, 1.5% and 2% respectively at basic pH). By increasing concentration of crosslinker over all swelling was reduced due to growing crosslinking density of polymer chain so drug release was also decreased given in Table 4.1.8. A number of authors have reported similar findings that by escalating the MBA concentration, there was a decline in drug release at all pH values owing to lessen in the mesh size of hydrogels, which hindered spreading out of the network and chain relaxation (Chen *et al*., 2005; Li *et al*., 2006; Sohail*et al*., 2014).

Different mathematical models have been applied for illustrating the kinetics of the drug release mechanism from CMAX-g-AA polymeric network. The technique that best fits the release data was estimated by the regression coefficient (r). For selection of the most suitable model criteria was based on the best fit values of regression coefficient (R^2) near to 1. Regression coefficient (r) values for Higuchi model, zero order, first order and KorsmeyarPeppas model were obtained from drug loaded CMAX-g-AA hydrogels at different contents of AA, CMAX and crosslinker have been given in the Table 4.1.9. For all formulations at alkaline pH the value of regression co-efficient (R^2) obtained for zero order release rate constants were found higher than those of others. Consequently it was deliberated that drug release from the formulations of varying acrylic acid, CMAX, and crosslinker contents were according to zero order release. Effect of formulation composition on release exponent 'n' values given in Table 4.1.9 between 0.5 and 1.0 are indication of non-Fickian or anomalous diffusion mechanism. Previous studies revealed that psyllium mucilage obtained from *Plantagoovata* has been modified by graft copolymerization by using N,N MBA as crosslinker and acrylic acid grafted onto mucilage employed as drug carrier. The release of model drugs salicylic acid and tetracycline from the hydrogels at alkaline pH occurred through non-Fickian diffusion mechanism (Singh *et al*., 2008). Release dynamics of insulin from psyllium–g-acrylamide has been studied for evaluation of release mechanism. It was found that drug release happened through non –fickian diffusion pattern (Singh *et al*., 2011).

5.2 Characterization of CMAX-g-MAA hydrogels

5.2.1: Effect of variation of pH, monomer, polymer and cross-linker on swelling behavior of CMAX-g-MAA hydrogel

5.2.1.1 Effect of monomer concentration on swelling

Swelling capacity of hydrogels depends on crosslinking density, hydrophilic contents, ionic contents of system and surroundings, environmental pH and temperature. The motivating force for swelling procedure is primarily equilibrium of osmotic pressure, electrostatic force and entropy-assisted dissolution of polymer in water. Elastic forces are specially made into the hydrogel structure to organize the entropy of the

dissolution process. These tailor made elasticity of hydrogels preclude absolute dissolution of hydrogel in swelling medium (Omidian and Park, 2008).

Swelling behavior of CMAX-g-MAA hydrogel of varying contents (monomer, polymer, cross linker) was investigated at acidic and alkaline pH given in Table (4.2.1-4.2.3). To evaluate the effect of methacrylic acid contents on swelling pattern series of formulations (M1, M2, and M3) with varying methacrylic acid contents from 20%w/w, 30%w/w and 35 %w/w respectively were analyzed at pH 1.2 and pH7.4. It was scrutinize that at alkaline pH swelling ratio (20.85, 16.70, and 14.28 of M1, M2 and M3 respectively) was higher than at low pH (5.03, 4.09 and 3.14 of M1, M2 and M3 respectively). pKa values of pH-sensitive polymers and buffer solutions perform major task in the swelling behavior. In literature it has been proposed that at basic pH, carboxyl groups of methacrylic acid repel each other, causing the swelling of the system. At acidic pH the carboxyl groups of methacrylic acid are unionized as a result, the polymer network remains in collapsed state avoid swelling. Phenomenon of electrostatic repulsion can also be explained by Donnan effect. Polymeric network is worthy of attracting counterions, causing a chemical potential gradient, osmotic pressure within the polymer's realm surmounts than that of the external solution, and therefore, the polymer is proficient of swelling. In the past it has been proclaimed, that polymeric networks containing methacrylic acid act like hydrophilic systems. Upon crosslinking they happen to insoluble, but are seemly to swell by protonation/de protonation of carboxyl group (Quintanar*et al*., 2008). Similar findings have been observed by Khare and Peppas in cross-linked poly (hydroxyethyl methacrylate-co-methacrylic acid) and poly (hydroxyethyl methacrylate-co-acrylic acid) hydrogels (Khare and Peppas, 1993). It has been observed that overall swelling (20.85, 16.70, and 14.28; 20%w/w, 30 %w/w and 35 %w/w methacrylic contents respectively) of CMAX-g-MAAwas reduced by increasing concentration of methacrylic acid. Hydrophobic nature of methacrylic acid was responsible for reduce swelling (Jafari and Hamid, 2005).

5.2.1.2 Effect of polymer concentration on swelling

Degree of swelling is highly pH dependent and increased by increasing concentration of CMAX as shown in Table 4.2.2. It may be assumed that increased contents of CMAX impart hydrophilicity to hydrogel. As it has been reported that carboxymethylation of Arabinoxylan modified its fundamental properties like hydrophilicity and anionic nature depending on degree of substitution (Saghir*et al*., 2008)

5.2.1.3 Effect of crosslinker concentration on swelling

Equilibrium swelling behavior of CMAX-g-MAA copolymer with varying degrees of cross-linking has been examined as a function of pH given in Table 4.2.3. It was ascertained that changing the degree of cross-linking has a significant effect on the swelling behavior. It has been shown in Figure 4.2.3 equilibrium swelling ratio by increasing N, N MBA concentration from 0.25%w/w to 0.85%w/w decrease swelling from 14.28 to 8.97. Decline swelling by increasing crosslinker contents could be mechanistically due to decreased mesh size of hydrogel and high degree of crosslinking obstruct ionization process. Our findings regarding relationship of swelling and crosslinker contents can be correlated with the results of Khalid *et al*., who prepared poly (methyl methacrylate-co-itaconic acid) hydrogels with varying contents of cross linker (Khalid *et al*., 2009).

5.2.2: Pulsatile behavior of hydrogel

Swelling equilibrium studies revealed that CMAX-g-MAA hydrogels are absolute pH sensitive system. For controlled drug delivery system, swelling process should be reversible to ensure that the release of drug could be triggered and stopped instantly. The proficiency of the contender polymer to manifest reversibility in swelling pattern was examined in the solutions of pH 1.2 and 7.4. It was detected that hydrogel at basic pH swell due to anion-anion repulsion of carboxylate ions, however, on exposing the swelled hydrogel in the solution of pH 1.2 it deswell with in few minutes due to protonation of carboxyl groups as shown in Figure 4.2.4. Now, again on immersing

the deswelled hydrogel in the solution of pH 7.4 swelled again, thus representing the pulsatile behavior.

This impulsive swelling-deswelling fashion at different pH values renders the system to be highly pH-responsive and thereby it may be a suitable candidate for designing controlled drug delivery systems. Similar pH dependency behavior has also been illustrated by other ionic hydrogels like Starch-Poly (Sodium Acrylate-co-Acrylamide) superabsorbent hydrogel; poly (acrylamide-co-methacrylic acid) grafted Gum ghatti based hydrogels (Sadeghi and Hosseinzadeh, 2008; Hemant *et al*., 2010).

5.2.3: Equilibrium water contents and gel fraction

It has been observed that the xerogel starts to drink water when it was placed in an aqueous media. Hence, determination of the extent of water gulped within the hydrogel is vital measure for illustrating the hydrogel for biomedical applications and is frequently symbolized equilibrium water contents, directly proportional to hydrophilicity of copolymeric network. Equilibrium water contents of CMAX-g-MAA was evaluated given in Table 4.2.4, revealed the effect of composition of hydrogel effect water absorbing capacity of hydrogels. It was scrutinizes that CMAX contents (1%w/w. 1.5%w/w and 2%w/w) promoted EWC (0.95), but increasing methacrylic acid contents (EWC=0.95-0.91) and crosslinker concentration (EWC= 0.92-0.81) obstruct water diffusion through hydrogels. Amount of water imbibed within the hydrogel impacts the diffusional characteristics of a drug through the hydrogel. Generally, the higher the equilibrium water contents, higher will be the diffusion rate of the solute. Micro-architecture of graft copolymer also one of the major controlling factor of EWC(Wei *et al*., 2009).

Figure 4.2.5 showed the effects of methacrylic acid, CMAX and crosslinking agent (N, N MBA) concentration on the gel fraction of different formulations of CMAX-g-MAA hydrogel. It was ascertained that by raising the concentration of MAA (M1toM3), and N, N MBA (M7 to M9) gel contents were increased while sol fraction decreased and by increasing the concentration of CMAX (M4 to M6) gel fraction increase upto 1.5% of polymer contents and above that remain constant. It has

been reported that reactivity of the monomers and radicals in copolymerization was determined by the nature of substituent in the double bond of the monomer. The methyl group of methacrylic acid may motivate the double bond, making the monomer more reactive than acrylic acid. Peppas and Klier prepared poly (methacrylic acid-g-ethylene glycol) hydrogels, and narrated that high MAA concentration formed efficient network (high gel contents) due to the higher concentration of reactive vinyl groups in monomer resulting in highly crosslinked matrix (Peppas and Klier, 1991).

5.2.4: Instrumental analysis

a) Scanning electron microscopy

The surface morphology of CMAX-g-MAA hydrogel was investigated by scanning electron microscopy (SEM). Figure 4.2.6presented SEM micrograph of the polymeric hydrogels. These photomicrographs confirm that synthesized polymer (CMAX-g-MAA) have a porous structure. At high magnification and lyophilized hydrogels (Figure 4.2.6) displayed a large, open, channel-like structure. Similar porous structure has been reported for crosslinked graft copolymer of methacrylic acid and gelatin (Sadeghi and Heidari, 2011). These interconnected pores could be suitable for controlling drug release by diffusion. Porosity of hydrogels depends on diverse factors like nature of monomer, reaction conditions, amount of diluent (water) and crosslinking density (Sadeghi, 2011).

b) FTIR spectral analysis

For polymer characterization one of preferred method is FTIR spectroscopy. To confirm grafting, FT-IR spectra of three samples (CMAX, MAA, and CMAX-g-MAA) were examined.

The FTIR spectrum of pure Carboxymethyl arabinoxylan (Figure 4.2.7) showed the characteristic peak at 3301 cm^{-1} due to –OH stretching, –C=O of –COOH at 1629 cm^{-1} and ether linkage at 1425 cm^{-1}. This can be related to the absorption of carboxymethyl groups in arabinoxylan and peaks at 1334, 1034, 895, 626, 618 cm^{-1} are due to polymer backbone. These results are in accordance with Saghir*et al*., work,

they prepared carboxymethylatedarabinoxylan by etherification method and characterized by FTIR spectra (Saghir*et al*., 2008).

Spectrum of CMAX-g-MAA(Figure 4.2.7) shown three new distinctive absorption peaks at 1692, 1536 and 1445 cm^{-1}authenticating the architecture of graft copolymer product. These new bands accredited to carbonyl stretching of the carboxylic acid groups and symmetric and asymmetric stretching modes of carboxylate anions, respectively. Similar findings have been illustrated for poly methacrylic acid grafted onto psyllium for confirmation of grafting (Ranvijay *et al*., 2013)

c) Thermal analysis

TGAthermogram of CMAX-g-MAA (Figure 4.2.8) illustrated that thermal degradation of graft copolymer was accomplished in two steps, 66 ^{o}C to 152 ^{o}C and 435 ^{o}C to 536 ^{o}C with weight loss 21.1%and 31.05% respectively. Middle thermal degradation temperature values, of both steps are 94 ^{o}C and 462 ^{o}C. Complete loss of pure methacrylic acid was detected below 200 ^{o}C as shown in Figure 4.2.8. Thermal decomposition of pure polymer CMAX was occurred in two steps initial degradation temperature of first segment is 266 ^{o}C and of second is 431 ^{o}C. Tdf of both steps are 382 ^{o}C and 562 ^{o}C with 44.8% and 25% weight loss. Total weight loss of graft copolymer is less than raw polymer, depicted thermal stability of graft copolymer. It has been illustrated in previous studies that weight loss in the range of 150–250 ^{o}C is due to the formation of anhydride with elimination of H_2O molecule from the two neighboring carboxylic group of the grafted chains. The second segment of degradation was credited to the decarboxylation of the anhydrides formed earlier. The change of thermal behaviors confirmed the formation of grafted copolymer. Xanthan gum grafted with methacrylic acid represented such type of thermal behavior (Kumar *et al*., 2007).

DSC curve of CMAX-g-MAA hydrogel revealed exothermic peak at 401 ^{o}C and endothermic peak at 517 ^{o}C as shown in Figure 4.2.9. These peaks confirm grafting because these are absent in polymer backbone DSC curve. Thermal stability and

endothermic–exothermic behaviors of graft copolymer related to the increase of molecular weight and addition of functional groups (Wang *et al*., 2011).

d) X-ray diffraction

Prepared hydrogel CMAX-g-MAA was investigated for amorphous or crystalline nature by X-ray diffraction as shown in figure 4.2.10. Diffractogram of XRD of prepared hydrogel proved that graft copolymerization imparted amorphous characteristics. Grafting was thought to be basic reason behind amorphous nature of hydrogels as grafting of monomer side chain on basic polymer back bone imparts amorphous regions to copolymer. Chandra also reported that hydrogel formulations did not have any peak on x-ray difractogram giving justification on its highly amorphous nature (Chandra *et al.,* 2013). The X-ray diffractograms of drug free hydrogel (M), drug (Rab) and drug loaded hydrogel (MD) were given in Figure 4.2.10. X-ray diffractograms documented for drug loaded and unloaded formulation did not express any distinctive peak, signifying that the captured drug was sustained amorphous state.

4.2.5:In vitro release kinetics of Rabeprazole sodium CMAX-g-MAA hydrogel

We were interested in developing a polymer which shows no swelling at low pH values and maximum swelling at higher pH value. In order to simulate the possible effect of pH on drug release rate, *in vitro* release studies were performed at acidic and alkaline pH values at physiological temperature of 37 °C. To explain release curves, three main factors have to be taken into account: pH sensitivity, graft copolymer composition and nature of individual constituent and crosslinking density of graft copolymer. *In vitro* release study has revealed that composition of the graft copolymer absolutely control release of drug. Figure 4.2.11 indicated that as contents of methacrylic acid raised (20%, 30% and 35 %), pH sensitivity enhanced (CPDR at basic pH is 84.19%, 75.9%, 71.26 and at acidic pH CPDR10.3%, 7.7% and 5.33%) but overall swelling reduced so percent cumulative drug release has been declined. Swelling analysis of CMAX-g-MAA hydrogel has been represented that overall swelling reduced by increasing concentration of methacrylic acid. Hydrophobic nature

of methacrylic acid was responsible for reduce swelling (Jafari and Hamid, 2005). The affirmative Rabeprazole sodium release depiction could be accredited to the pH-sensitivity of the hydrogel. Swelling of such hydrogels in the stomach was minimal so drug release consequently low. A similar practical approach has also been narrated by other researchers; pH sensitive methacrylic acid containing hydrogels can bypass the acidity of gastric fluid without liberating substantial amounts of the loaded drug (Lim and Lee, 2005).

Figure 4.2.12 revealed that by increasing concentration of CMAX (1%, 1.5% and 2%) percent cumulative release was increased at basic pH (79.78%, 87.93% and 90.06 % respectively) and become very low at acidic pH (4.91%, 3.17% and 2.93%). These results indicate that by increasing CMAX content of the hydrogels enhanced pH sensitivity, hence cumulative drug released at basic pH. This fact may be related with increased hydrophilicity of hydrogel by increasing CMAX contents, could be explained by free volume theory. This theory was suggested that solute diffuses only through aqueous region, so effective free volume available for transport of solute is free volume of water in gel in swollen state (Varshosaz and Koopaie, 2002).

Effect of MBA concentration on release of drug has been shown in Figure 4.2.13 revealed that high crosslinking density lead to low cumulative percent drug release i.e., 55%. This could be due to the fact that at higher crosslinking, reduced free volume of the matrix, thereby obstructing the transport of drug molecules through the matrix (Bhattarai *et al* 2010).

Numerous drug release models were practiced for analyzing the rabeprazole sodium release kinetics. Principles for choosing the apropos model were based on the ideal fit specified by the values of regression coefficient (R^2) near to 1. Regression coefficient (R^2) values obtained from CMAX-g-MAA hydrogels at varying contents of MAA, CMAX and N, N, MBA for zero order, first order, higuchi and korsemeyer peppas model are given in table 4.2.9. Values of R^2 obtained using zero order release model were viewed higher than other order release model, thus depicting that drug release from the series of hydrogels at varying amount of MAA, CMAX and N,N MBA was zero order. Release kinetics of drug from hydrogels have been used to describe the

relationship between drug dissolution and geometry of hydrogels on drug release patterns mathematically. It is apparent from the literature that no single approach was widely accepted to determine for similar dissolution profiles (Serraa *et al*., 2006).

5.3 Characterization of CMC-g-AA hydrogels

5.3.1: Effect of variation of pH, monomer, polymer and cross-linker on swelling behavior of CMC-g-AA hydrogel

5.3.1.1 Effect of monomer concentration on swelling

The rationale behind this study of grafting of acrylic acid on CMC was to increase the number of –COOH groups in CMC. These –COOH groups were expected to participate in minimizing the swelling at pH 1.2 and maximizing the swelling at pH 7.4. The limited swelling at low pH has consequently decreased the loss of loaded Rabeprazole sodium in gastric region.

Controlled release through oral drug delivery was usually based on the strong pH variations encountered when transitioning from the stomach to the intestine. The equilibrium swelling behavior of CMC-g-AA was studied as a function of pH and time at 37^{o}C. For this purpose , a series (CA1 to CA3) with varying contents of monomer (AA), (CA4 to CA6) with varying contents of CMC, (CA7 to CA9) with varying contents of cross-linker were synthesized. While altering the single constituent amount, other contents amount were kept constant.

It was observed that swelling ratio of the hydrogel was low in acidic medium and high at basic pH which was due to ionization of COOH groups of Acrylic acid at pH 7.4 (David *et al*., 2008). At low pH, anionic group remain protonated the gel exhibited syneresis and the swelling rate and ratio was low. Thus, as pH rose the carboxylic acid groups on the PAA became progressively more ionized. In these cases, the hydrogels swelled more rapidly due to a large swelling force created by the electrostatic repulsion between the ionized acidic groups. Thus CMC-g-AA revealed pH sensitive behavior and as the acrylic acid contents increased this response has been more pronounced. Huang *et al* (2007) prepared guar gum poly (acrylic acid) hydrogels and observed the similar swelling and drug release behavior. They reported that the

swelling and ketoprofen release was increased with increase of PAA content in the gel structure.

Parallel rise in swelling behavior was observed with concentration of acrylic acid. This phenomenon can be related to the increasing of anionic –COO- groups in the hydrogel. In addition, higher AA content enhanced the hydrophilicity of hydrogel, causing a higher absorption of buffer. Toledano *et al*, (2005) have also reported that the water absorption capacity of poly (acrylic acid) (PAA)-grafted-cellulose microfibers was found to be three times higher than that of original cellulose microfibers at alkaline pH. Water absorbing capacity will depend on degree of ionization, grafting percentage and ionic strength of swelling medium.

5.3.1.2 Effect of polymer concentration on swelling

It was observed that swelling of graft copolymer increased with an increasing concentration of CMC up to optimum level. Above that concentration swelling ratio was decreased. Figure 4.3.2 showed swelling ratio was increased (35.3, 37.8, and 43.3 of CA4, CA5 and CA6 respectively)with increased CMC concentration (0.5 %, 1%, and 1.5%) respectively but decreased(31.6) at 2% concentration of CMC. The increase in CMC content within the hydrogel shifts the position of the pH threshold to a lower values, as well as it reduces the magnitude of the phase transition. The effect of the increase of CMC content on position and magnitude of such phase transition might be attributed to the hydrophilic character of the CMC, as well as the crosslinking density. However, upon further increase in the polymer concentration, increase in the reaction medium viscosity, restricts the movements of macroradicals that was leading to decrease in grafting ratio.

Wang *et al* (2013) has been reported that with increasing content of CMC, the swelling ratio of the hydrogel increased up to optimum increment and then decreased. As the CMC concentration was increased the macromolecular radicals used to graft with monomers were increased and the grafting efficiency was enhanced. As a result, swelling ratio increased with increasing CMC content. Beyond this limit, increased contents of CMC may enhanced the viscosity of the reaction system the chain transfer

reaction was restricted, which decreases the grafting efficiency ultimately swelling decreased.

5.3.1.3 Effect of crosslinker concentration on swelling

Effect of crosslinker concentration (Cc**)** on rate of swelling of crosslinked CMC-g-(PAA) was investigated. As shown in Figure 4.3.3, more swelling ratio (32.3g/g) was obtained by lower Cc (0.4%) and less swelling ratio (23.8g/g) by higher Cc (0.8%). Higher crosslinker concentration increased crosslinking density of graft copolymer, that may resulted in more stabilization of the gel network. Crosslinked rigid structure cannot be expanded, resulted in less swelling when it was brought into contact with solvent. During the swelling process, it was also observed that the discs having relatively low concentration of cross linker were de-shaped at their boundaries, which could be attributed to the faster rate of swelling. Chandra *et al*., (2013) reported the good crosslinker concentration dependent swelling behavior of semi-IPN (interpenetrating network), as the crosslinker concentration was increased the swelling ratio decreased that was because the higher extent of crosslinking in the polymer network decrease diameter of pores of resultant hydrogels leading to decrease solvent mobility.

5.3.2: Pulsatile behavior of graft copolymer

The pH-dependent swelling reversibility of the CMC-g-AA was examined in buffered solutions of pH 1.2 and 7.4 as shown in Figure 4.3.4. It was evident from the plot that the swollen networks reverted to relatively collapsed networks whenever the pH decreased below pKa of the gel and that the deswelling time was faster than the swelling time. Swelling at pH 7.4 may take place due to anion-anion repulsion electrostatic forces and deswelling at low pH is due to protonation of carboxylate ions. After four On–Off cycles, the graft copolymer was still pH responsive. Swelling ratio was decreased and swelling time increased in every consecutive cycle, this may be due to some irreversible ionic complex. This pH reversibility makes the graft copolymer suitable candidates for controlled drug delivery systems. Sadeghi and Heidari (2011) described that hydrogels exhibited high pH responsive behavior by reversible

swelling- deswelling response in acidic and basic solutions renders hydrogels as a good candidate for controlled drug delivery systems.

5.3.3: Equilibrium water contents and gel fraction

Equilibrium water contents (EWC) were measured for hydrogels (CA1-CA9), composed of varying strength of acrylic acid, CMC and crosslinker. The data obtained for EWC was given in Table 4.3.4. It was shown that the amount of water taken in the hydrogel samples increased from 0.96-0.99. By increasing acrylic acid contents EWC value was increased (0.96-0.98), this may be strengthened by the fact that acrylic acid contain COOH functional groups. Ionization of these groups causes excessive repulsion between the coiled chains which is ultimately responsible for retaining more water. Another fact which can be used to explain the increased value of EWC was owing to more hydrophilic characteristics of acrylic acid. CMC also impart hydrophilic character to hydrogels also improve EWC value of hydrogels. Increasing crosslinker contents reduced EWC of hydrogel because of high crosslinking density may lead to depleting microchannels for water transport. Wang and Wu (2005) suggested that increasing hydrophobic contents in hydrogel leads to lower EWC in hydrogels.

Results of gel fraction of different formulations of CMC-g-AA were presented in Figure 4.3.5. It was perceived that by increasing hydrogels constituents enhanced gel fraction and reduced sol fraction of hydrogels. Amin *et al.*, (2014) have also reported that as the acrylic acid and crosslinker contents increased in hydrogel formulation gel fraction increased because of increased degree of grafting (Amin *et al.*, (2014).

5.3.4 Instrumental analysis

a)Scanning electron microscopy

SEM images showed dense three dimensional porous network structure. This picture verified that synthesized graft copolymer in this work have a porous structure. It was supposed that these pores were areas of solvent permeation responsible for swelling.

Figure 4.3.6 depicted that hydrogels at high magnification displayed large, open and channel like structure.

b) FTIR spectrum analysis

FTIR spectrum of the pure CMC, Figure 4.3.7 showed a broad absorption band at 3352 cm^{-1}, due to the stretching frequency of the –OH group and a band at 2924 cm^{-1} attributable to C H stretching vibration. The presence of strong absorption band at 1589 cm^{-1} confirmed the presence of COO^- group. The bands around 1420 and 1320 cm^{-1} are assigned to CH_2 scissoring and OH bending. FTIR spectrum assigned to stretching vibration of carbonyl is generally used for the confirmation of grafting. As the new bands at 1703 cm^{-1} (C=O stretching vibration of -COOH groups), and 1450 cm^{-1} (COO symmetrical stretching vibration of -COO groups) reveal that AA monomers were grafted onto the CMC chains.

c) Thermal analysis

The thermo gravimetric analysis (TGA) of hydrogel (CA) given in Figure 4.3.8 was depicted that the hydrogel was thermally stable. According to thermogram, the decomposition of hydrogel (CA) started at 300 ºC. The first step of degradation due to dehydration is observed up to 365ºC with 20 % weight loss. Second step of degradation is observed from 365-450 ºC with 15.17% weight loss and third step from 450ºC -586ºC with 21.782% weight loss due to degradation of functional groups of hydrogel.

DSC is the thermal analysis method practiced to evaluate the temperatures and heat flows linked with shifts as a function of time and temperature. Transition related with absorption or emission of heat created alteration in heat flow. Difference in energy recorded as peak. Area under the peak is directly related with enthalpy changes and direction of peak designates the thermal episode as endothermic or exothermic.

The endothermic peak of CMC below 100 ºC was evidently punier than that of CMC-g-AA, and the new endothermic peak at 450 ºC also seemed in the DSC curve of CMC-g-AA displayed in Figure 4.3.9. This signpost that the thermal decomposition

progression was comforted by grafting. Higher glass transition temperature value of prepared hydrogel (450 ºC) than pure parent polymer (325 ºC) can be accredited to the higher intermolecular hydrogen bonding as a result of grafting. Previous work has been described that shift to higher decomposition temperature could be accounted to formation of covalent bonds in the graft copolymers, and improved thermal stability (Wang *et al*., 2010).

4.3.5:In vitro release kinetics of Rabeprazole sodium CMC-g-AA hydrogel

Physiological variations of pH are present along gastrointestinal tract i.e. pH 1.2 to pH 7.4. (Chickpetty *et al.,* 2010). In the present study %cumulative drug release from CMC-g-Acrylic pH sensitive hydrogel ranges from 3.12% to 10.66% during early 24 hrs of dissolution release in simulated acidic pH medium of stomach (i.e. pH 1.2) while it range from 50.68% to 80.75% depending upon varying amounts of CMC, acrylic acid and cross linker as shown in Tables (4.3.5, 4.3.6 and 4.3.7 respectively). Percent drug release from pH sensitive gel increases by increasing amounts of polymer and monomer (i.e. Carboxymethyl cellulose and acrylic acid). While %cumulative drug release decreases with increasing concentration of cross linker as supported by values of decreasing %cumulative release of CA7 to CA9 i.e. 4.82 to 3.12 in 24 hrs of dissolution release in simulated acidic pH and 63.17 to50.68 in simulated intestinal medium.

Increase in % cumulative drug release can be justified by increasing molar ratio of polymer or monomer which was due to optimized swelling ratio of formulations with increasing concentration of polymer/monomer by polymer chain expansion. In fact by increasing polymer/monomer ratio enhanced swelling capacity at alkaline pH was imparted to formulations. These characteristics also imparts better swelling rates and smart swelling behavior in pH sensitive environment i.e. pH ranging from 1.2 to 7 which propose such formulations as good candidate for controlled drug delivery systems (Wang *et al.,* 2013).

Same type of study was conducted in 2013 which showed that swelling ratio enhanced with increasing CMC content until a maximum absorption which ultimately effects

drug release from formulation in same pattern. The approach behind was as molar ratio of CMC increased, macromolecular radicals that were used to graft with monomers were increased. As a result grafting efficiency was enhanced resulting in increased swelling ratio with increasing CMC content. Ultimately drug release is also effected by same pattern by increasing concentration of CMC (Wang *et al.*, 2013).

In present study pH sensitive behavior of formulations can be supported by another study conducted by other researchers where it was clearly elaborated that swelling coefficient was significantly higher at higher pH as compared to low pH. It was also worth mention that swelling of hydrogel was decreased by increasing the concentration of cross linker due to presence of more physical entanglements between hydrogels (Nazar and Umbreen 2014). Both factors supported the results of present study i.e. percent cumulative drug release increases from acid to basic pH and it decreased with increasing concentration of crosslinker.

To obtain a more quantitative understanding of the transport kinetics in the hydrogel, the drug release data was analyzed as a function of the time. The drug release data from a polymeric disc in glassy state is mainly modeled with the following empirical kinetic power equation to estimate the release kinetic parameters.

$$M_t/M_\infty = k \cdot t^n \qquad \text{Eq (3)}$$

$$\log (M_t/M_\infty) = n \cdot \log t + \log k \qquad \text{Eq (4)}$$

where M_t/M_∞ is the fractional release of drug in time t, k is a constant incorporating structural and geometric characteristic of the system, and n is an exponent indicative of the mechanism of drug release. The n and k values could be calculated from the slope and intercept of the plot of log (Mt/M∞) against log t using equation (4). We plotted log (Mt/M∞) against log t of the experimental data according to equation 3. A typical plot of log (Mt/M∞) versus log t for rabeprazole sodium at 37 ºC showed linearity, indicating that the Peppas equation is applicable to the present system. As a first approach, release exponents, n, regression coefficients, (R^2) from the drug delivery system were obtained by these plots and are listed in Table 4.3.8. The value of n for Rabeprazole sodium mentioned in Table 4.3.9 indicating

that the release of Rabeprazole sodium was an anomalous transport instead of a swelling-controlled transport (Huang and Brazel 2001, Ritger and Peppas , 1987, Korsmeyer *et al,*. 1983, Peppas *et al,*. 1987).

5.4 Characterization of CMC-g-MAA hydrogels

5.4.1 Effect of variation of pH, monomer, polymer and cross-linker on swelling behavior of CMC-g-MAA hydrogel

5.4.1.1 Effect of monomer concentration on swelling

The best exigent task in the development of drug delivery systems is to deal with instabilities of drugs in the cruel environment of the stomach. Swelling capacity in varying pH buffer solutions is of prime significance practical applications for controlled drug delivery system Equilibrium swelling capacity of hydrogels depends on hydrogel structure, crosslinking density, ionic contents and hydrophilicity of hydrogel (Omidian and Park 2008)

In present study dynamic swelling studies of CMC-g-MAA were executed to scrutinize the swelling behavior of hydrogels prepared using a different molar ratio of carboxymethyl cellulose, methacrylic acid and N, N MBA (crosslinker). Figure 4.4.1 showed swelling profile at different pHs for hydrogels prepared with varying methacrylic acid (monomer) contents. It was observed that hydrogels revealed pH sensitive behavior. At pH 1.2 hydrogels remained in collapsed state, showed less swelling. At alkaline pH swelling ratio was increased owing to dissociation of pendant acidic group (carboxylate group) of hydrogel. It has been proposed that as the methacrylic acid contents (20%, 30% and 35%) were increased, pH sensitivity of hydrogels augmented. At pH 7.4 exhibited chain relaxation process due to repulsion among –COO- groups sideways macromolecular chains formed from the ionization of carboxylic groups. Electrostatic repulsion caused the network to expand and solvent entered causing swelling at high pH. The equilibrium water absorption of hydrogel manifested its swelling capacity and was a function of the network configuration, the crosslinking ratio, hydrophilicity and the degree of dissociation of the functional groups. Similar swelling behavior has been depicted by HEMA-co-MAA hydrogel. HEMA-co-MAA revealed highly pH sensitive behavior but less equilibrium water

uptake because of methyl group, promoted hydrophobicity to polymeric network thus obstruct expansion (Khare and Peppas, 1995).

5.4.1.2 Effect of polymer concentration on swelling

Effect of carboxymethyl cellulose concentration on swelling capacity and pH sensitivity have been depicted in Figure 4.4.2. It was observed that increased contents of CMC (1%, 1.5%), there was decrease in swelling (26.45, 24.89). This fact may be related with increase gel fraction increased number of crosslinks per unit volume, thus causing a decrease in the free space for lodging of water molecule. Additionally, the increased firmness of the network also limited the relaxation of macromolecular chains in the matrix, thus directing to minor degree of swelling. Swelling profile of CMC-g-MAA hydrogels at alkaline pH revealed pH sensitivity, owing to negatively charged groups (carboxymethyl groups (-$COOCH_3$) in CMC increases the electrostatic repulsions between the polymer chains and permitted entry of fluid into hydrogel network thus enhance swelling ratio. Swelling at acidic pH was inhibited by collapsing the polymeric chains (protonation) and hindering the solvation of the hydrogel. Previous studies described similar CMC behavior in hydrogel swelling (Gabriela *et al*., 2011).

5.4.1.3 Effect of crosslinker concentration on swelling

In order to evaluate the effect of crosslinker contents on swelling three samples with varying concentration (0.2%, 0.3% and 0.4%) of N, N MBA has been prepared and observe their swelling profile. Figure 4.4.3 showed that increased crosslinker contents reduced swelling due to compact and dense polymeric network. Similar findings have been described by other researchers that high degree of crosslinking of hydrogels produce less porous network had a low swelling ratio (Lee *et al*., 2004).

5.4.2: Pulsatile behavior of hydrogels

To evaluate the pH responsive behavior of prepared hydrogels reversible oscillatory swelling experiment has been conducted. Pulsatile behavior of CMC-g-MAA has been shown in Figure 4.4.4, demonstrated that hydrogels undergo volume phase transition at acidic and basic pH due to protonation/and deprotonation of pendant groups

attached with copolymer chain leads to conformational changes. The pH-responsive swelling and collapsing style of CMC-g-MAA hydrogel was required for controlled release of acid sensitive model drug (rabeprazole sodium) in our study. Literature has been supported our findings that ionic hydrogels represent reversible swelling and deswelling behavior in response to pH transition due to electrostatic interactions of hydrogels and swelling medium. The most common pH-sensitive hydrogels were poly(acrylic acid) (PAA), poly (methacrylic acid) (PMAA), poly (diethylaminoethyl methacrylate) (PDEAEMA), and poly (dimethylaminoethyl methacrylate) (PDMAEMA), and their copolymers (Zhang and Peppas, 2000).

5.4.3: Equilibrium water contents and gel fraction

It has been reported that constituent that impart hydrophilic character to hydrogel improve water contents of hydrogels. Table 4.4.4 showed the variation of EWC of CMC-g-MAA hydrogels in varying quantities of CMC, MAA and croslinker. The values of EWC increased with increase of CMC content in the hydrogels. It was increased from 0.95-0.97 for the concentration of CMC in the range 1 to 2% in the hydrogels. CMC has high attraction to water due to existence of carboxyl group in it, as a result EWC of CMC-g-MAA hydrogels increased. Such characteristics of carboxymethyl cellulose (CMC) has also been reported that it improves EWC properties of poly (vinyl alcohol)/sago blend hydrogel due to the presence of the carboxylic group in the CMC molecules. Results also described that by increasing methacrylic acid amount and crosslinker contents decreased EWC values of hydrogels because of hydophobic nature (Dafader *et al*., 2009).

Figure 4.4.5 showed the effect of different concentrations of carboxymethyl cellulose, methacrylic acid and crosslinker (N, N MBA) on gel fraction. It can be explained on the basis of results that by increasing concentration of individual constituents increased gel fraction. Optimized reaction conditions and increased contents provide sufficient grafting site, monomers and crosslinking density favor high gel fraction. It was also reported that by increasing crosslinker contents in hydrogels resulted in high crosslinking density ultimately higher gel contents (Chen *et al*., 2010).

5.4.4: Instrumental analysis

a) Scanning electron microscopy analysis

Porous structure of hydrogel is prerequisite for their application in controlled drug delivery. Because porosity enhance the swelling capacity so, reduce drug transport resistance. CMC-g-MAA photomicrographs shown in Figure 4.4.6 were exhibiting that hydrogel was compact, smooth and dense surface at low magnification and at high magnification exhibited heterogeneous pore distribution in the structure. These morphological modifications related to grafting of methacrylic acid on to CMC accelerate penetration of water, promote swelling. The porosity plays the multiple role for drug loading and release from the hydrogels. Similar findings have been reported for pH-Sensitive Poly(ethylene oxide) grafted methacrylic acid and acrylic acid hydrogels (Lim and Lee, 2005).

b) FTIR spectrum analysis

In Figure 4.4.7 FTIR spectrum of pure sample showed, evidently exposes the major peaks allied with NaCMC. Previous studies have described that absorption bands seem at wave numbers of 1500-1700 cm^{-1} due to carboxyl groups and its salts respectively (Daniela *et al*., 2012).The band at 1030 cm^{-1} was due to carboxymethyl ether group (CH O CH_2-) stretching. Strong absorption band at 1589 cm^{-1} shown in Figure 4.4.7 confirmed the presence of C=O group, designated CMC. The band at 2924 cm^{-1} was due to C–H stretching of the $–CH_2$ and CH3 groups.The band around 1322 cm^{-1} was assigned to OH bending vibration. General absorption band at 3200 - 3600 cm^{-1}, due to the stretching frequency of the –OH group. (Auda *et al*., 2014)

FTIR spectrum in Figure 4.4.7 is associated with CMC-g-MAA (CMA) hydrogel.It can be perceived that important peaks at 1691, 1641 and 1443cm^{-1} authenticating the development of graft copolymer product. These peaks ascribed to carbonyl stretching of the carboxylic acid groups and symmetric and asymmetric stretching styles of carboxylate anions, respectively.This fact practically proved grafting of vinyl monomer onto carboxymethyl cellulose polymer backbone. Previous study revealed that FTIR spectra of the grafted (starch garfted with methacrylic acid) sample specify

the advent of identical absorption bands which were not observed in the spectrum of polymer backbone (Deepak and Reena, 2012).

c)Thermal analysis

Thermogram given in Figure4.4.8 CMC exhibited two distinct decomposition phases in its thermogravimetric curve. The first one was in temperature range of 51-89^{o}C allied with loss of moisture (4.76 wt %), and the second one was in the range 255-314^{o}C with maximum weight loss (36.08%), related with decomposition of carboxymethyl group. The maximum decomposition of the CMC-g-MAA hydrogels occurred in a temperature range of 447 - 531^{o}C, with approximately 21.79 % weight. Significantly, the remaining weight of the hydrogels at Tdf was far higher than the parent constituents. Higher remaining mass in the thermal profile of hydrogels designated higher thermal stability of the hydrogels than of the individual constituents. Preceding research has also been designated that graft copolymerization of natural polymer with vinyl monomers could augment their thermal stability (Silva *et al.*, 2007). DSC is the thermal analysis method practiced to evaluate the temperatures and heat flows linked with shifts as a function of time and temperature. Transition related with absorption or emission of heat created alteration in heat flow. Difference in energy recorded as peak. Area under the peak is directly related with enthalpy changes and direction of peak designates the thermal episode as endothermic or exothermic.

The endothermic peak of CMC below 100 ºC was evidently punier than that of CMC-g-MAA, and the new endothermic peak at 495ºC also seemed in the DSC curve of CMC-g-MAA (Figure 4.4.9).This signposts that the thermal decomposition progression was comforted by grafting. Previous work has been described that shift to higher decomposition temperature could be accounted to formation of covalent bonds in the graft copolymers, and improved thermal stability (Wang *et al*., 2010).

4.4.5:In vitro release kinetics of Rabeprazole sodium CMC-g-MAA hydrogel

Rabeprazole sodium release studies were conducted to a maximum period of 24 hrs in buffer of pH 1.2 and Tris buffer of pH 8 in accordance with the US Food and Drug

Administration. Results displayed in Figure 4.4.10showed rabeprazole sodium released from a gel containing 20 %, 30 % and 35 %w/w MAA at constant CMC and cross- linker contents. It was viewed that maximum drug released at pH 1.2 was (11.69 %, 7.80 %, and 5.59 % respectively) after 24 hrs with increasing contents of methacrylic acid. However, 63.11 % to 71.85 % of the total drug loaded was released at pH 8 in 24 hrs**.** These results are correlated with pH responive swelling of hydrogels. Analogous findings were depicted in previous studies, pH sensitive poly(methacrylic acid-g karaya gum) synthesized graft copolymer exhibited pH responsive swelling and drug release pattern (Momin *et al*., 2014).

Effect of carboxymethyl cellulose contents on percent cumulative drug reease have been studied. Results displayed in Figure 4.4.11 revealed that percent cumulative drug release at acidic pH (1.2) and at alkaline pH (8) were in accordence with swelling fashion of CMC-g-MAA hydrogels. High CMC contents increase hydrophilicity and dominent anionic properties to hydrogels, augment pH sensitivity and drug release accordingly.

Effect of concentration of crosslinker has also been studied, results presented in Table 4.4.8. Figure 4.4.12 revealed that by modulation in crosslinking density of hydrogels, decreased percent cumulative drug release due to compact and highly dense network restricted permeation of release medium ultimately declined swelling. Our findings are correlated with previous work that high crosslinker contents reduced free spaces for drug transport from meshwork of polymer (Varshosaz and Niloufar, 2002).

To evaluate the release mechanism from hydrogels drug release data was analysed by various release kinetics models, zero order kinetics, first order kinetics, Higuchi model, and Korsemeyer Peppas equation. Most appropriate mechanism was explained on the basis of best fitness of release model. The release model can be anticipated by deliberating the regression value nearby 1. The kinetics of drug release governed by comparative drive of the erosion and swelling/diffusion fronts.

To comprehend the rabeprazole sodium release from loaded graft copolymeric network, in vitro release studies data were fitted into release models as shown in Table 4.4.9, and release profile at basic pH was best explained by Higuchi model, as

plots expressed high linearity with regression value of between 0.992-0.998 of series of hydrogels with varying composition weight ratios. Drawback of Higuchi model was that it is unable to explain effect of swelling on matrix upon hydration. Therefore, *in vitro* release data were also fitted to exponential Korsmeyere Peppas equation and value of release exponent (n) explains the exact release mechanism. The detected 'n' values for release profiles of hydrogels were fall in between 0.50 and 1 indicated anomalous release behavior. Similar release kinetics have been exhibited by Poly (Vinyl caprolactam) grafted on to sodium alginate, the values of 'n' were in the range of 0.616-0.918 were accredited to the anomalous type of diffusive transport of drug (Madhusudana *et al*., 2013)

5.5: Characterization of PEG-g-MAA hydrogels

5.5.1 Effect of variation of pH, monomer and polymer on swelling behavior of PEG-g-MAA hydrogel

Swelling capacity in varying pH buffer solutions is of prime practical applications for controlled drug delivery system. Foremost dynamics that effect the swelling ratio of ionic hydrogels include polymer characteristics (charge, concentration and pKa of the ionizable group, degree of ionization, cross-link density and hydrophilicity or hydrophobicity) and features of the swelling medium (pH, ionic strength and the counterion and its valency) (Piyush *et al*., 2002).

Unique properties of PEG-based hydrogels renders them best nominee for drug delivery applications. Stimuli sensitive nature of PEG -based hydrogels referred as smart hydrogels. To evaluate the intelligent properties of PEG-based hydrogel we have prepared a series of hydrogels with varying PEG and methacrylic acid concentration by free radical polymerization technique. Swelling behavior of these hydrogel mentioned in Figure(4.5.1 and 4.5.2) and Table (4.5.1 and 4.5.2) revealed that swelling of the hydrogels was highly dependent on MAA contents and triggered a decrease in gel swelling in acidic buffer and increase in gel swelling in basic medium. MAA imparts pH sensitivity to hydrogels. The hydrogen-bonding and electrostatic interactions augmented with MAA content in the copolymer networks. Since, high

MAA contents in the hydrogels offers supplementary hydrogen bonds at low pH and more electrostatic repulsion at high pH. Present study has also been depicted that increasing concentration of PEG 600 increased swelling because of low crosslinking density. As high molecular weight PEG increased crosslinking density and reduced diffusion of solvent consequently reduced swelling. Similar results have been reported in previous study of poly (methacrylic acid-co-PEG) hydrogel (Bell and Peppas, 1996).

5.5.2: Pulsatile behavior of hydrogels

Equilibrium swelling analysis of PEG-g-MAA hydrogels revealed their pH sensitive attitude. Sharp swelling/deswelling pattern of pH sensitive hydrogels was studied to evaluate controlled drug release behavior from PEG-g-MAA hydrogel. Since hydrogel swells antagonistically at simulated gastric and intestinal pH as shown in Figure 4.5.3. At basic pH hydrogel swells because of repulsive electrostatic forces, while at acidic pH it contracts within a few minutes due to protonation of carboxyl groups. Similar pulsatile behavior exhibited other ionic hydrogels like chitosan-g-poly(Acrylic acid-co-HEMA) in acidic and alkaline solution (Sadeghi, 2010).

5.5.3: Equilibrium water contents and Gel fraction

EWC of hydrogels is the most substantial property, imparts them uniqueness for applications in biomedical fields. EWC of hydrogel be governed by the explicit interaction between water molecules and polymer chain. Table 4.5.3 denoted EWC of PEG-g-MAA hydrogels, as the PEG contents increased from 5-20% EWC values enhanced 0.89 to 0.95. Such propensity may be elucidated by a larger number of water molecules binding to the PEG chain through hydrogen bonds (Cursaru *et al*., 2010).

Sol-gel analysis is an important tool to measure crosslinking density or gelation which is related with its other physico-chemical properties. Sol–gel fraction analysis measures uncross linked or soluble residue of polymer or monomers and crosslinker in hydrogels. For this purpose sol–gel fraction analysis was performed on different series of hydrogels. Figure 4.5.4 showed the effect of varying amounts of PEG, and MAA

on gel fraction. Results showed that gel fraction was directly proportional to the concentration of individual constituents.

5.5.4: Instrumental analysis

a) Scanning electron microscopy

Scanning electron microscopy is an influential method extensively used to envisage the distinctive 'network' structure in hydrogels. The evidences attained through this technique explore the characteristics, useful for interaction of the hydrogels with living systems. Figure 4.5.5 displayed that PEG-g-MAA hydrogels having rough and porous surface morphology. SEM micrograph of PEG-g-MAA present high heterogeneity in pore size and shape. Numerous hydrogels with varying pore sizes and shapes have been published in the literature and pore size smart hydrogels can be controlled by external stimuli as temperature, pH, electrical discharge (You and Auguste, 2010; Li *et al*., 2010).

b) FTIR spectrum analysis

Hydrogels prepared by free radical polymerization were characterized by an ATR-FTIR spectroscopy. In Figure 4.5.6, ATR-FTIR spectra of the PEG, MAA, and PEG-g-MAA were presented. PEG exhibited the absorption peaks at 2914 cm^{-1} and around 1094 cm^{-1}. Other peaks were assigned to the $–CH_2$ scissoring band of ethylene glycol units at 1480 cm^{-1} and the antisymmetric and symmetric stretching bands (–O–R) of ethylene glycol units at 1160 cm^{-1}, respectively. FTIR spectrum of PEG-g-MAA an intense band (1710 cm^{-1}) conforming to the carbonyl group lifted by the hydrogen bonding between the ether group of the PEG and the hydroxyl group of the carboxyl group of Methacrylic acid (Bumsang and Peppas, 2003).

c) Thermal analysis

Thermal analysis of hydrogel is edifying regarding various features like, intrinsic crystallinity, melting behavior, flow properties, and nature of degradation. TGA was analyzed to explore the thermal stability of the PEG-g-MAA hydrogels in the

temperature range of 0–600°C under inert nitrogen atmosphere. Thermal degradation of copolymer (Figure 4.5.7) was shown by three phases befalling in the temperature ranges 60–110°C , 150–410°C and 450–543°C. First step of weight loss between 60°C and 110°C relates to a loss of moisture from the copolymer. The maximum weight loss occurred between 450°C and 543°C. DSC curve was shown in Figure4.5.8denoted first endothermic peak at 70°C indicated the loss of water molecules from the hydrogel. Furthermore, the copolymer revealed two endothermic transitions; one at 125°C and another at 135°C, owing to boosted intramolecular relations between carbonyl groups in the copolymer. However, endothermic peak at 490°C was endorsed to the melting of copolymeric hydrogel. Similarly novel pH-sensitive poly (methacrylamide-co-methacrylic acid) hydrogel system exhibited thermal behavior (Sunil and Surinderpal, 2006).

5.5.5: In vitro release kinetics of Rabeprazole sodium PEG-g-MAA hydrogel

Figure 4.5.9 showed the rabeprazole sodium release profile of the hydrogels at pH 1.2 and subsequently at pH 8. The amount of rabeprazole sodium released at pH 1.2 was below 15%, whereas released at pH 8 increased considerably (93%). The auspicious Rabeprazole sodium release pattern could be credited to the pH sensitivity of the hydrogel. On contrary to literature PEG-g-MAA revealed no burst release which might be due to the washing of hydrogels after preparation. Variations in the PEG and methacrylic acid concentration also have a significant effect on the drug release rate from the hydrogel formulations. It was noticed that by increasing PEG contents from 5 %-20 % cumulative drug release enhanced from 73% to 93%. Swelling analysis of hydrogels also behave in same fashion. Methacrylic acid as shown in Figure 4.5.10 act as swelling retardant because of hydrophobic methyl group, by increasing methacrylic acid contents hydrogels exhibited highly pH sensitive response but cumulative drug release was reduced due to low degree of swelling. Swelling of such hydrogel in the stomach was minimal and thus the drug release was also minimal. Attributable to increase in pH, the extent of swelling increased as the hydrogel passed down the intestinal tract, the hydrogel swelled and the controlled release of rabeprazole sodium

was influenced. Previous studies correlated with our findings that drug release increased by increasing the pH of the medium in cross-linked poly (hydroxyethyl methacrylate-co-methacrylic acid) and poly (hydroxyethyl methacrylate-co-acrylic acid) hydrogels (Khare and Peppas,1994)

PEG-g-MAA hydrogels showed good fit into higuchi order with the highest correlation coefficient (R^2=0.994). The value of n ranges from 0.5-0.715. Results presented in Table 4.5.6 showing that release in most of the conditions exhibit anomalous manner with a mixture of polymer swelling (relaxation) and drug diffusion (Fickian) mechanisms. Similar behavior has been depicted by other anionic hydrogels (Changez *et al*., 2003).

5.6: Characterization of PEG (HEMA-co-AA) hydrogels

5.6.1 Effect of variation of pH and individual constituents on swelling behavior of PEG (HEMA-co-AA) hydrogel

Water absorbing property of hydrogel is attractive for their biomedical application. The effect of HEMA and AA on the swelling curve of prepared hydrogels at acidic and basic pH was studied by varying concentrations. PEG concentration in the polymerization medium was fixed to 10% w/w. Swelling profile of hydrogels attained with different HEMA and AA contents were given in Figures 4.6.1 and 4.6.2. As seen in Figure 4.6.1 that with varying contents of AA (7.5 %, 10%, 12.5% and 15%) swelling ratio (q) in acidic medium decreased gradually (3.58, 3.30, 2.66, and 2.24 of PHA1, PHA2, PHA3 and PHA4 respectively) but at alkaline pH swelling ratio (12.89, 14.07, 16.13 and 19.72 of PHA1, PHA2, PHA3 and PHA4respectively) increased. Swelling profile indicated that increasing AA contents enhanced pH sensitivity and also swelling capacity of hydrogels. Hydrogels prepared with varying contents of HEMA (1%, 1.5%, 2% and 3%) showed low swelling ratio (4.03, 3.34, 3.16, 2.24 at acidic pH and 26.94, 24.65, 21.42 and 16.35 at high pH) with increasing its contents and concentration of other constituents keeping constant. Hence, HEMA promoted strong, mechanically strong hydrogels for drug delivery applications thus limiting swelling ratio of hydrogels. It could be concluded that swelling ratio is primarily

associated to features of the external stimuli, along with the nature of polymer, i.e. pliability of the network, existence of hydrophilic functional groups, and extent of crosslinking density. It has been described by previous work that HEMA/AA based hydrogels reveal similar swelling fashion (Belma, 2000).

5.6.2: Pulsatile behavior of hydrogel

To characterize the diverse nature of PEG (HEMA-co-AA) hybrid hydrogel, pH reversibility was studied in acidic and basic buffer. Ionic group present in matrix are responsible for abrupt swelling transition by pH modulation. Hydrogels collapsing/expanding behavior revealed in Figure 4.6.3 with pH transition. Such abrupt swelling/ deswelling behavior of hydrogels renders them as good candidate for controlled drug delivery application. Our results are related with previous work that ionic hydrogels showed more sensitive and reversible behavior under the oscillatory stimulus of pH (Lee *et al*., 2006)

5.6.3: Equilibrium water contents and Gel fraction

Equilibrium water contents of PEG(HEMA-co-AA)hydrogels summarized in Table 4.6.3 illustrated that AA contents enhanced EWC from 0.84 to 0.94 and decreased (0.92 to 0.53) with increased concentration of HEMA (1-3%) in copolymer hydrogel.The probableintentionsof HEMA and AA in hydrogels are stronger hydrophobic interactions and hydrogen bonding among them lead to modify EWC characteristics (De *et al*., 2002).Sol-gel fraction analysis of PEG (HEMA-co-AA) hydrogel was performed to determine the unreacted fraction of reactants. Figure 4.6.4 indicated % gel fraction of prepared hydrogels samples. It was detected that by raising contents of HEMA from 1-3 % gel fraction increased from 70-97 %. Gel fraction was also observed along with increased concentration of acrylic acid. Similar results were demonstrated by sung *et al.,* (Sung *et al*., 2010).

5.6.4: Instrumental analysis

a) Scanning electron microscopy

Surface morphologies of hydrogels PEG (HEMA-co-AA) swollen at different pH values were shown in Figure 4.6.5 although SEM is useful to describe the hydrogel structure. The hydrogel examined at low magnification showed a compact and collapsed structure with few pores. Polymeric network (Figure 4.6.5) showed a highly porous structure. Hydrogel composition defines surface morphology of hydrogel. In present study PEG (HEMA-co-AA)hydrogel the pore size in hydrogels with increasing HEMA concentrations reduced because of their compact structure and low water content. The morphology of PEG (HEMA-co-AA) can be varied with high crosslinking density. Our results are supported by Hana *et al.*, work, they prepared P(HEMA-co-SMA) hydrogels and studied surface morphology by SEM analysis, concluded that compact structure with varying contents of monomer and crosslinker modified surface morphology of hydrogels (Hana *et al*., 2009).

b) FTIR spectrum analysis

Figure 4.6.6demonstrated FTIR spectrum of HEMA which displayed distinctive peaks at 3394 cm^{-1} attributed to vibration of OH group, 2956 cm^{-1} from antisymetric vibration of CH_2 and CH_3, 1720 $cm^{-1}$of stretching C=O, a small shoulder around 1636 cm^{-1} from stretching C=C and 1164 cm^{-1} vibration of C-O-C.

FTIR spectroscopic analysis was used to elucidate the chemical structure modifications of prepared hydrogels and the nature of new bonds formation. All distinguishing bands of components (HEMA and AA), and polymer (PEG) of FTIR spectra have appeared into the FTIR spectrum of the resultant hydrogel (Figure 4.6.6). The spectral characteristics of PEG(HEMA-co-AA), shown the characteristic stretching vibration band of hydrogen-bonded alcohol (O–H) around 3281 cm^{-1}, the C=O stretching vibration of the ester group also appeared at 1712 cm^{-1}, and an absorption band with a weak shoulder around 2930 cm^{-1}, which relate to the stretching of aliphatic $–CH_2–$,C–H and $–CH_3$ groups, respectively. The increased peak intensity of the C=O group at 1712 cm^{-1} in the spectrum of

PEG(HEMA-co-AA), hydrogel was linked with further C=O groups from AA. Moreover, some peaks seemed in the fingerprint region for ethylene glycol units, instigating from PEG element, between 1555 and 1078 cm^{-1}.These bands were allotted to the $–CH_2$ scissoring band of ethylene glycol units at 1449 cm^{-1} and the antisymmetric and symmetric stretching bands (–O–R) of ethylene glycol units at 1148 cm^{-1},respectively. Other distinctive bands signify C–C and C–H vibrations of $–CH_3$ and $–CH_2–$ groups. Therefore, FTIR spectroscopy results confirmed the amalgamation of PEG and acrylic acid and HEMA into PHA hydrogel.

c) Thermal analysis.

The thermal characteristics of PEG (HEMA-co-AA) copolymers were deliberated by TGA and DSC analyses. The TGA curves of PEG (HEMA-co-AA) hydrogel contained two separate degradation steps. The first decomposition curve is detected in the range of 180 to 400°C with maximum weight loss. The second decomposition phase follows at 390 to 517 °C with 15% weight loss. It has been proposed that first decomposition phase related with ester bonds breakdown in the structure of copolymers, while the second one could be accredited to the entire degradation of copolymers. The TGA curves of PEG (HEMA-co-AA) as shown in Figure 4.6.7 indicated that resultant hydrogel was thermally more stable than its individual constituents (PEG, HEMA and acrylic acid). Generally it can be concluded that grafting improves thermal stability of copolymers. The DSC curves of parent components and resultant copolymer are presented in Figure 4.6.8 verified the above mentioned findings. One endothermic peak 83.3 to 125.4°C connected with loss of loose and bound water present in structure. However peak at 450°C showed the decomposition of cross-linked polymeric networks. Grafting evidence and thermal stability of hydrogels have been predicted by other researchers, thermal stability is due to the molecular rigidity of hosted crosslinkers (Hoffman, 2002).

5.6.5: In vitro release kinetics of Rabeprazole sodium PEG-g-MAA hydrogel

The drug release from hydrogels could be the result of macromolecular chain relaxation, since the swelling of glassy polymers is accompanied by chain relaxation processes. pH of external environment is controlling factor for chain relaxation and resultant swelling.

As PEG (HEMA-co-AA) hydrogels express pH sensitivity and pH responsive reversible behavior by swelling analysis and pulsatile behavior analysis. Cumulative drug release was also investigated at pH 1.2 and pH 8. Figures 4.6.9 & 4.6.10 showed the release profiles of rabeprazole sodium from the hydrogels containing different amount of HEMA and acrylic acid at two different pH (pH 1.2 and 8). At pH 1.2 the amount of drug released within 24 hrs was 7.04% with 7.5 % AA, 6.27% with 10% AA 5.15 % with 12.5% AA and 4.81% with 15% AA contents (Table 4.6.4). As described prior, the degree of swelling at pH 1.2 in 24hrs was found to be low. At lower pH, the carboxyl groups remain undissociated, results in compaction of polymeric matrix. Release of rabeprazole sodium from these hydrogels would be useful as matrix to protect the drug from the harsh environment of stomach. At high pH swelling of hybrid hydrogel increased due to ionization of carboxyl groups of acrylic acid, release of rabeprazole sodium also high. It was also observed that by increasing contents of acrylic acid cumulative drug release also increased, 71.99%, 77.09%, 82.61% and 90.06% from 7.5%, 10%, 12.5% and 15% acrylic acid concentration respectively. Previous studies demonstrated that drug release through hydrogels preferred pore mechanism. As hydrogels containing interconnecting microchannels through which drug molecules diffuse out. Diffusivity rises with gel water contents with increasing acrylic acid concentration (Dong and Hoffman, 1991).

Present study also investigated that by increasing HEMA contents while PEG and acrylic acid contents kept constant, drug release declined. These findings are correlated with swelling analysis of PEG(HEMA-co-AA). As HEMA is neutral monomer, which has no ionize able groups and exhibited very small swelling in buffer solution. But water swelling properties of HEMA could be improved by co-

polymerization with more hydrophilic monomer like acrylic acid (Hongyan *et al*., 2004).

Hydrogel polymeric network are reflected swelling-controlled systems, since the drug release is measured by the inward movement of solvent. Drug release kinetics of hydrogels are commonly scrutinized with Fickian and non-Fickian diffusional manner kinetics described by Peppas *et al*. On the basis of diffusion exponent 'n' release kinetics can be concluded. Present study demonstrated that by fitting in vitro release data into various release kinetics mathematical models, drug release follow the higuchi model (R^2 values of series of hydrogels are 0.991-0.995) as given in Table 4.6.6. Diffusion exponent 'n' was 0.5-0.6 that exhibited non Fickian diffusion (swelling and polymer relaxation pattern) (Peppas *et al*., 2000).

5.7 Acute oral toxicity study of prepared hydrogels

Most of the complications connected with hydrogel concerning toxicity, are the unreacted monomers, oligomers and initiators that percolate out during application. So it is compulsory to assess the toxicity of the hydrogel components like monomers, initiators and other building blocks involved in hydrogel synthesis. Meanwhile the safety assessment of the smart hydrogel can have a substantial inference on additional uses as a biocompatible carrier for oral drug delivery carrier.

Acute toxicity study of hydrogel is the knowledge of interaction of chemical composition of the biomaterial and tissue exposure. Hydrogels as oral drug delivery carrier must be safe, nontoxic and biocompatible matrix. Acute oral toxicity study of prepared hydrogels (CMC-g-AA, CMC-g-MAA, CMAX-g-MAA and CMAX-g-AA) were implemented consistent with the "Organization of Economic Co-operation and Development (OECD) guideline for chemicals toxicity study (Oecd, 2001).

5.7.1: Clinical observations

All groups of mice revealed a normal boost in body weight without radical alteration between both control and treated groups. The results publicized that, the vital organs such as kidney, liver, heart, lung, stomach and spleen were not harmfully affected throughout the treatment. Table 4.7.1 showed the effect of oral intake of hydrogels on

body weight, nutrients consumption, and other poisoning related symptoms. All of the mice gained weight and displayed no significant changes in behavior. Physical features such as skin, fur, eyes and physical activity of animals were found to be normal. All these observations depicted that the administration of the oral hydrogels have negligible level of toxicity on the growth and physical characteristics of the animals. Moreover, casual food and water intake evaluation of animals is an essential parameter for toxicity study, because proper consumption of nutrients is signal for normal physiological status. Present study illustrated that food intake and water consumption also was not influenced by hydrogels treatment. No mortality was found within study period. No signs of illness (vomiting, eye secretion, running nose, salivation) were observed after hydrogels administration. According to globally harmonized system (GHS), LD50 value of testing chemical is higher than the 2000 mg/kg dose then it will be categorize under the "Category 5" and toxicity score will be "zero." Therefore, prepared hydrogels (CMC-g-AA, CMC-g-MAA, CMAX-g-MAA and CMAX-g-AA) can be categorized under the Category 5 and toxicity grade is zero.

5.7.2: Biochemical blood analysis

The blood is the most sensitive target site for toxic chemicals and an imperative indication of physiological and pathological grade. Tables 4.7.2 and 4.7.3 showed complete blood chemistry, liver, kidney and lipid profile of control and hydrogel treated animals. Notch of boost of AST and ALT level were valuable in unique liver abnormalities direct linked with mutilation of liver parenchyma. It was observed that the ALT value of control animal was 54 IU/L, hydrogels treated animals were 53 IU/L (Group II), 66 (Group III), 63 IU/L (Group IV) and 55 IU/L (Group V). The reference range was 28–184 IU/L in mouse. Likewise, AST value of control group was 206 IU/L, animal treated with hydrogels revealed AST level 144 IU/L (Group II), 184 IU/L (Group III), 185 IU/L (Group IV), and 203 IU/L (Group V), reference range of AST level in mice was reported as 55-251 IU/L. Kidney function was assessed by creatinine, and urea level and lipid profile shown in Table 4.7.3 all values were in normal range illustrated that there was no sign of toxicity in blood, liver, kidney and lipid profile of mice was assessed. All vital organs of control and treated mice were in normal functioning mode. There was mild variations in WBCs count in

group IV and group V, may indicate stimulation of immune system. Such mild alterations are not considered to be adverse. Almost all hematological parameters in control and treated groups are comparable and in safe zone (Piyasi *et al*., 2014).

5.7.3: Histopathological Study

Microscopic examination of samples obtained from control and hydrogels treated groups of mice revealed that no clear histopathological lesions found in vital organs (heart, liver, kidney, stomach, intestine and spleen). Figure 4.7.2 described that section from the heart showed normal myocardium. No significant pathology was present with in myocardial tissues. Figure 4.7.3 revealed hepatic parenchyma with normal preserved lobular architecture, but there was focal mild inflammation in occasional portal tracts.Figure 4.7.4 described that there was no significant pathology present in spleen. Figure 4.7.5 demonstrated that no mild tube degenerative changes and focal mild interstitial inflammation. Figure 4.7.1 and 4.7.6 showed normal mucosa of stomach and intestine free from any significant pathology.

Thus, the maximal tolerance dose of hydrogels was estimated to be higher than 10 g/kg b.w. in mice. It was suggested that the tested hydrogel were nontoxic, safe and biocompatible following oral administration and it might be auspicious candidate as an innovative oral drug carrier.

5.8: Pharmacokinetic evaluation of rabeprazole sodium

Graft copolymeric networks (CMC-g-AA (CA), CMAX-g-AA (A)) have been prepared by free radical polymerization and characterized by swelling analysis, FTIR spectroscopy, thermal analysis, surface morphology study and *in vitro* cumulative drug release study. Equilibrium swelling studies and impulsive swelling-deswelling attitude at different pH values renders the system to be highly pH-responsive and thereby it may be a suitable candidate for controlled drug delivery systems. *In vitro* release study of these polymer matrices also represented their smart and sustained release fashion of Rabeprazole sodium. On the basis of preliminary investigations

these two formulations (CA5 and A6) with maximum *in vitro* cumulative drug release were selected for *in vivo* evaluation.

The pharmacokinetic parameters of Rabeprazole sodium from CMAX-g-AA, CMC-g-AA hydrogels and drug solution were analyzed from the plasma levels in rabbits by noncompartmental pharmacokinetic analysis using the software package kinetica v 4.4. The peak plasma concentration (C_{max}) and time to reach peak plasma concentration (T_{max}) was obtained from the visual inspection of the plasma concentration-time curves. The area under the plasma concentration curve (AUC_{0-t}) was determined using the trapezoidal rule.

Mean plasma concentration at specific time interval after administration of hydrogel formulations (CA5 and A6) to each group was depicted in Figure 4.8.2 and 4.8.3. Mean plasma concentration after oral drug solution of same strength as that of hydrogels was shown in Figure 4.8.6. Mean values of pharmacokinetic parameters of rabeprazole sodium after oral administration of hydrogel formulations and drug solution was shown in Table 4.8.5. Pharmacokinetic data was statistically analyzed by one way ANOVA, summarized in Table 4.8.6.

Graft copolymeric carrier networks (CMC-g-AA and CMAX-g-AA) and same oral dose of rabeprazole sodium drug solution showed significantly dissimilar ($P < 0.05$) C_{max} values of (CMC-g-AA) CA and (CMAX-g-AA) A and same oral dose of rabeprazole sodium were 87.28±12.671, 103.71±16.081 and 61.263±5.37 ng/ml, respectively. C_{max} values of rabeprazole sodium after administration of CA and A hydrogel formulations were also correlated with in vitro drug release (98.44 % of A6 and 80.75 % of CA5). Observed mean plasma AUC_{0-24} values for CA (952.25±191 ng.h/ml) and A(1084.57±148.68ng.h/ml) was significantly ($P < 0.05$) higher than drug solution (83.67±8.28ng.h/ml) which indicated improvement in relative bioavailability might be related to pH sensitive characteristics of graft copolymeric networks protect drug from harsh stomach environment. The T_{max} value of graft copolymer matrices CA(4.43 h) and A (4h) was significantly ($P < 0.05$) higher than drug solution (1h),

which indicated the slow absorption rate in graft copolymer due to extended release effect of polymer matrix (Zhang *et al*.,2011).

The elimination half life ($t_{½}$) of the CA (5.36 h) and A (4.5h) was more than drug solution (0.5h), which confirmed prolonged availability of rabeprazole sodium in body. The MRT and T_{max} of rabeprazole sodium in the plasma were significantly higher in hydrogels than oral drug solution. Therefore, therapeutic effective period for rabeprazole sodium were longer than for free rabeprazole sodium. It was also observed that Rabeprazole sodium was released from hydrogels in controlled manner with increased blood circulation time as well as drug concentration peak in rabbits (Bhavesh *et al.,* 2013).

The relative bioavailability of hydrogel formulations (CA and A) containing rabeprazole sodium than free rabeprazole sodium in drug solution, containing the same dose of the same drug, is obtained by comparing their respective AUCs (952.25 ng.l/hr for CA and 1084.57ng.l/hr for A hydrogel) were higher (Oprea *et al*., 2013).

CHAPTER # 6

CONCLUSION

6. Conclusion

Present research deals with development of graft copolymeric systems for acid labile drug, rabeprazole sodium to accomplish a lingering therapeutic outcome by continuously releasing the drug over extended period of time. To achieve desired drug carrier system, different hydrogel formulations were prepared with carboxymethyl arabin oxylan, carboxymethyl cellulose and polyethylene glycol (polymer), methacrylic acid and acrylic acid as monomer with varying concentrations of crosslinker by free radical polymerization technique were prepared and their potentials for controlled drug delivery have been premeditated.

Following conclusions have been assessed from present substantial research work.

- Carboxymethyl arabinoxyllan anionic polysaccharide obtained from Ispaghola husk by alkali extraction, exhibited variety of ideal characteristics for controlled drug delivery carrier. Free radical polymerization by KPS can be successfully employed to formulate pH responsive copolymeric network of carboxymethyl arabin oxylan with acrylic acid and methacrylic acid. FTIR, SEM and thermo gravimetric analysis verify graft copolymerization. Porous structure of hydrogel become more prominent at pH 7.4 by increasing contents of acrylic acid, as compared to methacrylic acid contents. CMAX-g-AA and CMAX-g-MAA underwent morphological changes during grafting which modified their structure and properties as well, which showed more thermal stability as compared to the raw back bone. Graft copolymers revealed highly pH responsive swelling, consequently drug release. At higher pH carboxylic acid group present in graft copolymer became progressively more ionized, hydrogels swelled more rapidly. Degree of swelling depends on crosslinked monomer concentration, polymer concentration and also on crosslinking density of hydrogels. Swelling of such hydrogels in the stomach is minimal so drug release consequently low at acidic pH. Values of R^2 obtained using zero order release model were viewed higher than other order

release model, thus depicting that drug release from the series of hydrogels at varying amount of polymer, monomer and crosslinker was zero order.

- Among various graft copolymer formulations prepared with varying contents of carboxymethyl cellulose, acrylic acid and N, N MBA CA4 present superior properties in regards with swelling, pulsatile behavior, mechanical strength, sustained, and pH responsive drug release. CMC-g- MAA hydrogels with high methacrylic acid concentration may lead to more efficient network formation (a lower sol fraction) due to the higher concentration of reactive vinyl groups in the polymer mixture. These hydrogels swelled slowly and give more sustained release.
- Polyethylene glycol is FDA accepted polymer for diverse biomedical functions because of biocompatibility, biodegradability, low toxicity, and non immunogenic nature. PEG-g-MAA hydrogels showed the rabeprazole sodium release profile of the hydrogels at pH 1.2 and subsequently at pH 8. The amount of rebeprazole sodium released at pH 1.2 was below 15%, whereas released at pH 8 increased considerably (93%). PEG is non ionic hydrophilic liquid. Other formulations prepared by other polymers (CMAX and CMC) released below 10% rabeprazole sodium at acidic pH. Therefore pH responsiveness of PEG hydrogels is low as compared to others.
- Acute toxicity study of hydrogel is the knowledge of interaction of chemical composition of the biomaterial and tissue exposure. Acute oral toxicity studies of prepared hydrogels suggested that the tested hydrogels were nontoxic, safe and biocompatible following oral administration and it might be auspicious candidate as a innovative oral drug carrier.
- Pharmacokinetic parameters evaluation indicated improvement in relative bioavailability of hydrogels as compared to drug solution, might be related to pH sensitive characteristics of graft copolymeric networks protect drug from harsh stomach environment. Also exhibited prolonged release owing to crosslinking of graft copolymer promote sustained effect.
- The concept of formulating graft copolymer containing Rabeprazole sodium offers a appropriate, sensible approach to accomplish a lingering

therapeutic outcome by continuously releasing the drug over extended period of time. Graft copolymerization is faster and more cost-effective technique to modify imperative properties of the existing drugs than developing new drug entities hence this research work will be windfall to novel drug carrier system.

- This Research work opens a new platform for potential use of chemically crosslinked smart materials for oral controlled release applications.

CHAPTER # 7

REFERENCES

References

1) Adeyanju O, Abayomi TG, Olajide O (2014). Carboxymethylation of Anacardium Occidentale L. Exudate Gum: Synthesis and Characterization. Scholars Academic Journal of Pharmacy. 3(2): 213-216.

2) Alessandro S, Christian D, Marta M (2009). Biodegradable Cellulose-based Hydrogels: Design and Applications. Materials. 2: 353-373.

3) Amitava G, Udaya KN, Prasant R, Tanusree N and Partha R (2008). Preparation, Evaluation and in vitro- in vivo Correlation (IVIVC) study of Lamivudine Loaded Microspheres. Research J. Pharm. and Tech. 1(4): 353-356.

4) Andersson T (1990). Pharmacokinetics and bioavailability of omeprazole after single and repeated oral administration in healthy subjects. British journal of clinical pharmacology. 29:557-63.

5) Andersson T, Reghdh CG, Dahl-Puustinen ML, Bertilsson L, (1990). Slow omeprazole metabolizers are also poor S-mephenytoin hydroxylators. Therapeutic Drug Monitoring, 12:415-6.

6) Arion H (2001). Carboxymethyl cellulose hydrogel-filled breast implants. Our experience in 15 years (in French). Annales de Chirurgie Plastique et Esthétique, 46: 55–59.

7) Arpit S, Mithilesh Y, Madan MM, Jasaswini T, Kunj B (2011). Studies on graft copolymerization of 2-acrylamidoglycolic acid on to partially carboxymethylated guar gum and physicochemical properties. Carbohydrate Polymers. 83: 14–21.

8) Auda JB, Sihama IS, Fadhel AH, Jaleel KA (2014). Proposed cross-linking model for carboxymethyl cellulose /starch superabsorbent polymer blend. International Journal of Materials Science and Applications. 3(6): 363-369.

9) Averitt RD, Westcott SL and Halas NJ (1996). Linear optical properties of gold nanoshells, J. opt Soc. Amer. B., 16(10): 1824-1832.

10) Bajpai SK (2001). Swelling–deswelling behavior of poly (acrylamide-co-maleic acid) hydrogels. Journal of Applied Polymer Science. 80(14): 2782–2789.

11) Baldwin RM, Ohlsson S, Pedersen RS, Mwinyi J, Ingelman SM, Eliasson E, Bertilsson L (2008). Increased omeprazole metabolism in carriers of the CYP2C19*17 allele; a pharmacokinetic study in healthy volunteers. British Journal of Clinical Pharmacology. 65:767–74.

12) Baljit S, Ritu B and Nirmala C (2008). In vitro release dynamics of model drugs from psyllium and acrylic acid based hydrogels for the use in colon specific drug delivery. Journal of Materials Science: Materials in Medicine. 19: 2771-2780.

13) Bardelmeijer HA, van TO, Schellens JH. & Beijnen JH (2000). The oral route for the administration of cytotoxic drugs: strategies to increase the efficiency and consistency of drug delivery. Investigational New Drugs. 18(3): 231-241.

14) Beierle I, Meibohm B, & Derendorf H (1999). Gender differences in pharmacokinetics and pharmacodynamics. International Journal of Clinical Pharmacology and Therapeutics. 37(11): 529-547.

15) Bell CL and Peppas NA (1996). Water, solute and protein diffusion in physiologically responsive hydrogels of poly(methacryli6 acid-g-ethylene glycol). Biomaterials. 17: 1203-1218.

16) Bellobono IR, Calgari S, Leonari MC, Selli E, Paglia ED (1981). Photochemical grafting of acrylated azo dyes onto polymeric surfaces. IV. Grafting of 4-(N-ethyl N-2-acryloxyethyl) amino-40 nitro azobenzene onto cellulose. Die Angewandte Makromolekurare Chemie. 100:135– 46.

17) Belma I (2000). Swelling Behavior of Acrylamide-2-Hydroxyethyl Methacrylate Hydrogels. Turkish Journal of Chemistry. 24: 147-156.

18) Bhavesh DK, Radheshyam RP,Shalini R, Rahul J, Yogesh KB,Heta J, Nisargin ee C, Navin RS, HariCB(2013).pH responsive MMT/Acrylamide Super Comp osite Hydrogel: Characterization, Anticancer Drug Reservoir and Controlled R elease Property.Biochemistry and Biophysics. 1(3): 43-60.

19) Bindu SM, Ashok V and Arkendu C (2012). As A Review on Hydrogels as Drug Delivery in the Pharmaceutical Field. International journal of pharmaceutical and chemical sciences. 1(2): 642-661.

20) Blanco FH, Anguiano IS, Otero EFJ and Blanco MJ (1996). *In vitro* bioadhesion of carbopol hydrogels. International Journal of Pharmacy. 146: 169-174.

21) Brittain RT and Jack D (1983). Histamine H_2-antagonistspast, present and future. Journal of Clinical Gastroenterology. 5(1):71-79.

22) Bromberg L, Temchenko M, Alakhov V, & Hatton TA (2004). Bioadhesive properties and rheology of polyether-modified poly (acrylic acid) hydrogels. International journal of pharmaceutics. 282(1): 45-60.

23) Bumsang K, Kristen LF, Peppas NA (2003). Dynamic Swelling Behavior of pH-Sensitive Anionic Hydrogels Used for Protein Delivery. Journal of Applied Polymer Science. 89:1606 –1613.

24) Bumsang K, and Peppas NA, (2003). Analysis of molecular interactions in poly(methacrylic acid-g-ethylene glycol) hydrogels. Polymer. 44: 3701–3707.

25) Carien E. Beneke AMV and Josias HH (2009). Polymeric Plant-derived Excipients in Drug Delivery. Molecules. 14: 2602-2620.

26) Chaaya RG, Feng L, MiroslavB and Sung WK (1999). Polymeric beads through polymer molecular weight. J Control Release,59: 287-298.

27) Chandra BA, Prabhakar MN, Suresh BA, Mallikarjuna B, Subha MCS, and Chowdoji RK (2013). Development and Characterization of Semi-IPN Silver Nanocomposite Hydrogels for Antibacterial Applications. International Journal of Carbohydrate Chemistry. 2013: 1-8.

28) Changez M, Krishna B, Veena K, Veena C (2003). The effect of composition of poly (acrylic acid)-gelatin hydrogel on gentamicin sulphate release: *in vitro*. Biomaterials. 24: 527-536

29) Chauhan S, Harikumar SL and Kanupriya (2012) .Hydrogels: a smart drug delivery system. International journal of research in pharmacy and chemistry. 2(3): 603-614.

30) Chen J, Iwata H, Maekawa Y, Yoshida M, Tsubokawa N (2003). Grafting of polyethylene byg-radiation grafting onto conductive carbon black and application as novel gas and solute sensors. Radiation Physics and Chemistry. 67(4): 397–401.

31) Chen KS, Ku YA, Lin HR, Yan TR, Sheu DC, Chen TM, Lin FH (2005). Preparation and characterization of pH sensitive poly (N-vinyl-2-pyrrolidone/itaconic acid) copolymer hydrogels. Materials Chemistry and Physics. 91(3): 484-489.

32) Chen S, Liu M, Jin S, Wang B (2008) Preparation of ionic crosslinked chitosan-based gel beads and effect of reaction conditions on drug release behaviors. International Journal of Pharmacy. 349: 180–187.

33) Chen X, Qian Z, Gou M, Chao G, Zhang Y, Gu Y, Huang M, Wang P Y, Wei Y, Chen I & Tu, M. (2008). Acute oral toxicity evaluation of biodegradable and pH-sensitive hydrogel based on polycaprolactone, poly (ethylene glycol) and methylacrylic acid (MAA).Journal of Biomedical Materials Research Part A. 84(3): 589-597.

34) Chickpetty SM and Raga B (2010). Studies on Design and In Vitro Evaluation of Compression-Coated Delivery Systems for Colon Targeting of Diclofenac Sodium. International Journal of PharmTech Research. 2(3): 1714-1722.

35) Chu Y, Varanasi PP, McGlade M.J and Varanasi S (1995). pH-induced swelling kinetics of polyelectrolyte hydrogels. Journal of Applied Polymer Sciences. 58: 2161-2176.

36) Cursaru B, Stănescu PO, and Teodorescu M (2010). The states of water in hydrogels synthesized from diepoxy-terminated poly (ethylene glycol) and aliphatic polyamines. UPB Sci Bull Ser B. 72: 99-114.

37) Dafader NC, Ganguli S, Sattar MA, Haque ME and Akhtar F (2009). Synthesis of Superabsorbent Acrylamide/Kappa-carrageenan Blend Hydrogel by Gamma Radiation. Malaysian Polymer Journal. 4(2): 37-45.

38) Daniela P, Milena DC and Rolando B (2012). Polysaccharide-Based Hydrogels: The Key Role of Water in Affecting Mechanical Properties. Polymers. 4: 1517-1534.

39) Das N (2013). Preparation methods and properties of hydrogel: a review. International Journal of Pharmacy and Pharmaceutical Sciences. 5(3): 112-117.

40) Davaran S, Rashidi MR and Hashemi M (2001). Synthesis and Characterization of Methacrylic Derivatives of 5-Amino salicylic Acid with pH-Sensitive Swelling Properties. AAPS Pharmaceutical Science and Technology. 2 (4): 1-6.

41) Davis KA and Anseth KS (2002). Controlled Release from Crosslinked Degradable Networks," Critical Reviews in Therapeutic Drug Carrier Systems. 19(4): 385-423.

42) De SK, Aluru NR, Johnson B, Crone WC, Beebe DJ and Moore J (2002). Equilibrium swelling and kinetics of pH-responsive hydrogels: models, experiments and simulations. Journal of Microelectromechanical Systems. 11: 544-555.

43) Deepak P and Reena S (2012). Synthesis and characterization of graft copolymers of methacrylic acid onto gelatinized potato starch using chromic acid initiator in presence of air. Advance Materials Letters. 3(2), 136-142

44) Dekkers CPM, Beker JA, Thjodleifsson B, Gabryelewicz A, Bell NE, and Humphries TJ (1999). Comparison of rabeprazole 20mg versus omeprazole 20 mg in the treatment of active duodenal ulcer: a European multicentre study. Alimentary Pharmacology and Therapeutics. 13: 179-186

45) Delhotal LB (1995). Clinical pharmacokinetics of lansoprazole. Clinical Pharmacokinetic. 28: 458-70. 33.

46) Devine DM, and Higginbotham CL (2005). Synthesis and characterisation of chemically crosslinked N-vinyl pyrrolidinone (NVP) based hydrogels. European polymer journal. 41(6): 1272-1279.

47) Dey P, Biswanath S and Sabyasachi M (2011). Carboxymethyl ethers of locust bean gum- a review International Journal of Pharmacy and Pharmaceutical Sciences. 3(2): 4-7.

48) Dirk S (2006). Thermo and pH-responsive polymers in drug delivery. Advanced Drug Delivery Reviews. 58: 1655–1670.

49) Dodi G, Hritcu D, and Popa MI (2011). Carboxymethylation of guar gum: synthesis and characterization. Cellulose chemistry and technology. 45(4):171-176.

50) Dong LC and Hoffman AS (1991). A novel approach for preparation of pH-sensitive hydrogels for enteric drug delivery. Journal of controlled Release. 15: 141-152.

51) Donini C, Robinson DN, Colombo P, Giordano F and Peppas NA (2002). Preparation of poly (methacrylic acid – g-poly (ethylene glycol)) nanospheres from methacrylic monomers for pharmaceutical applications. International Journal of Pharmacy. 245: 83-91.

52) Dumitriu S, 2002. Polymeric Biomaterials. Marcel Dekker, New York.

53) Edith M, Donald E and Chickeringand CL (1999). Bioadhesive drug delivery systems, fundamentals, novel approaches, and development, Informa HealthCare. 98: 125-135.

54) Edman P, Ekman B, Sjöholm I (1980) Immobilization of proteins in microspheres of biodegradable polyacryldextran. Journal of Pharmaceutical Sciences. 69: 838–842

55) Ekman L, Hansson E, Havu N, Carlsson E, Lundberg C (1985). Toxicological studies on omeprazole. Scandinavian Journal of Gastroenterology, 108:53-69

56) Eljarrat-Binstock E, Frederik R, Frucht-Pery J, and Abraham JD (2005). Transcorneal and transscleral iontophoresis of dexamethasone phosphate using drug loaded hydrogel. Journal of Controlled Release. 106(3): 386–390.

57) Eljarrat-Binstock E, Frederik R, David S, Abraham JD, and Frucht-Pery J (2004) Delivery of gentamicin to the rabbit eye by drug-loaded hydrogel iontophoresis. Investigative Ophthalmology and visual science. 45(8): 2543–2548.

58) Elliott JE, Macdonald M, Nie J, Bowman CN (2004). Structure and swelling of poly (acrylic acid) hydrogels: effect of pH, ionic strength, and dilution on the cross linked polymer structure. Polymer. 45: 1503-1510.

59) Fariba G and Ebrahim VF (2009). Hydrogels in controlled drug delivery systems. Iranian Polymer Journal. 18: 63-88.

60) Fischer MH, Yu, NG, Ralph GR, Anderson JL, & Marlett JA. (2004).The gel forming polysaccharide of psyllium husk (Plantago ovata Forsk). Carbohydrate Research. 339: 2009–2017.

61) Francesco MV and Gianfranco P (2005). PEGylation, Successful Approach to Drug Delivery. Drug Discovery Today. 10: 1451-1458.

62) Furuta T, Shirai N, Sugimoto M, Nakamura A, Hishida A, Ishizaki T (2005). Influence of CYP2C19 pharmacogenetic polymorphism on proton pump inhibitor-based therapies. Drug Metab Pharmacokinet. 20:153–67.

63) Furuta T, Ohashi K, Kosuge K, Zhao XJ, Takashima M, Kimura M, Nishimoto M, Hanai H, Kaneko E, Ishizaki T (1999).CYP2C19 genotype status and effect of omeprazole on intragastric pH in humans. Clinical Pharmacology and Therapeutic. 65: 552-561.

64) Gabriela T, Marcel P and Jacques D (2011). Microparticles of hydrogel type based on carboxymethylcellulose and gelatin for controlled release of water soluble drugs. Revue Roumaine de Chimie. 56(4): 399-410.

65) Gacesa P (1988) Alginates. Carbohydrate Polymer 8:161–182.

66) George S, Jai MS, Olga V, Nils L, Iskandar Y, Keith M (2007). The Gastric H,K ATPase as a Drug Target: Past, Present, and Future. Journal of Clinical Gastroenterology. 41(2): 226-242.

67) Gerson LB, & Triadafilopoulos G (2001). Proton pump inhibitors and their drug interactions: an evidence-based approach. European journal of gastroenterology & hepatology. 13(5): 611-616.

68) Geus W, Mulder PGH, Nicolai JJ, Van D, Boomgaard DM, Lamers CBHW, (1998). Acid-inhibitory effects of omeprazole and lansoprazole in Helicobacter pylori-negative healthy subjects. Alimentary Pharmacology and Therapeutics. 12:329-35.

69) Gombotz WR, Wee S (1998). Protein release from alginate matrices. Advance Drug Delivery and Review. 31:267–285.

70) Goosen MFA, Oshea GM, Gharapetian HM, Chou S, Sun AM (1985) Optimization of microencapsulation parameters: Semipermeable microcapsules as a bioartificial pancreas. Biotechnology Bioengneering. 27: 146–150.

71) Grootaert C, Delcour JA, Courtinb, CM, Broekaertb WF, Verstraetea W, Wiele, TV (2007). Microbial metabolism and prebiotic potency of arabinoxylan oligosaccharides in the human intestine. Trends in food sciences and technology. 18:64–71.

72) Guirguis OW and Moselhey MTH (2012). Thermal and structural studies of poly (vinyl alcohol) and hydroxypropyl cellulose blends. Natural Sciences. 4(1): 57-67.

73) Hana YA, Lee EM and Ji B C (2009). The physical properties of poly (2-hydroxyethyl methacrylate) copolymer hydrogels used as intravaginal rings. Chinese Journal of Polymer Science. 27(3): 359−366.

74) Hariharan D and Peppas NA (1993). Modelling of water transport and solute release in physiologically sensitive gels. Journal of Controlled Release. 23: 123-135.

75) Hassan AM (2000). Pharmacokinetics of esomeprazole after oral and intravenous administration of single and repeated doses to healthy subjects. European Journal of Clinical Pharmacology. 56(35): 665-70.

76) Hatakeyama T, Nakamura K (1982). Studies on heat capacity of cellulose and lignin by differential scanning calorimetry. Polymer 23:1801–1804.

77) Hemant M, Balbir SK and Rajeev J (2010). Synthesis, characterization and swelling behaviour of poly (acrylamide-comethacrylic acid) grafted Gum ghattibased superabsorbent hydrogels. Advances in Applied Science Research. 1(3): 56-66.

78) Hennink WE & Nostrum CFV (2002). Novel crosslinking methods to design hydrogels. Advanced Drug Delivery Reviews. 54: 13–36.

79) Hoare TR, Daniel SK (2008). Hydrogels in drug delivery: Progress and challenges. Polymer. 49:1993-2007.

80) Hoffman AS (2002) Hydrogels for biomedical applications. Advanced Drug Delivery Reviews. 43: 3–12.

81) Holtman G, Bytzer P, Metz M, Loeffler VA, and Blum L (2002). A randomized, doubleblind, comparative study of standard-dose rabeprazole and high-dose omeprazole in gastro-oesophageal reflux disease. Alimenaryt Pharmacology and Therapeutics. 16: 479–85

82) Hongyan H, Xia C, Lee LJ (2004). Design of a novel hydrogel-based intelligent system for controlled drug release. Journal of Controlled Release. 95: 391– 402.

83) Hosseinzadeh H (2010). Controlled release of diclofenac sodium from pH-responsive carrageenan-g-poly (acrylic acid) superabsorbent hydrogel. Journal of Chemical Sciences. 122(4): 651–659.

84) Huang JQ and Richard HH (2001). Pharmacological and pharmacodynamic essentials of H2-receptor antagonistsand proton pump inhibitors for the practising physician. Best Practice & Research Clinical Gastroenterology. 15(3): 355-370.

85) Huang Y, Yu H, Xiao C (2007). pH-sensitive cationic guargum/poly (acrylic acid) polyelectrolyte hydrogels: swelling and in vitro drug release. Carbohydrate Polymer. 69: 774–83.

86) Humphries TJ (1998). A review of the drug–drug interaction potential of rabeprazole sodium based on CYP-450 interference or absorption effects. Digestion. 59(3): 76

87) Humphries TJ, Nardi RV, Spera AC, et al (1996). Coadministration of rabeprazole sodium (E3810) and ketoconazole results in a predictable interaction with ketoconazole. Gastroentheterology. 110: 138

88) Ishizaki T, Chiba K, Manabe K, Koyama E, Hayashi M, Yasuda S, Horai Y, Tomono Y, Yamato C, Toyoki T (1995). Comparison of the interaction potential of a new proton pump inhibitor, E3810, versus omeprazole with diazepam in extensive and poor metabolizers of S-mephenytoin 4′-hydroxylation. Clinical Pharmacology and Therapeutics. 58: 155-64

89) Jafari S and Hamid M (2005). A Study on Swelling and Complex Formation of Acrylic Acid and Methacrylic Acid Hydrogels with Polyethylene Glycol. Iranian Polymer Journal. 14 (10): 863-873.

90) Jagadish N. Hiremath and Vishalakshi B (2012). Effect of Crosslinking on swelling behaviour of IPN hydrogels of Guar Gum & Polyacrylamide. Der Pharma Chemica. 4(3): 946-955.

91) Javad S and Zohre Z (2014). Advanced drug delivery systems: Nanotechnology of health design: a review. Journal of Saudi Chemical Society. 18: 85–99.

92) John P, Baker, Harvey W, Blanchand JM and Prausnitz (1995). Popcorn-polymer formation during hydrogel synthesis. Journal of Applied Polymer Sciences. 3: 47-58.

93) Kaith BS and Kiran K (2007). Preparation of Psyllium Mucilage and Acrylic Acid Based Hydrogels and their Application in Selective Absorption of Water fromDifferent Oil/Water Emulsions. Iranian Polymer Journal. 16(8): 529-538.

94) Katsura T and Inui K (2003). Intestinal absorption of drugs mediated by drug transporters: mechanisms and regulation. Drug Metabolism and Pharmacokinetic. 18(1): 1-15.

95) Kavitha R, Krishna MG, Shobharani S and Switi G (2011). Natural polysaccharides: versatile excipients for controlled drug delivery systems. Asian Journal of Pharmaceutical Sciences. 6(6): 275-286.

96) Kazimiera HB (2001). Evaluation of microcrystalline chitosan properties as a drug carrier. Part II. The influence of microcrystalline chitosan on release rate of ketoprofen. Acta Poloniae Pharmaceutica. 58(3): 185-194.

97) Khalid SH, Qadir MI, Massud A, Ali M, Rasool MH (2009). Effect of degree of cross-linking on swelling and drug release behaviour of poly (methyl methacrylate-co-itaconic acid) [P(MMA/IA)] hydrogels for site specific drug deliveryJournal of Drug Delivery Science and Technology.19(6): 413-418.

98) Khare AR and Peppas NA (1993). Release behaviour of bioactive agents from pH-sensitive hydrogels. Journal of Biomaterial Sciences Polymer Edition. 4: 275-289.

99) Khare AR and Peppas NA (1994). Swelling/deswelling of anionic copolymer gels. Biomaterials. 16: 559-567.

100) Khare AR and Peppas NA (1995). Swelling/deswelling of anionic copolymer gels. Biomaterials. 16: 559-567.

101) Knop K, Hoogenboom R, Fischer D, Schubert US (2010). Poly (ethylene glycol) in Drug Delivery: Pros and Cons as Well as Potential Alternatives.Angew. Chem. Int. Ed. 49, 6288-6308.

102) Kovanya M, Viness P, Yahya EC, Lisa CToit, Valence MKN, Pradeep K, Shivaan C and Priya B (2012). Oral Drug Delivery Systems Comprising Altered Geometric Configurations for Controlled Drug Delivery.International journal of molecular sciences. 13: 18-43.

103) Kuldeep HR, Nath LK (2012). Formulation, Evaluation and Optimization of Controlled Release Hydrogel Microspheres for Colon Targeted Drug Delivery. Journal of Pharmaceutical Sciences & Research. 4(2): 1739-1747.

104) Kulkarni RV and Sa B (2009). Electroresponsive polyacrylamide-graftedxanthan hydrogels for drug delivery. Journal of Bioactive and Compatible Polymer. 24: 368–84.

105) Kumar R, Srivastava A, Behari K (2007) Graft copolymerization of methacrylic acid ontoxanthan Gum by $Fe^{2+/}H_2O_2$redox initiator. Journal of Applied Polymer Science 105:1922–1929.

106) Langtry HD and Markham A (1999). Rabeprazole. Drugs. 58(4): 725-742.

107) Lee CF, Wen CJ, Lin CL, Wen YC (2004). Morphology and Temperature Responsiveness–Swelling Relationship of Poly (N-isopropylamide–chitosan) Copolymers and Their Application to Drug Release. Journal of Polymer Science. Polymer Chemistry. 42: 3029–3037.

108) Lee SB, Park EK, Lim YM, Seong KC, Kim SY, Lee YM, Nho YC (2006). Preparation of Alginate/Poly (N-isopropylacrylamide) SemiInterpenetrating and Fully Interpenetrating Polymer Network Hydrogels with g-Ray Irradiation and Their Swelling Behaviors. Journal of Applied Polymer Science. 100: 4439–4446.

109) Li Q, Wang J, Shahani S, Sun DDN, Sharma B, Elisseeff JH and Leong LK (2006). Biodegradable and Photocrosslinkable Polyphosphoester Hydrogel. Biomaterials. 27(17): 1027-1034.

110) Li X, Wu W, Wang J, Duan, Y (2006). The swelling behavior and network parameters of guar gum/poly (acrylic acid) semi-interpenetrating polymer network hydrogels. Carbohydr. Polym. 66(4): 473-479.

111) Li Y, Zhang L, Zuo Y, Yang WH, Shen J and Li Y (2010). Poly (N-isopropyl acrylamide)/chitosan composite membrane with smart thermoresponsive performance. Materials Research Innovations. 14: 252–257.

112) Lim Y M and Lee Y M (2005). Preparation and Characterization of pH-Sensitive Poly (ethylene oxide) Grafted Methacrylic Acid and Acrylic Acid Hydrogels by γ-ray Irradiation. Macromolecular Research. 13 (4): 327-333.

113) Lin CC, & Andrew TM (2006). Hydrogels in controlled release formulations: network design and mathematical modeling. Advanced Drug Delivery Review, 58(12): 1379 – 1408.

114) Lind T, Rydberg L, Kylebaèck A, Jonsson A, Andersson T, Hasselgrenà G, Holmbergà J& Roèhss K (2000). Esomeprazole provides improved acid control vs. omeprazole In patients with symptoms of gastro-oesophageal reflux disease. Alimentary Pharmacology Therapeutics. 14: 861-7.

115) Li-Wan PA, Girard T, Farndon P, Cooley C, & Lithgow J (2010). Pharmacogenetics of CYP2C19: functional and clinical implications of a new variant CYP2C19* 17. British journal of clinical pharmacology. 69(3): 222-230.

116) Lowman AM and Peppas NA (1999). Solute transport analysis in pH responsive, complexing hydrogels of poly (methacrylic acid-ethylene glycol). Journal of Biomaterial Science Polymer Edition. 10: 999–1009.

117) Madhusudana KR, Krishna R, Sudhakar P, Chowdoji KR, and Subha MCS (2013). Synthesis and Characterization of biodegradable Poly (Vinyl caprolactam) grafted on to sodium alginate and its microgels for controlled release studies of an anticancer drug. Journal of Applied Pharmaceutical Science. 3(6): 061-069.

118) Madolia H, and Sheo DM (2013). Preparation and evaluation of stomach specific ipn hydrogels for oral drug delivery: a review. Journal of Drug Delivery & Therapeutics. 3(2): 131-140.

119) Malana AM and Rubab Z (2013). The release behavior and kinetic evaluation of tramadol HCl from chemically cross linked Terpolymeric hydrogels. DARU Journal of Pharmaceutical Sciences. 21(10): 1-10.

120) Malfertheiner P, Chan FK, McColl KE (2009). Peptic ulcer disease. Lancet. 374: 1449-1461.

121) Mallikarjuna B, Madhu KSR, Prasad CV, Chowdoji KR, Krishana RKS and Subha MCS (2011). Synthesis, characterization and use of Poly (N-isopropylacrylamide-co-N-vinylcaprolactam) crosslinked thermoresponsive microspheres for control release of Ciproflaxin hydrochloride drug. Journal of Applied Pharmaceutical Science. 1(6): 171-177.

122) Mallikarjuna GM, Somashekar S, Putta RK and Shanta SMK (2010). Physico-chemical characterization, UV spectrophotometric analytical method development and validation studies of Rabeprazole Sodium. Journal of Chemical Pharmaceutical Research. 2(3):187-192.

123) Marina Z, Francesca C, Sara D and Gian MB (2011). Multimeric, Multifunctional Derivatives of Poly (ethylene glycol). Polymers. 3: 1076-1090.

124) Maryam A, Hosein A, Abolfazle B, Aliakbar S, Mehrdad B (2014). Experimental investigation and modeling of the anti-cancer drug delivery from poly (N-isopropylacrylamide-co Acrylic acid) copolymeric hydrogels. International Journal of Biosciences. 5(2): 183-191.

125) Matsuo ES, Tanaka T (1992) Patterns in shrinking gels. Nature 358:482–485.

126) Meenakshi B and Munish A (2015), Psyllium arabinoxylan: Carboxymethylation, characterization and evaluation for nanoparticulate drug delivery. International Journal of Biological Macromolecules. 72: 495–501.

127) Mehrdad H, Mohammad AS, Kobra R (2012). Copolymers: Efficient Carriers for Intelligent Nanoparticulate Drug Targeting and Gene Therapy. Macromolecular Biosciences. 12: 144–164.

128) Mejia A and Kraft WK (2009). Acid peptic diseases: pharmacological approach to treatment. Expert Review of Clinical Pharmacology. 2(3): 295–314.

129) Mishra BN, Mehta IK, Khetrapal RC (1984). Grafting onto cellulose. VIII. Graft copolymerization of poly (ethylacrylate) onto cellulose by use of redox initiators. Comparison of initiator reactivities. Journal of Polymer Science Polymer Chemistry. 22: 2767–75.

130) Misra BN, Dogra R, Mehta IK 1980. Grafting onto cellulose. V. Effect of complexing agents on Fenton's Reagent (Fe+2–H2O2) initiated grafting of poly (ethyl acrylate). Journal of Polymer Science Polymer Chemistry. 18:749–752.

131) Miwa H, Ohkura R, Murai T, Sato K, Nagahara A, Hirai S, Watanabe S and Sato N (1999). Impact of rabeprazole, a new proton pump inhibitor, in triple therapy for Helicobacter pylori infection comparison with omeprazole and lansoprazole. Alimentary Pharmacology and Therapeutics, 13:741-746

132) Momin M, Maria S, Sangshetti JN, Zahid Z (2014). Synthesis and characterization of ph-sensitive poly (methacrylic acid)-graft-karaya gum as a matrix for controlled release tablets. Indo American Journal of Pharmaceutical Research. 4(2): 1224-1237.

133) Mudassir J, & Ranjha NM (2008). Dynamic and equilibrium swelling studies: crosslinked pH sensitive methyl methacrylate-co-itaconic acid (MMA-co-IA) hydrogels. Journal of Polymer Research. 15(3): 195-203.

134) Mumper RJ, Huffman AS, Puolakkainen PA, Bouchard LS, Gombotz WR (1994) Calciumalginate beads for the oral delivery of transforming growth factor-β1 (TGF-β1): stabilization of TGF-β1 by the addition of polyacrylic acid within acid-treated beads. Journal of Controlled Release. 30:241–251.

135) Murdan S (2003). Electro-responsive drug delivery from hydrogels. Journal of Controlled Release. 92:1–17.

136) Mynatt RP, Davis GA, Romanelli F (2009). Peptic ulcer disease: clinically relevant causes and treatments. Orthopedics. 32(2):104.

137) Narayan B, Jonathan G, Miqin Z (2010). Chitosan-based hydrogels for controlled, localized drug delivery. Advanced Drug Delivery Reviews. 62: 83–99.

138) Nawaz M, Rohan DD, Gowda DV (2011). Modified polysaccharide as drug delivery: review. 11(1): 42-47.

139) Ndidi CN, Nelson AO and Okezie IA (2014). Naturapolyceutics: The Science of Utilizing Natural Polymers for Drug Delivery. Polymers. 6: 1312-1332.

140) Nho YC, Park JS and Lim YM (2014). Preparation of Poly (acrylic acid) Hydrogel by Radiation Crosslinking and Its Application for Mucoadhesives. Polymers. 6: 890-898.

141) Nihar S and Patel KR (2014). Formulation and Development of Hydrogel for Poly Acrylamide-Co-acrylic acid. Journal of pharmaceutical science and bioscientific research. 4 (1): 114-120.

142) Nihar S, Patel N, Patel KR (2013). A Sequential Review on Intelligent Drug Delivery System. Journal of Pharmaceutical Science and Bioscientific Research. 3(5): 158-162.

143) Omidian H and Park K (2008). Swelling agents and devices in oral drug delivery. Journal of drug delivery science and technology. 18(2): 83-93.

144) Onishi Y, Butler GB, Hogen-Esch TE (2004) 1, 2- propanediol cellulose acrylamide Graft Copolymers. Journal of applied Polymer Science. 92: 3022-3029.

145) Oprea AM, Ciolacu D, Neamtu A, Mungiu OC, Stoica B, & Vasile C. (2010). Cellulose/chondroitin sulfate hydrogels: Synthesis, drug loading/release properties and biocompatibility. Cellulose Chemistry & Technology. 44(9): 369-378.

146) Oprea AM, Manuela TN, Lenuta P, Marcel IP, Catalina EL, Cornelia V (2013). Evaluation of the Controlled Release Ability of Theophylline from Xanthan/Chondroitin Sulfate Hydrogels. Journal of Biomaterials and Nanobiotechnology. 4: 123-131.

147) Organization for Economic Cooperation and Development (OECD) Guidelines for Testing of Chemicals. (2001).Acute OralToxicity- Fixed Dose Procedure Annexure 420.

148) Organization for Economic Cooperation and Development (OECD) Guidelines for Testing of Chemicals. (2001).Acute OralToxicity- Fixed Dose Procedure Annexure 420.

149) Pace F, Stefano P, Stefania C, and Gabriele BP (2007).A review of rabeprazole in the treatment of acidrelated diseases. Therapeutics and Clinical Risk Management:3(3) 363–379.

150) Pankaj K, Ashok L, Bharat B S, Shubhanjali S (2014). Synthesis and characterization of pH sensitive ampiphillic new copolymer of methyl methacrylate grafted on modified starch: influences of reaction variables on grafting parameters. International Journal of Pharmacy and Pharmaceutical Sciences. 6(1): 868-880.

151) Peppas NA and Klier J (1991). Controlled release by using poly (methacrylic acid-g-ethylene glycol) hydrogels. Journal of Controlled Release. 16:203-214.

152) Peppas NA, Bures P, Leobandung W, Ichikawa H (2000). Hydrogels in pharmaceutical formulations. European Journal of Pharmaceutics and Biopharmaceutics. 50: 27-46

153) Peppas NA, Huang Y, Torres-Lugo M, Ward JH and Zhang J (2000). "Physicochemical, Foundations and Structural Design of Hydrogels in Medicine and Biology," Annual Review of Biomedical Engineering. 2: 9-29.

154) Peppas NA, Kristy MW & James OB (2004). Hydrogels for oral delivery of therapeutic proteins. Expert Opinion on Biology Ther. 4(6): 1-7.

155) Peppas NA, Zach HJ, Ali K, and Robert L (2006). Hydrogels in Biology and Medicine: From Molecular Principles to Bionanotechnology. Advanced Materials. 18: 1345–1360.

156) Petr K, Alfred JMY, Daniel M, Harryp Q, Clyde WB and Peter HS (1996). Subcutaneous hydrogel reservoir system for controlled drug delivery. Macromolecular Symposium. 109:15–26.

157) Petzold K, Schwikal K, & Heinze T (2006). Carboxymethyl xylan synthesis and detailed structure characterization. Carbohydrate Polymers. 64: 292–298.

158) Petzold K, Schwikal K, Günther W, & Heinze T. (2006). Carboxymethyl xylan control of properties by synthesis. Macromolecular Symposia. 232: 27–36.

159) Piyasi M, Kishor S, Sourav B, Aditi B, Roshnara M, Kundua PP (2014) . pH sensitive N-succinyl chitosan grafted polyacrylamide hydrogel for oral insulin delivery. Carbohydrate Polymers. 112: 627–637.

160) Piyush G, Kavita V and Sanjay G (2002). Hydrogels: from controlled release to pH-responsive drug delivery. Drug discovery today. 7(10): 569-579.

161) Pourjavadi A, Mahdavinia GR (2006). Superabsorbency: pH Sensitivity and Swelling Kinetics of Partially Hydrolyzed Chitosan-g-poly (Acrylamide) Hydrogels. Turkish Journal of Chemistry. 30: 595-608.

162) Pourjavadi A, Mehran K, Gholam RM, Hossein H (2006). Synthesis and super-swelling behavior of a novel protein based superabsorbent hydrogel. Polymer Bulletin. 57: 813–824.

163) Povea MB, Monal WA, Cauich-Rodríguez JV, Pat AM, Rivero NB, & Covas CP (2011). Interpenetrated chitosan-poly (acrylic acid-co-acrylamide) hydrogels. Synthesis, characterization and sustained protein release studies. Materials Sciences and Applications. 2(06): 509.

164) Prakash P and Kumar N (2013). Formulation, Evaluation and Comparison of Sustained Release Matrix Tablet of Diclofenac Sodium Using Natural Polymer. International Journal of Research in Pharmaceutical and Biomedical Sciences. 4(1): 367-379.

165) Qiu Y and Park K (2001). Environment-sensitive hydrogels for drug delivery. Advanced Drug Delivery Reviews. 53:321–339.

166) Quintanar-Guerrero D, Zorraquín-Cornejo BN, Ganem-Rondero A, Piñón-Segundo E, Nava-Arzaluz MG, & Cornejo-Bravo JM (2008). Controlled release of model substances from pH-sensitive hydrogels. Journal of the Mexican Chemical Society. 52(4), 272-278.

167) Raghavendra CM, Vidhya R and Tejraj MA (2011). Poly (N-vinylcaprolactam-co-methacrylic acid) hydrogel microparticles for oral insulin delivery. Journal of Microencapsulation. 28(5): 384–394.

168) Rakesh NT and Prashant KP (2011). Rabeprazole sodium delayed-release multiparticulates: Effect of enteric coating layers on product performance. Journal of Advanced Pharmaceutical Technology and Research. 2(3): 184–191.

169) Ramakrishnan K and Salinas RC (2007). Peptic ulcer disease. American Family Physician. 76:1005-1012.

170) Ranjha NM, Asadullah M, Abdullah AB, Nuzhat T, Saeed A and Hassan A (2014). Preparation and Characterization of Isosorbide Mononitrate Hydrogels Obtained by Free-Radical Polymerization for Site-Specific Delivery. Tropical Journal of Pharmaceutical Research. 13 (12): 1979-1985.

171) Ranvijay K, Kaushlendra S, Tiwary KP, Gautam S (2013). Polymethacrylic acid grafted psyllium (Psy-g-PMA): a novel material for waste water treatment. Applied Water Science. 3:285–291.

172) Richter JE (2005). The management of heartburn in pregnancy. Alimentary Pharmacology and Therapeutics. 22: 749-757.

173) Ritger PL, Peppas NA (1987). A Simple Equation for Description of Solute Release. II. Fickian and Anomalous Release from Swellable Devices. Journal of Controlled Release. 19: 37-42.

174) Robert L (1993). Polymer controlled drug delivery system. Accounts of chemical research. 26:537-542.

175) Rosiak JM & Yoshii F (1999) Hydrogels and their medical applications. Nuclear Instruments and Methods in Physics Research. 151: 56-64.

176) Rowe RC, Sheskey PJ, Quinn ME (2009). Handbook of Pharmaceutical Excipients. London Pharmaceutical Press.

177) Sabyasachi M, Somdipta R and Sa B (2010). Polysaccharide-based graft copolymers in controlled drug delivery. International Journal of Pharmaceutical Technology. 2: 1350-1358.

178) Sadeghi M (2010). Synthesis and Swelling Behaviors of graft copolymer Based on Chitosan-g-poly (AA-co-HEMA). International Journal of Chemical Engineering and Applications. 1(4): 354-358.

179) Sadeghi M (2011a). Pectin-Based Biodegradable Hydrogels with Potential Biomedical Applications as Drug Delivery Systems. Journal of Biomaterials and Nanobiotechnology. 2: 36-40.

180) Sadeghi M (2011b). Synthesis of starch-g-poly (acrylic acid-co-2-hydroxy ethyl methacrylate) as a potential pH-sensitive hydrogel-based drug delivery system.Turkish Journal of Chemistry. 35(5): 723-733.

181) Sadeghi M, & Hosseinzadeh H (2008). Synthesis and swelling behavior of starch-poly (sodium acrylate-co-acrylamide) superabsorbent hydrogel. Turkish Journal of Chemistry. 32(3): 375-388.

182) Sadeghi M, Hosseinzadeh H (2010). Studies on graft copolymerization of 2-hydroxyethylmethacrylate onto kappacarrageenan initiated by ceric ammonium nitrate, Journal of Chilean and chemical society. 55(4): 123-130.

183) Sadeghi M, Nahid G and Fatemeh S (2012). Graft Copolymerization Methacrylamide Monomer onto Carboxymethyl Cellulose in Homogeneous Solution and Optimization of Effective Parameters. World Applied Sciences Journal. 16 (1): 119-125.

184) Sadeghi M, Soleimani F, Yarahmadi M (2011). Chemical Modification of Carboxymethyl Cellulose via Graft Copolymerization and Determination of the Grafting Parameters. Oriental Journal of Chemistry, 27(3): 967 – 972.

185) Saghir S, Saeed MI, Ajaz MH, Andreas K, Thomas H (2008). Structure characterization and carboxymethylation of arabinoxylan isolated from Ispaghula (*Plantago ovata*) seed husk. Carbohydrate Polymers. 74(2):309–317.

186) Satish CS, Satish KP, Shivakumar HG (2006). Hydrogels as controlled drug delivery systems: Synthesis, crosslinking, water and drug transport mechanism. Indian journal of Pharmaceutical Sciences. 68: 133-140.

187) Savarino V, Mela GS, Zentilin P, Bisso G, Pivari M, Vigneri S, Termini R, Fiorucci S, Usai P, Malesci A, Celle G,(1998). Comparison of 24-h control of gastric acidity by three different dosages of pantoprazole in patients with duodenal ulcer. Alimentary Pharmacology Therapeutics. 12:1241-7.

189) Serraa L, Joseph D, Peppas N A (2006). Drug transport mechanisms and release kinetics from molecularly designed poly (acrylic acid-g-ethylene glycol) hydrogels. Biomaterials. 27: 5440–5451.

190) Siddhi G, Thomas JW, Arvind S (2011). Evolution of PVA gels prepared without crosslinking agents as a cell adhesive surface. Journal of Material Science. 22:1763–1772.

191) Siepman J and Peppas NA (2001). Modeling of drug release from delivery systems based on hydroxypropyl methylcellulose (HPMC). Advanced Drug Delivery Review. 48: 139–157.

192) Silva DA, Paula RCM, Feitosa JPA (2007). Graft copolymerization of acrylamide onto cashew gum. European Polymer Journal. 43: 2620-9.

193) Sim SC, Risinger C, Dahl ML, Aklillu E, Christensen M, Bertilsson L, Ingelman-Sundberg M (2006). A common novel CYP2C19 gene variant causes ultrarapid drug metabolism relevant for the drug response to proton pump inhibitors and antidepressants. Clinical Pharmacology Therapeutics. 79: 103–113.

194) Singh B, Sharma V and Kumar S (2011). Synthesis of smart hydrogels by radiation polymerisation for use as slow drug delivery devices. Canadian Journal of Chemical Engneering. 89: 1596–1605.

195) Singha AS and Ashvinder KR 2011. Kinetics of Graft Copolymerization of Acrylic Acid onto Cannabis indica Fibre. Iranian Polymer Journal. 20(11): 913-929.

196) Snežana IS, Ljubiša N, Vesna N, Slobodan P, Mihajlo S, Ivana MR (2001). Stimuli-sensitive hydrogels for pharmaceutical and medical applications. Physics, Chemistry and Technology. 9(1):37 – 56.

197) Sohail K, Khan IU, Shahzad Y, Hussain T, & Ranjha NM (2014). pH-sensitive polyvinylpyrrolidone-acrylic acid hydrogels: Impact of material parameters on swelling and drug release. Brazilian Journal of Pharmaceutical Sciences, 50(1): 173-184.

198) Soppimath KS, Aminabhavi TM, Dave AM, Kumbar SG, Rudzinski WE, (2002). Stimulus-responsive "smart" hydrogels as novel drug delivery systems. Drug Development and Industrial Pharmacy. 28: 957-974.

199) Stedman CA and Barclay ML (2000). Review article: comparison of the pharmacokinetics, acid suppression and efficacy of proton pump inhibitors. Aliment Pharmacology and Therapeutics. 14(34): 963-78.

200) Subham B, Gaurav C, Animesh G (2010). Smart polymers: around the cosmos. Asian Journal of Pharmaceutical and Clinical Research. 3(3): 135-141.

201) Sung JH, Hwang MR, Kim JO, Lee JH, Kim YI, Kim JH, Chang SW, Jin SG, Kim JA, Lyoo WS,Han SS, Ku SK, Yong SH, Choi HG (2010). Gel characterization and *in vivo* evaluation of minocycline-loaded wound dressing with enhanced wound healing using poly (vinyl alcohol) and chitosan. International Journal of Pharmacy. 392: 232–240.

202) Sunil KB and Surinderpal S (2006). Analysis of swelling behavior of poly (methacrylamide-co-methacrylic acid) hydrogels and effect of synthesis conditions on water uptake. Reactive & Functional Polymers. 66: 431–440.

203) Susana S, Ana F, Francisco V (2012). Modular Hydrogels for Drug Delivery. Journal of Biomaterials and Nanobiotechnology. 3: 185-199.

204) Suvakanta D, Padala NM, Lilakanta N and Prasanta C (2010). Kinetic modeling on drug release from controlled drug delivery systems. Drug Research. 67(3): 217-223.

205) Swan SK, Hoyumpa AM, Merritt GJ. 1999. Review article: the pharmacokinetics of rabeprazole in health and disease. Alimentary Pharmacology and Therapeutics. 13(3): 11–7.

206) Swathimutyam P and Bala P (2013). Review on Polymers in Drug Delivery. American Journal of Pharmaceutical Technology Research. 3(4): 900-917.

207) Tanaka T, Nishio I, Sun ST, & Ueno-Nishio S (1982). Collapse of gels in an electric field. Science. 218(4571): 467-469.

208) Tanaka T, Sun S-T, Hirokawa Y, Katayama S, Kucera J, Hirose Y, Amiya T (1987) Mechanical instability of gels at the phase transition. Nature 325:796–798.

209) Thakkar H, Patel B, Thakkar S (2010). A review on techniques for oral bioavailability enhancement of drugs. International Journal of Pharmaceutical Sciences Review and Research. 4(3): 203-223.

210) Thakur A, Wanchoo RK, and Singh P (2011). Hydrogels of Poly (acrylamide-co-acrylic acid): In-vitroStudy on Release of Gentamicin Sulfate. Chem. Biochem. Eng. Q.25(4) 471–482

211) Thjodleifsson B, Beker JA, Dekkers C,et al (2000).Rabeprazole versus omeprazole in preventing relapse of erosive or ulcerative gastroesophageal reflux disease: a double-blind, multicenter, European trial. Dig Dis Sci; 45: 845–53.

212) Togrul H and Arslan N (2003). Production of carboxymethyl cellulose from sugar beet pulp cellulose and rheological behaviour of Carboxymethyl cellulose. Carbohydrate Polymers. 54: 73-82.

213) Troy EG, Benjamin DG (2003). The Use of Proton Pump Inhibitors in Children. Pediatric drugs. 5(1): 25-40.

214) Uno T, Shimizu M, Yasui-Furukori N, Sugawara K, Tateishi T (2006). Different effects of fluvoxamine on rabeprazole pharmacokinetics in relation to CYP2C19 genotype status. Br J Clin Pharmacol. 61(3):309-14.

215) Varshosaz J and Niloufar K (2002). Cross-linked Poly (vinyl alcohol) Hydrogel: Study of Swelling and Drug Release Behaviour. Iranian Polymer Journal. 11(2): 123-131.

216) Veeran GK and Guru VB (2011). Water Soluble Polymers for Pharmaceutical Applications. Polymers. 3: 1972-2009.

217) Vilar G, Judit TP and Fernando A (2012). Polymers and Drug Delivery Systems. Current Drug Delivery. 9: 1-28.

218) Wang J and Wu W (2005). Swelling behaviors, tensile properties and thermodynamic studies of water sorption of 2-hydroxyethyl methacrylate/epoxymethacrylate copolymeric hydrogels. European Polymer Journal. 41: 1143-1151.

219) Wang WB, Xu JX, Wang AQ (2011). A pH-, salt- and solvent-responsive carboxymethylcellulose-g-poly (sodium acrylate)/medical stone superabsorbent composite with enhanced swelling and responsive properties. eXPRESS Polymer Letters.5(5) 385–400.

220) Wei L, Cai C, Lin J and Chen T (2009). Dual-drug delivery system based on hydrogel/micelle composites, Biomaterials. 30: 2606-2613.

221) Welage LS. (2003). Pharmacologic Properties of Proton Pump Inhibitors. Pharmacotherapy. 23: 745–805.

222) Wenbo W, Jiang W, Yuru K, Aiqin W (2011). Synthesis, swelling and responsive properties of a new composite hydrogel based on hydroxyethyl cellulose and medicinal stone. Composites. 42: 809–818.

223) Wichterle O, and Lim D (1960). Hydrophilic gels for biological use. Nature. 117-118.

224) Williams MP and Pounder RE (1999). Review article: the pharmacology of Rabeprazole. Alimentary Pharmacology and Therapeutics. 13(3): 3-10.

225) Yakup AM, Gülay B, Betül A, Emine Y, Koichi I and Yusuf Y (2005). Novel hydrogel membrane based on copoly (hydroxyethyl methacrylate/p-vinylbenzylpoly (ethylene oxide)) for biomedical applications: properties and drug release characteristics. Macromolecular Biosciences. 5(10): 983–992.

226) Yoshida R, Uchida K, Kaneko Y, Sakai K, Kikuchi A, Sakurai Y, Okano T (1995) Comb-type grafted hydrogels with rapid deswelling response to temperature changes. Nature. 374:240–242.

227) You JO and Auguste DT (2010). Conductive, physiologically responsive hydrogels. Langmuir. 26: 4607–4612.

228) You JO, Dariela A, George JCY and Debra TA (2010). Bioresponsive matrices in drug delivery. Journal of Biological Engineering. 4(15): 1-12.

229) Yuen SN, Choi SM, Phillips DL, Ma C (2009). Raman and FTIR spectroscopic study of carboxymethylated non-starch polysaccharides. Food chemistry. 114:1091-1098.

230) Zhang CH, Bing XZ, Yue H,Ying W, XiYK, Bo JZ, Xuan Z, and Qiang Z (2011). A Novel Domperidone Hydrogel: Preparation, Characterization, Pharmacokinetic, and Pharmacodynamic Properties. Journal of Drug Delivery. 2011: 1-9.

231) Zhang J and Peppas NA. (2000). Synthesis and Characterization of pH- and Temperature-Sensitive Poly (methacrylic acid)/Poly (N-isopropylacrylamide) Interpenetrating Polymeric Networks. Macromolecules, 33: 102-107

232) Zhe C, Xiaoyan L and Xuegang L (2011). Study on the synthesis of thermoplastic carboxymethyl cellulose with graft copolymerization. In Computer Distributed Control and Intelligent Environmental Monitoring (CDCIEM) International Conference on. 1224-1227).

PHARMACY RESEARCH ETHICS COMMITTEE
The Islamia University of Bahawalpur

Ref. No. 106-2014/PREC
Date: 12-02-2014

APPROVAL CERTIFICATE

The research project entitled "Development of Graft Co-polymeric Carrier Networks for Controlled Drug Delivery and its Evaluation" submitted by the applicant Ms. Ume Ruqia Tulain through application no. 110 dated November 28, 2013. Pharmacy Research Ethics Committee (PREC), in its meeting held on January 21, 2014, has recruited the research project and reviewed all aspects of ethical issues with reference to its policy. After the agreement of all members, the committee has approved above mentioned research study. Moreover the principal investigator has directed to assure the strict adherence to protocols recommended by the PREC during the conduct of study.

Prof. Dr. Mahmood Ahmad
Chairman,
Pharmacy Research Ethics Committee (PREC)

For any query please contact:
Department of Pharmacy, Khawaja Fareed Campus, Railway Road
The Islamia University of Bahawalpur, Bahawalpur-Punjab, Pakistan
Tel. +92629255565; Fax. +92629255565; E-mail. ma786_786@yahoo.com